Seeing through the clip of a fin: Comparing the salmonid liver and caudal fin transcriptome in demonstrating oil spill response

By

Jacob James Imbery
Diploma in Applied Chemistry and Biotechnology, Camosun College, 2014
B.Sc., University of Victoria, 2018

A Thesis Submitted in Partial Fulfillment
of the Requirements for the Degree of

MASTER OF SCIENCE

in the Department of Biochemistry and Microbiology

We acknowledge and respect the lək^{w}əŋən peoples on whose traditional territory the university stands and the Songhees, Esquimalt and W̱SÁNEĆ peoples whose historical relationships with the land continue to this day.

Supervisory Committee

Seeing through the clip of a fin: Comparing the salmonid liver and caudal fin transcriptome in demonstrating oil spill response

By

Jacob James Imbery
Diploma in Applied Chemistry and Biotechnology, Camosun College, 2014
B.Sc., University of Victoria, 2018

Dr Caren C. Helbing (Department of Biochemistry and Microbiology)

Supervisor

Dr. Lisa A. Reynolds (Department of Biochemistry and Microbiology)

Departmental Member

Dr. Ben F. Koop (Department of Biology)

Outside Member

Abstract

Effective tracking and management of an oil spill are crucial to mitigating deleterious effects on fish. Currently, the area covered by an oil spill is tracked primarily through satellite and aerial imaging of the top slick. However, this method of oil spill tracking fails to capture the dispersal of water-soluble compounds released from a spill, such as polycyclic aromatic hydrocarbons (PAH) and naphthenic acids (NA), that can be environmentally persistent. Transcriptomic biomonitoring of sentinel animals can be a powerful method for tracking and evaluating the impact of environmental toxicants, however, current sampling methods are lethal. Instead, the present thesis work evaluates the use of the caudal fin transcriptome as a nonlethal alternative to demonstrate salmon biological response to the water accommodated fraction (WAF) generated during an oil spill.

Most deleterious effects of WAF exposure presented in the literature were observed in fish embryos exposed to crude oil WAF under freshwater and/or warm marine conditions. As temperature, salinity, and oil type significantly impact oil WAF composition and toxicity, it is important to investigate effects of WAF exposure generated in cold-water marine conditions and with a variety of oil types. Herein, oil WAFs were generated at nonlethal concentrations with 100-to-1000 mg/L of one of four different oil types under cold-water marine conditions and juvenile coho smolts were exposed for 96 h. Paired caudal fin and liver tissues were collected from genotypically-sexed smolts and transcriptomic responses queried through gene-targeted quantitative real-time polymerase chain reaction (qPCR) and RNA-Seq assays. WAFs were characterized by the sum of 50 PAHS (tPAH-50) and measured using gas chromatography/triple quadrupole mass spectrometry.

WAFs generated with low sulfur marine diesel (LSMD) resulted in a significant and sex-biased change in gene transcript abundance relative to unexposed seawater controls in both the liver and caudal fin, demonstrating PAH exposure, general and oxidative stress, and estrogenic activity. In both female and male liver and caudal fin, *cyp1a1* exhibited the greatest increase in transcript abundance after 96 hours of LSMD WAF exposure, demonstrating that *cyp1a1* is a robust, sex-independent bioindicator of LSMD WAF exposure at this time point. Further evaluating transcript abundance of *ahr* and *cyp1a1* in the caudal fin significantly demonstrated response to WAFs generated with high sulfur fuel oil (HSFO), diluted bitumen (dilbit), and Alaskan crude oil relative to seawater controls. In contrast, response to Alaskan crude WAF exposure was not detected in the liver. HSFO WAF exposure induced the greatest *cyp1a1* response in both tissues, with the lowest response to Alaskan crude WAF despite containing the second highest tPAH50 concentration demonstrating a need for better PAH-responsive transcript bioindicators. RNA-Seq analysis of LSMD and HSFO WAF exposures revealed significant responses in the liver and caudal fin transcriptomes that were specific to oil type, tissue, and genetic sex. In addition to enrichment of transcripts involved in immunomodulation (LSMD WAF) and a cancer-like cell state (HSFO WAF), RNA-Seq analysis identified liver and caudal fin bioindicator candidates common across oil WAF types. Ultimately, this work demonstrates a robust response of the coho salmon caudal fin transcriptome to oil WAF exposure that is more consistent between sexes and different oil exposures than the conventional liver tissue. This improved consistency is ideal for biomonitoring assays and demonstrates promise for using the caudal fin transcriptome as a non-lethal alternative for assessing and tracking oil spill exposure in marine environments.

Table of Contents

Supervisory Committee ii

Abstract iii

Table of Contents v

List of Tables xi

List of Figures xii

List of Abbreviations xiv

Acknowledgements xvi

Dedication xvii

Thesis Format and Manuscript Claims xviii

1. Introduction 1

1.1. Tracking and managing oil spills is difficult 1

1.2. Biomonitoring of sentinel fish for environmental contaminant detection 3

1.3. Use of transcriptomics to detect sublethal deleterious effects of environmental contaminants 4

1.4. Transcriptomic sampling of the caudal fin as a non-lethal alternative to traditional methods 6

1.5. AhR-mediated pathway as a bioindicator for oil spill exposure 6

1.6. Coho salmon as an important test species 9

1.7. Objectives 11

2. Evaluation of gene bioindicators in the liver and caudal fin of juvenile Pacific coho salmon in response to low sulfur marine diesel seawater-accommodated fraction exposure 13

2.1. Introduction 13

2.2. Materials and methods 15

2.2.1. Source of seawater 15

2.2.2. WAF generation 15

2.2.3. Marine-acclimated coho salmon exposure tests 16

2.2.4. Chemistry subsampling 18

2.2.5. PAH analytical chemistry 19

2.2.6. Dissections 20

2.2.7. Isolation of total RNA and preparation of cDNA 20

2.2.8. qPCR analyses 21

2.2.9. Isolation of genomic DNA and sex genotyping 23

2.2.10. Statistical analyses 23

2.3. Results and Discussion 24

2.3.1. WAF tPAH50 concentration and chemical composition 24

2.3.2. Fish mortalities and morphometrics 27

2.3.3. Sex genotyping 27

2.3.4. Transcript abundance of biological indicators in liver and caudal fin 28

3. Evaluation of oil-responsive bioindicators in the caudal fin and liver in response to four different oil WAF exposures 40

3.1. Introduction 40

3.2. Materials and Methods 42

3.2.1. Source of seawater 42

3.2.2. WAF generation 42

3.2.3. Marine-acclimated coho salmon smolt exposure tests 43

3.2.4. PAH analytical chemistry 44

3.2.5. Isolation of total RNA, cDNA preparation, quantitation of mRNA abundance, and genotypic sexing 44

3.2.6. Statistical analyses 44

3.3. Results and Discussion 45

3.3.1. HSFO WAF 45

3.3.2. dilbit WAF 48

3.3.3. Alaskan crude WAF 51

3.3.4. Comparison of LSMD, HSFO, dilbit, and Alaskan crude oil WAFs……..54

3.3.5. Comparison of the liver and caudal fin in demonstrating biological response to oil WAF exposure 55

4. Near vs. far-shore fuels: Comparing the transcriptomic response of the salmonid caudal fin and liver to marine oil spills 58

4.1. Introduction 58

4.2. Materials and methods 60

4.2.1. Preparation of RNA for Illumina total RNA sequencing..... 60

4.2.2. RNA-Seq Assembly and Analysis 60

4.3. Results and Discussion..... 63

4.3.1. Evaluation of sex-biased baseline gene expression in control coho salmon smolts 63

4.3.2. LSMD WAF Exposure 63

4.3.3. HSFO WAF Exposure 68

4.3.4. Comparison between LSMD and HSFO WAF exposure responses of coho salmon smolts……72

5. Overall conclusions and future directions..... 81

5.1. Conclusions 81

5.2. Future directions..... 83

Bibliography 85

Appendices..... 100

Appendix 1. Water chemistry results for LSMD, HSFO, dilbit, and Alaskan crude WAFs…..100

Appendix 2. List of the 50 PAHs and alkylated PAHs included in the tPAH50 analysis……..101

Appendix 3. Comparison of the PAH selection used for tPAH50 analysis……..…..103

Appendix 4. qPCR primers validated for transcript and sex genotype analyses……105

Appendix 5. LSMD WAF normalizer C_t values……..……...106

Appendix 6. Primer efficiency scores of qPCR tools used……107

Appendix 7. Water chemistry results measuring PAHs (n=4) and volatile organic compounds (n=1) in the marine seawater supply……108

Appendix 8. The distribution of the PAHs grouped by number of aromatic rings…….110

Appendix 9. Weight and fork length of LSMD, HSFO, dilbit, and Alaskan crude WAF-exposed juvenile coho salmon prior to tissue sampling……..…111

Appendix 10. Distribution of male and female juvenile coho salmon from the LSMD, HSFO, dilbit, and Alaskan crude WAF exposures according to treatment condition…….112

Appendix 11. The qPCR amplification curves of juvenile coho salmon gDNA using *U-sdY* and *OtY2-WSU* primer sets…….113

Appendix 12. HSFO WAF normalizer C_t values…….…...114

Appendix 13. dilbit WAF normalizer C_t values……...…...115

Appendix 14. Alaskan crude WAF normalizer C_t values……...116

Appendix 15. PAH composition of HSFO WAF over time……...117

Appendix 16. PAH composition of dilbit WAF……..…118

Appendix 17. PAH composition of Alaskan crude WAF……...119

Appendix 18. Volcano plots contrasting 5 males to 5 female transcript profiles in the liver and caudal fin in the seawater control exposures……...120

Appendix 19. Six genes that are differentially expressed in all tissues with LSMD WAF……121

Appendix 20-1. Map of enriched GO terms from LSMD WAF……122

Appendix 20-2. Continued map of enriched GO terms from LSMD WAF exposure……..…123

Appendix 21. 312 genes that are differentially expressed in all tissues with HSFO WAF……124

Appendix 22-1. Map of enriched GO terms from HSFO WAF……...……...137

Appendix 22-2. Continued map of enriched GO terms from HSFO WAF……138

Appendix 22-3. Continued map of enriched GO terms from HSFO WAF……139

Appendix 22-4. Continued map of enriched GO terms from HSFO WAF……140

Appendix 23. *Cyp1a1* qPCR amplification and thermodenaturation peak…….141

Appendix 24. Liver primer efficiencies……..142

Appendix 25. Caudal fin primer efficiencies……..143

List of Tables

Table 1.1 Examples of commonly released compounds from oil spills.

Table 4.1. The number of differentially expressed genes from LSMD and HSFO WAF exposures.

Table 4.2. List of consistently responsive DETs in the liver to LSMD and HSFO WAF exposure.

Table 4.3. List of consistently responsive DETs in the caudal fin to LSMD and HSFO WAF exposure.

Table 4.4. Partial list of 21 DETs in the liver that respond to HSFO WAF, but not LSMD WAF, exposure.

Table 4.5. List of six DETs in the caudal fin that respond to LSMD WAF, but not HSFO WAF, exposure.

Table 4.6. Partial list of 20 DETs in the caudal fin that respond to HSFO WAF, but not LSMD WAF, exposure.

List of Figures

Figure 1.1. Cartoon depicting activation of the aryl hydrocarbon receptor-mediated pathway.

Figure 1.2. Diagram depicting the anadromous life cycle of Pacific salmon.

Figure 1.3. Cartoon depicting experimental parameters assessed in this thesis.

Figure 2.1. Schematic demonstrating tank setup for WAF exposures.

Figure 2.2. LSMD WAF tPAH50 concentrations over time.

Figure 2.3. Individual PAH concentrations from LSMD WAF.

Figure 2.4. Comparison of *OtY2-WSU* and *U-sdY* genetic sex markers.

Figure 2.5. qPCR of PAH-response gene transcript abundance after LSMD WAF exposure.

Figure 2.6. qPCR of stress-response gene transcript abundance after LSMD WAF exposure.

Figure 2.7. qPCR of estrogenic-response gene transcript abundance after LSMD WAF exposure.

Figure 2.8. qPCR of metal defense-response gene transcript abundance after LSMD WAF exposure.

Figure 3.1. HSFO WAF tPAH50 concentrations over time.

Figure 3.2. qPCR of PAH-response gene transcript abundance after HSFO WAF exposure.

Figure 3.3. dilbit WAF tPAH50 concentrations over time.

Figure 3.4. qPCR of PAH-response gene transcript abundance after dilbit WAF exposure.

Figure 3.5. Alaskan crude WAF tPAH50 concentrations over time.

Figure 3.6. qPCR of PAH-response gene transcript abundance after Alaskan crude WAF exposure.

Figure 4.1. A diagram depicting the RNA-Seq workflow used.

Figure 4.2. Venn-diagram and differential expression profile resulting from LSMD WAF exposure.

Figure 4.3. Top five largest clusters of GO terms enriched by LSMD WAF exposure.

Figure 4.4. Venn-diagram and differential expression profile resulting from HSFO WAF exposure.

Figure 4.5. Top five largest clusters of GO terms enriched by HSFO WAF exposure.

Figure 4.6. Venn-diagram comparing the overlap of DETs between LSMD and HSFO WAF exposure.

List of Abbreviations

Use of capitalization and italics for gene transcripts and proteins follows the scheme given below, which is derived from https://www.biosciencewriters.com/Guidelines-for-Formatting-Gene-and-Protein-Names.aspx

Class	Gene transcript	Protein
Mammalia	*Ahr*	AhR
Fish	*ahr*	AhR

%id	Percent identity
ahr	Aryl hydrocarbon receptor
ARNT	Ahr-Nuclear translocator
BAP	Benzo[a]pyrene
BTEX	Benzene, toluene, ethylbenzene, and xylene
CALA	Canadian Association for Laboratory Accreditation Inc
CAN	Acetonitrile
cDNA	Complementary DNA
CF	Caudal fin
cpm	Counts per million reads
cyp19	Cytochrome p450 family 19
cyp1a	Cytochrome P450-1a
DBF	Dibenzofulvene
DCM	Dichloromethane
DEG	Differentially expressed gene
DET	Differentially expressed transcript
dilbit	Diluted bitumen
ER	Estrogen receptor
EROD	7-ethoxy-resorufin O-deethylation
F	Females
FC	Fold-change
gapdh	Glyceraldehyde 3- phosphate dehydrogenase
GC-MS/MS	Gas chromatography/triple quadrupole mass spectrometry
gDNA	Genomic DNA
GO	Gene ontology
GSC	Genome sciences centre
GSI	Gonadosomatic index
HEPH	Heavy extractable petroleum hydrocarbons
HSFO	High sulfur fuel oil
hsp70	Heat shock protein 70

LC50	Median lethal concentrations of exposure
LEPH	Light extractable petroleum hydrocarbons
LI	Liver
LSMD	Low sulfur marine diesel
M	Males
Med	Medium
mta	Metallothionein A
NA	Naphthenic acids
NAP	Naphthalene
NCBI	National Center for Biotechnology Information
nr	Non-redundant
nt	Nucleotide
PAH	Polycyclic aromatic hydrocarbons
PYLET	Pacific & Yukon Laboratory for Environmental Testing
qPCR	Quantitative real-time polymerase chain reaction
RIN	RNA integrity number
rpl8	Ribosomal protein L8
rps10	Ribosomal protein S10
sod	Superoxide dismutase
SW	Seawater
tPAH	Sum of total PAH concentrations
tPAH50	Sum of 50 targeted PAH concentrations
ugt	UDP-glucuronosyltransferases
vepg	Vitelline envelope protein gamma
vtg	Vitellogenin
WAF	Water accommodated fraction

Acknowledgements

I would like to thank my supervisor, Dr. Caren Helbing, for her unwavering support and guidance throughout completing this thesis work and for a creating a truly enjoyable and unforgettable learning experience throughout my time in her lab. I would like to also thank my committee members, Dr. Lisa Reynolds and Dr. Ben Koop for their excitement and support over the course of this thesis work.

I would like to thank Emily Koide, for being a great mentor into graduate studies, and Meg Kempe for all her help running so many qPCR plates. I would also like to specifically thank Michael Allison, Lauren Bergman, Jessica Round, and Dr. Anita Thambirajah for providing valuable feedback and insight over the years, as well as the rest of the past and present members of the Helbing lab.

Dedication

For Kira Holder

For her unending patience and support during this thesis work

Thesis Format and Manuscript Claims

This thesis is presented in a manuscript format. Chapter 1 provides background information and introduces the rationale of the thesis. Chapters 2, 3, and 4 are written in a manuscript style containing an Introduction, Materials and Methods, and Results and Discussion. Chapter 5 synthesizes the major findings of the papers and suggests future experimental directions.

Chapter 2: **Imbery J**, Buday C, Miliano R, Shang D, Round J, Kwok H, Van Aggelen G, Helbing C. 2019. Evaluation of gene biomarkers in the liver and caudal fin of juvenile Pacific coho salmon in response to low sulphur marine diesel seawater-accommodated fraction exposure. Environ Sci Technol 53(3):1627-1638. Pilot experiments for validating the concept of this work were performed by Jessica Round. WAF exposures and tPAH50 analyses were completed by our collaborators at Environment and Climate Change Canada. Craig Buday and Rachel Miliano oversaw WAF exposures and tissue dissections. Honoria Kwok and Dayue Shang quantified PAH concentrations using GC-MS/MS. Jacob Imbery extracted gDNA and RNA from RNA-later preserved dissected tissues and performed all transcriptomic assays and data analysis. Jacob Imbery and co-authors prepared the manuscript.

Chapter 3: **Imbery J**, Kempe, M, Buday C, Miliano R, Shang D, Round J, Kwok H, Van Aggelen G, Helbing C. 2021. Evaluation of oil-responsive bioindicators in the caudal fin and liver in response to four different oil WAF exposures. Unpublished data. Distributions of labour regarding WAF exposures, analytical chemistry, and transcriptomic analyses are the same as in Chapter 2, with the addition of Meg Kempe assisting in qPCR analysis of HSFO WAF exposures. Manuscript was prepared by Jacob Imbery.

Chapter 4: **Imbery J**, Buday C, Miliano R, Shang D, Round J, Kwok H, Van Aggelen G, Helbing C. 2021. Near vs. far-shore fuels: Comparing the transcriptomic response of the salmonid caudal fin and liver to marine oil spills. Unpublished data. Distributions of labour regarding WAF exposures and analytical chemistry are the same as in Chapter 2. Total RNA sequencing was performed at the BC Cancer Michael Smith Genome Sciences Centre. RNA-Seq pipeline development and data analysis was performed by Jacob Imbery. Manuscript was prepared by Jacob Imbery and co-authors. This chapter will be combined with HSFO WAF results from Chapter 3 for manuscript submission.

1. Introduction

1.1. Tracking and managing oil spills is difficult

Large-scale petroleum oil spills (>30 tonnes) result in the reduction/closure of tourism and fishery activities, erosion/fouling of marine and coastal habitats, and death or impairment of exposed populations.[1–3] As it is estimated that 0.2-2.0 x 10^6 tonnes of petroleum oil are spilled into the global marine environment every year, it is important to have efficient and accurate tools to assess the extent of the environmental and economic impact of these oil spills.[1,2] In addition to managing the top slick, it is also important to consider the water-soluble molecules released from an oil spill that can exhibit high environmental persistence,[4] such as polycyclic aromatic hydrocarbons (PAH) and naphthenic acids (NA). Exposure to this water accommodated fraction (WAF) released from a spill can result in serious deleterious effects in fish populations, significantly impacting fish reproduction,[5–7] development,[8] cardiac function,[9] and social group adhesion.[10]

Due to ocean currents, the WAF can be distributed broadly from the initial site of an oil spill.[11] Unlike the top slick, an oil WAF is invisible to the naked eye and cannot be visually tracked. As satellite and aerial imaging are the primary tools for tracking oil spill dispersal, oil WAFs pose significant difficulties for oil spill management initiatives, as directing cleanup crews and shutting down fisheries activities is highly dependent on effective oil spill tracking.[12] This was particularly observed during the *Deepwater Horizon* blowout in the Gulf of Mexico, where responses were dictated by overhead imaging of the spill[13] only to find the effects of oil spill damage reaching far past initial estimates months and even years later.[12] There is a substantial need for reliable tools capable of tracking the dispersal of these water-soluble compounds.

Petroleum products are a complex mixture of chemical compounds estimated to be comprised of tens of thousands of hydrocarbons and other related hetero-compounds with only a fraction of the compounds released from an oil spill amenable to characterization using current analytical techniques.[14,15] Of those quantifiable, aliphatic hydrocarbons, monocyclic aromatics (BTEX; benzene, toluene, ethylbenzene, and xylene), PAHs, and NAs are cited as the most concerning pollutants from petroleum-based oil spills (**Table 1.1**).[16,17] Aliphatic hydrocarbons and BTEX are the most abundant fractions detected in source oil, however due to their high volatility they are not detected in high abundance in spilled oil.[18,19] Petrogenic PAHs are the most studied constituents released from oil spills that demonstrate increased persistence in aquatic environments with higher molecular weight.[20] NAs are more water soluble than PAHs and comprise up to 3-4% by weight of petroleum products.[17] NAs are also very persistent. For example, they can be detected in coastal marine sediments up to five years after an oil spill.[21]

Table 1.1. Examples of BTEX, PAHs, and NAs found commonly in petroleum products.

Aliphatic hydrocarbons	BTEX	PAH	NA
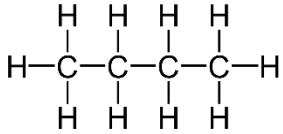 Butane	 Benzene	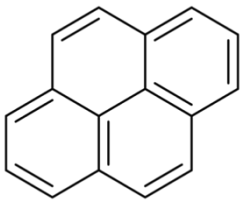 Pyrene	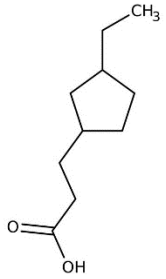 3-Naphthenic acid

The majority of oil WAF research focuses on Alaska North Slope and Macondo crude oils, which were involved in the *Exxon Valdez* and *Deepwater Horizon* oil spills.[2] Consequently, there is a lack of research on other non-conventional crude oils, like diluted bitumen (dilbit) or marine

diesels.[2] Furthermore, work studying the biological effects of WAF exposure is often performed in freshwater systems and/or at warm/temperate conditions. As temperature and salinity have been shown to significantly impact oil WAF composition,[22,23] it is important to study oil WAF generation and exposure under cold marine conditions as well.

Due to the low environmental persistence of aliphatic hydrocarbons and BTEX, these compounds are often not included in oil WAF characterization as they are rapidly weathered from solution.[4] Although NAs are abundant in oil WAFs, direct quantification of these molecules is challenging due to the extensive variation of the fatty acids chains between individual NAs.[24] Currently, quantification of PAHs via gas chromatography/triple quadrupole mass spectrometry(GC-MS/MS) is the best analytical chemistry-based method for characterization of the WAF dispersed from oil spills.[25] However, this method of PAH quantification is quite expensive and slow, leaving a need for a more cost-effective and rapid method that can be used to track WAF dispersal.[26]

1.2. Biomonitoring of sentinel fish for environmental contaminant detection

Biomonitoring of sentinel fish allows for the detection of environmental contaminants where direct detection of contaminants may be challenging.[27] An ideal bioindicator will provide a direct and specific response to external levels of toxicant exposure that can be empirically and reliably measured, although, it is not necessary that a bioindicator directly represent a deleterious response.[28] Instead, specificity of a bioindicator to a given toxicant is more important, particularly in large open ecosystems like the ocean, where other stressors may also be present

and confound the response seen from the toxicant of interest.[29] An ideal bioindicator should also exhibit low variation between biological replicates.[28]

Acute oil spill exposure is not always immediately lethal to fish, and obvious morphological effects like skin lesions can take months to develop.[30,31] Instead, these types of exposures result in sublethal deleterious effects that are difficult to measure. This presents a need for more subtle tools able to capture the biological response of these fish to oil WAF exposure. Through transcriptomic analysis, sublethal effects of oil spill exposure can be detected.[32]

1.3. Use of transcriptomics to detect sublethal deleterious effects of environmental contaminants

As the effects of toxicant exposure occur through molecular interactions with organisms, it is important to study toxicity at the molecular level.[32] Using transcriptomics, molecular response is measured by capturing a snapshot of gene expression through isolation and quantification of mRNA transcript abundance. mRNA transcripts are first reverse transcribed into complementary DNA (cDNA) strands which are more stable and serve as a template for analysis.[33] The cDNA generated can then be quantified either using gene-targeted assays (qPCR), multi-gene assays (microarray), and/or transcriptome-wide total RNA sequencing (RNA-Seq).

The use of qPCR and microarray assays comprise most of the ecotoxicology literature.[32] These methods have proven to be highly effective in detecting exposure to endocrine disrupting compounds and other harmful pollutants in aquatic environments. Estrogenic responses are observed using transcriptomics in a wide range of marine and freshwater fishes,[34] and quantification of hepatic vitellogenin (*vtg*) transcript abundance in fathead minnow, can detect estrogen exposure at concentrations below current analytical detection limits.[35] Transcriptomic response of fishes has even been used to identify unknown toxicant exposure. Through the use of

the Comparative Toxicogenomic Database, gene expression profiles from a population of wild largemouth bass (*Micropterus salmoides*) experiencing population decline were used to identify quercetin and tretinoin exposure response that was previously unknown.[36]

In addition to identifying toxicant exposure, transcriptomics is widely employed in ecotoxicology in identifying the mechanisms that underly toxicity.[32] Microarrays evaluating the response following exposure to the endocrine disrupting pesticide, toxaphene, identified novel immunosuppressing effects in largemouth bass.[37] Evaluating gene expression also identified key differences in the immune response to salmonid lice infections between susceptible (*Salmo salar*, *Oncorhynchus keta*) and resistant (*Oncorhynchus gorbuscha*) salmon.[38] Transcriptomic analysis also allows for the evaluation of toxicity-mitigating strategies, such as the use of silica nanoparticles to reduce the impacts of PAH exposure in embryonic fathead minnow.[39]

Due to the rapidly decreasing costs associated with RNA-Seq, whole transcriptome shotgun Illumina sequencing is becoming more commonly used in ecotoxicology.[40] Unlike qPCR and microarray assays, RNA-Seq does not require a prior selection of genes to evaluate and can even be performed without prior transcriptomic or genomic knowledge of the sequenced organism (*de novo* assembly).[40] The amount of RNA required is also less for RNA-Seq (nanogram quantities) compared to microarrays (microgram quantities), which can be very important when dealing with precious samples.[41] Also, RNA-Seq will quantify a greater dynamic range of transcripts than microarrays.[40] This non-selective method of transcriptomic querying is ideal for the identification of novel bioindicators of specific environmental conditions like hypoxia in Chinook salmon (*Oncorhynchus tshawytscha*).[42]

Measurement of hepatic transcript bioindicators have been used to demonstrate a significant biological response to WAF exposure in fishes.[17,43,44] Although as little as three mm^3 of tissue is needed, typical liver sampling methods still involve lethal dissections.[45] Requiring mortality as an endpoint of biomonitoring assays contrasts the efforts of conservation being employed and may even further stress a sampled ecosystem.

1.4. Transcriptomic sampling of the caudal fin as a non-lethal alternative to traditional methods

The caudal fin is a readily accessible tissue present on all fishes that can be sampled with minimal distress to the fish and allows for a catch-and-release method of sample collection. Furthermore, non-lethal caudal fin sampling allows for repeated measurements from a single fish during long-term exposures. Veldhoen *et al.* have previously demonstrated that in anurans, the tadpole tail fin can be a highly responsive to xenobiotics, specifically to endocrine disrupting compounds.[46] Further work from this lab have since demonstrated that the salmonid caudal fin transcriptome is also capable of indicating exposure to metals and estrogens.[45,47] Sensitive detection of sea lice infection in Atlantic salmon (*Salmo salar*) has also been observed in the salmonid skin transcriptome, demonstrating the responsiveness of external tissue transcriptomes and further supporting their use.[48] One primary hypothesis of the present thesis work proposes that the caudal fin is a reliable and accessible tissue to assess biological responses to oil WAFs.

1.5. AhR-mediated pathway as a bioindicator for oil spill exposure

To validate the use of the caudal fin transcriptome in demonstrating oil WAF exposure, it is important to identify and measure transcript expression that is specifically responsive to common WAF components. Due to the high presence of PAHs and other related hetero-compounds in petroleum-based oil products,[49] oil WAF exposed fish demonstrate a significant

response of the aryl hydrocarbon receptor (AhR)-mediated pathway.[50] AhR is a highly conserved nuclear receptor in metazoans[51] that primarily regulates the expression of xenobiotic metabolizing enzymes.[52] Other than PAHs, dioxins, PCBs, and phytochemicals are all known AhR agonists.[52]

The AhR-mediated pathway is activated when the cytosolic receptor, AhR, encounters an aromatic hydrocarbon ligand (**Figure 1.1)**.[52] Upon AhR-ligand binding, the receptor translocates to the nucleus and dimerizes with the AhR-Nuclear translocator (ARNT) forming the active heterodimer. This heterodimer then binds xenobiotic response elements and induces transcription of genes to manage the toxicant exposure.

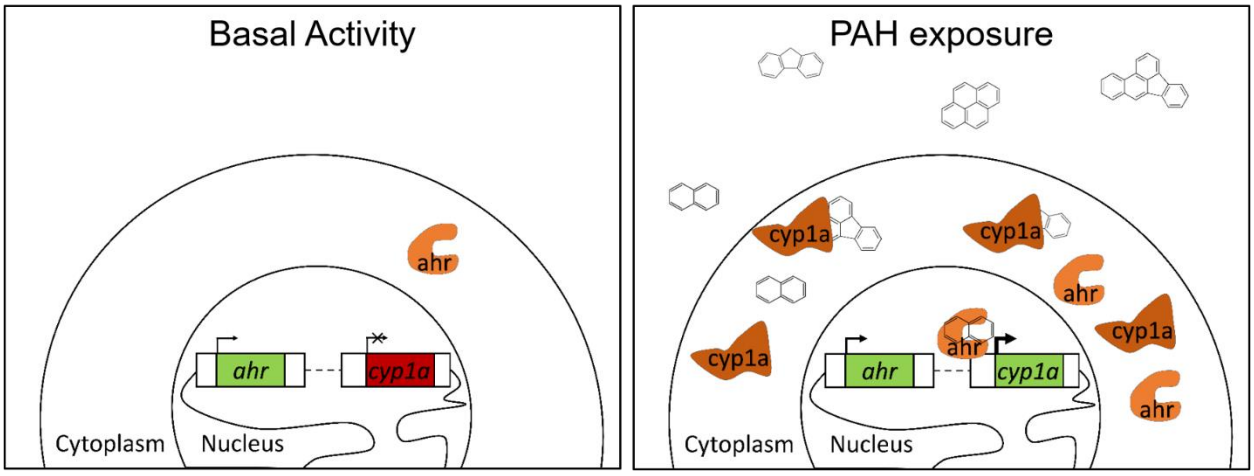

Figure 1.1. The AhR-mediated pathway is a xenobiotic response pathway which is induced during oil spill exposure due to high concentrations of AhR-agonists, PAHs. *Ahr* is constitutively expressed, whereas as AhR mediated genes like *cyp1a1* are only significantly expressed upon pathway activation.[52]

AhR activation appears to promote three major biological functions: xenobiotic processing, cell proliferation, and cell-cell/cell-extracellular matrix interaction.[52] One of the flagships responses of AhR induction is the expression of the *cyp1* family of genes.[53] These genes encode cytochrome p450 enzymes that initiate phase I metabolism of aromatic and

estrogenic compounds through the addition of highly reactive epoxide groups.[54] These genes exhibit low basal expression in the absence of AhR agonist, making *cyp1* genes excellent bioindicators of PAH exposure (**Figure 1.1.**).[53]

Due to the mass-epoxidation of PAHs by CYP1 enzymes, the resulting metabolites are potent mutagens, contributing to the observed carcinogenic effects of oil WAF exposure.[55] This has been observed in the form of hepatic neoplasms in killifish (*Fundulus heteroclitus*), winter flounder (*Pleuronectes americanus*), brown bullhead catfish (*Ameiurus nebulosus*), European flounder (*Platichthys flesus*), and English sole (*Parophrys vetulus*) after oil WAF exposure.[17]

In addition to carcinogenic effects, oil WAF exposure exhibits sex-specific endocrine disrupting effects, particularly in female fish.[17] In wild female killifish, there is a negative correlation between PAH concentration in local marine sediments and gonadosomatic index (GSI) as well as vitellogenin concentrations in killifish.[56,57] Similar effects are also observed in zebrafish (*Danio rerio*), that also exhibit reduced GSI and egg production after exposure to petrogenic PAH fractions, or the PAH, benzo[a]pyrene (BAP), alone.[58,59] In male humans and rats, the effects of PAH exposure are well documented in reducing sperm quantity and quality, however, conflicting research is observed concerning these effects in male fish.[17] NAs have also exhibited endocrine-disrupting capabilities in frogs, where exposure significantly alters thyroid hormone levels and disrupts thyroid hormone-mediated metamorphosis,[60] and act as estrogen receptor agonists in yeast cell assays.[61] Some research has also shown these endocrine-disrupting effects of NAs in fish, where fathead minnow (*Pimephales promelas*) exhibit a decrease in spawning rate with NA exposure.[62] The sex-biased nature of these responses emphasizes the need to take sex into consideration when analysing biological response, particularly with oil WAF exposure.

1.6. Coho salmon as an important test species

The effects of oil WAF exposure have been well characterized on freshwater (zebrafish and fathead minnow) and warm brackish/saltwater (killifish) fish species, however, there is a distinct lack of research investigating effects in cold saltwater fish species. As a family, salmonids represent a unique environmental, economic, and cultural significance worldwide.[63] All Pacific salmon follow an anadromous life cycle, with early life spent entirely in freshwater, followed by migration into saltwater where they will spend their adult life, and finally returning to their original rearing grounds in freshwater to spawn (**Figure 1.2**). As Pacific salmon are also semelparous, they will only complete this cycle once before becoming kelts and dying.

Smoltification is a critical process in a salmon's life cycle where it prepares to transition from a life in freshwater to saltwater (**Figure 1.2**).[64] Smoltification age differs with salmon species, but usually occurs in parr at around one to two years of age. This thyroid hormone-driven transition involves significant morphological, physiological, and behavioural changes such as a complicated remodeling of the gills and liver to adapt to the increased salt concentration in this new environment.[64] The recently smolted stage is the earliest point of coho salmon development where juveniles could encounter marine oil spill conditions and may be at a particular risk to oil spill exposure. Exposure to increasing salt concentrations[65] or to thyroid hormone[66] are sufficient to induce smoltification in parr.

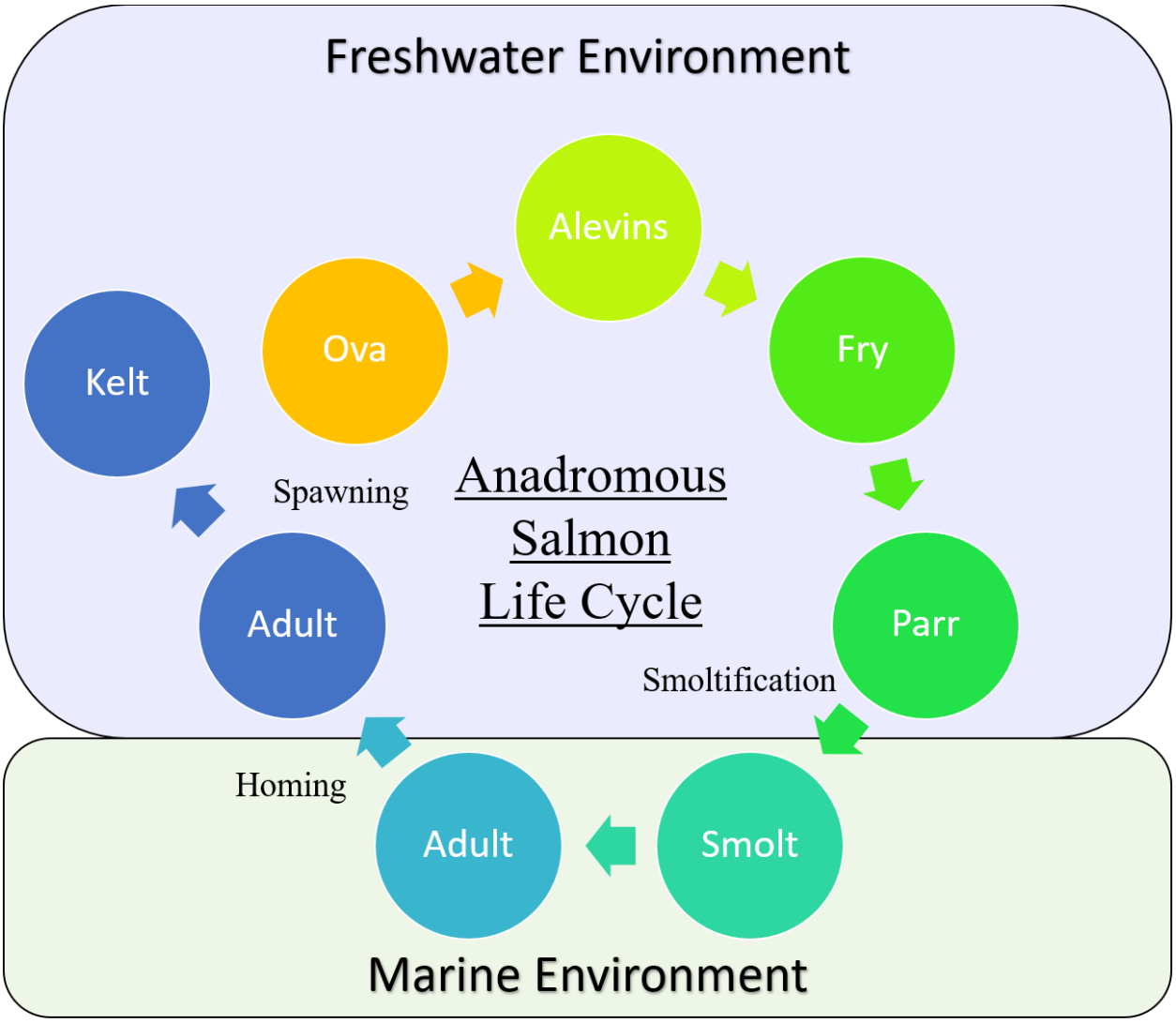

Figure 1.2. Diagram depicting the anadromous life cycle of Pacific salmon where they transition from freshwater to saltwater, then return to freshwater to spawn.[67,68]

Coho salmon (*Oncorhynchus kisutch*) inhabit a wide geographic distribution across the Pacific Northwest[69] and are currently threatened by over-fishing, climate change, and water pollution.[70] This region is also one of the busiest waterways in the world and a high-risk zone for oil spills.[71] As petroleum-derived pollutants significantly impact fish development,[72] examining the effects of oil WAF exposure to fish at developmental stages is important. For these reasons,

this thesis work investigated the effects of oil WAF exposure on recently smolted juvenile coho salmon.

1.7. Objectives

There are three main objectives of this thesis:

1) Assess the efficacy of non-lethal sampling of the caudal fin transcriptome as a bioindicator of oil spill exposure.
2) Evaluate potential sublethal deleterious effects of water-soluble fractions generated from four different oil types in juvenile salmon smolts in cold seawater.
3) Identify novel bioindicators of oil spill exposure in the salmonid caudal fin and liver.

The first data chapter will address the first objective. In Chapter 2, the use of caudal fin transcriptome for demonstrating oil spill exposure in salmon was validated. Genetically verified male and female juvenile coho salmon (*Onchorhynchus kisutch*) were exposed to a marine oil WAF generated at three sublethal concentrations using low sulfur marine diesel (LSMD), with transcriptomic response to oil exposure measured in the caudal fin and liver through qPCR (**Figure 1.3**).

The second data chapter will address the second objective. In Chapter 3, AhR-mediated bioindicators of oil spill exposure in coho salmon liver and caudal fin will be evaluated using qPCR after the exposure to WAFs generated with four different oil types: LSMD, high sulfur fuel oil (HSFO), dilbit, and Alaskan crude oil. This work identified HSFO WAF to be the most potent of the four oil types tested, with Alaskan crude oil eliciting the least response. This work also identified *cyp1a1* as insufficient to demonstrate oil responsiveness to lower concentration WAF exposures.

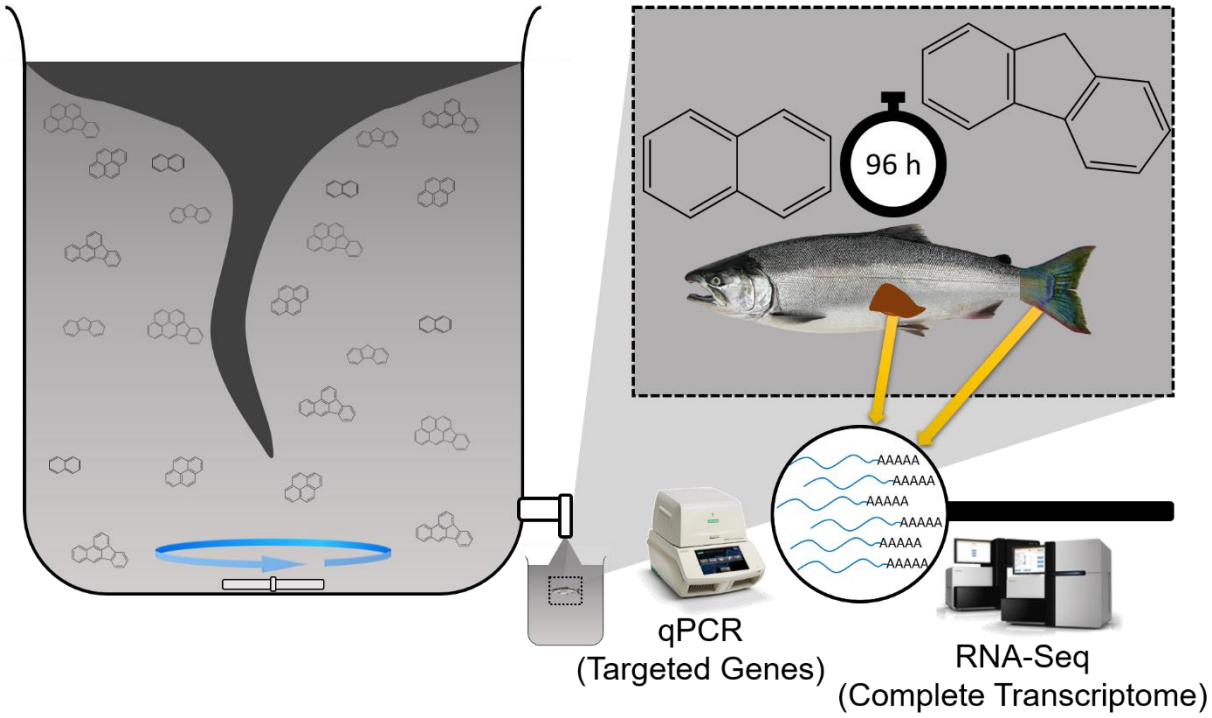

Figure 1.3. Liver and caudal fin samples were analysed from oil WAF exposed salmon to evaluate the caudal fin transcriptome in demonstrating toxicant response through known oil-responsive pathways, such as the AhR-mediated pathway. Oil spill conditions were simulated through WAF generation with a range of oil concentrations between 100-1000 mg/L. Juvenile coho salmon were exposed to oil WAFs for 96 hours prior to liver and caudal fin sampling. Total RNA was extracted from tissue samples and analysed through gene-targeted qPCR and total transcriptome RNA-Seq analyses.

The third data chapter will address the third objective. In Chapter 4, the total poly-adenylated transcriptomic response of the juvenile coho salmon liver and caudal fin were evaluated through RNA-Seq analysis after exposure to the highest concentration LSMD and HSFO WAFs. Novel liver and caudal fin oil spill bioindicators were identified and in-depth sublethal effects of these two exposures were characterized for both tissues.

2. Evaluation of gene bioindicators in the liver and caudal fin of juvenile Pacific coho salmon in response to low sulfur marine diesel seawater-accommodated fraction exposure

2.1. Introduction

Petroleum oil products are a complex mixture of chemical compounds of tens of thousands of hydrocarbons and other related hetero-compounds including PAHs.[1,49] The general toxic, mutagenic, and carcinogenic properties of PAHs have been well-documented[73,74] and analytical methods for quantifying many of the high-priority PAHs commonly dispersed from oil spills developed.[26] However, the complexity and diversity of petroleum products has made toxicological assessments challenging, particularly in determining sublethal deleterious effects on marine organisms.

Of particular note are identifying and monitoring biological effects as a consequence of exposure to petroleum oil-derived substances that partition into the aqueous phase after the spilled oil has been removed through clean-up efforts. Previous work has demonstrated that WAFs of various petroleum oil types induce endocrine disruption leading to reproductive consequences[5–7]; impaired growth, development, cardiac function, hypoxia tolerance, and modified behavior in marine fish[8,9,75,76]; and disturb microbiota[77] and coral populations.[78] During an oil spill response, there is a need to quickly and accurately determine whether or not clean-up efforts have been effective in mitigating biological effects.

PAHs induce transcription of downstream AhR-responsive genes in animals.[79] Cytochrome P450-1a (*cyp1a*) gene induction by AhR is a widely-used biomarker of PAH exposure in aquatic organisms.[43,53,80] Due to cross-talk between AhR and estrogen receptor (ER)

pathways,[81] PAH exposure also has a well-characterized estrogenic effect on exposed fish that induces differential expression of mRNA required for oocyte maturation.[82,83] Measuring the abundance of sensitive gene transcripts can therefore indicate biological responses to PAHs, endocrine disruption, as well as stress.[84–89] Typically, liver tissue is used to assess toxicological effects on these pathways, yet current methods of sampling require animal sacrifice or surgical methods that are not amenable to field sampling scenarios.[43]

Non-lethally obtained tissue samples are more desirable to detect and assess pollutant exposure. The caudal fin is a readily accessible tissue present on all fish that can be sampled with minimal distress to the animal and allows for their immediate release following sample collection. Furthermore, caudal fin sampling allows for repeated measurements from a single organism during long-term exposures or monitoring. The Helbing lab has previously demonstrated that the caudal fin transcriptome is capable of indicating exposure to metals and estrogens in salmonids.[45,47] It is plausible that the caudal fin could also be used to assess biological responses to oil spills.

In North America's Pacific northwestern coastal waters, LSMD is historically the primary petroleum oil product involved in large (>30 tonne) spills.[71,90] This region is one of the busiest marine routes in the world that shares critical habitats, migration routes, and diverse fisheries including salmonid species.[91] Compared to crude oils, relatively little is known about the toxic effects of LSMD in the context of seawater.

Herein, we generated LSMD WAF in seawater using multiple LSMD concentrations and then measured the extent of PAH solubilisation using our recently developed micro-extraction method.[92,93] To properly replicate ocean spill conditions, WAFs were made with seawater as salinity has a significant effect on PAH solubility.[22]

We also investigated the sublethal effects of LSMD WAF exposure on genetically verified male and female juvenile coho salmon (*Onchorhynchus kisutch*) by targeted gene transcript abundance changes indicative of PAH exposure, oxidative stress, general stress, estrogenic activity, and metal exposure in the liver and caudal fin. Coho salmon were chosen as they are an ecologically- and economically-relevant fish subject to the effects of oil spills. To our knowledge, this is the first report evaluating the effects of LSMD on gene transcript levels and the utility of the caudal fin in identifying LSMD exposure effects.

2.2. Materials and methods

2.2.1. Source of seawater

A fresh supply of seawater was used for the toxicity testing at the Pacific & Yukon Laboratory for Environmental Testing (PYLET) in North Vancouver, British Columbia. The seawater supply was continuously pumped into the laboratory from the Burrard Inlet, BC, at a depth of 33 m and sand filtered. The seawater typically has a salinity of 26.2 g/L and a pH of 7.7-7.9.

2.2.2. WAF generation

WAF preparation followed the method of Singer et al[94] with minor modifications[95] as indicated below. Each oil loading concentration to generate the WAF was prepared individually with three test concentrations and a control based on a logarithmic series of increasing loading concentrations. In a range finding experiment, we tested fish exposure concentrations of WAF prepared with up to 3200 mg/L LSMD which is higher that what would be expected during a marine oil spill. No mortality was observed when fish were exposed to WAF prepared with this high LSMD concentration during a 96-h exposure. Based upon this and logistical considerations

of available resources, three exposure concentrations were selected below this LSMD concentration and the WAFs were prepared as follows.

The WAF was prepared in a covered holding area outside the laboratory in four large Nalgene® mixing vats which had spigots on the bottom to draw off the WAF without disrupting the surface layer of oil. The mixing vats were placed on large magnetic stir plates with 10 cm spin bars at the bottom of each vat. On Day -1, the mixing vats were filled with 155 L of seawater. The mixing speed was set to 200 rpm, which did not create a vortex. Three LSMD-containing WAFs (low, medium, and high concentration) were prepared by adding 51.62, 165.39, and 516.62 g of LSMD to 155 L seawater for nominal loading concentrations of 333, 1067 and 3333 mg/L LSMD. A seawater only vat was also prepared. The lids were sealed with duct tape and there was approximately 5 cm of headspace in the mixing vat. The fuel oils in the mixing vats were mixed for 18 h and then the WAF was allowed to settle for 6 h.

On Day 0, a screw-on washer connected to Tygon® tubing was attached to the bottom spigot of each mixing vat. The WAF was drawn into four 90 L cubic vats lined with clear plastic, starting with the control and proceeding from the lowest concentration to highest concentration. At this time, the initial T = 0 h 40 mL subsamples (100% WAF) were sampled for chemistry analysis. The transfer vats were transported into the environmental test chambers where they were manually stirred with a Teflon® stir rod for several seconds.

2.2.3. Marine-acclimated coho salmon exposure tests

Adapted Environment Climate Change Canada standard methods[96] were used in this study with coho salmon smolt substituted for rainbow trout as the test species. The fish were fed daily with 100 mL of BioVita Fry 1.2 mm Nutra Plus pellets per tank of approximately 500 fish prior to the exposure. The fish were not fed during the exposure. All procedures were performed

under the University of Victoria Animal Use Protocol #2017-011 under the auspices of the Canadian Council for Animal Care. The certified disease-free salmon were obtained from the Department of Fisheries and Oceans Canada Chilliwack Hatchery on June 30, 2017. The smolts were acclimated to seawater at PYLET with a salinity of approximately 26±2 g/L and a temperature of 13±2 °C prior to testing. Fish mortalities during the acclimation and holding period did not exceed the maximum of 2% per week preceding the toxicity tests.

Using a submersible pump, the WAFs were transferred into the corresponding test vessels for the marine exposure tests arranged according to **Figure 2.1**. The test vessels contained 42 L of seawater and 18 L WAF for a final volume of 60 L at 15±1 °C corresponding to final nominal exposure loading concentrations of 0 (control), 100 (Low), 320 (Medium), and 1000 (High) mg/L LSMD. No mortalities were observed during the experiment. Eight replicate tanks were prepared per treatment with 5 smolts per tank. The tanks were covered with lids to minimize evaporation and the loss of volatile hydrocarbons from the WAFs. The test solutions were aerated at 6.5±1 mL/min·L to maintain adequate levels of dissolved oxygen saturation for the smolts. The following water quality parameters were measured: pH, dissolved oxygen, temperature, and salinity (**Appendix 1**). Phenol reference toxicant tests ensured that the organism sensitivity was within acceptable quality control warning chart limits.

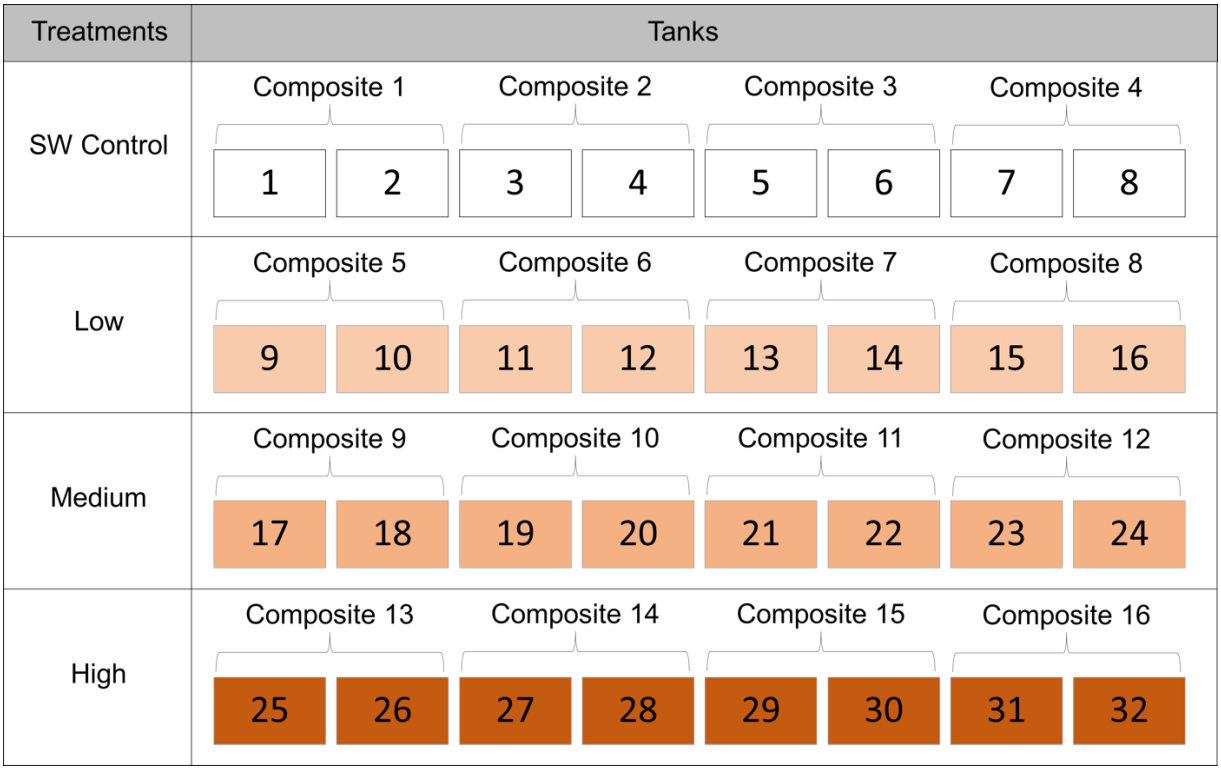

Figure 2.1. Schematic demonstrating the setup used for the 32 tanks involved in the present study for fish exposure to the four treatment conditions: seawater control (SW control), 100 (Low), 320 (Medium), and 1000 (High) mg/L LSMD. A total of four (50 mL) composite samples were taken from each treatment condition for analytical chemistry analyses, for a total of 16 composite samples taken per day.

2.2.4. Chemistry subsampling

Chemistry subsamples were taken at T = 0, 24, 48, 72, and 96 h. Twenty-five mL was taken from each tank and samples were pooled from paired tanks (**Figure 2.1**) for a total of four aliquots of 50 mL collected per concentration per day. Samples were collected into 60 mL trace clean clear glass vials using 10 mL Eppendorf automatic pipettes. Following sample collection, 2 mL of dichloromethane (DCM) was added immediately and then vortexed for sample preservation. All the samples were held between 1-23 days at 4 °C in the dark until analysis.

For sample extraction, 2 mL of acetonitrile (ACN) was added to each sample vial. Samples were vortexed and then centrifuged to separate the aqueous and organic layers. The bottom organic layer was transferred into a 4 mL liquid chromatography vial using a glass Pasteur pipette and the sample was made up to 2 mL with DCM. The samples were vortexed and then transferred into 2 mL amber glass gas chromatography vials for instrument analysis using gas chromatography/triple quadrupole mass spectrometry.[26]

2.2.5. PAH analytical chemistry

Our ability to completely characterize oil spill contaminants dispersed into the aqueous phase is limited due to the complexity of the sample and the limited number of available standards. Furthermore, the cocktail of compounds dispersed in an oil spill can vary greatly depending on the type of oil involved. Consequently, the extent of aqueous oil contamination is often quantified using a limited subset of more readily characterized hydrocarbons, such as BTEX, or a broader subset including LEPH/HEPHs, PAHs, and related alkylated compounds. These subsets are considered to be the most important indicators of oil toxicity.[97]

Because PAHs are typically more persistent in the environment than their monocyclic counterparts, oil contamination and exposure are often described in terms of individual PAH concentrations or by a sum of those individual PAH concentrations (*i.e.*, tPAH).[18]

A total of 50 PAHs (tPAH50) (23 parents and 27 alkyl homologs) were targeted for analysis (**Appendix 2**). This list includes all PAH and related hetero-polycyclic compounds reported as part of the standard PAH analysis performed for the Deepwater Horizon Natural Resource Damage Assessment (**Appendix 3**).[98]

Our collaborators have developed a micro-extraction method[92,93] to deliver timely analysis of 320 samples that were collected from the four WAF concentrations. Traditional PAH

analysis requires mixing of 1 L water matrix with 200 mL of toxic DCM as the extraction solvent. Use of such large sample volumes would have compromised the exposure study due to volume loss in the fish tanks and long turn-around times. This trace level tPAH50 method requires only 50 mL of sample matrix and 2 mL of DCM as extraction solvent. Our method has passed eight separate rounds of proficiency testing organized by the Canadian Association for Laboratory Accreditation Inc. (CALA) and has been accredited under ISO17025. For several alkylated PAHs, we reported concentrations for both individual PAHs and grouped alkyl homolog PAHs (i.e., 1-methylnaphthalene and C1-naphthalenes, which includes 1-methylnaphthalene). To avoid double counting in the present study, the individual alkylated PAHs were excluded in the tPAH50 summations.

The measurement and consideration of volatile petroleum hydrocarbons (BTEX), light extractable and heavy extractable petroleum hydrocarbons (LEPH/HEPHs) are discussed in the Supporting Information.

2.2.6. Dissections

At 96 h, fish were individually euthanized using 0.3% sodium bicarbonate buffered (pH 7) tricaine methane sulfonate (Aqua Life, Syndel Laboratories, Nanaimo, BC, Canada). The weight and fork length of each fish was measured and recorded immediately prior to dissection. Whole liver and caudal fin were collected into separate 1.5 mL microfuge tubes containing 1 mL RNALater (Ambion, Foster City, CA, USA). The tissues were stored at 4 °C overnight, then kept at -20 °C prior to the delivery to the University of Victoria for RNA isolation and sex genotyping.

2.2.7. Isolation of total RNA and preparation of cDNA

Caudal fin and liver tissue samples were randomized to remove processing bias. RNA was isolated from 2 cm tail tips or 3 mm^3 liver samples using 700 µL TRIzol reagent, then homogenized for 6 min at 24 Hz in a Retsch MM301 mixer mill (ThermoFisher Scientific Inc., Ottawa, ON, Canada) in microtubes containing a 3 mm tungsten carbide bead (Mixer mill rack was rotated 180 degrees halfway through homogenization). In order to increase RNA yield, 20 µg glycogen was added to caudal fin samples prior to alcohol precipitation. RNA concentration was determined using a Nanodrop ND-1000 (ThermoFisher Scientific) with minimal DNA contamination confirmed based on $A_{260/280}$ values. The extracted RNA was stored at -80 ^{o}C, and 1 µg was converted into cDNA for qPCR using the Applied Biosystems Inc. (ThermoFisher) High-Capacity cDNA reverse transcription kit with RNase inhibitor. cDNA samples were diluted 20-fold with RNase- and DNase-free water prior to qPCR analysis.

2.2.8. qPCR analyses

Primer sets that were previously used on Chinook and sockeye salmon[99,100] were rigorously validated for use on coho liver and caudal fin samples as outlined in Veldhoen *et al.* with reference to MIQE guidelines (**Appendix 4**).[101,102] The primer sets chosen amplify transcripts sensitive to (1) PAH exposure: aryl hydrocarbon receptor α (*ahr*) and 3-methylcholanthrene responsive cytochrome P450 CYP1A1 (*cyp1a*); (2) oxidative stress: superoxide dismutase (*sod*); (3) general stress: heat shock protein 70 (*hsp70*); (4) estrogenic activity: vitellogenin A (*vtg*), vitelline envelope protein gamma (*vepg*), and cytochrome p450 family 19 (*cyp19*); and (5) metal exposure: metallothionein A (*mta*). Glyceraldehyde 3-phosphate dehydrogenase (*gapdh*), ribosomal protein L8 (*rpl8*), and ribosomal protein S10 (*rps10*) were used in a geometric mean normalization. The *mta* primer set did not pass our validation criteria for use with caudal fin samples so it was only used to assay transcript

abundance in the liver. Where possible, primers were designed to span intron/exon boundaries (**Appendix 4**).

All qPCR reactions were run in quadruplicate and reactions were performed in a 15 μL volume consisting of 10 mM Tris-HCl (pH 8.3 at 20 °C), 50 mM KCl, 3 mM $MgCl_2$, 0.01% Tween 20, 0.8% glycerol, 40,000-fold dilution of SYBR Green I (Life Technologies), 69.4 nM ROX (Life Technologies), 5 pmol of each primer, 200 μM dNTPs (Bioline USA Inc, Taunton, MA, USA), 2 μL of 20-fold diluted cDNA, and one unit of Immolase Hot Start Taq DNA polymerase (Bioline). Amplification reactions were subject to the following thermocycle conditions: an initial 9 min activation step at 95 °C, followed by 40 cycles of 15 sec denaturation at 95 °C, 30 sec annealing at 60 °C, and 30 sec polymerization at 72 °C. Specificity of target amplification was measured by the inclusion of reactions lacking cDNA (no DNA template control) and by subjecting completed runs to thermodenaturation analysis to confirm correct single product amplification. An additional inter-plate control comprising a universal cDNA sample present in all qPCR runs was included for each gene target. Replicate data for each cDNA sample were averaged and test gene targets normalized to the geometric mean of *gapdh*, *rps10*, and *rpl8* during application of the comparative C_t method ($\Delta\Delta C_t$).[103] Suitability of these normalizer transcripts was determined using Cronbach's α (http://languagetesting.info/statistics/spreadsheets/Alpha.xls), Norm Finder (moma.dk/normfinder-software), and Best Keeper analysis (www.gene-quantification.com/bestkeeper.html). Stability of normalizer C_t values are presented in **Appendix 5**. Primer set efficiencies are presented in **Appendix 6**.

2.2.9. Isolation of genomic DNA and sex genotyping

Genomic DNA (gDNA) was isolated from RNAlater-preserved caudal fin tissue and analysed as previously described[100] with the following modifications: gDNA concentration and integrity was determined by Nanodrop quantification and agarose gels, respectively (data not shown). To determine the genotypic sex of the juvenile coho salmon, we used two different primer sets: *U-sdY* and *OtY2-WSU* that have been developed to target the male-specific Y chromosome of salmonids (**Appendix 4**).[104–106] qPCR genotyping was performed on gDNA samples in duplicate and followed the same reaction conditions as described above. A fragment of the *gapdh* gene was used to normalize the presence or absence of the Y chromosome markers for all gDNA samples (**Appendix 4**). Assay performance was verified using multiple gDNA samples of visually confirmed male and female coho salmon obtained from Hartley Bay, Kitimat River, and Salmon River, BC (n=4 fish of each sex per site, a generous gift from Dr. Ben Koop, University of Victoria).

2.2.10. Statistical analyses

For all statistical analyses, $p \leq 0.05$ was used to denote significance. Genetic sex was used to separate the fish into male and female groups. Distribution of male and female coho salmon across the four treatment conditions was evaluated using the Fisher Exact test (http://www.quantitativeskills.com/sisa/statistics/fiveby2.htm). Statistical analyses of the mRNA abundance data were performed using R version 3.4.1 (R Foundation for Statistical Computing, Vienna, Austria). Relative fold changes were examined for normal distribution (Shapiro-Wilk) and unequal variances (Levene's) and the data were non-parametric. Significance was determined using the Kruskal-Wallis test and pairwise comparisons using the Mann-Whitney U test.

2.3. Results and Discussion

2.3.1. WAF tPAH50 concentration and chemical composition

All measured tPAH50 concentrations were ~90 µg/L in the 100% WAF regardless of the initial LSMD loading concentration,[107] which suggest that saturation of these components can be easily reached within the context of a spill scenario. These concentrations are lower than tPAH50 concentrations of WAFs derived from heavier oils made under the same concentrations and conditions.[26]

Each WAF was diluted to 30% for the fish exposures which translated to similar tPAH50 concentrations at approximately 30 µg/L tPAH50 (**Figure 2.2**)[107]. The most dramatic reduction in hydrocarbons occurred in all three concentrations between 0 and 24 h, with a 60 to 70% loss. PAH concentrations continued to drop 86-90% during the exposure, resulting in a final tPAH50 concentration of ~2 µg/L by 96 h (**Figure 2.2**). Monthly water quality sampling and chemical analysis of the seawater confirmed very low concentrations of volatile hydrocarbon compounds and PAHs prior to WAF generation.[107]

The primary PAH class observed in LSMD WAF was the water-soluble, two-ringed naphthalenes while the three-ringed and larger compounds were minor constituents (**Figure 2.3**)[107]. This is in contrast to heavier, high-sulfur oils in which greater quantities of three- to five-ringed compounds partition into WAF due to the surfactant effects of sulfur on hydrophobic PAHs.[26,108] Over time, the lighter hydrocarbons (i.e., naphthalenes) showed the greatest loss. This loss occurred as the result of several processes, including dissolution, evaporation, and biodegradation.[109] In the field of oil spill forensics, the term "weathering" has been used to describe such a loss of the lighter hydrocarbons. The extent of weathering is often represented by the total mass loss in comparison to the starting point. Based on the tPAH50 results, the WAF

experienced a faster weathering rate compared to heavier oils[26] due to the relatively high amount of volatile compounds found in the sample.

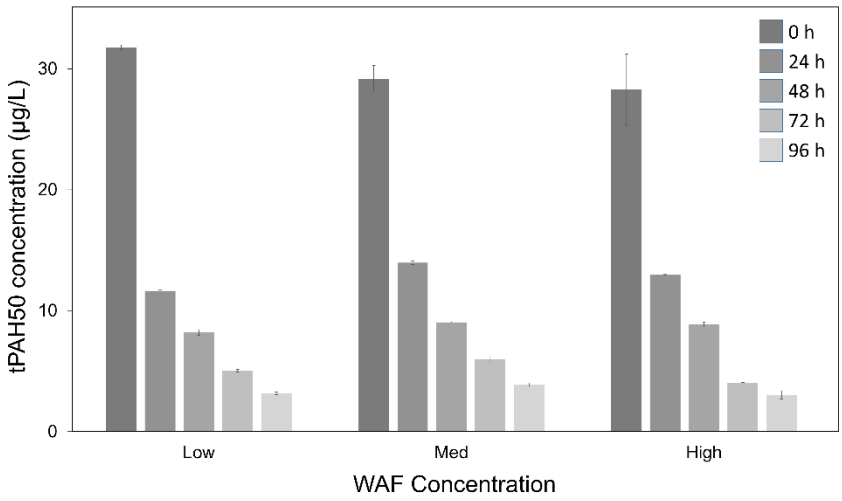

Figure 2.2. Similar tPAH50 concentrations were observed for all LSMD WAF concentrations: Low, medium (Med), and High concentration WAF (equivalent to 100, 320, and 1000 mg/L LSMD, respectively), over a test period of 96 h. PAHs were quantified from WAF subsamples taken every 24 h from start to end of the exposure. Decreasing grey scale intensity indicate progression of time from 0-96 h of exposure in 24 h increments. Bars represent the median concentration observed from composite samples from 8 different tanks of the same WAF concentration. Error bars represent the median absolute deviation.

BTEX, comprised of benzene, toluene, ethylbenzene, and xylenes, are usually detected in source oil, but often not in spilled oils due to their high volatility.[110] BTEX concentration was not measured in the present study due to probable loss during WAF preparation and exposure execution. During WAF preparation, steps such as mixing, transferring, vortexing solutions in unsealed containers, and subsequent dilutions would have led to significant loss of BTEX

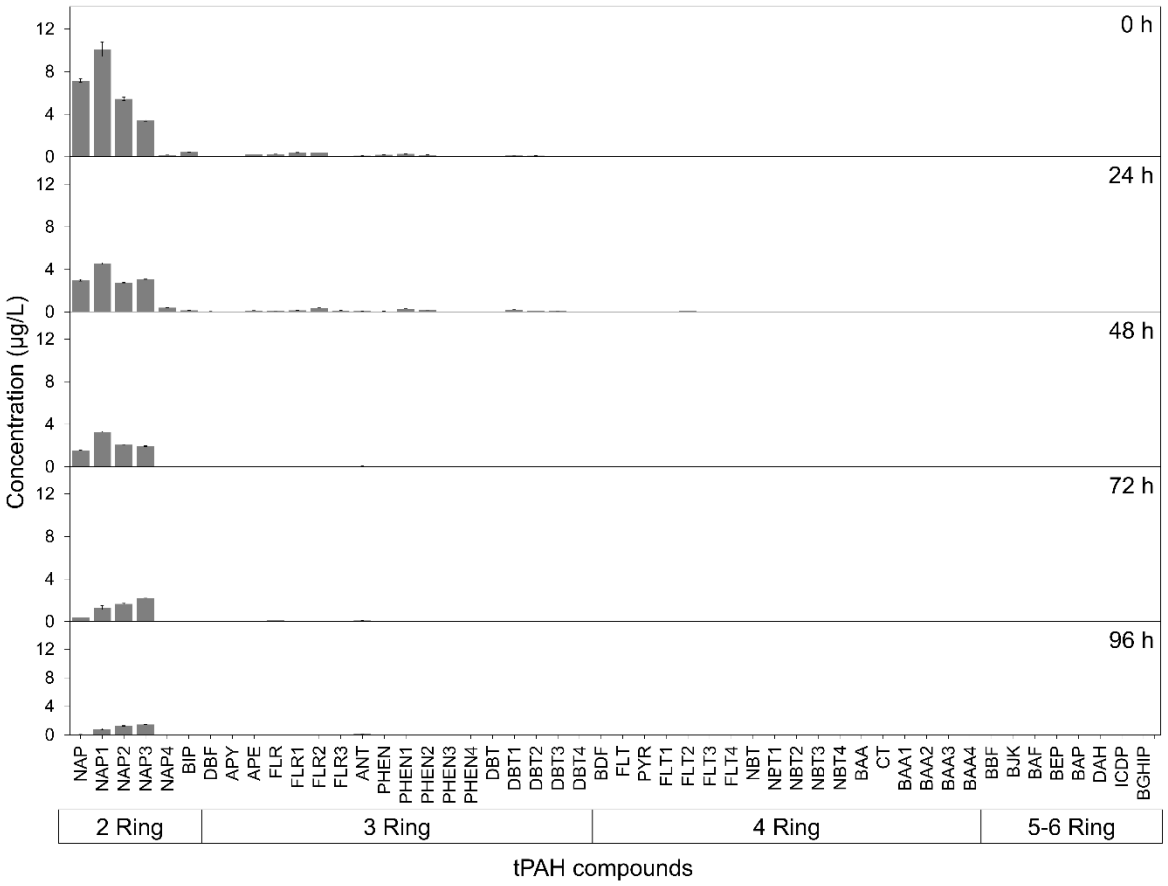

Figure 2.3. LSMD WAF is mostly composed of diaromatic hydrocarbons. The concentrations of PAH analytes grouped by number of rings quantified from the Medium (320 mg/L LSMD) WAF concentration over time are shown. The minimum quantifiable limit of PAH concentration was 0.04 µg/L. The low and high WAF concentrations show similar PAH profiles as grouped by ring size (**Appendix 8**). Refer to **Appendix 2** for compound identification. Medians (bars) and median absolute deviation (whiskers) are depicted.

compounds. In addition, any remaining BTEX would be further reduced to below the limit of quantitation during the WAF sampling and long-term storage before the final analysis.

LEPH/HEPHs are associated with the oil spill contaminated water body and their determination is often used in the initial stage of oil spills to semi-quantitatively determine the contamination level. However, LEPH/HEPH determination has limited value in the current study due to the quick evaporation of high volatile petroleum compounds (LEPHs) and poor solubility

of less volatile oil products (HEPHs). Additionally, the LEPH/HEPH analysis is based on GC flame ionization detection, a non-specific method, and is prone to various contaminants from the fish tanks. To verify this point, LEPH/HEPHs were measured in one batch of WAF samples and the results indicated very low concentration of extractable petroleum hydrocarbons in the LSMD WAF (**Appendix 7**).

2.3.2. Fish mortalities and morphometrics

There were no fish mortalities in any of the exposure conditions during the experiment. The weight and fork length were similar between treatment groups and ranged between 6.7-7.4 g and 8.4-8.6 cm on average, respectively (**Appendix 9**).

2.3.3. Sex genotyping

The proportion of males and females was approximately 50:50 within each treatment group with no significant difference in overall distribution of sex between treatment groups (**Appendix 10**). The *OtY2-WSU* and the *U-sdY* qPCR results correctly identified known male and female controls (**Figure 2.4**). Although these primers target genomic regions that should not be present in female fish, some amplification is observed in females due to off-target amplification likely due to recombination between sex-associated loci and the sex-determining gene.[111] The *OtY2-WSU* primer set was able to sex-genotype with a greater resolution between male and females (minimum 3 C_t difference in transcript abundance) than the *U-sdY* primer set (minimum 2 C_t difference in transcript abundance). Thus, for coho salmon, the *OtY2-WSU* primer set provided greater certainty in differentiating between males and females than the *U-sdY* primer set (**Appendix 11**).

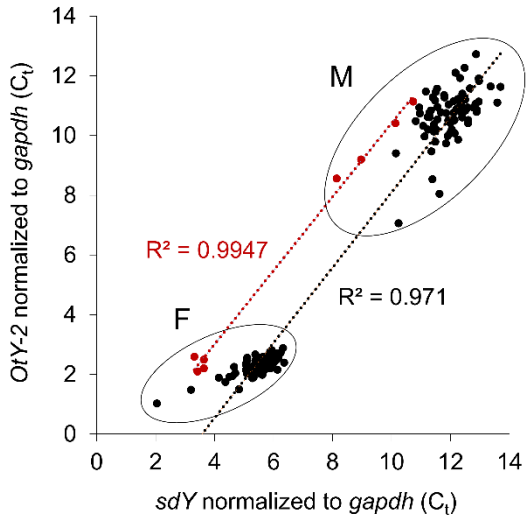

Figure 2.4. Use of *OtY2-WSU* and *U-sdY* genotypic sex markers clearly separates fish into two groups corresponding to males (M) and females (F). Each black circle represents an individual and the ovals indicate individuals grouped into either M or F categories for gene expression analysis. Red circles represent confirmed adult male and female coho salmon.

Sex genotyping is important in interpreting phenotype and can substantially impact transcriptomic results.[100] This information is often overlooked in the evaluation of pollutant exposure effects, particularly in juvenile fish as they lack obvious physical sex characteristics. Despite the lack of phenotypic difference between juvenile males and females, sex-based differential response to WAF exposure is possible. The results from the sex genotyping were used to group juvenile fish as male or female for subsequent targeted transcript analyses.

2.3.4. Transcript abundance of biological indicators in liver and caudal fin

Assuming that PAH toxicity is proportional to PAH concentration[112] and given the apparent equivalency in tPAH concentrations of the three WAF concentrations, we expected to see equivalent molecular responses between the fish exposed to the three LSMD WAF

concentrations. Using routine qPCR methods,[45] we examined established gene transcripts that are indicators of PAH exposure, general and oxidative stress, estrogenic activity, and metal exposure.[99,100] We analysed paired liver and caudal fin samples to assess the efficacy of the caudal fin response to the response of a conventional tissue used for monitoring purposes.

To assess the responsiveness of the liver and caudal fin tissues to PAH exposure, two well-documented PAH-responsive genes, *ahr* and *cyp1a*, were amplified (**Figure 2.5**). *Ahr* is a constitutively expressed gene that encodes the AhR protein which binds planar aromatic hydrocarbons.[53] Upon PAH binding, the ligand-receptor complex translocates into the nucleus and dimerizes with ARNT inducing changes in the transcription of target genes such as *cyp1a*.[113] The *cyp1a* gene encodes the cytochrome P450 CYP1A protein involved in PAH metabolism.[43]

Significant *ahr* response to WAF exposure was observed in both the liver and caudal fin although the observed patterns differed between sexes and tissues (**Figure 2.5**). The liver was the most responsive tissue (~2-fold increase) with similar significant increases observed in males at all WAF concentrations. A similar magnitude significant increase was also observed in female liver in the medium WAF concentration while the low and high WAF concentration results were approaching significance (p=0.1 and 0.08, respectively). Transcript abundance of *ahr* was significantly increased by ~2-fold in the male caudal fin at all WAF concentrations whereas female caudal fin *ahr* transcript levels were not significant at any WAF concentration although the medium concentration approached significance (p=0.09). Our results are consistent with a modest induction of *ahr* transcript abundance reported in the liver of juvenile rainbow trout[114] and Japanese medaka embryos exposed to diluted bitumen WAF[115] but neither study separated sexes.

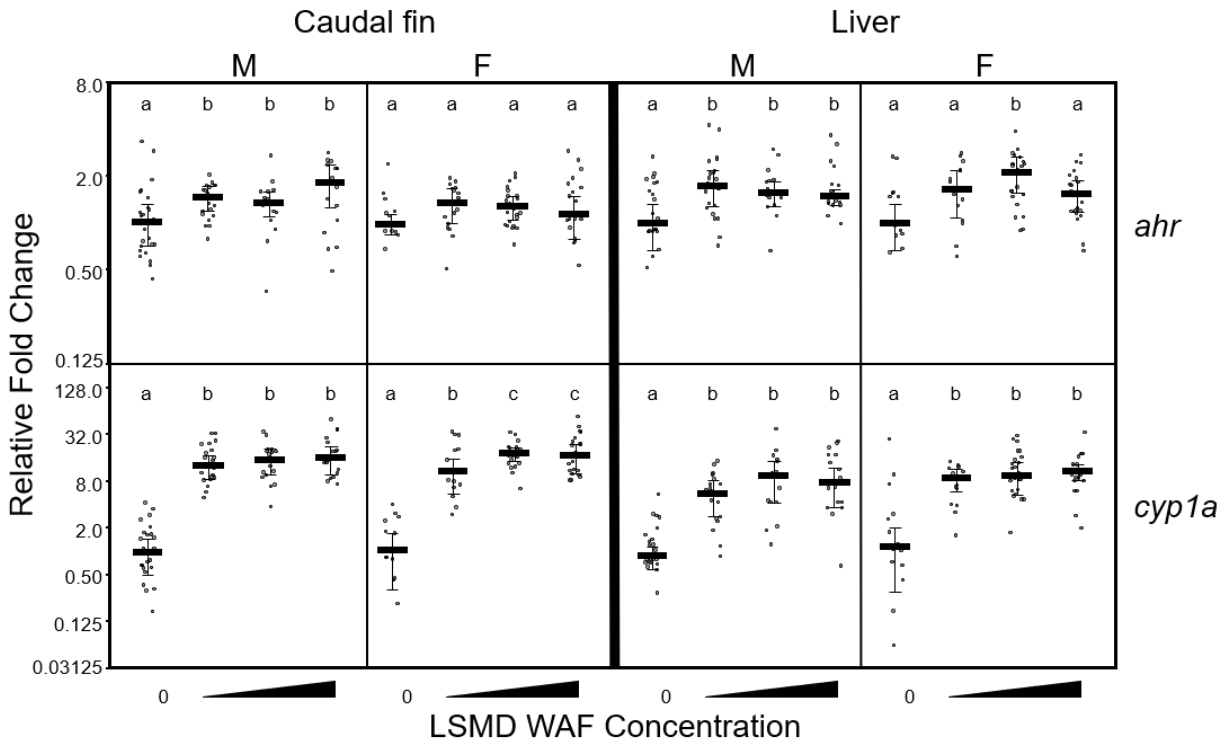

Figure 2.5. The abundance of *ahr* and *cyp1a* transcripts in both caudal fin and liver tissue is significantly affected by WAF exposure but the response patterns differ by sex and tissue type. The normalized relative fold change of PAH-response gene transcript abundance is shown after exposure to different WAF concentrations as determined by qPCR analysis. The bevel represents increasing WAF concentrations (equivalent to 100, 320, and 1000 mg/L LSMD, respectively). Each open circle represents an individual animal, the median is represented by a horizontal bar, and the median absolute deviation is defined by the whiskers. Relative fold changes are expressed in a $\log_2$ scale. Different letters indicate significant differences between groups ($p < 0.05$). For example, "b" denotes significant difference from "a". "c" denotes significant different from "a" and "b".

We found a significant increase between 6- to 10-fold in *cyp1a* transcript abundance in the liver of male and female juveniles with no significant difference between WAF concentrations (**Figure 2.5**). The *cyp1a* abundance levels were more strongly induced (11- to 18-fold) in the caudal fin compared to the liver by LSMD WAF exposure regardless of sex.

The *cyp1a* transcript responses observed are consistent with previous findings of diesel, diluted bitumen, and crude oil WAF exposure in rainbow trout liver, Atlantic cod larvae and liver, and Japanese medaka embryos.[80,114–116] Madison et al observed a strong relationship

between developmental malformations and *cyp1a* mRNA level in newly hatched Japanese medaka.[115] While reasonable concordance between hepatic *cyp1a* mRNA and CYP1A protein induction as a consequence of marine diesel WAF exposure has been observed in rainbow trout and Atlantic cod[80,114], these studies both noted the difficulties in relating abundances to 7-ethoxy-resorufin O-deethylation (EROD) activity; an assay that is commonly used to assess CYP1A enzyme activity. These authors pointed out the difficulties in relating EROD activity to transcript and protein levels due to the effects of antagonists present in the complex oil mixtures on EROD activity.[80,114] Regardless of the relationship, activation of the AhR-CYP1A pathway is indicative of a biological response to diesel exposure requiring energetic resources allocated to this detoxification pathway perhaps to deal with the reduced capacity to metabolize oil components. The fact that the caudal fin shows a stronger *cyp1a* transcript induction than the liver indicates that this tissue may be more sensitive to WAF exposure than the liver for testing, without the need for animal sacrifice. These results are very promising for use of the caudal fin as a quick, non-lethal sampling method that would be a great advantage for biological assessment of fish in the environment.

In male caudal fin, a similar strength *cyp1a* transcript response was observed in all WAF concentrations (**Figure 2.5**). However, a distinctive induction pattern was observed in the female caudal fin. While the *cyp1a* gene transcripts were also significantly elevated in all three WAF concentrations, a significantly greater response was observed in the medium and high WAF concentrations relative to the low concentration. This result is intriguing because of the apparent PAH saturation in all of the LSMD WAFs (**Figure 2.2**). This observation suggests that while the overall tPAH50 values may be the same between the LSMD WAF concentrations tested, it is possible that the application amount influenced partitioning of individual PAHs or other

components (e.g., acid extractable organics) in such a way to lead to differential biological effects. For example, anthracene levels are consistently 4-6 times higher in the low concentration WAF compared to the high concentration WAF throughout the experiment (**Figure 2.3**). Further analyses of WAF composition and the relationship to biological effects are warranted.

To evaluate WAF exposure-induced stress, we measured the transcript levels of genes involved in general and oxidative stress pathways: *hsp70* and *sod* (**Figure 2.6**). The *hsp70* gene encodes a chaperone protein involved in stabilizing partially folded proteins and protein remodeling and has been linked to general stress pathways.[117] The *sod* gene encodes superoxide dismutase which catalyses the conversion of superoxide to less toxic hydrogen peroxide.[118] General and oxidative stress in fish is strongly associated with *hsp70* and *sod* biomarker up-regulation and can cause reduced disease resistance and growth, and increased mortality.[119]

No significant difference between male and female fish in seawater alone was observed for *hsp70* or *sod* transcripts in either liver or caudal fin (**Figure 2.6**). WAF exposure induced a significant increase in both *hsp70* (1.4-fold) and *sod* (2-fold) response in the liver of males at all concentrations. Male caudal fin showed no significant response in *hsp70* transcript levels and a 1.4-fold increase in *sod* transcript abundance at the high WAF concentration. The medium WAF concentration for male caudal fin *sod* transcripts was approaching significance ($p=0.1$).

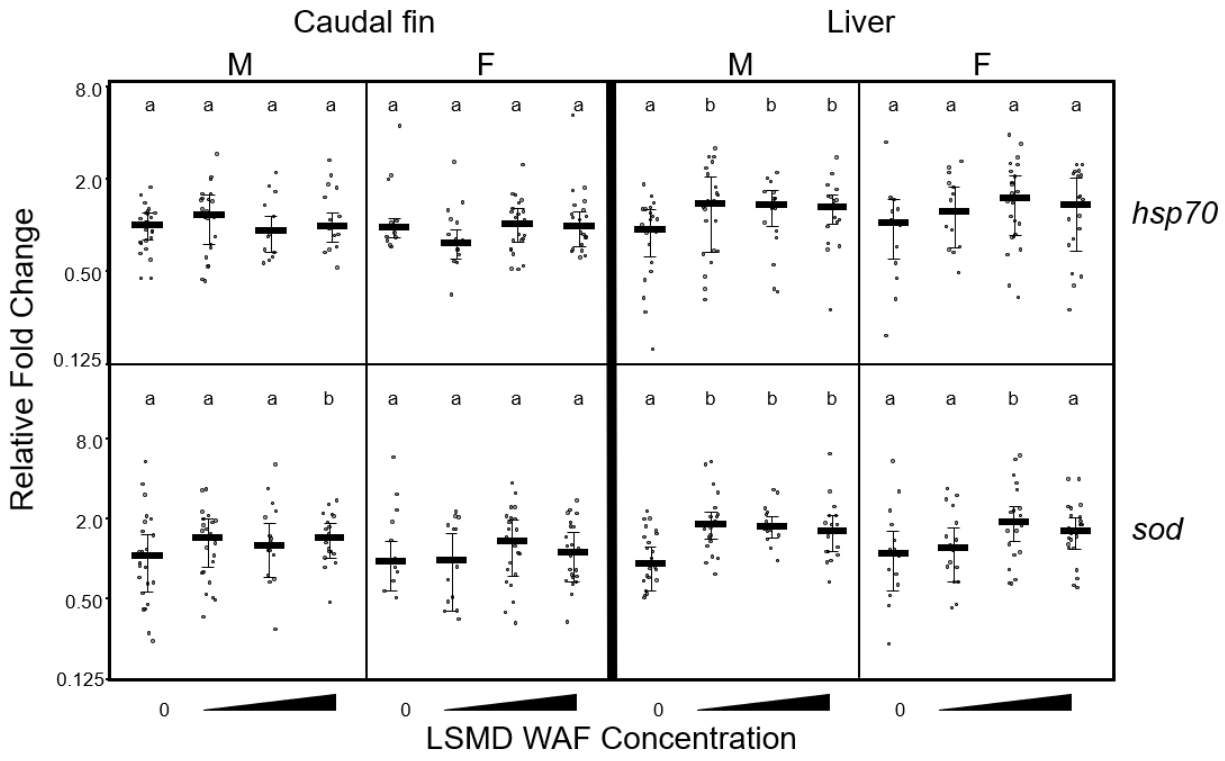

Figure 2.6 The abundance of *hsp70* and *sod* transcripts is significantly affected by WAF exposure in male liver with reduced responsiveness in the caudal fin. Female liver and caudal fin are generally non-responsive. The normalized relative fold change is shown of general stress-related gene transcript abundance after exposure to different WAF concentrations as determined by qPCR analysis. See **Figure 2.5** legend for additional details.

Female livers had a similar magnitude increase in *hsp70* transcript abundance relative to the controls in the medium and high WAF concentrations, but these values did not quite reach significance (p=0.07 and p=0.1, respectively; **Figure 2.6**). A significant 1.7-fold increase in *sod* transcript levels was observed in female livers at only the medium WAF concentration with a trend towards a similar increase at the high WAF concentration (p=0.08). WAF exposure did not induce a significant response in either of these gene transcripts in the female caudal fin although the low WAF concentration approached a significant 0.8-fold decrease for *hsp70* transcript levels compared to the control (p=0.09).

Previous work on Atlantic cod larvae and juveniles and Japanese medaka embryos evaluated exposures to WAF prepared from heavier oils and found evidence of general and oxidative stress using a variety of bioindicators including increased abundance of *hsp70* and *sod* transcripts.[80,116,120] Holth et al also examined the effects of ship-diesel WAF on mixed-sex juvenile Atlantic cod and found evidence for increased glutathione S-transferase antioxidant enzyme activity and lipid peroxidation in the gill; both indicators of oxidative stress.[80]

The present study indicates a modest stress response induced by LSMD WAF with males being more sensitive than females. While previous fish studies did not distinguish between sexes, increased sensitivity of oxidative stress pathways to PAH exposure has previously been reported in male Nile crocodiles compared to females.[121] As the genotypic sex is not often reported in juvenile fish studies, our results indicate that sex should be taken into account when evaluating stress responses to PAHs.

These stress bioindicator results also indicate possible tissue-specific differences as the liver had a greater response than the caudal fin. The caudal fin is in direct contact with the WAF, so it is possible that a stress response did occur in this tissue, but at a much earlier time point than that selected in the present study. Another possibility is that the caudal fin may not be as sensitive to stress induced by LSMD WAF exposure. Based on previous studies mentioned above, we expect that exposure to WAFs prepared from other oil types with different compositions (such as heavy oils) may induce a stronger stress response in this tissue. Further analyses of earlier time points and comparison of LSMD to other oil WAF exposures are needed to address these possibilities.

The effect of WAF exposure on estrogenic activity was evaluated by measuring female-biased gene transcripts encoding proteins involved in egg (*vtg*: vitellogenin A, *vepg*: vitelline

envelope protein gamma) and estrogen (*cyp19*: cytochrome p450 family 19) production (**Figure 2.7**). Adult female salmon express substantially higher levels of these three gene transcripts in the liver than adult males.[100] All three transcripts were detected and validated in both liver and caudal fin in both sexes. Of these transcripts, only *cyp19* abundance in the caudal fin showed a female bias with a 1.5-fold significantly higher abundance in female caudal fin compared to males in the seawater controls. The liver did not show this female bias in these immature juvenile fish.

A 2-fold increase in *vepg* transcript abundance in the liver tissue of males was induced at the low and medium WAF concentrations (**Figure 2.7**). The abundance of *vepg* transcripts in female liver or caudal fin of either sex were not affected by WAF exposure. However, at high WAF concentrations, the *vepg* transcript levels trended downwards to 0.6-fold in the caudal fin ($p=0.08$) and upwards to 1.4-fold in the liver ($p=0.1$) compared to controls in female fish.

There was no significant effect of LSMD WAF exposure on *vtg* transcripts in any condition, sex, or tissue although the female caudal fin showed a tendency toward a 0.6-fold reduction in *vtg* transcript levels at the high WAF concentration ($p=0.08$; **Figure 2.7**).

While there were no significant changes in *cyp19* transcript levels in male or female livers or male caudal fin (**Figure 2.7**), a significant decrease in *cyp19* transcript abundance up to 2.5-fold was observed in the female caudal fin. The low WAF concentration just missed the significance cut-off at $p=0.07$ due to slightly higher variation in the data compared to the other WAF concentrations.

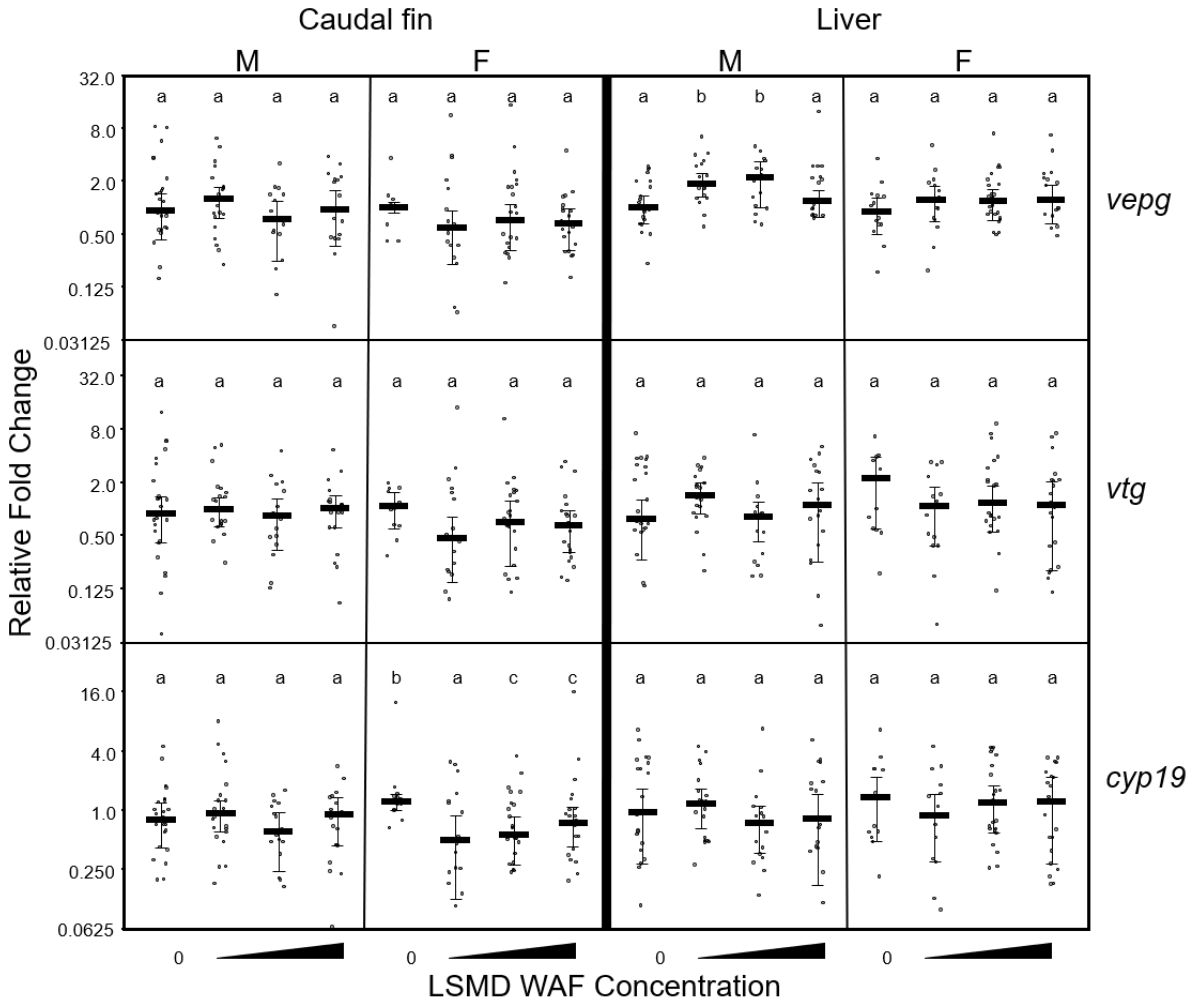

Figure 2.7. WAF exposure elicits a modest response in male liver and female caudal fin to some estrogen-responsive transcripts. The normalized relative fold changes are shown of estrogen response gene transcripts, *vepg*, *vtg*, and *cyp19*, in caudal fin and liver tissue after exposure to different WAF concentrations as determined by qPCR analysis. See **Figure 2.5** legend for additional details.

Previous work on individual PAHs indicates that these substances can act as estrogen receptor agonists possibly due to cross-talk between the AhR- and ER-mediated pathways.[81,82,122] The significant and nearly-significant differences compared to controls observed in these estrogen-responsive gene transcripts (i.e. increase in *vepg* mRNA in male livers, decrease of *cyp19* mRNA in female caudal fin, and near significant decrease of *vtg* mRNA in female liver) is suggestive that there was a perturbation in the estrogen signaling pathway. Previous work using

subtractive suppressive hybridization on the liver of female guppies, *Poecilia vivipara*, after a 24 h exposure to 10% (v/v) diesel WAF[123] identified 27 differentially expressed gene fragments that included increased *cyp1a* and decreased *vtg* consistent with our findings.

As the majority of information regarding xenoestrogen effects on these gene transcripts in differentiated tissues has come from adult male livers, it is becoming increasingly evident that juvenile fish are responsive to estrogenic substances, perhaps more so than adult males.[45,124] We previously examined the response of juvenile rainbow trout liver and caudal fin to a concentration range of 17α-ethinyl estradiol and established that, while the liver was more sensitive, both the liver and caudal fin responded to this potent estrogen with increased *vtg* and *vepg* transcript abundance while *cyp19* transcripts were not affected.[45] It is currently unclear how these rainbow trout responses relate to the juvenile coho salmon in the present study as the rainbow trout work did not distinguish between genetic sexes and the juveniles were different ages. Further elucidation of the juvenile response to other estrogens and PAHs, again keeping genotypic sex in mind, through analysis of additional time points and a broader range of response gene transcripts is warranted.

The extent of heavy metal interaction resulting from WAF exposure was evaluated through measurement of metallothionein A (*mta*) transcript levels (**Figure 2.8**). Our *mta* primer set only passed our validation for use with the liver tissue and not for use with the caudal fin (**Appendix 6**). In the liver, there was no significant change in *mta* transcript abundance following exposure to WAF. Although not significant, there was a slight trend (up to 1.3-fold) toward increased *mta* transcript abundance at low and high WAF concentrations (p=0.08; **Figure**

2.8). These results suggest that the trace elements of heavy metals in LSMD WAF did not affect the exposed fish to an appreciable degree.

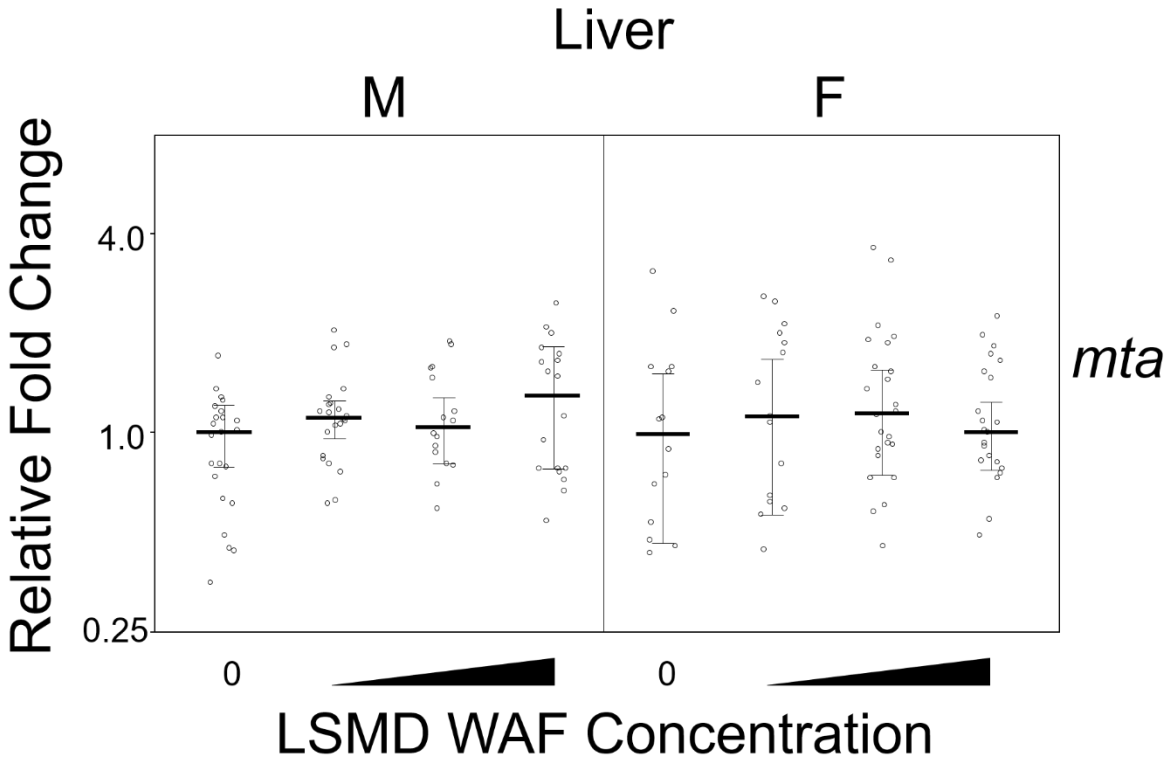

Figure 2.8. There is no response in the abundance of the metal exposure responsive *mta* gene transcript in liver tissue relative to seawater controls. The relative fold change of transcript abundance after exposure to different WAF concentrations as determined by qPCR analysis is shown. The bevel represents increasing low, medium, and high WAF concentrations (equivalent to 100, 320, or 1000 mg/L LSMD, respectively). Each open circle represents an individual animal, the median is represented by a horizontal bar, and the median absolute deviation is defined by the whiskers. Relative fold changes are expressed in a $\log_2$ scale.

In summary, LSMD WAF exposure clearly showed effects on PAH detoxification, stress, and estrogenic pathways and the liver showed a broader range of significant transcript responses compared to the caudal fin. Male salmon were particularly sensitive, accentuating the importance of taking genotypic sex into account in biological effects assessments in juvenile fish. Our data showed that when *cyp1a* is up-regulated in the liver of juvenile coho salmon, that this up-

regulation is apparent and even enhanced in the caudal fin of the same individuals. However, the other limited targeted gene transcripts used in the present study did not show this relationship and rather accentuated the differences in responsiveness between tissue types. Nevertheless, the qPCR-based tools developed and validated herein for both liver and caudal fin are poised for broader comparative WAF effects analyses with different oils. With the limited targeted gene transcript approach presented herein, it is likely that additional affected pathways were not identified with the targeted approach taken so far. For example, there is some suggestion that diesel exposure can affect immune system components and metabolic functioning in guppies and coral reef fish.[123,125] Further in-depth RNA-seq analyses are in progress to identify additional transcripts and pathways affected in the liver and caudal fin upon LSMD WAF exposure.

Given the results of this present study and from previous experiments, the salmonid caudal fin is a useful tissue for assessing response to a variety of contaminant exposures, such as: estradiol, cadmium, heavy metals field contamination, and now LSMD WAF exposure.[45,47] As we learn more about how the caudal fin responds to different scenarios, the utility of this easily accessible tissue for non-lethal biomonitoring assays will further increase with the anticipated discovery of more bioindicators to monitor pollutant exposure in the environment. Pending further validation on the kinetics of caudal fin transcriptomic response and recovery, caudal fin sampling may become a great boon, not only for oil spill cleanup initiatives, but for tracking aquatic pollutant effects on fish while preserving their populations.

3. Evaluation of oil-responsive bioindicators in the caudal fin and liver in response to four different oil WAF exposures

3.1. Introduction

Due to the complex nature of petroleum oil products, the resulting oil WAF released from a spill can significantly vary between different oil types.[126] This difference in oil WAF generation can result in significant differences in the persistence of WAF components and the resulting health effects on exposed fish.[127] This highlights the importance to characterize the composition and health effects of multiple types of oil, especially those that are not already extensively covered in the literature.[2] Furthermore, temperature and salinity significantly affect WAF composition,[22,23] yet there is little work investigating oil WAF composition and biological impact in cold marine climates.

Historically, oil toxicity has been assessed based on median lethal concentrations of exposure (LC50 assays).[71,128] These assays are useful for establishing the acute lethality of exposure, but fail to capture the potential for sublethal deleterious effects that may significantly impact long term fish health and survival.[72] It is important when considering toxicity, to take these sublethal effects into consideration.

Transcriptomics has been widely used in ecotoxicology to identify these sublethal effects that cannot be captured through acute LC50 assays.[32] Analysis of bioindicator transcripts (typically in the liver) has been effectively used to demonstrate the sublethal effects of oil WAF exposure, however, the majority of these studies focus on crude oils that have recently been involved in large spills.[2] In Chapter 2, the sublethal effects of LSMD WAF exposure were

assessed, but there are many other oil types that are underrepresented in the literature yet still abundantly used and present high risks of marine spills.

In addition to LSMDs, HSFOs are used in large vessels worldwide and found to be frequently involved in large (>30 tonne) spills, particularly off the North American Pacific coast.[71,129] HSFOs are typically restricted to use beyond 200 nautical miles offshore (far-shore fuel), whereas LSMDs can be used in vessels closer to shore (near-shore fuel). Despite distinct differences in regulation, there is little research directly comparing the sublethal deleterious effects resulting from the exposure of these two oils, specifically in cold marine environments.

In order to transport crude oil extracted from Canadian oil sands, bitumen is diluted (dilbit) using natural gas condensate, naptha, or other mixtures of lighter hydrocarbons to allow more efficient pipeline transportation.[130] Dilbit and crude oil are considered to exhibit similar properties, however, the resulting WAF generated using dilbit does differ from crude oils.[16] With increased oil sands production in Northern Alberta directing dilbit to be transported in tankers off British Columbia's coast, there is a significant risk of dilbit spills affecting marine fish.[16] A direct comparison of WAFs generated with dilbit and crude oils is warranted to further evaluate the effects of exposure.

In addition to evaluating the PAH dispersal and resulting biological effects of LSMD WAF exposure in Chapter 2, this present thesis work evaluated WAFs generated with three other ubiquitous oil types, HSFO, dilbit, and Alaskan crude oil. The work presented in this chapter focused on characterizing the tPAH50 of each resulting WAF and investigating the resulting sublethal exposures on juvenile coho smolt.

We have previously demonstrated in Chapter 2 that measurement of transcript abundance in the liver and caudal fin of coho salmon smolt significantly demonstrated response to LSMD WAF exposure generated under cold marine conditions. As *cyp1a1* response (referred to as *cyp1a* in chapter 2) is the most used bioindicator of oil WAF and PAH exposure,[50] the present work will continue to evaluate its responsiveness to these three new WAF exposures in these juveniles, also under cold marine conditions. The change of *cyp1a* naming in this chapter is to acknowledge that we are specifically measuring *cyp1a1* transcript abundance as teleost fish are known to contain several unique *cyp1a* paralogues.[131] *Cyp1a1* transcript abundance was also specifically being measured in Chapter 2, yet the term "*cyp1a*" was used as we were unaware of the presence of multiple paralogues in these fish. The response of constitutively expressed *ahr* will also be included for evaluation as a comparison to AhR-mediated *cyp1a1* expression. Transcript abundance will be measured in both the conventional liver tissue and caudal fin to compare the responsiveness to oil WAF exposure of these tissues.

3.2. Materials and Methods

3.2.1. Source of seawater

A fresh supply of seawater was used for the toxicity testing at PYLET in North Vancouver, British Columbia. The seawater supply was continuously pumped into the laboratory from the Burrard Inlet, BC, at a depth of 33 m and sand filtered. The seawater typically has a salinity of 26.2 g/L and a pH of 7.7-7.9.

3.2.2. WAF generation

WAF generation follows the same methods presented in Chapter 2 of this thesis. Prior to WAF preparation, smaller scale 96 h exposures involving WAF concentrations up to 3200 mg/L of HSFO, dilbit, and Alaskan crude oil were conducted. No fish mortalities were observed.

Given these data and logistical considerations, we prepared three WAFs per oil type by adding 51.62, 165.39, and 516.62 g of oil to 155L seawater for nominal loading concentrations of 333, 1067, and 3333 mg/L of oil respectively. Oil WAFs were prepared with Bunker C - 1994 (HSFO), cold lake blend lightly weathered diluted bitumen from the Canadian oil sands (dilbit), and Alaska North Slope crude oil (Alaskan crude). A seawater only vat was also prepared for each oil type.

3.2.3. Marine-acclimated coho salmon smolt exposure tests

Exposures and dissections were conducted as described in Chapter 2, following adapted Environment Climate Change Canada standard methods[132] with seawater acclimated coho salmon smolt substituted for rainbow trout as the test species. Smoltification was induced in coho salmon parr as described in Chapter 2: using seawater with a salinity of approximately 26±2 g/L and a temperature of 13±2 °C. Exposure vessels contained 42L of seawater and 18L WAF for a final volume of 60L at 15±1°C corresponding to final nominal exposure loading concentrations of 0 (control), 100 (Low), 320 (Medium), and 1000 (High) mg/L LSMD. A total of 40 salmon were exposed for each exposure concentration, except for the medium concentration dilbit exposure (n=39). HSFO WAF exposures took place two weeks after the initial LSMD WAF exposure, on September 28th, 2017, with dilbit WAF exposures starting on November 16th, 2017, and Alaskan crude WAF exposures starting on December 14th, 2017. The following water quality parameters were measured: pH, dissolved oxygen, temperature, and salinity for HSFO WAF exposures, dilbit WAF, and Alaskan crude WAF, with LSMD WAF parameters previously described (**Appendix 1**). Weights and fork length were recorded for each fish after exposures were completed and were similar between treatments for all WAF exposures (**Appendix 9**).

3.2.4. PAH analytical chemistry

Measurement of tPAH50 (23 parents and 27 alkyl homologs) was used for analytical chemistry analysis (**Appendix 2**) as described in Chapter 2.

3.2.5. Isolation of total RNA, cDNA preparation, quantitation of mRNA abundance, and genotypic sexing

Total RNA and gDNA isolation, as well as cDNA preparation of caudal fin and liver tissue samples were processed according to the methods described in Chapter 2. Liver and caudal fin samples were taken from the same fish. The methods used for qPCR analysis are described in Chapter 2, with qPCR primers presented in **Appendix 4.** Stability of normalizer C_t values are presented in **Appendices 12-14**. Sex genotyping of salmon via qPCR amplification of the male Y-chromosome marker, *oty2*, revealed the proportion of males and females was approximately 50:50 within each treatment group of all WAF exposures (**Appendix 10).** The results from the sex genotyping were used to group juvenile fish as male or female for subsequent targeted transcript analyses.

3.2.6. Statistical analyses

Significance was set at $p \leq 0.05$. Genetic sex was used to separate the fish into male and female groups. Statistical analyses of the mRNA abundance data were performed using R version 3.4.1 (R Foundation for Statistical Computing, Vienna, Austria). Relative fold changes were examined for normal distribution (Shapiro-Wilk) and unequal variances (Levene's) and the data were non-parametric. Significance was determined using the Kruskal-Wallis test and pairwise comparisons between treatments and sexes using the Mann-Whitney U test.

3.3. Results and Discussion

3.3.1. HSFO WAF

3.3.1.1. tPAH50 Concentrations

In the second chapter of this thesis, it was identified that LSMD WAFs became saturated at ~90 µg/L tPAH50 concentrations with nominal loading concentrations as low as 320 mg/L of LSMD. This resulted in all three WAF exposure concentrations being ~30 µg/L tPAH50 after a 30% dilution, with 2-ring PAHs making up most PAHs quantified (**Figure 2.2**). The WAFs generated with HSFO resulted in much higher tPAH50 concentrations when using the same nominal loading concentrations compared to LSMD WAF preparations. Initial PAH concentrations for the concentrated low, medium, and high concentration WAFs were 195.49, 374.64, and 731.84 µg/L tPAH50 (**data not shown**). Following a 30% dilution, the median exposure concentrations of the low, medium, and high concentration WAFs were 58.41 $\pm$ 0.75, 182.27 $\pm$ 1.26, and 635.42 $\pm$ 243.43 µg/L tPAH50 (**Figure 3.1**). This increased tPAH50 concentration is partially due to the increased amount of sulfur- and nitrogen-containing compounds in HSFO, allowing larger and more hydrophobic PAHs to be solubilized[18] that are not present abundantly in LSMD WAFs. The ability of HSFO WAFs to solubilize larger PAHs is demonstrated in the individual PAH profile, where 19 to 33% of the initial tPAH50 concentration is made up of four-ring and larger PAHs (**Appendix 15**).

Over the course of the 96-h exposure, HSFO WAF tPAH50 concentrations dropped ~91% PAHs weathered (**Figure 3.1**). Rapid weathering of PAHs is a frequently observed phenomenon that is likely caused by a combination of bioaccumulation in fish gills, adherence to exposure tank walls, evaporation of more volatile PAHs, and the precipitation of heavier PAHs.[133] There is also significant evidence of microbial involvement in the biodegradation of

PAH compounds.[23] As the HSFO WAF weathered, there was also an enrichment in the percent composition of larger PAHs. This is particularly evident in the highest concentration HSFO WAF, where the percent composition of four-ring and larger PAHs increases from 33% to 48% at the end of the 96 h exposure (**Appendix 15**) demonstrating their environmental persistence relative to smaller PAHs.[20]

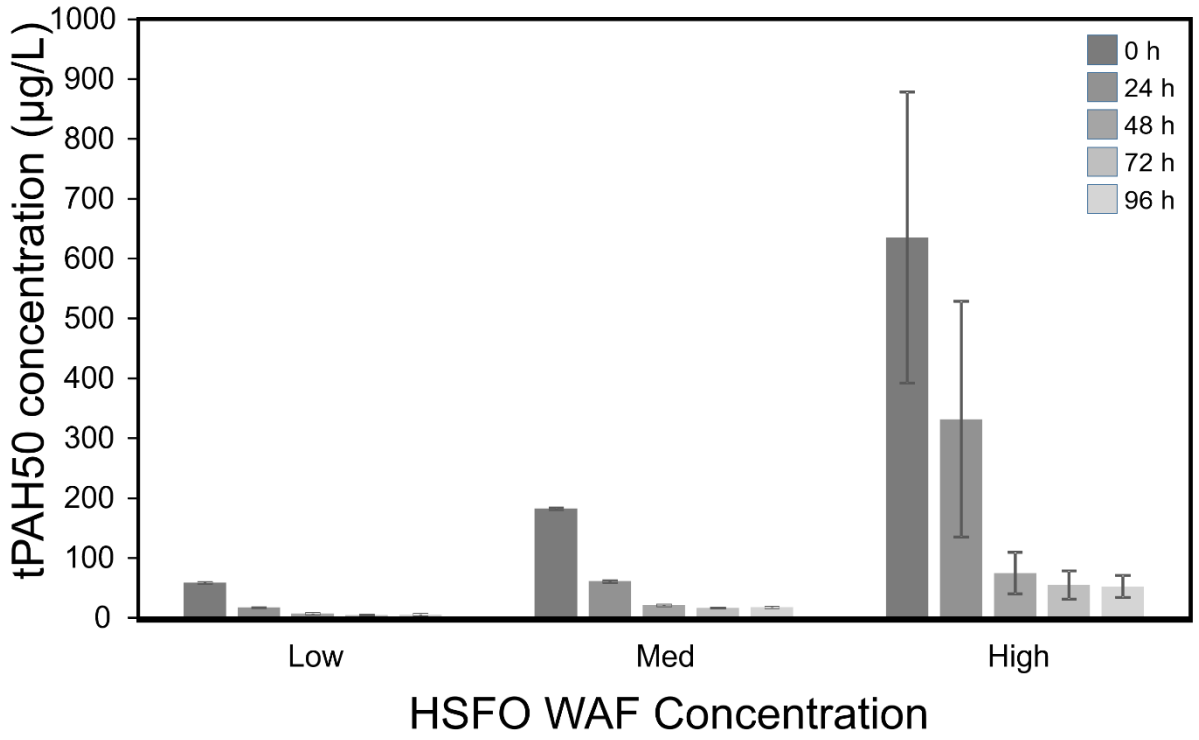

Figure 3.1. HSFO WAF tPAH50 profiles over time. Low, medium (Med), and High concentration WAF (equivalent to 100, 320, and 1000 mg/L HSFO, respectively), over a test period of 96 h. PAHs were quantified from WAF subsamples taken every 24 h from start to end of the exposure. Decreasing grey scale intensity indicate progression of time from 0-96 h of exposure in 24 h increments. Bars represent the median concentration observed from composite samples from 8 different tanks of the same WAF concentration. Error bars represent the median absolute deviation.

3.3.1.2. Fish mortalities and morphometrics

There were no fish mortalities. The weight and fork length were similar between treatment groups and medians ranged between 7.3-8.2 g and 8.8-9.0 cm, respectively (**Appendix 9)**.

3.3.1.3. *Ahr* and *cyp1a1* response

In Chapter 2, we identified that LSMD WAF exposure resulted in significant increases in *cyp1a1* and *ahr* transcript abundance. Therefore, we expected to see a greater response of these classically PAH-responsive genes to HSFO WAF exposure as the initial median tPAH50 concentrations are 2 to 20-fold greater than the LSMD WAFs. As previously observed in the LSMD WAF exposures, HSFO WAF exposure induced *ahr* only at the higher concentration WAF exposures (up to 2-fold difference) in both the caudal fin and liver (**Figure 3.2**). This response is also sex dependent as female *ahr* transcript abundance is significantly responsive only to the high concentration HSFO WAF, where male *ahr* significantly responds to the medium concentration WAF as well. The *ahr* response in the male liver to high HSFO WAF is also significantly greater than the medium concentration WAF exposure. A larger *cyp1a1* response with HSFO WAF exposure was observed with up to 125- and 35-fold increase in transcript abundance in the liver and caudal fin, respectively. This is a considerable increase from the maximum 18-fold increase in *cyp1a1* transcript abundance from LSMD WAF exposures (**Figure 2.5**). A dose/response relationship was observed in all sex/tissue combinations except for the male caudal fin, where the response reached a threshold at the medium concentration (**Figure 3.2**). This indicates that *cyp1a1* response to HSFO WAF is sexually dimorphic in the caudal fin, and not the liver. Overall, these data indicate an increased

potency of the HSFO WAF exposure compared to LSMD WAF likely due to the ~20-fold greater PAH concentration in the HSFO WAF.

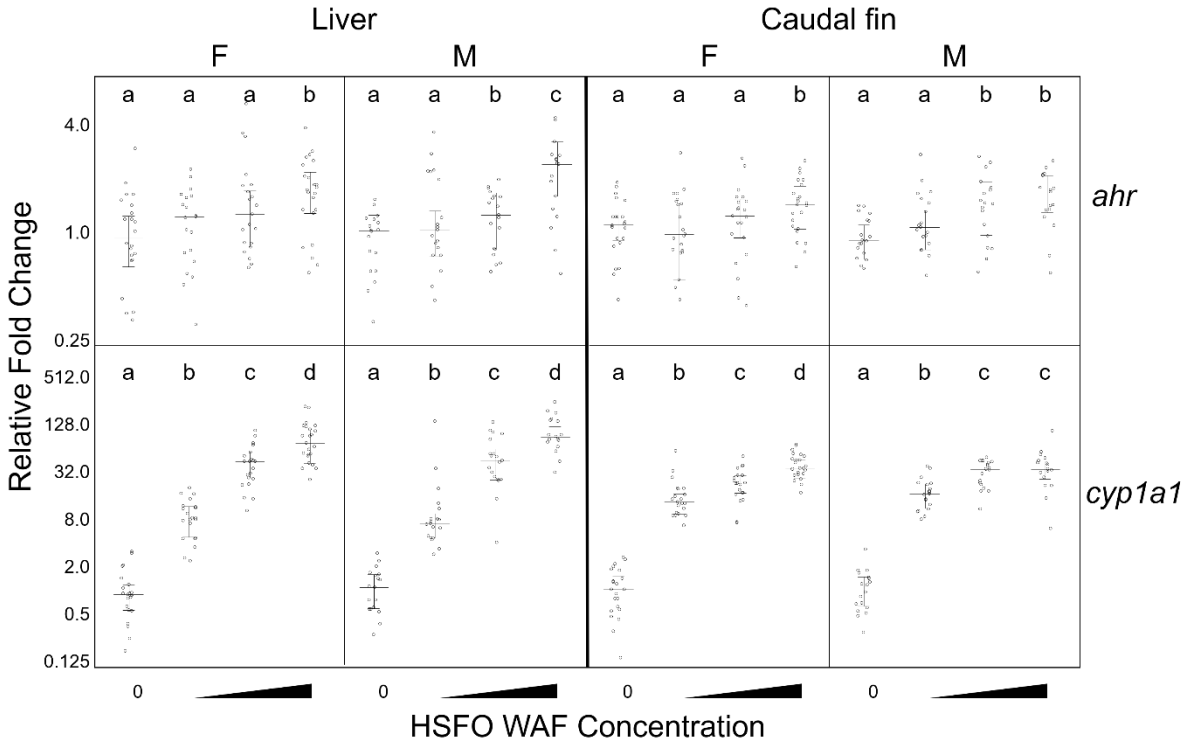

Figure 3.2. The abundance of *ahr* and *cyp1a* transcripts in both caudal fin and liver tissue is significantly affected by HSFO WAF exposure but the response patterns differ by sex and tissue type. The normalized relative fold change of PAH-response gene transcript abundance is shown after exposure to different WAF concentrations as determined by qPCR analysis. The bevel represents increasing WAF concentrations (equivalent to 100, 320, and 1000 mg/L HSFO, respectively). Each open circle represents an individual animal, the median is represented by a horizontal bar, and the median absolute deviation is defined by the whiskers. Relative fold changes are expressed in a $\log_2$ scale. For more details, see **Figure 2.5** legend.

3.3.2. dilbit WAF

3.3.2.1. tPAH50 Concentrations

The initial PAH concentrations of the low, medium, and high concentration dilbit WAF exposures were 9.24 $\pm$ 0.18, 21.45 $\pm$ 0.26, and 26.70 $\pm$ 0.03 µg/L tPAH50 (**Figure 3.3**). The composition of PAHs at the beginning of WAF exposure demonstrate a similar abundance of two- and three-ring PAHs, as well as four-ring PAHs (**Appendix 16**). Over the course of the 96-

h exposure, dilbit WAF PAH concentrations decreased by 93% with a similar distribution of two- to four-ring PAHs. Dilbit WAFs resulted in the lowest abundance of PAHs generated compared to WAFs generated with the same volume of all other oil types examined.

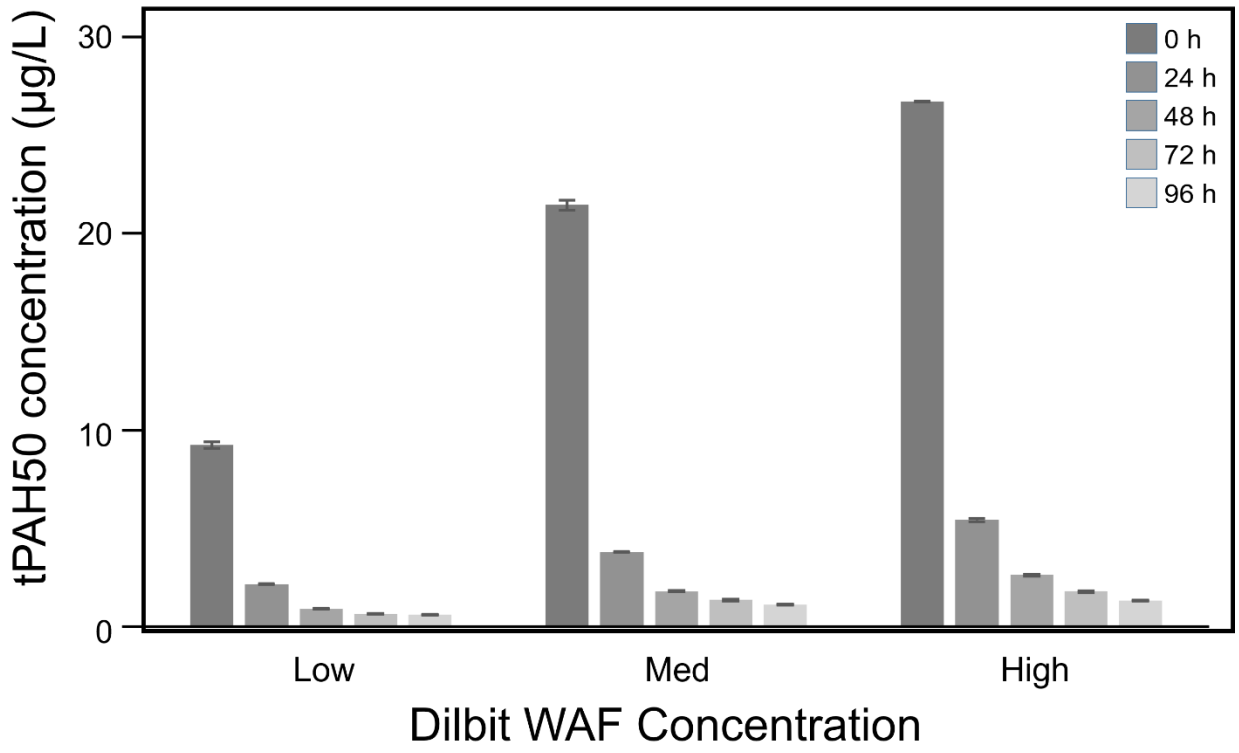

Figure 3.3. Dilbit WAF tPAH50 profiles over time. Low, medium (Med), and High concentration WAF (equivalent to 100, 320, and 1000 mg/L dilbit, respectively), over a test period of 96 h. For more details see **Figure 3.1** legend.

3.3.2.2. Fish mortalities and morphometrics

No fish mortalities were observed upon dilbit WAF exposure. The weight and fork length were similar between treatment groups and medians ranged between 9.9-11 g and 9.6-10 cm, respectively (**Appendix 9**).

3.3.2.3. *Ahr* and *cyp1a1* response

Although *ahr* transcript abundance was significantly responsive to the highest concentration LSMD (**Figure 2.5**) and HSFO (**Figure 3.2**) WAF exposures, this transcript does

not significantly respond to dilbit WAF exposure in either tissue (**Figure 3.4**). In the liver, *cyp1a1* transcript abundance significantly increases in the medium and high concentration WAF exposures in both sexes (females-1.6- to 1.8-fold; males-1.7-fold), but not the lowest concentration dilbit WAF. In contrast, caudal fin *cyp1a1* transcript abundance significantly responded to all dilbit WAF concentrations and demonstrated a greater fold change response to all dibit WAF exposures in both sexes (females-3.1- to 3.7-fold; males-2.4 to 3.7-fold). As with HSFO WAF, these data demonstrate that *cyp1a1* response to dilbit WAF is sexually dimorphic in the caudal fin, and not the liver. This supports separating biological replicates by sex when examining *cyp1a1* response in the caudal fin but not the liver. These data also demonstrate that caudal fin *cyp1a1* transcript abundance was more sensitive to these low PAH WAF exposures than in the liver. In comparison, freshwater dilbit WAF exposures generated at similar tPAH50 concentrations resulted in mortality of some sockeye salmon (*Oncorhynchus nerka*) embryos, and salmon alevins reared to swim-up stage exhibited up to 40-fold increases in *cyp1a1* transcript abundance from whole head samples.[8]

Caudal fin *cyp1a1* transcript abundance also exhibited a U-shaped dose response curve in response to increasing dilbit WAF concentration (**Figure 3.4**). This type of hormetic response is well observed in biology,[134] where middling dose ranges may exhibit inhibitive properties compared to low or high doses. This type of response has also been observed on copepod metabolism with pyrogenic PAH exposure,[135] and may be indicative of an evolutionary response to environmental PAH concentrations.[136]

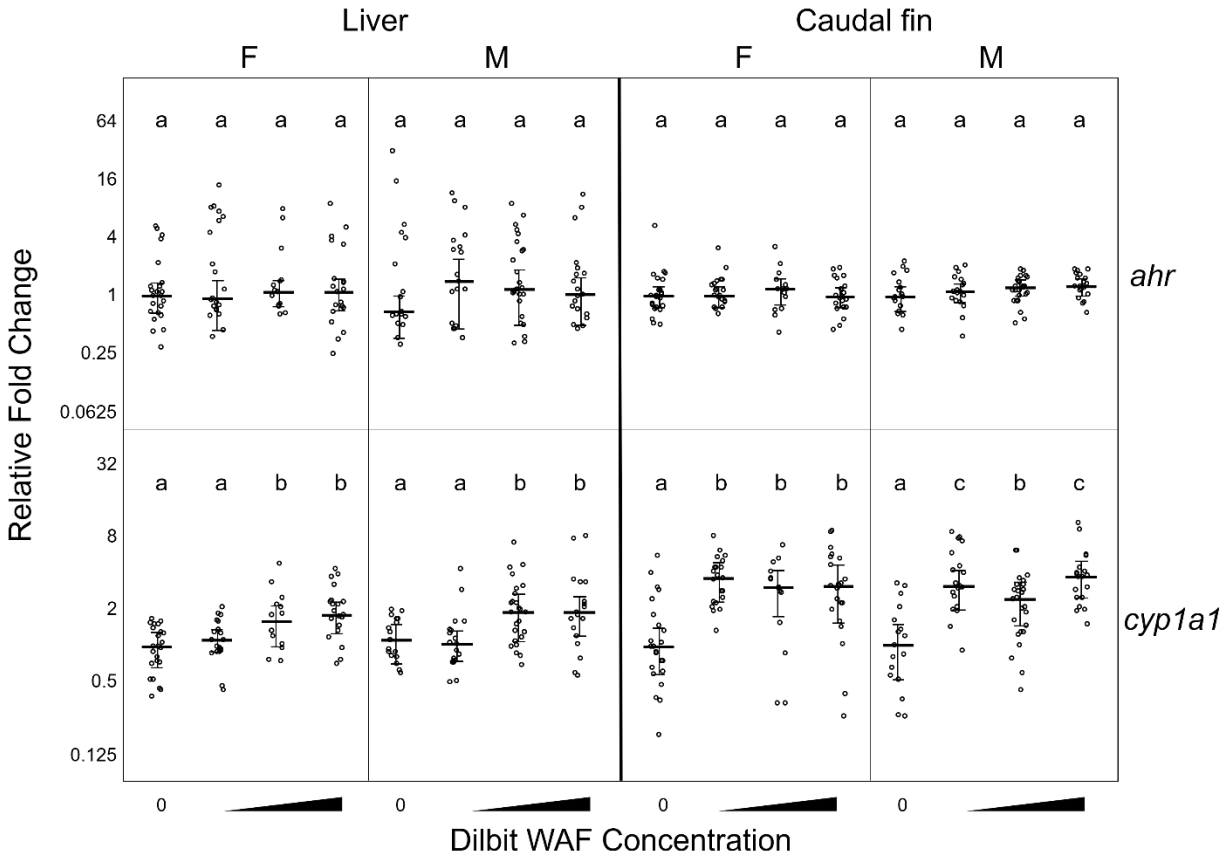

Figure 3.4. Caudal fin *cyp1a1* responds to all dilbit WAF exposures where liver *cyp1a1* only responds to the medium and high concentration WAFs. The normalized relative fold change of PAH-response gene transcript abundance is shown after exposure to different dilbit WAF concentrations as determined by qPCR analysis. For more details, see **Figure 2.5** legend.

3.3.3. Alaskan crude WAF

3.3.3.1. tPAH50 Concentrations

The initial tPAH50 concentrations between the low, medium, and high concentration Alaskan crude WAF exposures were 94.56 $\pm$ 3.19, 94.60 $\pm$ 3.04, and 103.94 $\pm$ 3.45 µg/L, respectively (**Figure 3.5**). About 86% of this WAF is comprised of the two-ring PAH, naphthalene (NAP) and its alkylated homologues, as well as very few three-ring PAHs (**Appendix 17**). After 96 hours, 82-85% of the WAFs tPAH50 concentration were weathered out of solution, although maintaining a similar individual PAH distribution. The apparent saturation

of these Alaskan crude WAFs at ~95 µg/L tPAH50 and significant Naphthalene composition are very similar to the tPAH50 profiles observed in LSMD WAFs (**Figure 2.2**, **Figure 2.3**), although three-times as concentrated. Although the tPAH50s of the Alaskan crude WAFs were greater than the dilbit WAFs, the dilbit WAFs contained more three- and four-ring PAHs which are more environmentally persistent than two-ring PAHs.[20]

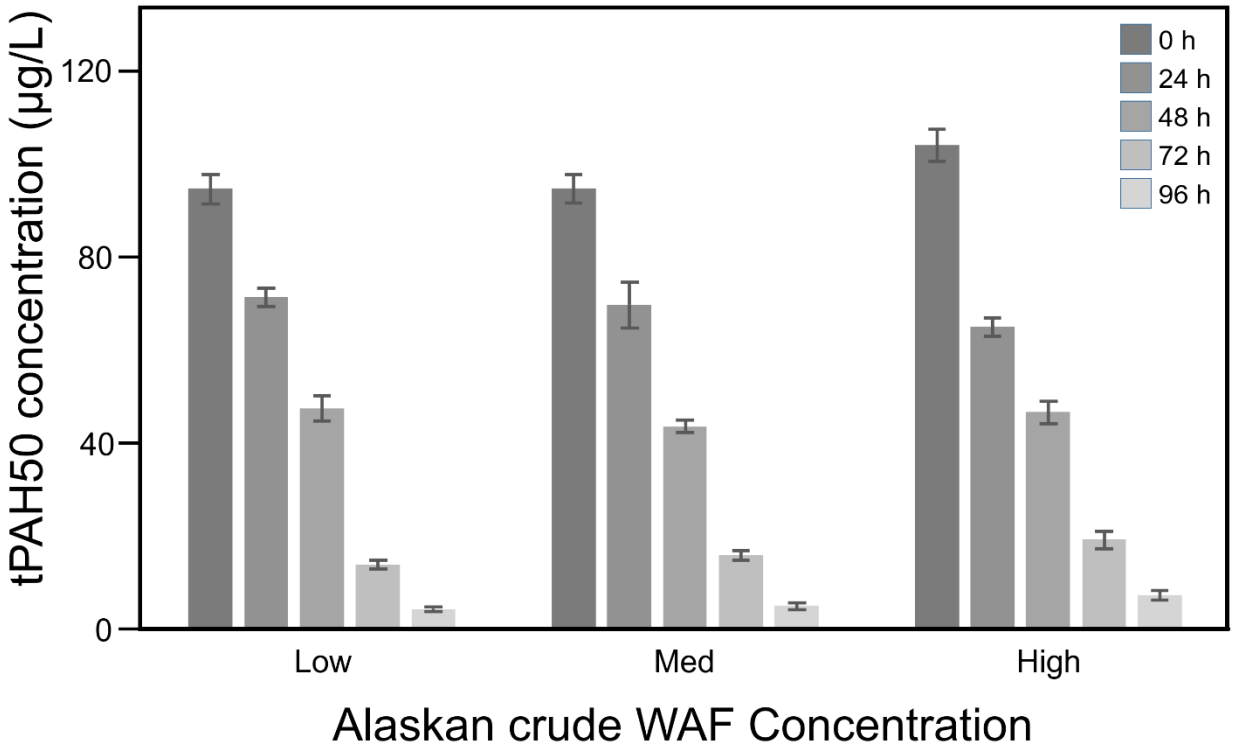

Figure 3.5. Alaskan WAF tPAH50 profiles over time. Low, medium (Med), and High concentration WAF (equivalent to 100, 320, and 1000 mg/L dilbit, respectively), over a test period of 96 h. For more details see **Figure 3.1** legend.

3.3.3.2. Fish mortalities and morphometrics

There were no mortalities with any of the Alaskan crude WAF exposures and the weight and fork length were similar between treatment groups and medians ranged between 11.6-13.2 g and 10.1-10.5 cm, respectively (**Appendix 9**).

3.3.3.3. *Ahr* and *cyp1a1* response

Although the tPAH50 concentration of Alaskan crude WAF exposure was at least three-fold higher than dilbit WAFs, *ahr* and *cyp1a1* transcript abundance was not responsive in the liver and only responsive to the highest concentration in the caudal fin (**Figure 3.6**). The response observed to the highest concentration Alaskan crude WAF was also sex-specific, where caudal fin *ahr* transcript abundance only significantly increased in males (1.6-fold change) and *cyp1a1* in females (1.4-fold change), following a trend of sexual dimorphism in the caudal fin response to these WAF exposures. Despite exhibiting similar PAH distributions to LSMD WAFs (**Appendix 17**, **Figure 2.3**) and having a minimum three-fold higher tPAH50 concentration, LSMD WAF exposure resulted in a completely different *ahr* and *cyp1a1* response in both the liver and caudal fin. This is potentially due to the presence of toxicants not captured by the tPAH50 analysis, such as NAs. This reduced effect of WAFs generated with Alaska North Slope crude oil has been previously observed in larval and juvenile Atlantic cod and Atlantic salmon where it was suggested that these WAFs were unlikely to pose an acute risk to these cold-water marine fishes.[137] In contrast, warm-water crude oil WAFs containing similar tPAH50 concentrations significantly increased hepatic *cyp1a1* expression in mahi, highlighting the temperature dependence of WAF generation.[30] Overall, these data demonstrate that between these two tissues, only the caudal fin was able to demonstrate significant response to Alaskan crude WAF exposure when measuring *ahr* and *cyp1a1* response.

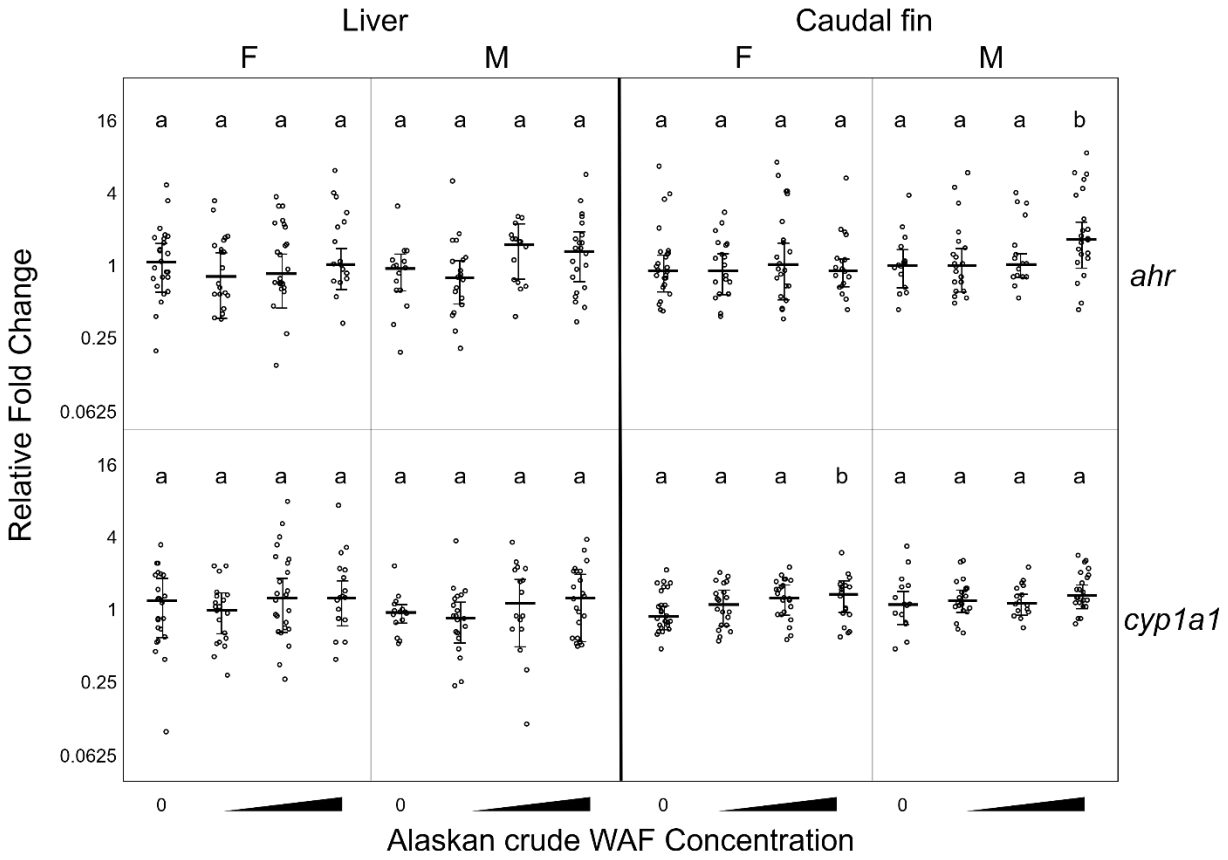

Figure 3.6. A significant response of caudal fin *ahr* (males only) and *cyp1a1* (females only) transcript abundance is observed to the highest concentration Alaskan crude WAF, but not in the liver. The normalized relative fold change of PAH-response gene transcript abundance is shown after exposure to different Alaskan crude WAF concentrations as determined by qPCR analysis. For more details, see **Figure 2.5** legend.

3.3.4. Comparison of WAFs generated with LSMD, HSFO, dilbit, and Alaskan crude oil.

Between the four oil types, HSFO WAF had the highest tPAH50 concentrations (**Figure 3.1**) and dilbit resulted in the lowest tPAH50 WAFs (**Figure 3.3**). Each WAF demonstrated a weathering of 82-93% of tPAH50 concentrations after 96 h in the presence of fish, with the HSFO and Alaskan crude WAFs remaining at notable levels of PAHs.[133] The LSMD and Alaskan crude WAFs were dominated mostly by Naphthalenes, whereas dilbit and HSFO WAFs contained more four-ring and larger PAHs (**Appendix 15**, **Appendix 16)**. In comparison to the

total PAH concentrations found in the warm marine waters of the Gulf of Mexico after the *Deepwater Horizon* oil spill (189 µg/L),[20] the tPAH50 concentration observed in these WAF exposures were lower in all oil WAFs examined, except for the medium and high concentration HSFO WAFs, which then dropped below this level within 48 hours. These results demonstrate that these cold-water marine WAF exposures are comparable to real-world oil spill scenarios based on PAH concentrations. These PAH concentrations are still of concern, as warm-water marine tPAH50 concentrations as low as 33 µg/L significantly impact behaviour in Atlantic croaker (*Micropogonias undulatus*), such as social group adhesion.[10] The effects of exposure to similar PAH concentrations under cold-water marine conditions are not well characterized in the literature.

3.3.5. Comparison of the liver and caudal fin in demonstrating biological response to oil WAF exposure

These exposures significantly differ from the majority of WAF exposures found in the literature as they were performed in cold marine conditions (which tends to lower potential PAH toxicity relative to warm marine conditions)[17] and with salmon smolts instead of early life stages that are typically assessed.[17,112] Overall, both the liver and caudal fin demonstrated a significant response in *ahr* and *cyp1a1* transcript abundance to these cold marine WAF exposures in most circumstances, however only the caudal fin elicited a significant response to WAFs generated with all four oil types. Between the four oil types, HSFO WAF exposure resulted in the greatest response in *cyp1a1* transcript abundance, with up to 118- and 125-fold increase in the female and male liver, respectively, and up to 35- and 33-fold increase in the female and male caudal fin, respectively (**Figure 3.2**). The response of *ahr* transcript abundance was weaker than *cyp1a1* measured in the same fish, and typically non-responsive in lower concentration WAF exposures.

This is as expected, as *ahr* is constitutively expressed whereas *cyp1a1* expression is only induced upon AhR activation.[52] However, significant response to dilbit WAF exposure in males was only observed with *ahr* transcript abundance in the caudal fin and not in the liver. Comparing *cyp1a1* response to the lowest WAF exposure concentrations (low dilbit WAF; 9.2 µg/L tPAH50), only the caudal fin demonstrated a significant response with 3.7- and 3.1-fold changes in females and males respectively.

In order of *cyp1a1* response in the caudal fin and liver, HSFO WAFs (**Figure 3.2**) induced the greatest response, followed by LSMD (**Figure 2.5**), dilbit (**Figure 3.4**), and Alaskan crude (**Figure 3.6**) WAFs. This trend mostly follows an order of decreasing tPAH50 WAF concentration, except for the Alaskan crude WAFs that, despite exhibiting the second highest tPAH50 concentrations, hardly elicited a *cyp1a1* response in the caudal fin, and no response in the liver. As described above, this decreased responsiveness to Alaskan crude WAF may be due to the presence of compounds other than PAHs, like NAs. Alaskan crude WAF exposures were also the last exposure conducted resulting in larger smolts involved (**Appendix 9**). As larger smolt size has been attributed to likelihood of survival during the transition of coho smolts to adulthood,[138] this size difference might contribute to a reduced response to Alaskan crude WAF exposure, although these salmon are still expected to exhibit similar physiology.

Although *cyp1a1* transcript abundance has been demonstrated to be an effective tool for demonstrating salmon response to oil spill exposure in the liver[8,112,139] and caudal fin, the response of this transcript does not appear to directly correlate with tPAH50 concentrations measured. This demonstrates a clear need for better transcript bioindicators that are specifically PAH responsive. Moreover, sex-biased responses were observed for each WAF type, highlighting the importance of taking sex into consideration when analysing transcriptomic

responses. These data also accentuate the need for directly testing biological response rather than relying on tPAH50 measurements for these complex mixtures.

Overall, the data presented herein demonstrate valuable insight into the effects of cold-water marine oil WAF exposure in juvenile salmon. These data also demonstrate that the caudal fin more sensitively detected exposure to very low tPAH50 concentration WAFs than the liver as seen with the lowest concentration dilbit WAF exposure (**Figure 3.4**). The caudal fin transcriptome also demonstrated significant response to Alaskan crude WAF exposure that was not detected in the liver indicating a broader range of responsiveness in the caudal fin (**Figure 3.6**). This improved sensitivity in the caudal fin, in combination with the ability to be sampled non-lethally, projects a promising future for the caudal fin in demonstrating biological response to oil spill exposure and tracking the effectiveness of clean up efforts.

4. Near vs. far-shore fuels: Comparing the transcriptomic response of the salmonid caudal fin and liver to marine oil spills

4.1. Introduction

The water soluble organic chemical compounds released during an oil spill, such as PAHs, significantly impact fish reproduction,[5–7] development,[8] cardiac function,[9] and social group adhesion.[10] Acute exposure does not typically result in immediate lethality or obvious morphological changes in exposed fish, yet these sublethal effects still pose a significant threat to fish health.[31] There is a clear need for tools that can sensitively and conveniently evaluate fish health and track oil spill exposure.

Difficulties in evaluating oil spill toxicity are magnified considering the heterogeneity of petroleum products.[127] LSMDs and HSFOs are very different oil types and are frequently involved in large (>30 tonne) spills, particularly off the North American Pacific coast.[71,129] HSFOs are typically restricted to use beyond 200 nautical miles offshore (far-shore fuel), whereas LSMDs can be used in vessels closer to shore (near-shore fuel). Despite distinct differences in regulation, limited research has been carried out directly comparing the sublethal deleterious effects resulting from the exposure of these two oils, specifically in cold marine environments.

Measuring the response of hepatic transcriptomic bioindicators has been widely implemented in evaluating oil spill toxicity. However, these methods typically require lethal sampling through labor-intensive dissection and is not compatible with conservation. In contrast, the caudal fin is a readily accessible tissue that can be sampled rapidly through minimal distress to the fish and allows for rapid catch-and-release methods of fish sampling. The benefits of

reduced lethality in biomonitoring cannot be overstated, and non-lethal sampling methods also allow for repeated measures of single organisms which is very important for accounting for differences between biological replicates. Using qPCR methods, we have previously demonstrated that the caudal fin can be highly responsive to a range of different contaminants using transcript targets originally identified in the liver.[45,47,107] This previous work suggested that there may be a suite of caudal fin-specific transcripts that are highly responsive with low variation in the caudal fin but have not yet been identified as they may not be expressed or respond in the liver.

In this present chapter, exposure effects involving near-shore fuel, LSMD, and far-shore fuel, HSFO WAFs from Chapter 2 and 3, respectively, are directly compared. As salinity and temperature can significantly impact the aqueous phase of an oil spill,[22,23] we ensured all exposures and WAF preparations were performed with cold marine conditions. We measured 50 individually quantified PAHs and their alkylated homologues that are found to be commonly released during oil spills. Exposures were conducted on seawater acclimated coho smolts. Smolting salmon undergo intense developmental restructuring as they are transitioning from freshwater to marine environments.[140] Little is known of how oil spill exposure may impact salmon during this sensitive stage.

The effects of acute WAF exposures were characterized through measuring the transcriptomic responses observed within the liver and caudal fin from exposed smolt, with specific attention to separating genetic females and males to account for potential sex-bias. In addition to qPCR analysis of PAH-responsive gene transcripts performed in Chapter 3, we performed in-depth RNA-Seq analysis on the liver and caudal fin of females and males exposed to the highest concentration WAFs. Herein we report a comparison of the effects of near- and

far-shore fuel oils in both the caudal fin and the liver of juvenile salmon and identify novel bioindicator candidates that may be used for identifying exposure to oil spills. We define strong bioindicators as those with a high fold change compared to unexposed controls with low variation.

4.2. Materials and methods

4.2.1. Preparation of RNA for Illumina total RNA sequencing

In preparation for RNA-Seq, the integrity of isolated RNA from fish exposed to seawater controls and the highest concentration WAF exposures were analyzed using a Bioanalyzer 2100 (Agilent Technologies), and samples with RNA integrity number (RIN) of > 7 were used for RNA-Seq analyses (5 biological replicates per treatment and tissue). Liver and caudal fin samples were taken from the same fish. RNA samples were shipped on dry ice to Canada's Michael Smith Genome Sciences Centre (GSC, BC Cancer Research, Canada), where strand-specific mRNA libraries were constructed and sequenced using Illumina HiSeq 2500 (paired-end platform generating 2 x 75 base pair reads for each sample).

4.2.2. RNA-Seq Assembly and Analysis

Read quality was assessed using FastQC[141] to ensure high read quality in all samples. Reads were aligned to *Oncorhynchus kisutch* genome assembly, oki_ref_Okis_V1 (GCF_002021735.1) using STAR two-pass alignment (version 2.6.1)[142]. Mapped reads were assembled and counted using StringTie (version 1.3.4) with a minimum read coverage of 1 for most transcripts, and 4.75 for single-exon transcripts.[143] Gene counts were exported as transcript count tables comparing individual transcript counts from the treated animals to transcript counts from the control animals. Transcripts were annotated using BLASTn and BLASTx against National Center for Biotechnology Information (NCBI) nucleotide (nt) and non-redundant (nr)

protein database. Differential gene expression analysis was performed using DESeq2 (version 1.28.1)[144] as described previously[145] with a $p_{adj} \leq 0.05$ cut-off for significance. To identify the function of the differentially expressed genes and to investigate the corresponding enriched pathways, we performed gene annotation enrichment analysis. A hypergeometric test was performed to evaluate whether the overlap in commonly DEGs between sexes is significantly greater ($p \leq 0.05$) than the overlap drawn from two independent groups. To perform functional annotation analysis, genes were annotated with gene ontology (GO) terms using Trinotate (version 3.2.0).[146] The GO terms annotated to DEGs from each treatment were compared against the distribution of GO terms annotated to all significantly expressed from their respective tissue (counts per million reads; cpm > 0.1) using GOseq (version 1.42.0)[147] to identify GO term enrichment ($p_{adj} \leq 0.05$, FDR ≤ 0.05). A cpm > 0.1 in more than 50% of genes were excluded to remove low level expressed transcripts that produced a high fold change but still had very low overall expression. Due to the high abundance of enriched GO terms observed, an 'extremes' filter was applied using Gogadget (version 2.1)[148] to remove overly specific or general GO terms for clearer visualization of enriched processes. GO terms annotating fewer than 10 or more than 300 DEGs were excluded from LSMD WAF treated animals and fewer than 20 or more than 100 DEGs were excluded from HSFO WAF treated animals. Enrichment maps were then generated from the filtered lists of enriched GO terms using Cytoscape (version 3.8.2).[149]

This RNA-seq protocol has been prepared as a semi-automated RNA-Seq pipeline that uses bash scripts requiring simplified user inputs to interact with the Slurm workload manager of Compute Canada superclusters to take advantage of its advanced computing power. A simple diagram detailing the workflow of this pipeline is demonstrated in **Figure 4.1**.

Figure 4.1. A diagram depicting the RNA-Seq workflow used.

4.3. Results and Discussion

4.3.1. Evaluation of sex-biased baseline gene expression in control coho salmon smolts

We first compared transcript levels between genetic male and female controls to evaluate sex-based differences in baseline gene expression of coho salmon smolts (**Appendix 19**). In the liver, there were 17 differentially expressed genes (DEGs) between genetic males and females from LSMD controls and 377 DEGs from HSFO controls. This increase in sexual dimorphism in the liver of HSFO WAF control fish appears in tandem with fish development, as HSFO WAF salmon are longer and heavier than LSMD WAF salmon (**Appendix 9**) as the exposures were two weeks apart. Despite this, the caudal fin is steady as both sets of control fish exhibited fewer than ten DEGs between genetic males and females in this tissue.

4.3.2. LSMD WAF Exposure

The second chapter of this present thesis demonstrated that LSMD WAF exposure results in the differential expression of genes associated with xenobiotic metabolism, general stress, oxidative stress, and estrogen-mediated pathways in the caudal fin and liver (**Figure 2.5, Figure 2.6, Figure 2.7**). To obtain a broader profile of DEGs, total RNA-Seq was performed on paired caudal fin and liver tissues to quantify the abundance of significantly expressed transcripts from salmon smolts exposed to a seawater control or the highest concentration LSMD WAF. We noted a significant sex-biased response to LSMD WAF exposure, so we analyzed genetic males and females separately.

4.3.2.1. Comparing DEGs with LSMD WAF exposure

In the liver, LSMD WAF results in 509 DEGs in females with a substantially lower number in males (86 DEGs; **Table 4.1**). LSMD WAF exposure results in a similar number of

DEGs in both the female and male caudal fin, with 495 and 545 DEGs, respectively. Across the four tissue types, there were 1,600 unique genes that were differentially expressed with only 10% differentially expressed in more than one tissue (**Figure 4.2 b**). In total, six genes were commonly differentially expressed in all tissues which all shared similar functions of xenobiotic metabolism (**Appendix 19**). These data indicate that the response to LSMD WAF exposure is highly tissue- and sex-dependent. Overall, comparable levels of response were found in three of the four tissue sets, with the male liver exhibiting fewer DEGs. This level of sex-biased transcriptomic variation is not unusual in salmonids.[150]

Table 4.1. Comparison of the number of genes from the LSMD and HSFO RNA-Seq datasets that were carried through the differential expression analysis workflow. CF, caudal fin; DETs, differentially expressed transcripts ($p<0.05$); DEGs, differentially expressed genes; F, genetic female; GO, gene ontology; LI, liver; M, genetic male.

LSMD WAF exposure				
Tissue Type	LI-F	LI-M	CF-F	CF-M
Total number of genes	28,014	28,301	33,916	33,745
Number of DETs	323	125	704	442
Number of DEGs	509	86	495	545
Number of DEGs with a Blastn annotation	507	86	488	540
Number of DEGs with Uniprot annotation	490	83	445	485
Number of DEGs generating a GO term	479	83	438	481
Number of enriched GO terms	79	21	69	167
Number of enriched GO terms after filtering (min 10, max 300)	43	2	58	89
HSFO WAF exposure				
Tissue Type	LI-F	LI-M	CF-F	CF-M
Total number of genes	27,395	27,096	34,206	34,172
Number of DETs	11,246	6,745	9,831	3,401
Number of DEGs	11,864	7,229	10,119	2,125
Number of DEGs with a Blastn annotation	11,864	7,229	10,119	2,125
Number of DEGs with Uniprot annotation	11,276	6,882	9,572	2,010
Number of DEGs generating a GO term	11,041	6,764	9,386	1,981
Number of enriched GO terms	233	337	196	514
Number of enriched GO terms after filtering (min 20, max 100)	157	150	91	138

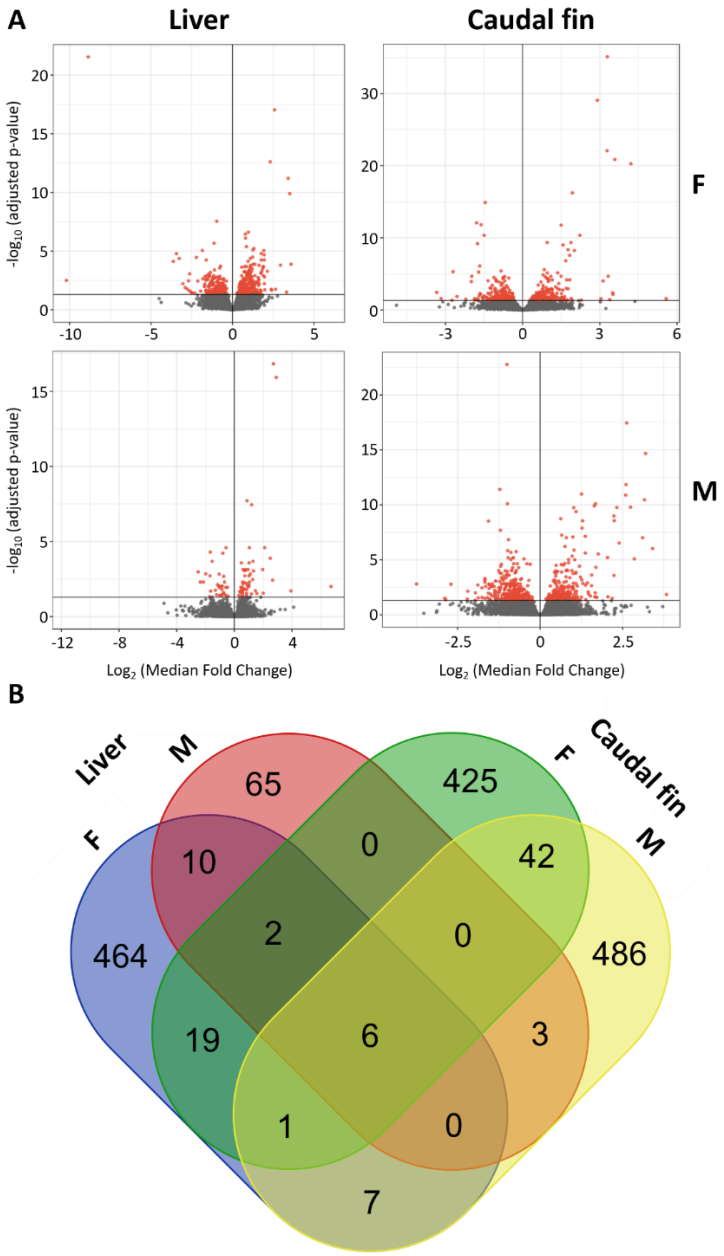

Figure 4.2. LSMD WAF exposure induces a unique, sex-specific transcriptomic response in the coho salmon caudal fin and liver. **A.** Volcano plots depicting the differential expression of sequenced RNA transcripts from the caudal fin or liver of 10 male or 10 female salmon exposed to either seawater control or high concentration marine diesel WAF are shown. Differentially expressed genes as determined by DESEQ2 are represented by red dots and not differentially expressed genes are represented by grey dots ($p_{adj} < 0.05$). Individual isoform abundance was grouped to give counts of gene expression rather than individual transcript expression. Significance cut-off is represented by the horizontal bar separating the red and grey dots. Degree of differential expression is depicted by an increasing –log10 of the p_{adj} value for each transcript. Median fold change in transcript abundance is expressed in a log2 scale. **B.** Venn-diagram

demonstrating the overlap of differentially expressed genes ($p_{adj} < 0.05$) because of high-concentration LSMD WAF exposure. Transcriptomic profiles were quantified using RNA-Seq analysis of the liver (left) and caudal fin (right) of 10 females (blue and green) and 10 males (red and yellow). Abundance displayed combines individual transcript isoform abundance to give counts for overall transcript abundance.

Of the 1,600 unique DEGs represented between the liver and caudal fin, only 28 are differentially expressed in both. This highlights the need for caudal fin-specific gene bioindicators to fully evaluate the utility of the caudal fin transcriptome for detection of oil spill exposure. This overlap in differential expression between males and females in the liver and caudal fin was significant with 11.5-fold ($p < 1.7e-14$) and 6.2-fold ($p < 2.8e-24$) greater overlap, respectively, than what is randomly expected using the hypergeometric test. For this reason, males and females were analyzed separately.

4.3.2.2. GO term enrichment analysis with LSMD WAF exposure

In the liver, LSMD WAF exposure results in the enrichment of 79 GO terms in females and 21 GO terms in males (**Table 4.1**). Enriched GO terms in the female liver highlight regulation of the ERAD pathway, protein misfolding, and cellular redox activity (**Figure 4.3 C**). The few enriched terms in the male liver also showcase the enrichment of redox management highlighting a conserved response between sexes (**Appendix 20**). Outside of major clusters, N-linked glycosylation GO terms are also strongly enriched in the female liver with LSMD WAF exposure. The significant response of the ERAD pathway is likely representative of hepatic cytochrome activity required to manage the exposure of aryl xenobiotics such as PAHs.[151] The enrichment of N-linked protein glycosylation also indicates that wnt/β-catenin signalling and cell-adhesion may also be modulated in the liver.[152]

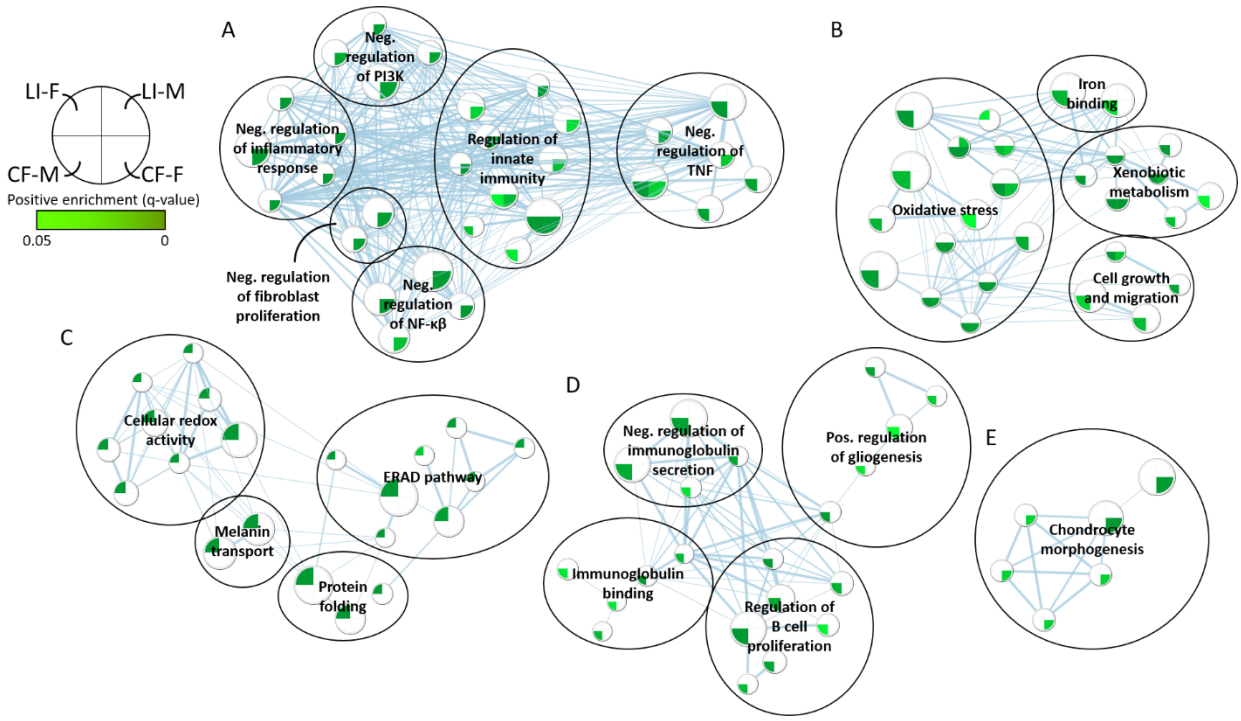

Figure 4.3. LSMD WAF exposure primarily results in the enrichment of these five processes: A. Negative regulation of innate immunity; B. Xenobiotic metabolism and oxidative stress; C. ERAD pathways and protein folding; D. B-cell proliferation and gliogenesis. E. Chondrocyte morphogenesis. The 5 largest clusters of enriched GO terms in male and female liver and caudal fin as a result of LSMD WAF exposure. LSMD WAF appears to influence the following biological factors: Significantly enriched GO terms (FDR<0.05) were visualized using the Cytoscape Enrichment Map plugin. An "extremes" filter was applied to remove overly specific or general GO terms (minimum 10 or maximum 300 genes annotated). Enrichment is relative to a background containing GO-terms represented from all genes expressed from their respective tissue-types (males and females combined). Each node represents a GO term. Each tissue is represented by a single quadrant of GO term nodes. If a tissues quadrant is a shade of green, this indicates this GO-term was enriched in that tissue set where a darker shade of green indicates a lower q-value enrichment. Node size is indicative of the number of genes annotated with that GO term. The thickness of each line is indicative of the number of genes shared between the connected gene sets (minimum 50% overlap). White shading indicates that the GO term was missing for a given tissue.

In the caudal fin, 69 GO terms are enriched in females and 167 in males. The caudal fin features the largest clusters of enriched GO terms with LSMD WAF exposure, demonstrating conserved innate and adaptive immune responses (**Figure 4.3 A, D**), as well as oxidative stress,

xenobiotic metabolism, and morphogenesis (**Figure 4.3 B, E**). These data indicate LSMD WAF exposure results in extensive immunomodulatory effects in the caudal fin as well as unfolded protein response and chondrocyte morphogenesis highlighting a potential for chondrodysplasias that could contribute to developmental defects like small size and/or abnormal body proportions.[153] These effects are particularly observed in teleost fish, where PAH exposure results in hyperdorsalized embryos.[154] The significant enrichment of defense response observed here has also been captured in channel catfish, where an influx of inflammation cascade occurred with increased expression of cytochrome P450 genes.[155]

Overall, the response in the liver tissue contrasts greatly from the caudal fin tissue from the same fish. In addition to the differences in cell-types, this may be explained, in part, by the different modes of exposure: the caudal fin is directly exposed, and the liver is exposed through internal processing of LSMD WAF contaminants. Despite their differences, both demonstrate activation of the AhR-mediated pathway. This is apparent through enrichment of xenobiotic metabolism[52] and Wnt/β-catenin signaling[156] in the liver. This presents a clear risk to these juvenile coho as chronic activation of this pathways has been shown to exhibit cancer-promoting activity.[52]

4.3.3. HSFO WAF Exposure

4.3.3.1. Comparing DEGs with HSFO WAF exposure

Given the greater response of the *cyp1a1* gene to all HSFO WAF exposures, we anticipated that the HSFO WAF would also induce a greater overall transcriptomic response compared to the LSMD WAF with equivalent volumes of oil. Indeed, we observed the most DEGs in the liver, with 11,864 DEGs in females and 7,229 DEGs in males (**Table 4.1**). There

were also many DEGs in the caudal fin with HSFO WAF exposure with 9,572 and 3,401 DEGs in females and males, respectively.

HSFO WAF resulted in 23- and 84-fold more DEGS in the female and male liver, respectively, compared to LSMD WAF exposure with a 20- and four-fold increase in the female and male caudal fin, respectively. Compared to LSMD WAF (**Figure 4.2**), HSFO WAF resulted in substantially more overlap in differential expression (**Figure 4.4 b**). Across the four data sets (two tissues and two sexes), 19,261 unique DEGs are represented with 46 percent being commonly differentially expressed in more than one tissue set and 312 genes in all four data sets. These 312 genes represent a mixture of biological processes, featuring mostly xenobiotic metabolism, oxidative stress response, and morphogenesis (**Appendix 21**). Despite this larger overlap in differential expression, the response profiles to HSFO WAF in each tissue set is still distinct, as with the LMSD WAF exposures (**Figure 4.2 a, Figure 4.4 a**). Like in the LSMD WAF-exposed fish, this overlap in differential expression between males and females in the liver and caudal fin was also significant, although only 1.6-fold ($p < 6.6e\text{-}183$) and 1.8-fold ($p < 6.6e\text{-}183$) greater overlap, respectively, than what is randomly expected using the hypergeometric test. For this reason, males and females were analyzed separately.

In both tissues, HSFO WAF exposure resulted in fewer DEGs in genetic males than females. To our knowledge, this sex-based differential responsiveness is not captured in the literature and should be kept into consideration when performing transcriptomic analyses.

.

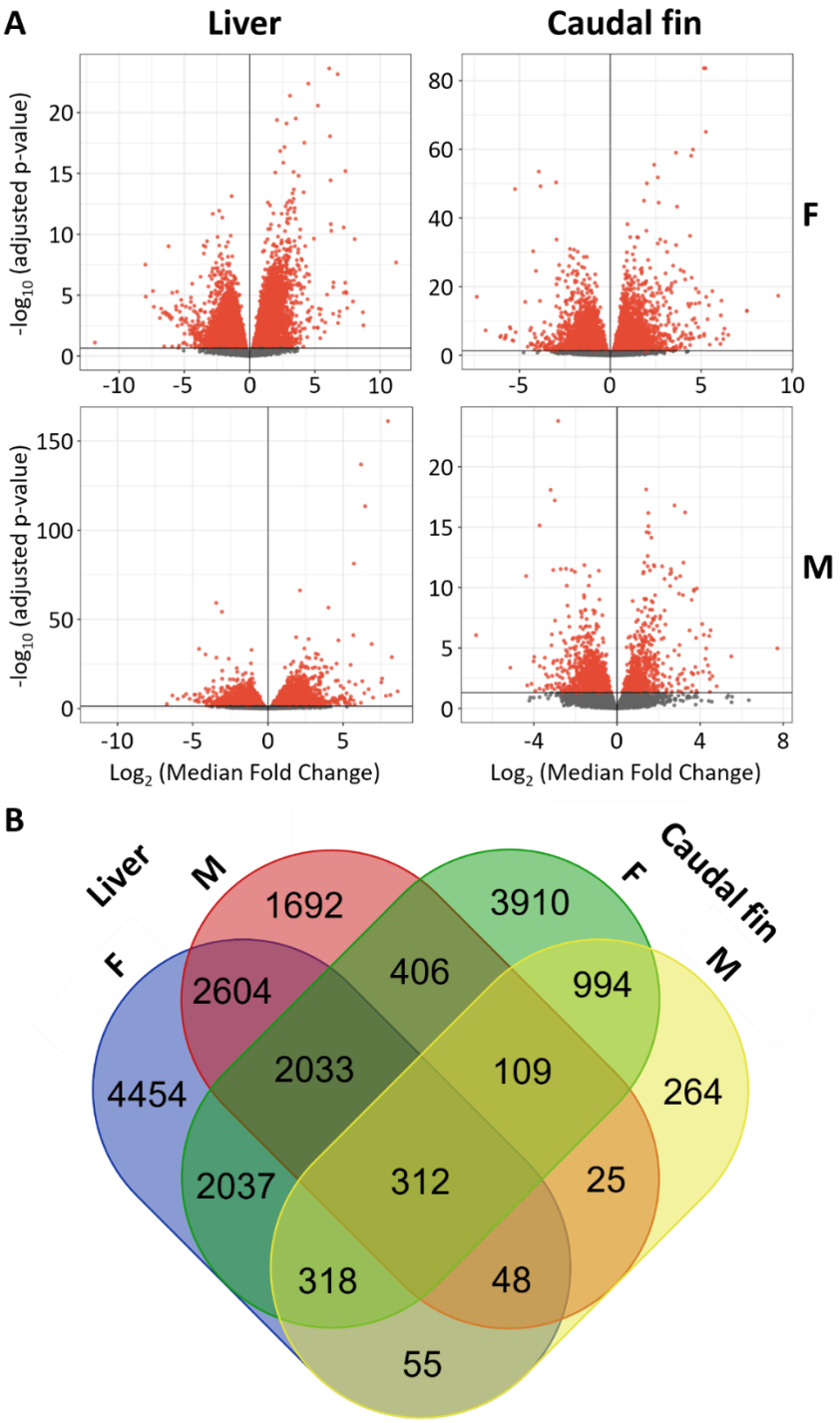

Figure 4.4. Compared to LSMD WAF exposure, HSFO WAFs prepared at the same concentration result in a much greater transcriptome-wide response in coho salmon caudal fin and liver that is similarly sex- and tissue-specific. A. Volcano plots depicting the differential expression of sequenced RNA transcripts from the caudal fin or liver of 10 male or 10 female salmon exposed to either seawater control or high concentration HSFO WAF are shown. B. Venn-diagram demonstrating the overlap of differentially expressed genes ($p_{adj} < 0.05$) because of high-concentration HSFO WAF exposure. See **Figure 4.2** legend for more details.

4.3.3.2. GO term enrichment analysis with HSFO WAF exposure

In the liver, HSFO WAF exposures enriched 233 and 337 GO terms in females and males, respectively (**Table 4.1**). In the caudal fin, 196 GO terms were enriched in females and 514 in males. Comparing GO term enrichment in both the caudal fin and liver, the largest clusters of commonly enriched GO terms are related to MHC processing, protein degradation, transmembrane transport, and mRNA splicing (**Figure 4.5**). In the liver, HSFO WAF also resulted in a significant cluster of enriched GO terms involving ATP (females) and pyrimidine-containing compound (males) metabolism. HSFO WAF also significantly affected NADH dehydrogenase complex activity in the female liver and complement activation in the male liver (**Appendix 22**). HSFO WAF exposure in the female caudal fin resulted in similar GO term enrichment as the liver, (**Figure 4.5**) but also resulted in the additional enrichment of clusters related to tRNA aminoacylation and morphogenesis (**Appendix 22**). GO terms enriched in the male caudal fin are not abundantly represented in the five largest clusters featured, however, common enrichment of morphogenesis and cell adhesion with the female caudal fin is still seen.

HSFO WAF exposure resulted in increased indicators of disease states including cancerous cells[52] with modulation of nucleotide metabolism and enrichment of cell proliferation in the liver indicating the potential for DNA adduct formation.[55] Changes to alternative splicing has also been linked to disease states[157,158] suggesting further potential health impact on these juvenile salmon.

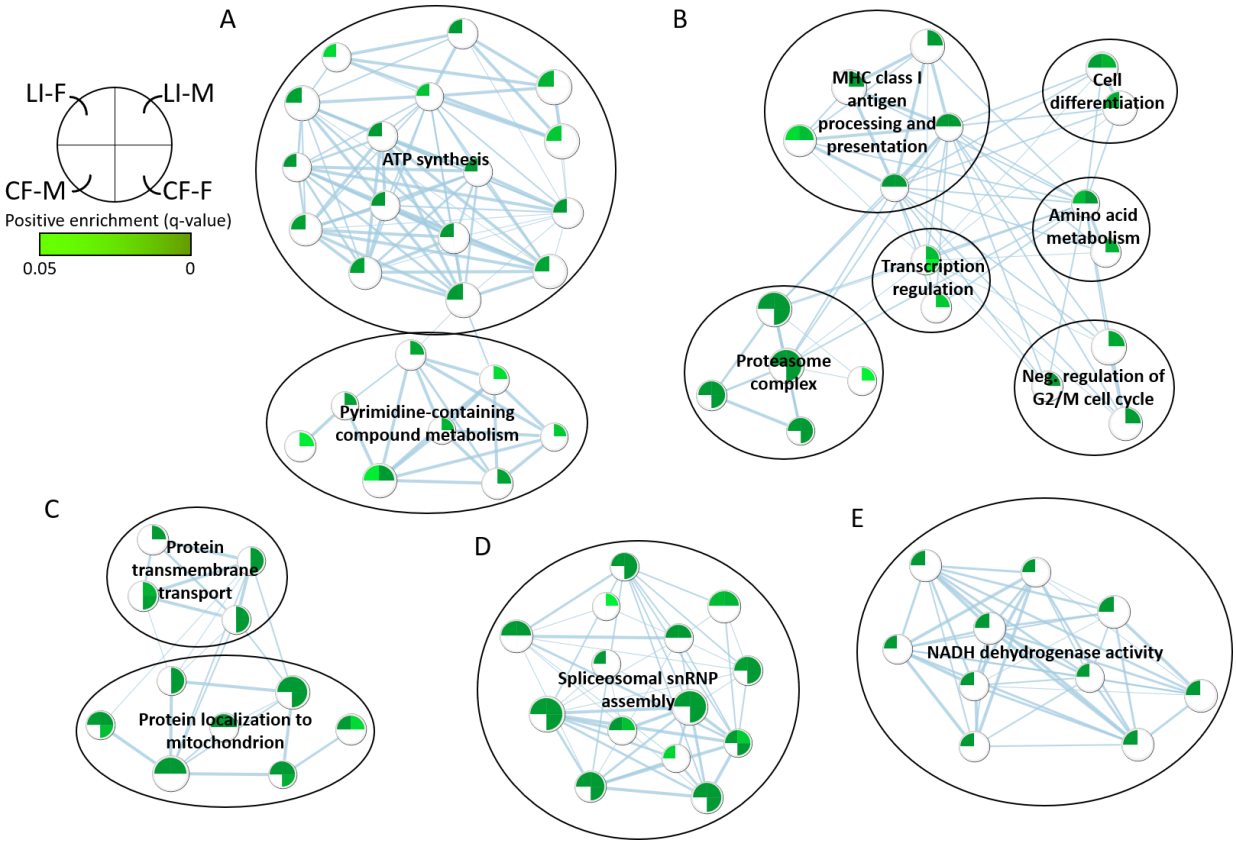

Figure 4.5. HSFO WAF exposure results in the enrichment of GO term clusters primarily associated with these functions: A. Nucleotide-containing compound metabolism; B. MHC class I processing and proteasome complex; C. Transmembrane protein transportation; D. mRNA Splicing; E. NADH dehydrogenase Complex. See **Figure 4.3** legend for more details.

4.3.4. Comparison between LSMD and HSFO WAF exposure responses of coho salmon smolts

The RNA-Seq data presented up until this point was generated using gene counts, merging the total counts of all transcript isoforms under a given gene. This is appropriate for GO term-based analyses but does not capture the data inherent in individual isoforms.[159] As one of the goals of the present study is to identify transcript-specific bioindicator candidates for high throughput qPCR methods, it is important to also examine differential expression at the level of individual transcript isoform counts.

In the liver, nine differentially expressed transcripts (DETs) respond to both LSMD and HSFO WAF regardless of sex (**Figure 4.6 a**), with most transcripts encoding proteins involved

in xenobiotic metabolism and cellular redox (**Table 4.2**). Of these transcripts, the most promising candidates were selected based on fold-change and statistical significance of differential expression encode for CYP1 proteins.

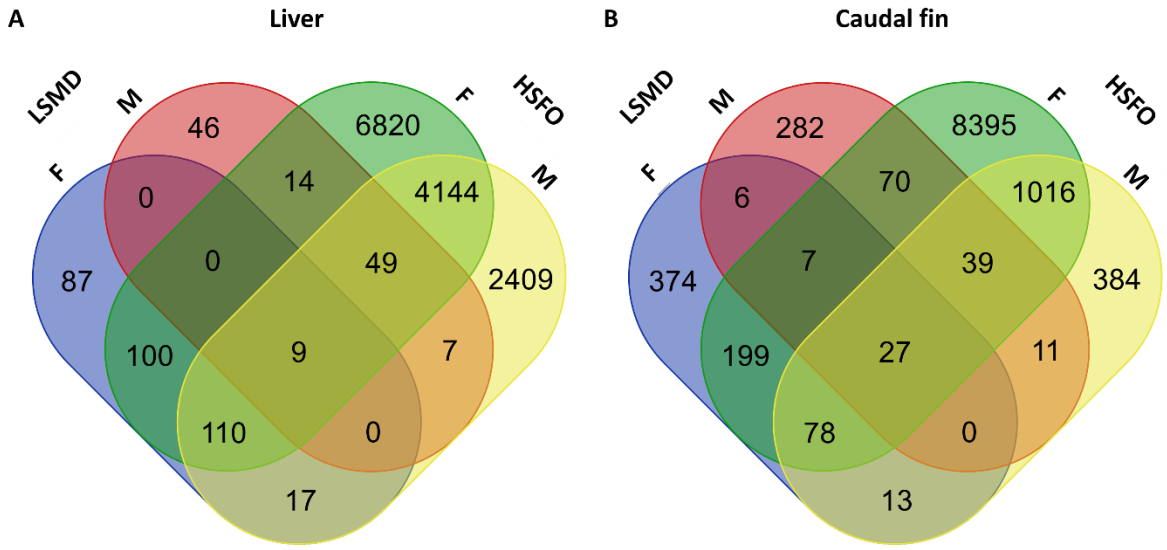

Figure 4.6. Venn-diagrams comparing the overlap of DETs between LSMD and HSFO WAF exposures in (A) liver and (B) caudal fin. There are 27 transcripts in the caudal fin and only nine in the liver that are consistently differentially expressed upon exposure to both LSMD and HSFO WAF in both sexes. See **Figure 4.2** legend for more details.

The *cyp1* family, specifically *cyp1a1*, are important first responders of the AhR-mediated pathway and the most used indicators of oil and PAH exposure in the liver.[52] These genes encode cytochrome P450 enzymes involved initiate the metabolism of fused ring structures, such as PAHs, through formation of highly reactive epoxides.[151] Although the role of sex-bias is occasionally mentioned, often bioindicator evaluation does not take sex into consideration.[28,29] The present work indicates that hepatic *cyp1* family response to WAF exposure in juvenile coho is robust regardless of sex. Moreover, this extends to *cyp1* family expression in the caudal fin, which maintains that robustness across sex.

Table 4.2. List of nine transcripts that are differentially expressed in the liver in response to both LSMD and HSFO exposure regardless of sex. Annotations are based on Blastn results of each transcript against NCBI's nucleotide (nt) database. Fold-change (FC) and adjusted p-value (p_{adj}) are displayed for each transcript.

Annotation	ContigID	LI-F				LI-M			
		LSMD		HSFO		LSMD		HSFO	
		FC	p_{adj}	FC	p_{adj}	FC	p_{adj}	FC	p_{adj}
Cytochrome P450 1A1	rna15507	6	4.55E-14	69	6.46E-32	10	3.79E-14	84	7.45E-115
	rna6745	6	2.04E-10	61	7.12E-44	8	1.79E-15	69	7.10E-153
Cytochrome P450 1B1	gene18523	14	4.98E-08	81	5.61E-40	5	5.95E-03	49	7.83E-88
Glutathione S-transferase P	rna37359	3	1.02E-03	13	3.14E-23	3	5.23E-04	7	6.31E-09
Heat shock protein HSP 90-alpha	rna23625	11	2.63E-02	97	6.01E-17	6	2.76E-02	23	4.10E-10
Metallothionein B	rna40663	3	3.40E-02	17	5.79E-31	3	2.02E-02	9	2.45E-12
Thioredoxin reductase 1	rna726	3	1.62E-02	6	3.67E-35	2	5.15E-03	4	5.95E-14
UDP-glucuronosyltransferase	gene36783	2	2.08E-02	7	1.49E-23	2	1.73E-02	12	2.76E-18
	rna64043	1	4.96E-02	7	2.55E-18	2	3.15E-02	11	6.34E-14

Compared to the liver, the caudal fin exhibits three-fold more DETs that respond to both exposures regardless of sex (**Figure 4.6 b**), featuring transcripts primarily associated with xenobiotic metabolism, cell redox, and morphogenesis. In addition to these, three consistently differentially expressed transcripts are currently uncharacterized in the coho salmon genome, highlighting the limitation the limitation of BLASTn/BLASTx annotation methods standard for RNA-Seq methods. In the caudal fin, transcripts encoding CYP1B appeared to more consistently respond than CYP1A-encoding transcripts (**Table 4.3**). CYP1A and CYP1B are closely related P450 subfamilies exhibiting unique metabolic capabilities.[54] Unlike CYP1A1, CYP1B1 can metabolize aromatic amines[54] and shows enhanced metabolic activation of some PAHs, such as BAP in humans,[160] and dibenzofulvene (DBF) in zebrafish.[54] Although neither of those PAHs

are significantly represented in either WAF, the enrichment CYP1Bs seen may indicate the presence of other CYP1B-specific metabolites in these WAF exposures.

Table 4.3. Table of 27 transcripts that are differentially expressed in the caudal fin in response to both LSMD and HSFO exposure regardless of sex. See **Table 4.2** legend for more information.

		CF-F				CF-M			
		LSMD		HSFO		LSMD		HSFO	
Transcript Annotation (Blastn)	**ContigID**	**FC**	**p_{adj}**	**FC**	**p_{adj}**	**FC**	**p_{adj}**	**FC**	**p_{adj}**
Aryl hydrocarbon receptor repressor	rna47187	3	7.81E-09	11	4.13E-24	3	1.40E-04	10	2.73E-13
Cadherin-13	rna33088	-2	2.64E-11	-8	4.41E-52	-3	3.28E-11	-8	3.64E-09
Coiled-coil domain-containing protein 80	rna60329	1	1.66E-02	2	2.78E-16	1	1.87E-02	2	2.96E-07
Cytochrome P450 1B1	gene18523	4	4.97E-07	10	1.04E-17	6	1.05E-14	9	9.83E-08
	rna64606	5	1.46E-09	9	2.33E-22	6	2.48E-09	14	2.88E-07
Cytochrome P450 1B1a	gene18522	4	5.59E-08	8	5.97E-17	7	3.23E-05	10	2.29E-08
Cytochrome P450 1B1 pseudogene	rna15010	3	6.16E-13	17	2.79E-19	3	7.69E-09	11	6.92E-10
	rna15011	4	4.25E-17	38	1.72E-78	7	1.19E-08	58	1.68E-08
Cytosolic sulfotransferase 2	rna44151	8	1.81E-27	46	9.49E-14	6	3.34E-07	45	3.45E-04
Dickkopf-related protein 1	rna8841	-2	1.76E-02	-4	1.70E-23	-2	4.20E-29	-5	2.21E-06
Ectonucleoside triphosphate diphosphohydrolase 5	rna28258	2	2.46E-05	10	6.50E-32	3	6.32E-08	8	1.50E-14
Fibroblast growth factor 7	rna58523	11	7.02E-37	23	1.65E-31	8	3.28E-11	29	9.42E-05
	rna58531	9	1.55E-21	22	1.07E-53	8	3.06E-08	33	7.98E-04
Keratin, type I cytoskeletal 13-like	rna252	-2	3.88E-02	-3	1.39E-07	-2	3.69E-02	-5	9.86E-04
Mitogen-activated protein kinase 14A	rna9745	-1	6.08E-03	-2	1.81E-05	-2	2.01E-02	-2	9.94E-09
Netrin-4	rna10181	2	2.18E-03	7	4.37E-19	2	8.55E-06	8	1.86E-09
NOTUM, palmitoleoyl-protein carboxylesterase	rna60321	2	5.40E-03	4	8.91E-14	1	3.26E-02	4	2.29E-08
Protein sprouty homolog 1	rna44914	2	2.09E-04	1	9.80E-03	2	1.18E-02	3	2.75E-02
Protocadherin-16	rna30259	2	1.13E-05	4	5.34E-15	2	1.60E-02	3	2.89E-08
R-spondin-1	rna3139	2	2.43E-03	3	3.40E-08	2	1.56E-02	3	4.96E-03
UDP-glucuronosyltransferase	gene36783	3	1.18E-06	46	1.65E-76	4	5.09E-07	43	9.35E-07
	rna45831	3	6.84E-05	48	3.35E-09	5	4.04E-03	52	3.11E-05
	rna63216	3	5.48E-08	47	1.04E-58	4	7.62E-08	37	4.68E-08
	rna64043	2	4.13E-02	26	1.63E-56	3	4.61E-04	25	5.29E-07
Uncharacterized LOC109867258	rna40575	1	4.48E-02	2	2.26E-03	2	1.73E-04	2	5.85E-04
Uncharacterized LOC109884259	rna61047	-2	4.90E-05	-4	2.85E-11	1	4.91E-05	-3	1.54E-04
Uncharacterized LOC109899381	rna21192	2	1.09E-02	4	1.41E-28	2	1.23E-04	6	1.36E-08

There is also a distinct lack of *cyp1a1* DETs in the caudal fin, despite the transcript demonstrating significant differential expression in response to all LSMD and HSFO WAFs in chapter 2. In fact, RNA-Seq detected significant *cyp1a1* differential expression in most caudal fin tissues except for the male caudal fin after HSFO WAF exposure. Although a large fold-change in *cyp1a1* transcript abundance is observed in the male caudal fin with HSFO WAF exposure, in all *cyp1a1* transcripts quantified, excessive variation between replicates as determined by the DESeq2 R-package. This lack of significant differential expression observed in the RNA-Seq is overcome in the qPCR data sets of Chapter 2 of this thesis, as statistical significance of the qPCR results is evaluated across 40 individual biological replicates as opposed to five in the RNA-Seq data. This increase in biological replicates allows for an increased robustness of statistical evaluations to mitigate factors such as variation between biological replicates, as seen with the RNA-Seq data, for detecting significant differences.

Several transcripts encoding UDP-glucuronosyltransferases (UGT) were also consistently differentially expressed in the caudal fin (**Table 4.3**). Previous work reported increases in *ugt* transcript abundance in the gills[161] and liver[162] of Gulf killifish upon oil spill exposure. UGTs are also regulated by AhR and important during phase 2 PAH metabolism, involving the glucuronidation of dihydrodiols and phenols, inhibiting secondary oxidation and the generation of more mutagenic metabolites.[163] This may have implications in salmon farming, as UGTs are widely known for their inactivation of drug therapies[164] and may decrease the effectiveness of some antibiotics.[165]

Although no LSMD WAF-specific DETs were identified in the liver, there were 4,144 transcripts that were uniquely differentially expressed compared to LSMD upon HSFO WAF exposure regardless of sex (**Table 4.4, remaining DETs not shown**). The lack of LSMD-

specific DETs in the liver is likely attributed to the relatively modest-response compared to HSFO WAF exposure. Despite this, six DETs were able to differentiate LSMD WAF exposure in the caudal fin (**Table 4.5**), and 1,016 DETs only responsive to HSFO WAF (**Table 4.6, remaining DETs not shown**). The majority of LSMD WAF-specific DETs are related to wnt/β-catenin signaling, and HSFO WAF-specific DETs encompass a wide range of functions such as xenobiotic metabolism, inflammatory/immune response, oxidative stress, and wnt/β-catenin signaling.

Table 4.4. Top 21 of 4,144 DETs in the liver that were uniquely DE with HSFO but not LSMD. Transcripts exhibit a minimum nine-fold change in transcript abundance, and $p_{adj} < 0.0000005$. Fold-change (FC) and adjusted p-value (p_{adj}) are displayed for each transcript. Annotations are based on Blastn results against NCBI's nt database with Accesion number, percent identity (%id) of the query sequence to the result, and the annotated name represented.

ContigID	LI-F		LI-M		Accession number	%id	Blastn Annotation
	FC	p_{adj}	FC	p_{adj}			
COHO.359.1	167	2.43E-08	109	8.43E-23	XM024139013.1	100	PREDICTED: Salvelinus alpinus thioredoxin-like (LOC112071572), mRNA
gene36776	16	8.23E-10	14	1.1E-19	XM014198687.1	95.5	PREDICTED: Salmo salar heat shock 70 kDa protein 4-like (LOC106604228), transcript variant X2, mRNA
rna10576	23	4.43E-09	44	1.75E-13	XM020483514.1	100	PREDICTED: Oncorhynchus kisutch glutathione peroxidase 2-like (LOC109891177), mRNA
rna13707	10	0.000000222	12	8.78E-09	XM020484419.1	100	PREDICTED: Oncorhynchus kisutch ribonucleoprotein PTB-binding 1-like (LOC109891977), mRNA
rna15010	201	1.2E-15	327	5.52E-223	XM002255881.1	100	PREDICTED: Oncorhynchus kisutch cytochrome P450 1B1 pseudogene (LOC109894532), misc RNA
rna20195	17	5.11E-14	12	4.82E-08	XM020493404.1	100	PREDICTED: Oncorhynchus kisutch coiled-coil domain-containing protein 43-like (LOC109898436), mRNA
rna22496	9	1.8E-17	9	1.13E-28	XM020495671.1	100	PREDICTED: Oncorhynchus kisutch desumoylating isopeptidase 1-like (LOC109899982), transcript variant X1, mRNA
rna26406	14	7.39E-16	10	2.14E-10	XM020499414.1	100	PREDICTED: Oncorhynchus kisutch proteasome subunit alpha type-7-like (LOC109902778), mRNA
rna28459	9	1.65E-10	10	1.03E-18	XM020501343.1	100	PREDICTED: Oncorhynchus kisutch ornithine decarboxylase 1-like (LOC109904160), mRNA
rna31136	30	2.66E-12	31	1.04E-14	XM020504111.1	100	PREDICTED: Oncorhynchus kisutch thioredoxin-like (LOC109906425), mRNA
rna3178	13	8.2E-12	9	1.15E-10	XM020452010.1	100	PREDICTED: Oncorhynchus kisutch yrdC domain-containing protein, mitochondrial-like (LOC109864299), mRNA
rna37531	11	7.53E-31	9	4.84E-12	XM020509379.1	100	PREDICTED: Oncorhynchus kisutch thiosulfate sulfurtransferase/rhodanese-like domain-containing protein 1 (LOC109910248), mRNA
rna38099	19	5.81E-13	11	2.53E-23	XM020453546.1	100	PREDICTED: Oncorhynchus kisutch 26S proteasome non-ATPase regulatory subunit 11B-like (LOC109865405), mRNA
rna41335	9	9.77E-19	10	1.02E-12	XM020457151.1	100	PREDICTED: Oncorhynchus kisutch caveolin-2-like (LOC109867831), mRNA
rna41719	16	1.75E-17	9	1.52E-09	XM020457936.1	100	PREDICTED: Oncorhynchus kisutch proteasome subunit beta type-7-like (LOC109868402), transcript variant X1, mRNA
rna41720	9	6.81E-12	9	6.14E-09	XM020457937.1	100	PREDICTED: Oncorhynchus kisutch proteasome subunit beta type-7-like (LOC109868402), transcript variant X2, mRNA
rna58993	19	1.2E-43	13	5.3E-17	XM020474289.1	100	PREDICTED: Oncorhynchus kisutch glutamate--cysteine ligase regulatory subunit-like (LOC109882206), mRNA
rna59191	15	6.72E-19	9	0.000000135	XM020474484.1	100	PREDICTED: Oncorhynchus kisutch proteasome maturation protein-like (LOC109882385), mRNA
rna64606	16	9.14E-17	25	3.05E-47	XM020479494.1	100	PREDICTED: Oncorhynchus kisutch cytochrome P450 1B1-like (LOC109888318), mRNA
rna8192	18	1.72E-10	20	6.56E-11	XM020481255.1	100	PREDICTED: Oncorhynchus kisutch vesicle transport protein GOT1B (LOC109889666), mRNA
rna8480	41	5.96E-38	75	3.78E-33	XM020481515.1	100	PREDICTED: Oncorhynchus kisutch cytochrome P450 1B1-like (LOC109889798), transcript variant X1, mRNA

Table 4.5. Six transcripts in the caudal fin that were uniquely DE with LSMD but not HSFO. FC and adjusted p-value (p_{adj}) are displayed for each transcript. For more details, see **Table 4.4** legend.

ContigID	CF-F		CF-M		Accession number	%id	Blastn Annotation
	FC	p_{adj}	FC	p_{adj}			
COHO.10317.1	4	2.33E-02	3	1.34E-02	EU621899.1	86.6	Salmo salar clone 63I10 growth hormone 2 gene, complete cds; and skeletal muscle sodium channel alpha subunit-like, myosin alkali light chain-like, and microtubule-associated protein Tau-like genes, complete sequence
rna3183	-2	4.17E-02	-2	1.90E-02	XM020509397.1	100	PREDICTED: Oncorhynchus kisutch thymocyte selection associated family member 2 (themis2), mRNA
rna3217	-2	1.59E-02	-2	1.06E-02	XM020509449.1	99.9	PREDICTED: Oncorhynchus kisutch T-cell surface glycoprotein CD4-like (LOC109910298), mRNA
rna45908	1	4.27E-02	1	2.94E-04	XM020462252.1	100	PREDICTED: Oncorhynchus kisutch protein Wnt-10a (LOC109871395), mRNA
rna48015	-8	1.54E-04	-8	9.57E-03	XM020463655.1	100	PREDICTED: Oncorhynchus kisutch heterogeneous nuclear ribonucleoprotein A/B-like (LOC109872444), transcript variant X1, mRNA
rna6672	2	1.64E-03	2	3.98E-02	XM020479600.1	100	PREDICTED: Oncorhynchus kisutch kinesin family member 18A (kif18a), transcript variant X1, mRNA

Herein, we have identified that both LSMD and HSFO WAF exposure in cold-water marine conditions result in effects primarily driven by induction of the AhR-mediated pathway, with a greater response to HSFO WAF exposure. We also demonstrated that this tissue-specific response in juvenile coho salmon is heavily influenced by sex, which is often overlooked in the evaluation of oil spill effects. Despite this, the caudal fin readily and more consistently elicited a transcriptomic response across genetic sexes and yielded both specific and generic oil WAF bioindicator candidates. This improved consistency in addition to that ability to be sampled non-lethally further attests to the use of the caudal fin transcriptome as a means for tracking oil spill exposure and remediation effectiveness.

Table 4.6. Top 20 of 1,016 differentially expressed transcripts in the caudal fin that were uniquely DE with HSFO but not LSMD. Criteria for selecting these transcripts required a minimum of four-fold increase or decrease in transcript abundance, and $p_{adj} < 0.0000005$. For more details, See **Table 4.4** legend.

ContigID	CF-F		CF-M		Accession number	%id	Blastn Annotation
	FC	p_{adj}	FC	p_{adj}			
COHO.5388.1	7	7.12E-26	7	2.70E-10	XM020483996.1	100	PREDICTED: Oncorhynchus kisutch APC down-regulated 1 like (apcdd1l), mRNA
rna11161	8	5.42E-15	8	1.31E-08	XM020483996.1	100	PREDICTED: Oncorhynchus kisutch APC down-regulated 1 like (apcdd1l), mRNA
rna13199	-5	1.01E-07	-5	1.36E-09	XM020486311.1	100	PREDICTED: Oncorhynchus kisutch complement C1q tumor necrosis factor-related protein 1-like (LOC109893204), mRNA
rna15554	4	5.28E-22	4	2.94E-12	XM020488970.1	100	PREDICTED: Oncorhynchus kisutch plakophilin-3-like (LOC109895343), transcript variant X1, mRNA
rna19410	9	1.68E-28	9	8.17E-09	XM020492757.1	100	PREDICTED: Oncorhynchus kisutch ras-like protein family member 11B (LOC109898022), mRNA
rna19713	9	1.04E-14	9	1.57E-07	XM020493004.1	100	PREDICTED: Oncorhynchus kisutch beta-1,3-galactosyltransferase 2-like (LOC109898164), mRNA
rna20750	-6	1.07E-28	-6	1.44E-15	XM020493844.1	100	PREDICTED: Oncorhynchus kisutch transcription factor Sox-9-B-like (LOC109898744), transcript variant X2, mRNA
rna20751	-5	1.36E-08	-5	1.06E-08	XM020493843.1	100	PREDICTED: Oncorhynchus kisutch transcription factor Sox-9-B-like (LOC109898744), transcript variant X1, mRNA
rna24108	51	5.61E-15	51	1.92E-07	XM020497206.1	100	PREDICTED: Oncorhynchus kisutch complexin-1-like (LOC109901159), mRNA
rna250	-8	1.75E-15	-8	3.50E-07	XR002255233.1	100	PREDICTED: Oncorhynchus kisutch keratin, type I cytoskeletal 13-like (LOC109889145), misc RNA
rna25658	-4	7.14E-39	-4	4.77E-14	XM020498796.1	100	PREDICTED: Oncorhynchus kisutch C-C motif chemokine 25-like (LOC109902446), transcript variant X1, mRNA
rna33419	-6	1.02E-23	-6	9.06E-10	XM020506266.1	100	PREDICTED: Oncorhynchus kisutch WAP four-disulfide core domain protein 3-like (LOC109907951), mRNA
rna3348	6	6.31E-22	6	9.87E-11	XM020453112.1	100	PREDICTED: Oncorhynchus kisutch discoidin, CUB and LCCL domain-containing protein 1-like (LOC109864994), transcript variant X2, mRNA
rna35861	-4	2.29E-08	-4	2.81E-10	XM020508492.1	100	PREDICTED: Oncorhynchus kisutch homeobox protein BarH-like 2 (LOC109909455), mRNA
rna37528	5	1.34E-07	5	2.45E-10	XM020453046.1	100	PREDICTED: Oncorhynchus kisutch coagulation factor VIII-like (LOC109864950), mRNA
rna38007	-7	1.05E-32	-7	1.19E-15	XM020454039.1	100	PREDICTED: Oncorhynchus kisutch transcription factor Sox-9-B-like (LOC109865673), mRNA
rna39379	4	2.67E-60	4	2.83E-07	XM020455592.1	100	PREDICTED: Oncorhynchus kisutch DBH-like monooxygenase protein 1 homolog (LOC109866755), mRNA
rna49532	12	1.15E-58	12	1.61E-09	XM020466304.1	100	PREDICTED: Oncorhynchus kisutch prostaglandin E synthase-like (LOC109874417), mRNA
rna51521	8	4.00E-09	8	4.05E-07	XM020466731.1	100	PREDICTED: Oncorhynchus kisutch aryl hydrocarbon receptor repressor-like (LOC109874706), mRNA
rna6305	5	9.46E-13	5	6.24E-11	XM020477980.1	100	PREDICTED: Oncorhynchus kisutch neuropilin and tolloid-like protein 2 (LOC109886256), mRNA

5. Overall conclusions and future directions

5.1. Conclusions

The first objective of this thesis was to evaluate the use of the caudal fin transcriptome as a bioindicator of oil spill exposure. Indeed, the caudal fin demonstrated a significant response in *cyp1a1* transcript abundance to WAFs generated from all four oil types tested. In contrast, hepatic *cyp1a1* only significantly responded to WAFs from three out of four oil types tested. Not only did the present thesis work demonstrate that the caudal fin transcriptome can detect significant biological response to oil spill exposure, but that the caudal fin exhibited increased sensitivity in comparison to the liver. The responsiveness of the caudal fin transcriptome was not limited to a few gene transcripts but rather involved hundreds (LSMD) to thousands (HSFO) of genes. These data also demonstrated that the caudal fin of juvenile smolts exhibited less sex-bias than the liver when comparing the number of overlapping differentially expressed genes and GO term enrichment. This reduction in sex-bias is ideal when trying to establish a fish-sampling-based biomonitoring assay, as it reduces the need to sample a specific sex to deal with high variation. Together, these data validate that transcriptomic sampling of the juvenile coho salmon caudal fin is a viable method for identifying salmon biological response to oil spill exposure, and support using sampling of this tissue as a non-lethal alternative to liver sampling.

The second objective of this thesis was to evaluate potential sublethal deleterious effects resulting from four oil types in juvenile salmon under cold marine conditions. The WAFs generated from these oil types demonstrated unique PAH profiles when using equivalent volumes of oil that varied widely in tPAH50 concentrations and individual PAH composition. Significant biological response was detected in the salmon smolt to WAFs generated with as little as 100 mg/L dilbit, LSMD, or HSFO, and 1000 mg/L Alaskan crude oil. All WAF

exposures also elicited significant differences between male and female responses, demonstrating that sex-bias to WAF exposure occurs even at this juvenile stage. In general, dilbit, LSMD, and HSFO WAF exposures resulted in a proportional elevation in liver and caudal fin *cyp1a1* transcript abundance response in salmon with increasing PAH concentrations. However, Alaskan crude WAF, which contained the second highest PAH concentrations of WAFs tested, induced a significant salmon biological response only at the highest concentration WAF exposure that was weaker in comparison to other WAFs. These results contrast a dose-dependent response relationship between *cyp1a1* transcript abundance and PAH concentration and suggests that better transcript bioindicators of PAH exposure are required in these juvenile salmon.

A further probe into the overall transcriptomic response using RNA-Seq demonstrated a complex network of differentially expressed genes due to LSMD and HSFO WAF exposure that was sex- and tissue-specific. Combining the effects observed in the liver and caudal fin, LSMD WAF exposure resulted in the significant enrichment of immune system-, oxidative stress-, and cell proliferation/morphogenesis-related GO terms highlighting a potential for altered immune function in smolts upon LSMD WAF exposure and a risk for chondrodysplasias development. While many of the genes and GO categories overlapped between HSFO WAF and LSMD WAF exposures, it is notable that HSFO WAF exposed smolts exhibited a stronger response in the number and fold-change relative to controls. HSFO WAF-induced differential gene expression suggested potential for the development of disease states associated with cancer and altered mRNA splicing. Overall, this present work has identified that although tPAH50 WAF concentrations are usually proportional to induced salmon-response, this is not always true, and

suggests the need to extend WAF characterization to the measurement of other known toxicants present in oil WAFs like NAs.

The third objective of this thesis was the identification of novel transcript bioindicators of oil spill exposure in both the liver and caudal fin of juvenile coho smolts. The need for this third objective is clearly demonstrated in the evaluation of WAF exposure, as the classically used *cyp1a1* bioindicator was insufficient to demonstrate biological response proportional to PAH concentrations measured in these WAFs. Herein, several novel transcript bioindicator candidates were identified in both the liver and caudal fin to be significantly responsive to exposure to both nearshore LSMD and far-shore HSFO WAF exposures, regardless of sex. In addition to identifying bioindicator candidates that were commonly differentially expressed in both exposures, bioindicators that differentiate between LSMD or HSFO WAF exposures were also identified in the caudal fin but were conspicuously absent in the liver. This host of bioindicator candidate tools identified are a significant finding for more effectively monitoring oil spill exposure in cold water marine environments.

5.2. Future directions

The novel transcript bioindicators identified herein will act as a foundation for future research involving caudal fin transcriptomics and the investigation of biological effects of cold-water marine oil spills in juvenile salmon smolts.

The present work identified thousands of bioindicator candidates that may be used to demonstrate oil spill exposure independent of sex. However, all bioindicators may not be needed to characterize a response. Further work should focus on evaluating the degree of specificity or universality of transcript bioindicators in identifying oil WAF exposure. For example, *cyp1b1* and *ugt1* transcripts may be suitable cross-tissue indicators of general oil WAF exposures while a

selection of other transcripts may be able to reliably differentiate between oil WAF exposure types. Expression of these transcripts should be further queried against LSMD, HSFO, dilbit, and Alaskan crude WAF exposures at multiple concentrations.

The transcriptomic responses presented here represent a single snapshot of the state of differential expression captured at the end of a 96-h exposure. Toxicokinetic studies are also important to map the transcriptomic response to acute WAF exposure over time to evaluate the consistency of salmon transcriptomic response and identify key time points of exposure, such as the earliest point at which biological response can be measured. In addition to these studies, evaluation of salmon depuration after oil WAF exposure is critical to establish the time required for liver and caudal fin transcriptome to recover. This is very important in establishing bioindicator assays, as biological response should reflect exposure within a defined timeframe of sentinel animal sampling.[166] Currently, the examination of the depuration of juvenile coho smolt liver and caudal fin following 96 h LSMD WAF exposure is ongoing.

Finally, the caudal fin response should be further evaluated in adult salmon and in other fishes significantly impacted by oil spill exposure, such as Pacific herring[167] and bluefin tuna.[168] This will broaden the caudal fin's scope of application and further support conservation efforts.

Bibliography

(1) Li, P.; Cai, Q.; Lin, W.; Chen, B.; Zhang, B. Offshore Oil Spill Response Practices and Emerging Challenges. *Marr Pollut Bull* **2016**, *110* (1), 6–27. https://doi.org/10.1016/j.marpolbul.2016.06.020.

(2) Murphy, D.; Gemmell, B.; Vaccari, L.; Li, C.; Bacosa, H.; Evans, M.; Gemmell, C.; Harvey, T.; Jalali, M.; Niepa, T. H. R. An In-Depth Survey of the Oil Spill Literature since 1968: Long Term Trends and Changes since Deepwater Horizon. *Marr Pollut Bull* **2016**, *113* (1), 371–379. https://doi.org/10.1016/j.marpolbul.2016.10.028.

(3) Silliman, B. R.; Koppel, J. van de; McCoy, M. W.; Diller, J.; Kasozi, G. N.; Earl, K.; Adams, P. N.; Zimmerman, A. R. Degradation and Resilience in Louisiana Salt Marshes after the BP–Deepwater Horizon Oil Spill. *Proc Natl Acad Sci USA* **2012**, *109* (28), 11234–11239. https://doi.org/10.1073/pnas.1204922109.

(4) Brakstad, O. G.; Davies, E. J.; Ribicic, D.; Winkler, A.; Brönner, U.; Netzer, R. Biodegradation of Dispersed Oil in Natural Seawaters from Western Greenland and a Norwegian Fjord. *Polar Biol* **2018**, *41* (12), 2435–2450. https://doi.org/10.1007/s00300-018-2380-8.

(5) Vrabie, C. M.; Candido, A.; Duursen, M. B. M. van; Jonker, M. T. O. Specific in Vitro Toxicity of Crude and Refined Petroleum Products: II. Estrogen (α and β) and Androgen Receptor-Mediated Responses in Yeast Assays. *Envirol Toxicol Chem* **2010**, *29* (7), 1529–1536. https://doi.org/10.1002/etc.187.

(6) Vrabie, C. M.; Candido, A.; Berg, H. van den; Murk, A. J.; Duursen, M. B. M. van; Jonker, M. T. O. Specific in Vitro Toxicity of Crude and Refined Petroleum Products: 3. Estrogenic Responses in Mammalian Assays. *Envirol Toxicol Chem* **2010**, *30* (4), 973–980. https://doi.org/10.1002/etc.463.

(7) Kim, S.; Sohn, J. H.; Ha, S. Y.; Kang, H.; Yim, U. H.; Shim, W. J.; Khim, J. S.; Jung, D.; Choi, K. Thyroid Hormone Disruption by Water-Accommodated Fractions of Crude Oil and Sediments Affected by the Hebei Spirit Oil Spill in Zebrafish and GH3 Cells. *Environ Sci Technol* **2016**, *50* (11), 5972–5980. https://doi.org/10.1021/acs.est.6b00751.

(8) Alderman, S. L.; Lin, F.; Gillis, T. E.; Farrell, A. P.; Kennedy, C. J. Developmental and Latent Effects of Diluted Bitumen Exposure on Early Life Stages of Sockeye Salmon (Oncorhynchus Nerka). *Aquat Toxicol* **2018**, *202*, 6–15. https://doi.org/10.1016/j.aquatox.2018.06.014.

(9) Cox, G. K.; Crossley, D. A.; Stieglitz, J. D.; Heuer, R. M.; Benetti, D. D.; Grosell, M. Oil Exposure Impairs In Situ Cardiac Function in Response to β-Adrenergic Stimulation in Cobia (Rachycentron Canadum). *Environ Sci Technol* **2017**, *51* (24), 14390–14396. https://doi.org/10.1021/acs.est.7b03820.

(10) Armstrong, T.; Khursigara, A. J.; Killen, S. S.; Fearnley, H.; Parsons, K. J.; Esbaugh, A. J. Oil Exposure Alters Social Group Cohesion in Fish. *Sci Rep* **2019**, *9*. https://doi.org/10.1038/s41598-019-49994-1.

(11) Ji, H.; Xu, M.; Huang, W.; Yang, K. The Influence of Oil Leaking Rate and Ocean Current Velocity on the Migration and Diffusion of Underwater Oil Spill. *Sci Rep* **2020**, *10*, 9226. https://doi.org/10.1038/s41598-020-66046-1.

(12) Berenshtein, I.; Paris, C. B.; Perlin, N.; Alloy, M. M.; Joye, S. B.; Murawski, S. Invisible Oil beyond the Deepwater Horizon Satellite Footprint. *Sci Adv* **2020**, *6* (7). https://doi.org/10.1126/sciadv.aaw8863.

(13) Macfadyen, A.; Watabayashi, G. Y.; Barker, C. H.; Beegle-Krause, C. J. Tactical Modeling of Surface Oil Transport During the Deepwater Horizon Spill Response. In *Monitoring and Modeling the Deepwater Horizon Oil Spill: A Record-Breaking Enterprise*; American Geophysical Union (AGU), 2011; pp 167–178. https://doi.org/10.1029/2011GM001128.
(14) McKenna, A. M.; Purcell, J. M.; Rodgers, R. P.; Marshall, A. G. Heavy Petroleum Composition. 1. Exhaustive Compositional Analysis of Athabasca Bitumen HVGO Distillates by Fourier Transform Ion Cyclotron Resonance Mass Spectrometry: A Definitive Test of the Boduszynski Model. *Energy Fuels* **2010**, *24* (5), 2929–2938. https://doi.org/10.1021/ef100149n.
(15) McKenna, A. M.; Blakney, G. T.; Xian, F.; Glaser, P. B.; Rodgers, R. P.; Marshall, A. G. Heavy Petroleum Composition. 2. Progression of the Boduszynski Model to the Limit of Distillation by Ultrahigh-Resolution FT-ICR Mass Spectrometry. *Energy Fuels* **2010**, *24* (5), 2939–2946. https://doi.org/10.1021/ef1001502.
(16) Ruberg, E. J.; Elliott, J. E.; Williams, T. D. Review of Petroleum Toxicity and Identifying Common Endpoints for Future Research on Diluted Bitumen Toxicity in Marine Mammals. *Ecotoxicology* **2021**, *30* (4), 537–551. https://doi.org/10.1007/s10646-021-02373-x.
(17) Collier, T. K.; Anulacion, B. F.; Arkoosh, M. R.; Dietrich, J. P.; Incardona, J. P.; Johnson, L. L.; Ylitalo, G. M.; Myers, M. S. 4 - Effects on Fish of Polycyclic Aromatic HydrocarbonS (PAHS) and Naphthenic Acid Exposures. In *Fish Physiology*; Tierney, K. B., Farrell, A. P., Brauner, C. J., Eds.; Organic Chemical Toxicology of Fishes; Academic Press, 2013; Vol. 33, pp 195–255. https://doi.org/10.1016/B978-0-12-398254-4.00004-2.
(18) Stout, S. A.; Wang, Z. 3 - Chemical Fingerprinting Methods and Factors Affecting Petroleum Fingerprints in the Environment. In *Standard Handbook Oil Spill Environmental Forensics (Second Edition)*; Academic Press: Boston, 2016; pp 61–129. https://doi.org/10.1016/B978-0-12-803832-1.00003-9.
(19) Macaya, C. C.; Durán, R. E.; Hernández, L.; Rodríguez-Castro, L.; Barra-Sanhueza, B.; Dorochesi, F.; Seeger, M. Bioremediation of Petroleum. In *Reference Module in Life Sciences*; Elsevier, 2019. https://doi.org/10.1016/B978-0-12-809633-8.20810-8.
(20) Duran, R.; Cravo-Laureau, C. Role of Environmental Factors and Microorganisms in Determining the Fate of Polycyclic Aromatic Hydrocarbons in the Marine Environment. *FEMS Microbiol Rev* **2016**, *40* (6), 814–830. https://doi.org/10.1093/femsre/fuw031.
(21) Wan, Y.; Wang, B.; Khim, J. S.; Hong, S.; Shim, W. J.; Hu, J. Naphthenic Acids in Coastal Sediments after the Hebei Spirit Oil Spill: A Potential Indicator for Oil Contamination. *Environ Sci Technol* **2014**, *48* (7), 4153–4162. https://doi.org/10.1021/es405034y.
(22) Kuhl, A. J.; Nyman, J. A.; Kaller, M. D.; Green, C. C. Dispersant and Salinity Effects on Weathering and Acute Toxicity of South Louisiana Crude Oil. *Environ Toxicol Chem* **2013**, *32* (11), 2611–2620.
(23) Ribicic, D.; McFarlin, K. M.; Netzer, R.; Brakstad, O. G.; Winkler, A.; Throne-Holst, M.; Størseth, T. R. Oil Type and Temperature Dependent Biodegradation Dynamics - Combining Chemical and Microbial Community Data through Multivariate Analysis. *BMC Microbiol* **2018**, *18* (1), 83. https://doi.org/10.1186/s12866-018-1221-9.
(24) Dias, H. P.; Pereira, T. M. C.; Vanini, G.; Dixini, P. V.; Celante, V. G.; Castro, E. V. R.; Vaz, B. G.; Fleming, F. P.; Gomes, A. O.; Aquije, G. M. F. V.; Romão, W. Monitoring the

Degradation and the Corrosion of Naphthenic Acids by Electrospray Ionization Fourier Transform Ion Cyclotron Resonance Mass Spectrometry and Atomic Force Microscopy. *Fuel* **2014**, *126*, 85–95. https://doi.org/10.1016/j.fuel.2014.02.031.

(25) Park, G.; Brunswick, P.; Kwok, H.; Yan, J.; Kim, M.; Helbing, C.; Buday, C.; van Aggelen, G.; Shang, D. Novel TPAH-50 Multi-Level Surrogate Calibration Quantitation Method by Gas Chromatography Tandem Mass Spectrometer for Surface Water Analysis. *To be submitted*.

(26) Park, G.; Brunswick, P.; Kwok, H.; Haberl, M.; Yan, J.; MacInnis, C.; Kim, M.; Helbing, C.; Aggelen, G. van; Shang, D. A Rapid Gas Chromatography Tandem Mass Spectrometry Method for the Determination of 50 PAHs for Application in a Marine Environment. *Anal Methods* **2018**, *10* (46), 5559–5570. https://doi.org/10.1039/C8AY02258E.

(27) *Aquatic Ecotoxicology: Advancing Tools for Dealing with Emerging Risks*; Amiard-Triquet, C., Amiard, J.-C., Mouneyrac, C., Eds.; Elsevier, 2015. https://doi.org/10.1016/C2013-0-15592-4.

(28) Kroon, F.; Streten, C.; Harries, S. A Protocol for Identifying Suitable Biomarkers to Assess Fish Health: A Systematic Review. *PLoS One* **2017**, *12* (4). https://doi.org/10.1371/journal.pone.0174762.

(29) Hook, S. E.; Gallagher, E. P.; Batley, G. E. The Role of Biomarkers in the Assessment of Aquatic Ecosystem Health. *Integr Environ Assess Manag* **2014**, *10* (3), 327–341. https://doi.org/10.1002/ieam.1530.

(30) Edmunds, R. C.; Gill, J. A.; Baldwin, D. H.; Linbo, T. L.; French, B. L.; Brown, T. L.; Esbaugh, A. J.; Mager, E. M.; Stieglitz, J.; Hoenig, R.; Benetti, D.; Grosell, M.; Scholz, N. L.; Incardona, J. P. Corresponding Morphological and Molecular Indicators of Crude Oil Toxicity to the Developing Hearts of Mahi Mahi. *Sci Rep* **2015**, *5*. https://doi.org/10.1038/srep17326.

(31) Hedgpeth, B. M.; Redman, A. D.; Alyea, R. A.; Letinski, D. J.; Connelly, M. J.; Butler, J. D.; Zhou, H.; Lampi, M. A. Analysis of Sublethal Toxicity in Developing Zebrafish Embryos Exposed to a Range of Petroleum Substances. *Environ Toxicol Chem* **2019**, *38* (6), 1302–1312. https://doi.org/10.1002/etc.4428.

(32) Schirmer, K.; Fischer, B. B.; Madureira, D. J.; Pillai, S. Transcriptomics in Ecotoxicology. *Anal Bioanal Chem* **2010**, *397* (3), 917–923. https://doi.org/10.1007/s00216-010-3662-3.

(33) Chan, L. Y.; Mugler, C. F.; Heinrich, S.; Vallotton, P.; Weis, K. Non-Invasive Measurement of MRNA Decay Reveals Translation Initiation as the Major Determinant of MRNA Stability. *eLife 7*, e32536. https://doi.org/10.7554/eLife.32536.

(34) Martyniuk, C. J.; Feswick, A.; Munkittrick, K. R.; Dreier, D. A.; Denslow, N. D. Twenty Years of Transcriptomics, 17alpha-Ethinylestradiol, and Fish. *Gen Comp Endocrinol* **2020**, *286*, 113325. https://doi.org/10.1016/j.ygcen.2019.113325.

(35) Gómez, L.; Niegowska, M.; Navarro, A.; Amendola, L.; Arukwe, A.; Ait-Aissa, S.; Balzamo, S.; Barreca, S.; Belkin, S.; Bittner, M.; Blaha, L.; Buchinger, S.; Busetto, M.; Carere, M.; Colzani, L.; Dellavedova, P.; Denslow, N.; Escher, B. I.; Hogstrand, C.; Khan, E. A.; König, M.; Kroll, K. J.; Lacchetti, I.; Maillot-Marechal, E.; Moscovici, L.; Potalivo, M.; Sanseverino, I.; Santos, R.; Schifferli, A.; Schlichting, R.; Sforzini, S.; Simon, E.; Shpigel, E.; Sturzenbaum, S.; Vermeirssen, E.; Viarengo, A.; Werner, I.; Lettieri, T. Estrogenicity of Chemical Mixtures Revealed by a Panel of Bioassays. *Sci Total Environ* **2021**, *785*, 147284. https://doi.org/10.1016/j.scitotenv.2021.147284.

(36) Basili, D.; Zhang, J.-L.; Herbert, J.; Kroll, K.; Denslow, N. D.; Martyniuk, C. J.; Falciani, F.; Antczak, P. In Silico Computational Transcriptomics Reveals Novel Endocrine Disruptors in Largemouth Bass (Micropterus Salmoides). *Environ Sci Technol* **2018**, *52* (13), 7553–7565. https://doi.org/10.1021/acs.est.8b02805.
(37) Martyniuk, C. J.; Mehinto, A. C.; Colli-Dula, R. C.; Kroll, K. J.; Doperalski, N. J.; Barber, D. S.; Denslow, N. D. Transcriptome and Physiological Effects of Toxaphene on the Liver-Gonad Reproductive Axis in Male and Female Largemouth Bass (Micropterus Salmoides). *Comparative Biochemistry and Physiology Part D: Genomics and Proteomics* **2020**, *36*, 100746. https://doi.org/10.1016/j.cbd.2020.100746.
(38) Braden, L. M.; Barker, D. E.; Koop, B. F.; Jones, S. R. M. Comparative Defense-Associated Responses in Salmon Skin Elicited by the Ectoparasite Lepeophtheirus Salmonis. *Comp Biochem Physiol Part D: Genomics Proteomics* **2012**, *7* (2), 100–109. https://doi.org/10.1016/j.cbd.2011.12.002.
(39) Kurita-Oyamada, H.; Brown, C. L.; Kroll, K. J.; Walley, S. E.; Keller, C.; Ejaz, M.; Kozuch, M.; Reed, W.; Grayson, S.; Savin, D. A.; Denslow, N. D. Toxicity Assessment of a Novel Oil Dispersant Based on Silica Nanoparticles Using Fathead Minnow. *Aquat Toxicol* **2020**, *229*, 105653. https://doi.org/10.1016/j.aquatox.2020.105653.
(40) Qian, X.; Ba, Y.; Zhuang, Q.; Zhong, G. RNA-Seq Technology and Its Application in Fish Transcriptomics. *OMICS* **2014**, *18* (2), 98–110. https://doi.org/10.1089/omi.2013.0110.
(41) Lowe, R.; Shirley, N.; Bleackley, M.; Dolan, S.; Shafee, T. Transcriptomics Technologies. *PLoS Comput Biol* **2017**, *13* (5), e1005457. https://doi.org/10.1371/journal.pcbi.1005457.
(42) Akbarzadeh, A.; Houde, A. L. S.; Sutherland, B. J. G.; Günther, O. P.; Miller, K. M. Identification of Hypoxia-Specific Biomarkers in Salmonids Using RNA-Sequencing and Validation Using High-Throughput QPCR. *G3 (Bethesda)* **2020**, *10* (9), 3321–3336. https://doi.org/10.1534/g3.120.401487.
(43) Olsvik, P. A.; Lie, K. K.; Saele, Ø.; Sanden, M. Spatial Transcription of CYP1A in Fish Liver. *BMC Physiol* **2007**, *7*, 12. https://doi.org/10.1186/1472-6793-7-12.
(44) Mos, L.; Cooper, G. A.; Serben, K.; Cameron, M.; Koop, B. F. Effects of Diesel on Survival, Growth, and Gene Expression in Rainbow Trout (*Oncorhynchus Mykiss*) Fry. *Environ Sci Technol* **2008**, *42* (7), 2656–2662. https://doi.org/10.1021/es702215c.
(45) Veldhoen, N.; Stevenson, M. R.; Skirrow, R. C.; Rieberger, K. J.; van Aggelen, G.; Meays, C. L.; Helbing, C. C. Minimally Invasive Transcriptome Profiling in Salmon: Detection of Biological Response in Rainbow Trout Caudal Fin Following Exposure to Environmental Chemical Contaminants. *Aquat Toxicol* **2013**, *142–143*, 239–247. https://doi.org/10.1016/j.aquatox.2013.08.016.
(46) Veldhoen, N.; Helbing, C. C. Detection of Environmental Endocrine-Disruptor Effects on Gene Expression in Live Rana Catesbeiana Tadpoles Using a Tail Fin Biopsy Technique. *Environ Toxicol Chem* **2001**, *20* (12), 2704–2708. https://doi.org/10.1002/etc.5620201208.
(47) Veldhoen, N.; Beckerton, J. E.; Mackenzie-Grieve, J.; Stevenson, M. R.; Truelson, R. L.; Helbing, C. C. Development of a Non-Lethal Method for Evaluating Transcriptomic Endpoints in Arctic Grayling (Thymallus Arcticus). *Ecotoxicol Environ Saf* **2014**, *105*, 43–50. https://doi.org/10.1016/j.ecoenv.2014.03.030.
(48) Sutherland, B. J. G.; Covello, J. M.; Friend, S. E.; Poley, J. D.; Koczka, K. W.; Purcell, S. L.; MacLeod, T. L.; Donovan, B. R.; Pino, J.; González-Vecino, J. L.; Gonzalez, J.; Troncoso, J.; Koop, B. F.; Wadsworth, S. L.; Fast, M. D. Host–Parasite Transcriptomics during Immunostimulant-Enhanced Rejection of Salmon Lice (Lepeophtheirus Salmonis)

by Atlantic Salmon (Salmo Salar). *FACETS* **2017**, *2*, 477–495. https://doi.org/10.1139/facets-2017-0020.
(49) Haritash, A. K.; Kaushik, C. P. Biodegradation Aspects of Polycyclic Aromatic Hydrocarbons (PAHs): A Review. *J Hazard Mater* **2009**, *169* (1), 1–15. https://doi.org/10.1016/j.jhazmat.2009.03.137.
(50) Dubansky, B.; Rice, C. D.; Barrois, L. F.; Galvez, F. Biomarkers of Aryl-Hydrocarbon Receptor Activity in Gulf Killifish (Fundulus Grandis) From Northern Gulf of Mexico Marshes Following the Deepwater Horizon Oil Spill. *Arch Environ Contam Toxicol* **2017**, *73* (1), 63–75. https://doi.org/10.1007/s00244-017-0417-6.
(51) Hahn, M. E. Aryl Hydrocarbon Receptors: Diversity and Evolution11Invited Review for Chemico-Biological Interactions. *Chem Biol* **2002**, *141* (1), 131–160. https://doi.org/10.1016/S0009-2797(02)00070-4.
(52) Larigot, L.; Juricek, L.; Dairou, J.; Coumoul, X. AhR Signaling Pathways and Regulatory Functions. *Biochim Open* **2018**, *7*, 1–9. https://doi.org/10.1016/j.biopen.2018.05.001.
(53) Fujii-Kuriyama, Y.; Mimura, J. Molecular Mechanisms of AhR Functions in the Regulation of Cytochrome P450 Genes. *Biochem Biophys Res Commun* **2005**, *338* (1), 311–317. https://doi.org/10.1016/j.bbrc.2005.08.162.
(54) Scornaienchi, M. L.; Thornton, C.; Willett, K. L.; Wilson, J. Y. Functional Differences in the Cytochrome P450 1 Family Enzymes from Zebrafish (Danio Rerio) Using Heterologously Expressed Proteins. *Arch Biochem Biophys* **2010**, *502* (1), 17–22. https://doi.org/10.1016/j.abb.2010.06.018.
(55) Baird, W. M.; Hooven, L. A.; Mahadevan, B. Carcinogenic Polycyclic Aromatic Hydrocarbon-DNA Adducts and Mechanism of Action. *Environ Mol Mutagen* **2005**, *45* (2–3), 106–114. https://doi.org/10.1002/em.20095.
(56) Pait, A. S.; Nelson, J. O. A Survey of Indicators for Reproductive Endocrine Disruption in Fundulus Heteroclitus (Killifish) at Selected Sites in the Chesapeake Bay. *Mar Environ Res* **2009**, *68* (4), 170–177. https://doi.org/10.1016/j.marenvres.2009.06.006.
(57) Bugel, S. M.; Bonventre, J. A.; White, L. A.; Tanguay, R. L.; Cooper, K. R. Chronic Exposure of Killifish to a Highly Polluted Environment Desensitizes Estrogen–Responsive Reproductive and Biomarker Genes. *Aquat Toxicol* **2014**, *152*, 222–231. https://doi.org/10.1016/j.aquatox.2014.04.014.
(58) Hoffmann, J. L.; Oris, J. T. Altered Gene Expression: A Mechanism for Reproductive Toxicity in Zebrafish Exposed to Benzo[a]Pyrene. *Aquat Toxicol* **2006**, *78* (4), 332–340. https://doi.org/10.1016/j.aquatox.2006.04.007.
(59) Vignet, C.; Larcher, T.; Davail, B.; Joassard, L.; Le Menach, K.; Guionnet, T.; Lyphout, L.; Ledevin, M.; Goubeau, M.; Budzinski, H.; Bégout, M.-L.; Cousin, X. Fish Reproduction Is Disrupted upon Lifelong Exposure to Environmental PAHs Fractions Revealing Different Modes of Action. *Toxics* **2016**, *4* (4), 26. https://doi.org/10.3390/toxics4040026.
(60) Thambirajah, A. A.; Koide, E. M.; Imbery, J. J.; Helbing, C. C. Contaminant and Environmental Influences on Thyroid Hormone Action in Amphibian Metamorphosis. *Front Endocrinol (Lausanne)* **2019**, *10*, 276. https://doi.org/10.3389/fendo.2019.00276.
(61) Effect-Directed Identification of Naphthenic Acids As Important in Vitro Xeno-Estrogens and Anti-Androgens in North Sea Offshore Produced Water Discharges | Environmental Science & Technology https://pubs-acs-org.ezproxy.library.uvic.ca/doi/10.1021/es9014212 (accessed 2021 -06 -30).

(62) Kavanagh, R.; Frank, R.; Burnison, B.; Young, R.; Fedorak, P.; Solomon, K.; Kraak, G. Fathead Minnow (Pimephales Promelas) Reproduction Is Impaired When Exposed to a Naphthenic Acid Extract. *Aquat toxicol (Amsterdam, Netherlands)* **2012**, *116–117*, 34–42. https://doi.org/10.1016/j.aquatox.2012.03.002.
(63) Macqueen, D. J.; Primmer, C. R.; Houston, R. D.; Nowak, B. F.; Bernatchez, L.; Bergseth, S.; Davidson, W. S.; Gallardo-Escárate, C.; Goldammer, T.; Guiguen, Y.; Iturra, P.; Kijas, J. W.; Koop, B. F.; Lien, S.; Maass, A.; Martin, S. A. M.; McGinnity, P.; Montecino, M.; Naish, K. A.; Nichols, K. M.; Ólafsson, K.; Omholt, S. W.; Palti, Y.; Plastow, G. S.; Rexroad, C. E.; Rise, M. L.; Ritchie, R. J.; Sandve, S. R.; Schulte, P. M.; Tello, A.; Vidal, R.; Vik, J. O.; Wargelius, A.; Yáñez, J. M.; Primmer, C. R.; Macqueen, D. J.; Houston, R. D.; Nowak, B. F.; Davidson, W. S.; Lien, S.; Koop, B. F.; The FAASG Consortium. Functional Annotation of All Salmonid Genomes (FAASG): An International Initiative Supporting Future Salmonid Research, Conservation and Aquaculture. *BMC Genom* **2017**, *18* (1), 484. https://doi.org/10.1186/s12864-017-3862-8.
(64) Gallagher, E. P.; LaVire, H. M.; Bammler, T. K.; Stapleton, P. L.; Beyer, R. P.; Farin, F. M. Hepatic Expression Profiling in Smolting and Adult Coho Salmon (Onchorhynchus Kisutch). *Environ Res* **2008**, *106* (3), 365–378. https://doi.org/10.1016/j.envres.2007.10.001.
(65) Stefansson, S.; BTh, B.; Ebbesson, L.; McCormick, S. Smoltification. In *Fish Larval Physiology*; 2008; pp 639–681. https://doi.org/10.1201/9780429061608-27.
(66) Barron, M. G. Endocrine Control of Smoltification in Anadromous Salmonids. *J Endocrinol* **1986**, *108* (2), 313–319. https://doi.org/10.1677/joe.0.1080313.
(67) Salmon Life Cycle | Marine Institute https://www.marine.ie/Home/site-area/areas-activity/fisheries-ecosystems/salmon-life-cycle (accessed 2021 -07 -03).
(68) Fisheries, N. Coho Salmon | NOAA Fisheries https://www.fisheries.noaa.gov/species/coho-salmon (accessed 2021 -07 -03).
(69) Tuor, K. M. F.; Heath, D. D.; Shrimpton, J. M. Spatial and Environmental Effects on Coho Salmon Life History Trait Variation. *Ecol Evol* **2020**, *10* (23), 13198–13210. https://doi.org/10.1002/ece3.6912.
(70) Lavado, R.; Aparicio-Fabre, R.; Schlenk, D. Effects of Salinity Acclimation on the Expression and Activity of Phase I Enzymes (CYP450 and FMOs) in Coho Salmon (Oncorhynchus Kisutch). *Fish Physiol Biochem* **2014**, *40* (1), 267–278. https://doi.org/10.1007/s10695-013-9842-2.
(71) Marty, J.; Potter, S. Risk Assessment for Marine Spills in Canadian Waters, Phase 1: Oil Spills South of the 60th Parallel. https://www.researchgate.net/publication/274081547_Risk_Assessment_for_Marine_Spills_in_Canadian_Waters_Phase_1_Oil_Spills_South_of_the_60th_Parallel (accessed 2018 -12 -12).
(72) Cherr, G. N.; Fairbairn, E.; Whitehead, A. Impacts of Petroleum-Derived Pollutants on Fish Development. *Annu Rev Anim Biosci* **2017**, *5* (1), 185–203. https://doi.org/10.1146/annurev-animal-022516-022928.
(73) Reynaud, S.; Deschaux, P. The Effects of Polycyclic Aromatic Hydrocarbons on the Immune System of Fish: A Review. *Aquat Toxicol* **2006**, *77* (2), 229–238. https://doi.org/10.1016/j.aquatox.2005.10.018.

(74) Eom, I. C.; Rast, C.; Veber, A. M.; Vasseur, P. Ecotoxicity of a Polycyclic Aromatic Hydrocarbon (PAH)-Contaminated Soil. *Ecotoxicol Environ Saf* **2007**, *67* (2), 190–205. https://doi.org/10.1016/j.ecoenv.2006.12.020.
(75) Wang, Y.; Shen, C.; Wang, C.; Zhou, Y.; Gao, D.; Zuo, Z. Maternal and Embryonic Exposure to the Water Soluble Fraction of Crude Oil or Lead Induces Behavioral Abnormalities in Zebrafish (Danio Rerio), and the Mechanisms Involved. *Chemosphere* **2018**, *191*, 7–16. https://doi.org/10.1016/j.chemosphere.2017.09.096.
(76) Mauduit, F.; Domenici, P.; Farrell, A. P.; Lacroix, C.; Le Floch, S.; Lemaire, P.; Nicolas-Kopec, A.; Whittington, M.; Zambonino-Infante, J. L.; Claireaux, G. Assessing Chronic Fish Health: An Application to a Case of an Acute Exposure to Chemically Treated Crude Oil. *Aquat Toxicol* **2016**, *178*, 197–208. https://doi.org/10.1016/j.aquatox.2016.07.019.
(77) Brussaard, C. P. D.; Peperzak, L.; Beggah, S.; Wick, L. Y.; Wuerz, B.; Weber, J.; Samuel Arey, J.; van der Burg, B.; Jonas, A.; Huisman, J.; van der Meer, J. R. Immediate Ecotoxicological Effects of Short-Lived Oil Spills on Marine Biota. *Nat Commun* **2016**, *7*. https://doi.org/10.1038/ncomms11206.
(78) Negri, A. P.; Brinkman, D. L.; Flores, F.; Botté, E. S.; Jones, R. J.; Webster, N. S. Acute Ecotoxicology of Natural Oil and Gas Condensate to Coral Reef Larvae. *Sci Rep* **2016**, *6*. https://doi.org/10.1038/srep21153.
(79) Schmidt, J. V.; Bradfield, C. A. Ah Receptor Signaling Pathways. *Annu Rev Cell Dev Biol* **1996**, *12* (1), 55–89. https://doi.org/10.1146/annurev.cellbio.12.1.55.
(80) Holth, T. F.; Eidsvoll, D. P.; Farmen, E.; Sanders, M. B.; Martínez-Gómez, C.; Budzinski, H.; Burgeot, T.; Guilhermino, L.; Hylland, K. Effects of Water Accommodated Fractions of Crude Oils and Diesel on a Suite of Biomarkers in Atlantic Cod (Gadus Morhua). *Aquat Toxicol* **2014**, *154*, 240–252. https://doi.org/10.1016/j.aquatox.2014.05.013.
(81) Bemanian, V.; Male, R.; Goksøyr, A. The Aryl Hydrocarbon Receptor-Mediated Disruption of Vitellogenin Synthesis in the Fish Liver: Cross-Talk between AHR- and ERα-Signalling Pathways. *Comp Hepatol* **2004**, *3* (1), 2. https://doi.org/10.1186/1476-5926-3-2.
(82) Fertuck, K. C.; Kumar, S.; Sikka, H. C.; Matthews, J. B.; Zacharewski, T. R. Interaction of PAH-Related Compounds with the Alpha and Beta Isoforms of the Estrogen Receptor. *Toxicol Lett* **2001**, *121* (3), 167–177.
(83) Mortensen, A. S.; Arukwe, A. Estrogenic Effect of Dioxin-like Aryl Hydrocarbon Receptor (AhR) Agonist (PCB Congener 126) in Salmon Hepatocytes. *Mar Environ Res* **2008**, *66* (1), 119–120. https://doi.org/10.1016/j.marenvres.2008.02.041.
(84) Amiri, B. M.; Xu, E. G.; Kupsco, A.; Giroux, M.; Hoseinzadeh, M.; Schlenk, D. The Effect of Chlorpyrifos on Salinity Acclimation of Juvenile Rainbow Trout (Oncorhynchus Mykiss). *Aquat Toxicol* **2018**, *195*, 97–102. https://doi.org/10.1016/j.aquatox.2017.12.011.
(85) Heerema, J. L.; Jackman, K. W.; Miliano, R. C.; Li, L.; Zaborniak, T. S. M.; Veldhoen, N.; van Aggelen, G.; Parker, W. J.; Pyle, G. G.; Helbing, C. C. Behavioral and Molecular Analyses of Olfaction-Mediated Avoidance Responses of Rana (Lithobates) Catesbeiana Tadpoles: Sensitivity to Thyroid Hormones, Estrogen, and Treated Municipal Wastewater Effluent. *Horm Behav* **2017**, *101*, 85–93. https://doi.org/10.1016/j.yhbeh.2017.09.016.
(86) Feswick, A.; Isaacs, M.; Biales, A.; Flick, R. W.; Bencic, D. C.; Wang, R.-L.; Vulpe, C.; Brown-Augustine, M.; Loguinov, A.; Falciani, F.; Antczak, P.; Herbert, J.; Brown, L.; Denslow, N. D.; Kroll, K. J.; Lavelle, C.; Dang, V.; Escalon, L.; Garcia-Reyero, N.;

Martyniuk, C. J.; Munkittrick, K. R. How Consistent Are We? Interlaboratory Comparison Study in Fathead Minnows Using the Model Estrogen 17α-Ethinylestradiol to Develop Recommendations for Environmental Transcriptomics: Fathead Minnow Microarray Interlaboratory Comparison. *Environ Toxicol Chem* **2017**, *36* (10), 2614–2623. https://doi.org/10.1002/etc.3799.

(87) Diamante, G.; do Amaral e Silva Müller, G.; Menjivar-Cervantes, N.; Xu, E. G.; Volz, D. C.; Dias Bainy, A. C.; Schlenk, D. Developmental Toxicity of Hydroxylated Chrysene Metabolites in Zebrafish Embryos. *Aquat Toxicol* **2017**, *189*, 77–86. https://doi.org/10.1016/j.aquatox.2017.05.013.

(88) Huang, S. S. Y.; Benskin, J. P.; Veldhoen, N.; Chandramouli, B.; Butler, H.; Helbing, C. C.; Cosgrove, J. R. A Multi-Omic Approach to Elucidate Low-Dose Effects of Xenobiotics in Zebrafish (Danio Rerio) Larvae. *Aquat Toxicol* **2017**, *182*, 102–112. https://doi.org/10.1016/j.aquatox.2016.11.016.

(89) Brown, T. M.; Hammond, S. A.; Behsaz, B.; Veldhoen, N.; Birol, I.; Helbing, C. C. De Novo Assembly of the Ringed Seal (*Pusa Hispida*) Blubber Transcriptome: A Tool That Enables Identification of Molecular Health Indicators Associated with PCB Exposure. *Aquat Toxicol* **2017**, *185*, 48–57. https://doi.org/10.1016/j.aquatox.2017.02.004.

(90) Stephens, C. *Summary of West Coast Oil Spill Data, Calendar Year 2017*; Pacific States/British Columbia Oil Spill Task Force: Seattle, WA, 2018; p 27.

(91) Gilkeson, L.; Bonner, L.; Brown, R.; Francis, K.; Johanneson, D.; Canessa, R.; Alder, J.; Bernard, D.; Mattu, G.; Wong, C.; Paynter, R. Alive and Inseparable : British Columbia's Coastal Environment : 2006.

(92) Yan, J.; Kim, M.; Haberl, M.; Kwok, H.; Brunswick, P.; MacInnis, C.; Aggelen, G. van; Shang, D. Determination of Polycyclic Aromatic Hydrocarbons in Surface Water Using Simplified Liquid–Liquid Micro-Extraction and Pseudo-MRM GC/MS/MS. *Anal Methods* **2018**, *10* (4), 405–416. https://doi.org/10.1039/C7AY01902E.

(93) Shang, D.; Kim, M.; Haberl, M. Rapid and Sensitive Method for the Determination of Polycyclic Aromatic Hydrocarbons in Soils Using Pseudo Multiple Reaction Monitoring Gas Chromatography/Tandem Mass Spectrometry. *J Chromatogr A* **2014**, *1334*, 118–125. https://doi.org/10.1016/j.chroma.2014.01.074.

(94) Singer, M. M.; Aurand, D.; Bragin, G. E.; Clark, J. R.; Coelho, G. M.; Sowby, M. L.; Tjeerdema, R. S. Standardization of the Preparation and Quantitation of Water-Accommodated Fractions of Petroleum for Toxicity Testing. *Mar Pollut Bull* **2000**, *40* (11), 1007–1016. https://doi.org/10.1016/S0025-326X(00)00045-X.

(95) Blenkinsopp, S. Guidance Document for the Preparation of Water Accommodated Fractions (WAF) from Oil and Refined Products for Use in Aquatic Toxicity Testing. Environment Canada 1998.

(96) Canada, E. *Environment Canada, Biological Test Methods: Acute Lethality Test Using Rainbow Trout*; Report EPS 1/RM/9; Ottawa, Canada, 1990.

(97) Forth Heather P.; Mitchelmore Carys L.; Morris Jeffrey M.; Lipton Joshua. Characterization of Oil and Water Accommodated Fractions Used to Conduct Aquatic Toxicity Testing in Support of the Deepwater Horizon Oil Spill Natural Resource Damage Assessment. *Environ Toxicol Chem* **2016**, *36* (6), 1450–1459. https://doi.org/10.1002/etc.3672.

(98) Brown-Peterson, N. J.; Krasnec, M.; Takeshita, R.; Ryan, C. N.; Griffitt, K. J.; Lay, C.; Mayer, G. D.; Bayha, K. M.; Hawkins, W. E.; Lipton, I.; Morris, J.; Griffitt, R. J. A

Multiple Endpoint Analysis of the Effects of Chronic Exposure to Sediment Contaminated with Deepwater Horizon Oil on Juvenile Southern Flounder and Their Associated Microbiomes. *Aquat Toxicol* **2015**, *165*, 197–209. https://doi.org/10.1016/j.aquatox.2015.06.001.

(99) Veldhoen, N.; Ikonomou, M. G.; Dubetz, C.; Macpherson, N.; Sampson, T.; Kelly, B. C.; Helbing, C. C. Gene Expression Profiling and Environmental Contaminant Assessment of Migrating Pacific Salmon in the Fraser River Watershed of British Columbia. *Aquat Toxicol* **2010**, *97* (3), 212–225. https://doi.org/10.1016/j.aquatox.2009.09.009.

(100) Veldhoen, N.; Ikonomou, M. G.; Rehaume, V.; Dubetz, C.; Patterson, D. A.; Helbing, C. C. Evidence of Disruption in Estrogen-Associated Signaling in the Liver Transcriptome of in-Migrating Sockeye Salmon of British Columbia, Canada. *Comp Biochem Physiol C Toxicol Pharmacol* **2013**, *157* (2), 150–161. https://doi.org/10.1016/j.cbpc.2012.10.007.

(101) Veldhoen, N.; Propper, C. R.; Helbing, C. C. Enabling Comparative Gene Expression Studies of Thyroid Hormone Action through the Development of a Flexible Real-Time Quantitative PCR Assay for Use across Multiple Anuran Indicator and Sentinel Species. *Aquat Toxicol* **2014**, *148*, 162–173. https://doi.org/10.1016/j.aquatox.2014.01.008.

(102) Bustin, S. A.; Benes, V.; Garson, J. A.; Hellemans, J.; Huggett, J.; Kubista, M.; Mueller, R.; Nolan, T.; Pfaffl, M. W.; Shipley, G. L.; Vandesompele, J.; Wittwer, C. T. The MIQE Guidelines: Minimum Information for Publication of Quantitative Real-Time PCR Experiments. *Clin Chem* **2009**, *55* (4), 611–622. https://doi.org/10.1373/clinchem.2008.112797.

(103) Livak, K. J.; Schmittgen, T. D. Analysis of Relative Gene Expression Data Using Real-Time Quantitative PCR and the $2^{-\Delta\Delta CT}$ Method. *Methods* **2001**, *25* (4), 402–408. https://doi.org/10.1006/meth.2001.1262.

(104) Brunelli, J. P.; Thorgaard, G. H. A New Y-Chromosome-Specific Marker for Pacific Salmon. *Trans Am Fish Soc* **2004**, *133* (5), 1247–1253. https://doi.org/10.1577/T03-049.1.

(105) Anglès d'Auriac, M. B.; Urke, H. A.; Kristensen, T. A Rapid QPCR Method for Genetic Sex Identification of *Salmo Salar* and *Salmo Trutta* Including Simultaneous Elucidation of Interspecies Hybrid Paternity by High-Resolution Melt Analysis: *Salmo* Sex and Hybrid Paternity Identification. *J Fish Biol* **2014**, *84* (6), 1971–1977. https://doi.org/10.1111/jfb.12401.

(106) Yano, A.; Nicol, B.; Jouanno, E.; Quillet, E.; Fostier, A.; Guyomard, R.; Guiguen, Y. The Sexually Dimorphic on the Y-Chromosome Gene (*SdY*) Is a Conserved Male-Specific Y-Chromosome Sequence in Many Salmonids. *Evol Appl* **2013**, *6* (3), 486–496. https://doi.org/10.1111/eva.12032.

(107) Imbery, J. J.; Buday, C.; Miliano, R. C.; Shang, D.; Round, J. M.; Kwok, H.; Van Aggelen, G.; Helbing, C. C. Evaluation of Gene Bioindicators in the Liver and Caudal Fin of Juvenile Pacific Coho Salmon in Response to Low Sulfur Marine Diesel Seawater-Accommodated Fraction Exposure. *Environ Sci Technol* **2019**, *53* (3), 1627–1638. https://doi.org/10.1021/acs.est.8b05429.

(108) Stout, S. A.; Payne, J. R.; Emsbo-Mattingly, S. D.; Baker, G. Weathering of Field-Collected Floating and Stranded Macondo Oils during and Shortly after the Deepwater Horizon Oil Spill. *Mar Pollut Bull* **2016**, *105* (1), 7–22. https://doi.org/10.1016/j.marpolbul.2016.02.044.

(109) Short, J. W.; Heintz, R. A. Identification of Exxon Valdez Oil in Sediments and Tissues from Prince William Sound and the Northwestern Gulf of Alaska Based on a PAH

Weathering Model. *Environ Sci Technol* **1997**, *31* (8), 2375–2384. https://doi.org/10.1021/es960985d.
(110) Wang, Z.; Stout, S. *Oil Spill Environmental Forensics - 1st Edition*, first.; Academic Press, 2007.
(111) Larson, W. A.; McKinney, G. J.; Seeb, J. E.; Seeb, L. W. Identification and Characterization of Sex-Associated Loci in Sockeye Salmon Using Genotyping-by-Sequencing and Comparison with a Sex-Determining Assay Based on the SdY Gene. *J Hered* **2016**, *107* (6), 559–566. https://doi.org/10.1093/jhered/esw043.
(112) Page, D. S.; Chapman, P. M.; Landrum, P. F.; Neff, J.; Elston, R. A Perspective on the Toxicity of Low Concentrations of Petroleum-Derived Polycyclic Aromatic Hydrocarbons to Early Life Stages of Herring and Salmon. *Hum Ecol Risk Assess* **2012**, *18* (2), 229–260. https://doi.org/10.1080/10807039.2012.650569.
(113) Le Beau, M. M.; Carver, L. A.; Espinosa, R.; Schmidt, J. V.; Bradfield, C. A. Chromosomal Localization of the Human AHR Locus Encoding the Structural Gene for the Ah Receptor to 7p21-->p15. *Cytogenet Cell Genet* **1994**, *66* (3), 172–176. https://doi.org/10.1159/000133694.
(114) De Anna, J. S.; Leggieri, L. R.; Arias Darraz, L.; Cárcamo, J. G.; Venturino, A.; Luquet, C. M. Effects of Sequential Exposure to Water Accommodated Fraction of Crude Oil and Chlorpyrifos on Molecular and Biochemical Biomarkers in Rainbow Trout. *Comp Biochem Physiol Part C Toxicol Pharmacol* **2018**, *212*, 47–55. https://doi.org/10.1016/j.cbpc.2018.07.003.
(115) Madison, B. N.; Hodson, P. V.; Langlois, V. S. Cold Lake Blend Diluted Bitumen Toxicity to the Early Development of Japanese Medaka. *Environ Pollut* **2017**, *225*, 579–586. https://doi.org/10.1016/j.envpol.2017.03.025.
(116) Olsvik, P. A.; Lie, K. K.; Nordtug, T.; Hansen, B. H. Is Chemically Dispersed Oil More Toxic to Atlantic Cod (Gadus Morhua) Larvae than Mechanically Dispersed Oil? A Transcriptional Evaluation. *BMC Genom* **2012**, *13*, 702. https://doi.org/10.1186/1471-2164-13-702.
(117) Krøvel, A. V.; Søfteland, L.; Torstensen, B. E.; Olsvik, P. A. Endosulfan in Vitro Toxicity in Atlantic Salmon Hepatocytes Obtained from Fish Fed Either Fish Oil or Vegetable Oil. *Comp Biochem Physiol Part C Toxicol Pharmacol* **2010**, *151* (2), 175–186. https://doi.org/10.1016/j.cbpc.2009.10.003.
(118) Habibi, M.; Rottler, J.; Plotkin, S. S. The Unfolding Mechanism of Monomeric Mutant SOD1 by Simulated Force Spectroscopy. *Biochim Biophys Acta* **2017**, *1865* (11 Pt B), 1631–1642. https://doi.org/10.1016/j.bbapap.2017.06.009.
(119) Eissa, N.; Wang, H.-P.; Yao, H.; Shen, Z.-G.; Shaheen, A. A.; Abou-ElGheit, E. N. Expression of Hsp70, Igf1, and Three Oxidative Stress Biomarkers in Response to Handling and Salt Treatment at Different Water Temperatures in Yellow Perch, Perca Flavescens. *Front Physiol* **2017**, *8*. https://doi.org/10.3389/fphys.2017.00683.
(120) Madison, B. N.; Hodson, P. V.; Langlois, V. S. Diluted Bitumen Causes Deformities and Molecular Responses Indicative of Oxidative Stress in Japanese Medaka Embryos. *Aquat Toxicol* **2015**, *165*, 222–230. https://doi.org/10.1016/j.aquatox.2015.06.006.
(121) Arukwe, A.; Røsbak, R.; Adeogun, A. O.; Langberg, H. A.; Venter, A.; Myburgh, J.; Botha, C.; Benedetti, M.; Regoli, F. Biotransformation and Oxidative Stress Responses in Captive Nile Crocodile (Crocodylus Niloticus) Exposed to Organic Contaminants from the

Natural Environment in South Africa. *PLoS ONE* **2015**, *10* (6). https://doi.org/10.1371/journal.pone.0130002.
(122) Lee, S.; Hong, S.; Liu, X.; Kim, C.; Jung, D.; Yim, U. H.; Shim, W. J.; Khim, J. S.; Giesy, J. P.; Choi, K. Endocrine Disrupting Potential of PAHs and Their Alkylated Analogues Associated with Oil Spills. *Environ Sci Process Impacts* **2017**, *19* (9), 1117–1125. https://doi.org/10.1039/c7em00125h.
(123) Mattos, J. J.; Siebert, M. N.; Luchmann, K. H.; Granucci, N.; Dorrington, T.; Stoco, P. H.; Grisard, E. C.; Bainy, A. C. D. Differential Gene Expression in Poecilia Vivipara Exposed to Diesel Oil Water Accommodated Fraction. *Mar Environ Res* **2010**, *69*, S31–S33. https://doi.org/10.1016/j.marenvres.2009.11.002.
(124) Esterhuyse, M. M.; Venter, M.; Veldhoen, N.; Helbing, C. C.; van Wyk, J. H. Characterization of Vtg-1 MRNA Expression during Ontogeny in Oreochromis Mossambicus (PETERS). *J Steroid Biochem Mol Biol* **2009**, *117* (1–3), 42–49. https://doi.org/10.1016/j.jsbmb.2009.07.001.
(125) Baum, G.; Kegler, P.; Scholz-Böttcher, B. M.; Alfiansah, Y. R.; Abrar, M.; Kunzmann, A. Metabolic Performance of the Coral Reef Fish Siganus Guttatus Exposed to Combinations of Water Borne Diesel, an Anionic Surfactant and Elevated Temperature in Indonesia. *Mar Pollut Bull* **2016**, *110* (2), 735–746. https://doi.org/10.1016/j.marpolbul.2016.02.078.
(126) Adams, J.; Charbonneau, K.; Tuori, D.; Brown, R. S.; Hodson, P. V. *Review of Methods for Measuring the Toxicity to Aquatic Organisms of the Water Accommodated Fraction (WAF) and Chemically-Enhanced Water Accommodated Fraction (CEWAF) of Petroleum*; Research Document 2017/064; Canadian Science Advisory Secretariat (CSAS), 2017.
(127) Hodson, P. V.; Adams, J.; Brown, R. S. Oil Toxicity Test Methods Must Be Improved. *Environ Toxicol Chem* **2019**, *38* (2), 302–311. https://doi.org/10.1002/etc.4303.
(128) Buday, C.; Schroeder, G. *Biological Assessment of Diesel and Gasoline Using Various Freshwater and Saltwater Toxicity Tests*; 2008.
(129) Stephens, C. *Summary of West Coast Oil Spill Data, Calendar Year 2017*; Pacific States/British Columbia Oil Spill Task Force, 2017.
(130) Diluted Bitumen https://www.api.org:443/oil-and-natural-gas/wells-to-consumer/exploration-and-production/oil-sands/diluted-bitumen (accessed 2021 -07 -01).
(131) Råbergh, C. M.; Vrolijk, N. H.; Lipsky, M. M.; Chen, T. T. Differential Expression of Two CYP1A Genes in Rainbow Trout (Oncorhynchys Mykiss). *Toxicol Appl Pharmacol* **2000**, *165* (3), 195–205. https://doi.org/10.1006/taap.2000.8941.
(132) *Environment Canada, Biological Test Methods: Acute Lethality Test Using Rainbow Trout*; Report Report EPS 1/RM/9 July 1990, amended May 1996 and May 2007.
(133) Park, G.; Brunswick, P.; Kwok, H.; Haberl, M.; Yan, J.; MacInnis, C.; Kim, M.; Helbing, C.; Aggelen, G. van; Shang, D. A Rapid Gas Chromatography Tandem Mass Spectrometry Method for the Determination of 50 PAHs for Application in a Marine Environment. *Anal Methods* **2018**, *10* (46), 5559–5570. https://doi.org/10.1039/C8AY02258E.
(134) Calabrese, E. J.; Baldwin, L. A. U-Shaped Dose-Responses in Biology, Toxicology, and Public Health. *Annu Rev Public Health* **2001**, *22* (1), 15–33. https://doi.org/10.1146/annurev.publhealth.22.1.15.

(135) Thor, P.; Granberg, M. E.; Winnes, H.; Magnusson, K. Severe Toxic Effects on Pelagic Copepods from Maritime Exhaust Gas Scrubber Effluents. *Environ Sci Technol* **2021**, *55* (9), 5826–5835. https://doi.org/10.1021/acs.est.0c07805.
(136) Toxicity Effects Of Dispersed Alaska North Slope Oil On Fish - Final Report, March 2013- Appendices A-H. *Prince William Sound*.
(137) Lee, K.; King, T.; Robinson, B.; Li, Z.; Burridge; Lyons; Wong; MacKeigan; Courtenay; Johnson; Boudreau, M.; Hodson; Greer; Venosa, A. Toxicity Effects of Chemically-Dispersed Crude Oil on Fish; 2011; Vol. 2011. https://doi.org/10.7901/2169-3358-2011-1-163.
(138) Bilton, H. T.; Alderdice, D. F.; Schnute, J. T. Influence of Time and Size at Release of Juvenile Coho Salmon (Oncorhynchus Kisutch) on Returns at Maturity. *Can J Fish Aquat Sci* **1982**, *39* (3), 426–447. https://doi.org/10.1139/f82-060.
(139) Browne, E.; Kelley, M.; Zhou, G.-D.; He, L. Y.; McDonald, T.; Wang, S.; Duncan, B.; Meador, J.; Donnelly, K.; Gallagher, E. In Situ Biomonitoring of Juvenile Chinook Salmon (Onchorhynchus Tshawytscha) Using Biomarkers of Chemical Exposures and Effects in a Partially Remediated Urbanized Waterway of the Puget Sound, WA. *Environ Res* **2010**, *110* (7), 675–683. https://doi.org/10.1016/j.envres.2010.06.007.
(140) Finn, R. N. *Fish Larval Physiology*; CRC Press, 2020.
(141) Andrews, S. FastQC: A Quality Control Tool for High Throughput Sequence Data https://www.bioinformatics.babraham.ac.uk/projects/fastqc/ (accessed 2020 -10 -06).
(142) Dobin, A.; Davis, C. A.; Schlesinger, F.; Drenkow, J.; Zaleski, C.; Jha, S.; Batut, P.; Chaisson, M.; Gingeras, T. R. STAR: Ultrafast Universal RNA-Seq Aligner. *Bioinformatics* **2013**, *29* (1), 15–21. https://doi.org/10.1093/bioinformatics/bts635.
(143) Pertea, M.; Pertea, G. M.; Antonescu, C. M.; Chang, T.-C.; Mendell, J. T.; Salzberg, S. L. StringTie Enables Improved Reconstruction of a Transcriptome from RNA-Seq Reads. *Nat Biotech* **2015**, *33* (3), 290–295. https://doi.org/10.1038/nbt.3122.
(144) Love, M. I.; Huber, W.; Anders, S. Moderated Estimation of Fold Change and Dispersion for RNA-Seq Data with DESeq2. *Genome Biol* **2014**, *15* (12), 550. https://doi.org/10.1186/s13059-014-0550-8.
(145) Jackman, K. W.; Veldhoen, N.; Miliano, R. C.; Robert, B. J.; Li, L.; Khojasteh, A.; Zheng, X.; Zaborniak, T. S. M.; van Aggelen, G.; Lesperance, M.; Parker, W. J.; Hall, E. R.; Pyle, G. G.; Helbing, C. C. Transcriptomics Investigation of Thyroid Hormone Disruption in the Olfactory System of the Rana [Lithobates] Catesbeiana Tadpole. *Aquat Toxicol* **2018**, *202*, 46–56. https://doi.org/10.1016/j.aquatox.2018.06.015.
(146) Bryant, D. M.; Johnson, K.; DiTommaso, T.; Tickle, T.; Couger, M. B.; Payzin-Dogru, D.; Lee, T. J.; Leigh, N. D.; Kuo, T.-H.; Davis, F. G.; Bateman, J.; Bryant, S.; Guzikowski, A. R.; Tsai, S. L.; Coyne, S.; Ye, W. W.; Freeman, R. M.; Peshkin, L.; Tabin, C. J.; Regev, A.; Haas, B. J.; Whited, J. L. A Tissue-Mapped Axolotl De Novo Transcriptome Enables Identification of Limb Regeneration Factors. *Cell Rep* **2017**, *18* (3), 762–776. https://doi.org/10.1016/j.celrep.2016.12.063.
(147) Young, M. D.; Wakefield, M. J.; Smyth, G. K.; Oshlack, A. Gene Ontology Analysis for RNA-Seq: Accounting for Selection Bias. *Genome Biol* **2010**, *11* (2), R14. https://doi.org/10.1186/gb-2010-11-2-r14.
(148) Nota, B. Gogadget: An R Package for Interpretation and Visualization of GO Enrichment Results. *Mol Inform* **2017**, *36* (5–6), 1600132. https://doi.org/10.1002/minf.201600132.

(149) Shannon, P.; Markiel, A.; Ozier, O.; Baliga, N. S.; Wang, J. T.; Ramage, D.; Amin, N.; Schwikowski, B.; Ideker, T. Cytoscape: A Software Environment for Integrated Models of Biomolecular Interaction Networks. *Genome Res* **2003**, *13* (11), 2498–2504. https://doi.org/10.1101/gr.1239303.
(150) Sutherland, B. J. G.; Prokkola, J. M.; Audet, C.; Bernatchez, L. Sex-Specific Co-Expression Networks and Sex-Biased Gene Expression in the Salmonid Brook Charr Salvelinus Fontinalis. *G3 (Bethesda)* **2019**, *9* (3), 955–968. https://doi.org/10.1534/g3.118.200910.
(151) Kim, S.-M.; Wang, Y.; Nabavi, N.; Liu, Y.; Correia, M. A. Hepatic Cytochromes P450: Structural Degrons and Barcodes, Posttranslational Modifications and Cellular Adapters in the ERAD-Endgame. *Drug Metab Rev* **2016**, *48* (3), 405–433. https://doi.org/10.1080/03602532.2016.1195403.
(152) Vargas, D. A.; Sun, M.; Sadykov, K.; Kukuruzinska, M. A.; Zaman, M. H. The Integrated Role of Wnt/β-Catenin, N-Glycosylation, and E-Cadherin-Mediated Adhesion in Network Dynamics. *PLoS Comput Biol* **2016**, *12* (7). https://doi.org/10.1371/journal.pcbi.1005007.
(153) Hughes, A.; Oxford, A. E.; Tawara, K.; Jorcyk, C. L.; Oxford, J. T. Endoplasmic Reticulum Stress and Unfolded Protein Response in Cartilage Pathophysiology; Contributing Factors to Apoptosis and Osteoarthritis. *Int J Mol Sci* **2017**, *18* (3). https://doi.org/10.3390/ijms18030665.
(154) Honda, M.; Suzuki, N. Toxicities of Polycyclic Aromatic Hydrocarbons for Aquatic Animals. *Int J Environ Res Public Health* **2020**, *17* (4). https://doi.org/10.3390/ijerph17041363.
(155) Zhang, J.; Yao, J.; Wang, R.; Zhang, Y.; Liu, S.; Sun, L.; Jiang, Y.; Feng, J.; Liu, N.; Nelson, D.; Waldbieser, G.; Liu, Z. The Cytochrome P450 Genes of Channel Catfish: Their Involvement in Disease Defense Responses as Revealed by Meta-Analysis of RNA-Seq Datasets. *Biochim Biophys Acta* **2014**, *1840* (9), 2813–2828. https://doi.org/10.1016/j.bbagen.2014.04.016.
(156) Procházková, J.; Kabátková, M.; Bryja, V.; Umannová, L.; Bernatík, O.; Kozubík, A.; Machala, M.; Vondrácek, J. The Interplay of the Aryl Hydrocarbon Receptor and β-Catenin Alters Both AhR-Dependent Transcription and Wnt/β-Catenin Signaling in Liver Progenitors. *Toxicol Sci* **2011**, *122* (2), 349–360. https://doi.org/10.1093/toxsci/kfr129.
(157) Bhadra, M.; Howell, P.; Dutta, S.; Heintz, C.; Mair, W. B. Alternative Splicing in Aging and Longevity. *Hum Genet* **2020**, *139* (3), 357–369. https://doi.org/10.1007/s00439-019-02094-6.
(158) Scotti, M. M.; Swanson, M. S. RNA Mis-Splicing in Disease. *Nat Rev Genet* **2016**, *17* (1), 19–32. https://doi.org/10.1038/nrg.2015.3.
(159) Yi, L.; Pimentel, H.; Bray, N. L.; Pachter, L. Gene-Level Differential Analysis at Transcript-Level Resolution. *Genome Biol* **2018**, *19* (1), 53. https://doi.org/10.1186/s13059-018-1419-z.
(160) Shimada, T.; Gillam, E. M. J.; Oda, Y.; Tsumura, F.; Sutter, T. R.; Guengerich, F. P.; Inoue, K. Metabolism of Benzo[a]Pyrene to Trans-7,8-Dihydroxy-7,8-Dihydrobenzo[a]Pyrene by Recombinant Human Cytochrome P450 1B1 and Purified Liver Epoxide Hydrolase. *Chem Res Toxicol* **1999**, *12* (7), 623–629. https://doi.org/10.1021/tx990028s.
(161) Pilcher, W.; Miles, S.; Tang, S.; Mayer, G.; Whitehead, A. Genomic and Genotoxic Responses to Controlled Weathered-Oil Exposures Confirm and Extend Field Studies on

Impacts of the Deepwater Horizon Oil Spill on Native Killifish. *PLoS One* **2014**, *9* (9). https://doi.org/10.1371/journal.pone.0106351.
(162) Whitehead, A.; Dubansky, B.; Bodinier, C.; Garcia, T. I.; Miles, S.; Pilley, C.; Raghunathan, V.; Roach, J. L.; Walker, N.; Walter, R. B.; Rice, C. D.; Galvez, F. Genomic and Physiological Footprint of the Deepwater Horizon Oil Spill on Resident Marsh Fishes. *Proc Natl Acad Sci U S A* **2012**, *109* (50), 20298–20302. https://doi.org/10.1073/pnas.1109545108.
(163) Grove, A. D.; Llewellyn, G. C.; Kessler, F. K.; White, K. L.; Crespi, C. L.; Ritter, J. K. Differential Protection by Rat UDP-Glucuronosyltransferase 1A7 against Benzo[a]Pyrene-3,6-Quinone- versus Benzo[a]Pyrene-Induced Cytotoxic Effects in Human Lymphoblastoid Cells. *Toxicol Appl Pharmacol* **2000**, *162* (1), 34–43. https://doi.org/10.1006/taap.1999.8815.
(164) Allain, E. P.; Rouleau, M.; Lévesque, E.; Guillemette, C. Emerging Roles for UDP-Glucuronosyltransferases in Drug Resistance and Cancer Progression. *Br J Cancer* **2020**, *122* (9), 1277–1287. https://doi.org/10.1038/s41416-019-0722-0.
(165) Moise, P. A.; Birmingham, M. C.; Schentag, J. J. Pharmacokinetics and Metabolism of Moxifloxacin. *Drugs Today (Barc)* **2000**, *36* (4), 229–244. https://doi.org/10.1358/dot.2000.36.4.570201.
(166) *Water Quality Monitoring: A Practical Guide to the Design and Implementation of Freshwater Quality Studies and Monitoring Programmes*, 1st ed.; Bartram, J., Ballance, R., United Nations, World Health Organization, Eds.; E & FN Spon: London ; New York, 1996.
(167) Twenty-Five Years After the Exxon Valdez Oil Spill: NOAA's Scientific Support, Monitoring, and Research. 78.
(168) Summary of Information Concerning the Ecological and Economic Impacts of the BP Deepwater Horizon Oil Spill Disaster https://www.nrdc.org/resources/summary-information-concerning-ecological-and-economic-impacts-bp-deepwater-horizon-oil (accessed 2021 -07 -03).
(169) Veldhoen, N.; Ikonomou, M. G.; Rehaume, V.; Dubetz, C.; Patterson, D. A.; Helbing, C. C. Evidence of Disruption in Estrogen-Associated Signaling in the Liver Transcriptome of in-Migrating Sockeye Salmon of British Columbia, Canada. *Comp Biochem Physiol C Toxicol Pharmacol* **2013**, *157* (2), 150–161. https://doi.org/10.1016/j.cbpc.2012.10.007.
(170) Veldhoen, N.; Beckerton, J. E.; Mackenzie-Grieve, J.; Stevenson, M. R.; Truelson, R. L.; Helbing, C. C. Development of a Non-Lethal Method for Evaluating Transcriptomic Endpoints in Arctic Grayling (Thymallus Arcticus). *Ecotoxicol Environ Saf* **2014**, *105*, 43–50. https://doi.org/10.1016/j.ecoenv.2014.03.030.
(171) Anglès d'Auriac, M. B.; Urke, H. A.; Kristensen, T. A Rapid QPCR Method for Genetic Sex Identification of *Salmo Salar* and *Salmo Trutta* Including Simultaneous Elucidation of Interspecies Hybrid Paternity by High-Resolution Melt Analysis: *Salmo* Sex and Hybrid Paternity Identification. *J Fish Biol* **2014**, *84* (6), 1971–1977. https://doi.org/10.1111/jfb.12401.
(172) Brunelli, J. P.; Thorgaard, G. H. A New Y-Chromosome-Specific Marker for Pacific Salmon. *Trans Am Fish Soc* **2004**, *133* (5), 1247–1253. https://doi.org/10.1577/T03-049.1.
(173) Yano, A.; Nicol, B.; Jouanno, E.; Quillet, E.; Fostier, A.; Guyomard, R.; Guiguen, Y. The Sexually Dimorphic on the Y-Chromosome Gene (*SdY*) Is a Conserved Male-Specific Y-

Chromosome Sequence in Many Salmonids. *Evol Appl* **2013**, *6* (3), 486–496. https://doi.org/10.1111/eva.12032.

Appendices

Appendix 1. Water chemistry results for LSMD, HSFO, dilbit, and Alaskan crude WAFs are shown across 8 tanks per WAF concentration before and after exposure. Average ± standard deviation is shown. SW, seawater.

Treatment	Time (h)	Salinity (mg/L)	pH	DO (mg/L)	Temperature (°C)
LSMD WAF					
SW Control	0	26.6±0.1	7.9±0.0	8.5±0.0	14.5±0.1
	96	26.7±0.0	8.0±0.1	8.5±0.0	14.6±0.0
Low	0	26.6±0.0	7.9±0.0	8.5±0.1	14.4±0.1
	96	26.7±0.0	8.0±0.0	8.5±0.0	14.5±0.0
Medium	0	26.5±0.0	7.9±0.0	8.6±0.0	14.5±0.1
	96	26.7±0.0	8.0±0.0	8.5±0.2	14.4±0.1
High	0	26.5±0.0	7.9±0.0	8.6±0.0	14.5±0.0
	96	26.7±0.0	8.0±0.0	8.5±0.1	14.5±0.1
HSFO WAF					
SW Control	0	26.6±0.1	7.9±0.0	8.5±0.0	14.5±0.1
	96	26.7±0.0	8.0±0.1	8.5±0.0	14.6±0.0
Low	0	26.6±0.0	7.9±0.0	8.5±0.1	14.4±0.1
	96	26.7±0.0	8.0±0.0	8.5±0.0	14.5±0.0
Medium	0	26.5±0.0	7.9±0.0	8.6±0.0	14.5±0.1
	96	26.7±0.0	8.0±0.0	8.5±0.2	14.4±0.1
High	0	26.5±0.0	7.9±0.0	8.6±0.0	14.5±0.0
	96	26.7±0.0	8.0±0.0	8.5±0.1	14.5±0.1
dilbit WAF					
SW Control	0	26.6±0.1	7.9±0.0	8.5±0.0	14.5±0.1
	96	26.7±0.0	8.0±0.1	8.5±0.0	14.6±0.0
Low	0	26.6±0.0	7.9±0.0	8.5±0.1	14.4±0.1
	96	26.7±0.0	8.0±0.0	8.5±0.0	14.5±0.0
Medium	0	26.5±0.0	7.9±0.0	8.6±0.0	14.5±0.1
	96	26.7±0.0	8.0±0.0	8.5±0.2	14.4±0.1
High	0	26.5±0.0	7.9±0.0	8.6±0.0	14.5±0.0
	96	26.7±0.0	8.0±0.0	8.5±0.1	14.5±0.1
Alaskan crude WAF					
SW Control	0	26.6±0.1	7.9±0.0	8.5±0.0	14.5±0.1
	96	26.7±0.0	8.0±0.1	8.5±0.0	14.6±0.0
Low	0	26.6±0.0	7.9±0.0	8.5±0.1	14.4±0.1
	96	26.7±0.0	8.0±0.0	8.5±0.0	14.5±0.0
Medium	0	26.5±0.0	7.9±0.0	8.6±0.0	14.5±0.1
	96	26.7±0.0	8.0±0.0	8.5±0.2	14.4±0.1
High	0	26.5±0.0	7.9±0.0	8.6±0.0	14.5±0.0
	96	26.7±0.0	8.0±0.0	8.5±0.1	14.5±0.1

Appendix 2. List of the 50 PAHs and alkylated PAHs included in the tPAH50 analysis

#	Analyte	Abbreviation	Ring #	Molecular Formula	Monoisotopic Mass	CAS#	Pictorial Example
1	Naphthalene	NAP	2	C10H8	128.0626	91-20-3	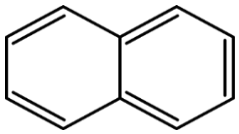 **e.g. Naphthalene**
2	C1-Naphthalene	NAP1	2	C11H10	142.0782	-	
3	C2-Naphthalene	NAP2	2	C12H12	156.0939	-	
4	C3-Naphthalene	NAP3	2	C13H14	170.1095	-	
5	C4-Naphthalene	NAP4	2	C14H16	184.1252	-	
6	Biphenyl	BIP	2	C12H10	154.0782	92-52-4	
7	Dibenzofuran	DBF	3	C12H8O	168.0575	132-64-9	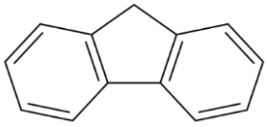 **e.g., Fluorene**
8	Acenaphthylene	APY	3	C12H8	152.0626	208-96-8	
9	Acenaphthene	APE	3	C12H10	154.0782	83-32-9	
10	Fluorene	FLR	3	C13H10	166.0782	86-73-7	
11	C1-Fluorene	FLR1	3	C14H12	180.0939	-	
12	C2-Fluorene	FLR2	3	C15H14	194.1095	-	
13	C3-Fluorene	FLR3	3	C16H16	208.1252	-	
14	Anthracene	ANT	3	C14H10	178.0782	120-12-7	
15	Phenanthrene	PHEN	3	C14H10	178.0782	1985-01-08	
16	C1-Phenanthrene/ Anthracene	PHEN1	3	C15H12	192.0939	-	
17	C2-Phenanthrene/ Anthracene	PHEN2	3	C16H14	206.1095	-	
18	C3-Phenanthrene/ Anthracene	PHEN3	3	C17H16	220.1252	-	
19	C4-Phenanthrene/ Anthracene	PHEN4	3	C18H18	234.1409	-	
20	Dibenzothiophene	DBT	3	C12H8S	184.0347	132-65-0	
21	C1-Dibenzothiophene	DBT1	3	C13H10S	198.0503	-	
22	C2-Dibenzothiophene	DBT2	3	C14H12S	212.066	-	
23	C3-Dibenzothiophene	DBT3	3	C15H14S	226.0816	-	
24	C4-Dibenzothiophene	DBT4	3	C16H16S	240.0972	-	
25	Benzo(b)fluorene	BDF	4	C17H12	216.0939	243-17-4	
26	Fluoranthene	FLT	4	C16H10	202.0782	206-44-0	
27	Pyrene	PYR	4	C16H10	202.0782	129-00-0	
28	C1-Fluoranthene/Pyrene	FLT1	4	C17H12	216.0939	-	
29	C2-Fluoranthene/Pyrene	FLT2	4	C18H14	230.1095	-	

30	C3-Fluoranthene/Pyrene	FLT3	4	C19H16	244.1251	-	
31	C4-Fluoranthene/Pyrene	FLT4	4	C20H18	258.1407	-	
32	Naphthobenzothiophene	NBT	4	C16H10S	234.0503	239-35-0	
33	C1-Naphthobenzothiophene	NBT1	4	C17H12S	248.066	-	
34	C2-Naphthobenzothiophene	NBT2	4	C18H14S	262.0816	-	
35	C3-Naphthobenzothiophene	NBT3	4	C19H16S	276.0972	-	
36	C4-Naphthobenzothiophene	NBT4	4	C20H18S	290.1128	-	
37	Benzo(a)anthracene	BAA	4	C18H12	228.0939	56-55-3	
38	Chrysene+Triphenylene	CT	4	C18H12	228.0939	218-01-9, 217-59-4	
39	C1-Benzo[a]anthracene/ Chrysene	BAA1	4	C19H14	242.1095	-	
40	C2-Benzo[a]anthracene/ Chrysene	BAA2	4	C20H16	256.1252	-	
41	C3-Benzo[a]anthracene/ Chrysene	BAA3	4	C21H16, C21H18	268.1252, 270.1408*	-	
42	C4-Benzo[a]anthracene/ Chrysene	BAA4	4	C22H20	284.1565	-	
43	Benzo(b)fluoranthene	BBF	5	C20H12	252.0939	205-99-2	
44	Benzo(j+k)fluoranthene	BJK	5	C20H12	252.0939	205-82-3, 207-08-9	
45	Benzo(a)fluoranthene	BAF	5	C20H12	252.0939	203-33-8	
46	Benzo(e)pyrene	BEP	5	C20H12	252.0939	192-97-2	
47	Benzo(a)pyrene	BAP	5	C20H12	252.0939	50-32-8	
48	Dibenzo(a,h)anthracene	DAH	5	C22H14	278.1096	53-70-3	
49	Indeno(1,2,3-cd)pyrene	ICDP	6	C22H12	276.0939	193-39-5	
50	Benzo(g,h,i)perylene	BGHIP	6	C22H12	276.0939	191-24-2	

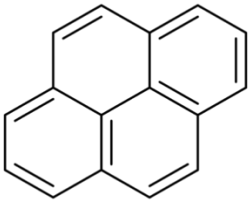

e.g., Pyrene

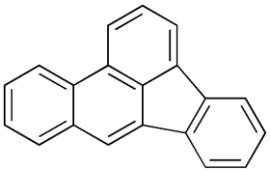

e.g. Benzo(e)fluoranthene

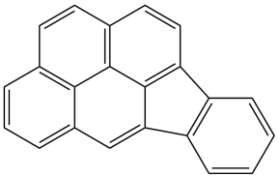

e.g. Indeno(1,2,3-cd)pyrene

*Note: Molecular weight differs depending on alkyl group position and structure

Appendix 3. Comparison of the PAH selection used in our tPAH50 analysis with lists generated by the US Environmental Protection Agency (EPA) and National Oceanic and Atmospheric Administration (NOAA). The EPA first listed 16 PAH compounds on their priority pollutant list in the 1980s (EPA 16).[110] In 1991, NOAA introduced a list of 24 PAHs for their monitoring programs (NOAA 24).[110] The EPA later introduced a more comprehensive list of 34 PAHs (EPA 34) and suggested it as the minimum list to use in establishing equilibrium partitioning sediment benchmarks for PAHs.[18] The tPAH50 list is based on the extensive analyses done by many labs following the Deepwater Horizon oil spill. The list includes all PAH and related hetero-polycyclic compounds reported as part of the standard PAH analysis performed for the Deepwater Horizon Natural Resource Damage Assessment.[98]

Analyte	EPA 16	NOAA 24	EPA 34	tPAH50
Naphthalene	X	X	X	X
C1-Naphthalene			X	X
C2-Naphthalene			X	X
C3-Naphthalene			X	X
C4-Naphthalene			X	X
Biphenyl		X		X
Dibenzofuran				X
Acenaphthylene	X	X	X	X
Acenaphthene	X	X	X	X
Fluorene	X	X	X	X
C1-Fluorene			X	X
C2-Fluorene			X	X
C3-Fluorene			X	X
Anthracene	X	X	X	X
Phenanthrene	X	X	X	X
C1-Phenanthrene/Anthracene			X	X
C2-Phenanthrene/Anthracene			X	X
C3-Phenanthrene/Anthracene			X	X
C4-Phenanthrene/Anthracene			X	X
Dibenzothiophene				X
C1-Dibenzothiophene				X
C2-Dibenzothiophene				X
C3-Dibenzothiophene				X
C4-Dibenzothiophene				X
Benzo(b)fluorine				X
Fluoranthene	X	X	X	X
Pyrene	X	X	X	X

C1-Fluoranthenes/Pyrene			X	X
C2-Fluoranthenes/Pyrene				X
C3-Fluoranthenes/Pyrene				X
C4-Fluoranthenes/Pyrene				X
Naphthobenzothiophene				X
C1-Naphthobenzothiophene				X
C2-Naphthobenzothiophene				X
C3-Naphthobenzothiophene				X
C4-Naphthobenzothiophene				X
Benzo(a)anthracene	X	X	X	X
Chrysene+Triphenylene	X	X	X	X
C1-Chrysenes			X	X
C2-Chrysenes			X	X
C3-Chrysenes			X	X
C4-Chrysenes			X	X
Benzo(b)fluoranthene	X	X	X	X
Benzo(j+k)fluoranthene	X	X	X	X
Benzo(a)fluoranthene				X
Benzo(e)pyrene		X	X	X
Benzo(a)pyrene	X	X	X	X
Dibenzo(a,h)anthracene	X	X	X	X
Indeno(1,2,3-c,d)pyrene	X	X	X	X
Benzo(g,h,i)perylene	X	X	X	X
1-Methylnaphthalene		X		
2,6-Dimethylnaphthalene		X		
1,6,7-Trimethylnaphthalene		X		
1-Methylphenanthrene		X		
Perylene		X	X	

Appendix 4. qPCR primers validated for transcript and sex genotype analyses in the present study.

Primer Set	Gene Target	Target ID	Primer Name	Primer Sequence	Amplicon Size	Reference
Normalizers						
gapdh	*Glyceraldehyde 3-phosphate dehydrogenase*	ONQ12	ONQ12 up	CCRCCAGAACATYATCCC	81	[99]
			ONQ12 dn	GTCAGCTTGCCRTTSAGC		
rpl8[a]	*Ribosomal protein L8*	ONQ11	ONQ11 up	TTGGTAATGTTCTGCCTGTG	130	[99]
			ONQ11 dn	GGGTTGTGGGAGATGACTG		
rps10[a]	*Ribosomal protein S10*	ONQ22b	ONQ 22b up	TTGTTCCTGCCACTCTGC	176	[169]
			ONQ 22a dn	ACCTGCCTCTGCTTTCTT		
Target Gene Transcripts						
ahr[a]	*Aryl hydrocarbon receptor alpha*	ONQ5	ONQ5 up	GCTCCAGATGTGGTCAAGT	123	[99]
			ONQ5 dn	GAGTTTGTCCAGGCGAGA		
cyp1a1[a]	*Cytochrome P450, family 1, subfamily A*	ONQ6	ONQ6 up	TCATCAACGACGGCAAGA	317	[169]
			ONQ6 dn	GTTCACCAAGCCCAACAG		
cyp19	*Cytochrome p450, family 19*	ONQ4.1	ONQ4.1 up	AGCGGACAGTAGGGATCT	77	[99]
			ONQ4.1 dn	TCCAGAGGGGTCAGTCAT		
hsp70	*Heat shock protein 70*	ONQ24	ONQ24 up	GCACCACCTACTCCTGTG	359	[170]
			ONQ24 dn	AGCGATCTCCYTCATCTT		
mta	*Metallothionein A*	ONQ7	ONQ7 up	ATCTTGCAACTGCGGTGG	83	[99]
			ONQ7 dn	GACAGCAGTCGCAGCAAC		
sod	*Superoxide dismutase*	ONQ23	ONQ23 up	CGGGACCGTATTCTTTGA	357	[99]
			ONQ23 dn	TCCTCGTTGYCTCCTTTT		
vepg	*Vitelline envelope protein gamma*	ONQ2	ONQ2 up	AGCCAGAGCCCAAGATTA	308	[99]
			ONQ2 dn	GGTGTTTGCCAGAGGTTT		
vtg	*Vitellogenin A*	ONQ1	ONQ1 up	GTCTATGAGTTGCAGGAGG	223	[99]
			ONQ1 dn	TGAGGTAKTTGTAAGTGGC		
Sex Genotyping						
gapdh	*Glyceraldehyde 3-phosphate dehydrogenase*	*gapdh*	Gapdh-f2	AAGGCCATGCCAGTCAGCT	256	[171]
			Gapdh-r	GTAATGCATCTTGCACGAGT		
OtY2	*Salmonid Y-chromosome marker*	*OtY2-WSU*	OTY2-f2	CTGGTTCGAGCCTAAGTAG	260	[172]
			OTY2-r2	GATGCAGTAGGAGCAGATG		
sdY	*Sexually dimorphic on the Y-chromosome*	*U-sdY*	UsdY-Fw	CCCAGCACTSTTTTCTTYTCTCA	220	[173]
			UsdY-Rv2	CTTAAAACRACTCCACCCTCCAT		

[a]Primer amplicons confirmed to span gene intron/exon boundary.

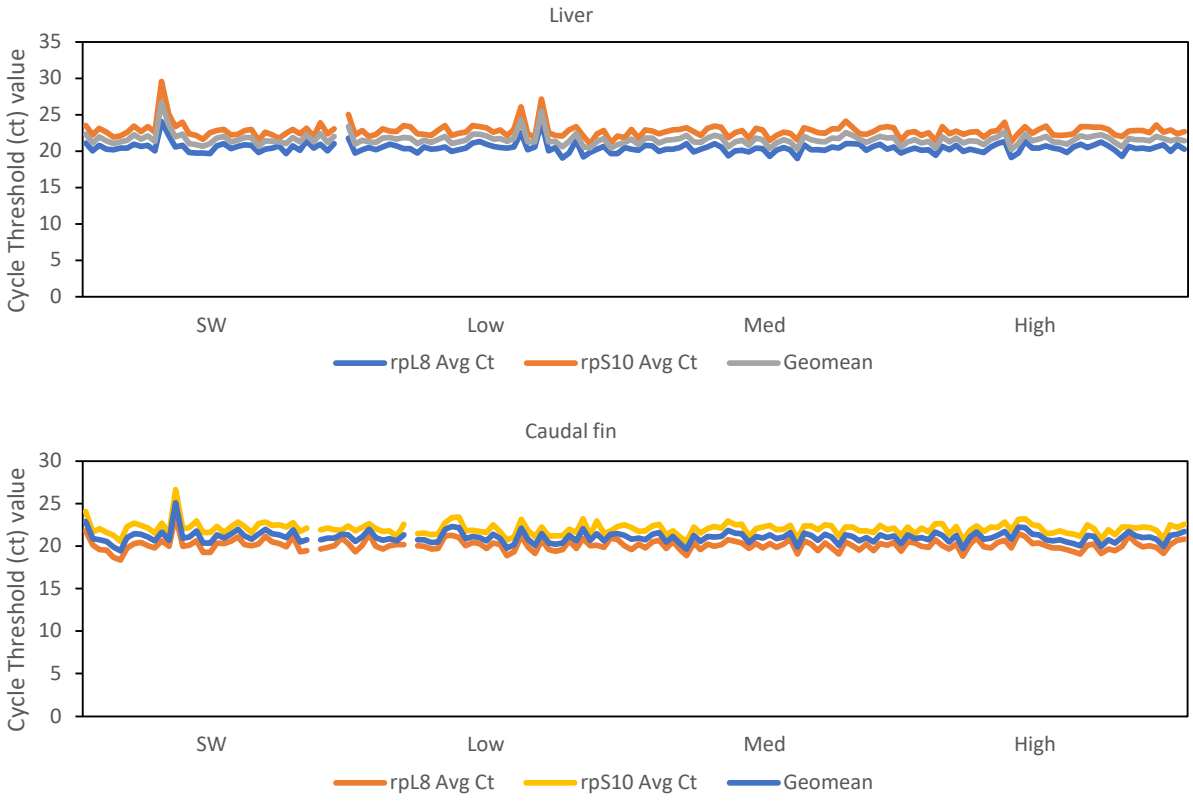

Appendix 5. Distribution of C_t values of normalizer genes used for the LSMD WAF exposure.

Appendix 6. Primer efficiency scores of qPCR tools used in the present study. The primer pair efficiencies for normalizers are reported as a ratio between 0 and 1. The normalizers were used to obtain a geometric mean which was used in the $\Delta\Delta C_t$ analysis. Target gene primer pair efficiencies are reported as the absolute value of the $\log_2$ cDNA concentration versus ΔC_t (test gene – geometric mean) where 100% efficiency = 0. "-" indicates that the tool failed quality control with that tissue. Primer efficiency curves are presented in **Appendix 24** and **Appendix 25.**

Primer Set	Gene Target	Assay Criteria	
		Liver	Caudal Fin
Normalizers		Normalizer Efficiency	
gapdh	*Glyceraldehyde 3- phosphate dehydrogenase*	0.99	0.98
rpl8	*Ribosomal protein L8*	1.00	1.00
rps10	*Ribosomal protein S10*	0.99	0.99
Target Gene Transcripts		[cDNA] vs Normalized ΔCt	
ahr	*Aryl hydrocarbon receptor alpha*	0.04	0.02
cyp1a	*Cytochrome P450, family 1, subfamily A*	0.11	0.11
cyp19	*Cytochrome p450, family 19*	0.14	0.00
hsp70	*Heat shock protein 70*	0.05	0.01
mta	*Metallothionein A*	0.09	-
sod	*Superoxide dismutase*	0.01	0.02
vepg	*Vitelline envelope protein gamma*	0.10	0.08
vtg	*Vitellogenin A*	0.14	0.04

Appendix 7. Water chemistry results measuring PAHs (n=4) and volatile organic compounds (n=1) in the marine seawater supply used in the present study. Median ± median absolute deviation is shown.

Analyte	Concentration in Seawater (µg/L)
Naphthalene	0.0084±0.0002
C1-Naphthalene	0.0070±0.0003
C2-Naphthalene	<LOQ
C3-Naphthalene	<LOQ
C4-Naphthalene	<LOQ
Biphenyl	<LOQ
Dibenzofuran	0.0041±0.0000
Acenaphthylene	<LOQ
Acenaphthene	<LOQ
Fluorene	<LOQ
C1-Fluorene	<LOQ
C2-Fluorene	<LOQ
C3-Fluorene	<LOQ
Anthracene	<LOQ
Phenanthrene	0.0068±0.0003
C1-Phenanthrene/Anthracene	<LOQ
C2-Phenanthrene/Anthracene	<LOQ
C3-Phenanthrene/Anthracene	<LOQ
C4-Phenanthrene/Anthracene	<LOQ
Dibenzothiophene	<LOQ
C1-Dibenzothiophene	<LOQ
C2-Dibenzothiophene	<LOQ
C3-Dibenzothiophene	<LOQ
C4-Dibenzothiophene	<LOQ
Benzo(b)fluorene	<LOQ
Fluoranthene	<LOQ
Pyrene	<LOQ
C1-Fluoranthene/Pyrene	<LOQ
C2-Fluoranthene/Pyrene	<LOQ
C3-Fluoranthene/Pyrene	<LOQ
C4-Fluoranthene/Pyrene	<LOQ
Naphthobenzothiophene	<LOQ
C1-Naphthobenzothiophene	<LOQ
C2-Naphthobenzothiophene	<LOQ
C3-Naphthobenzothiophene	<LOQ
C4-Naphthobenzothiophene	<LOQ
Benzo(a)anthracene	<LOQ

Chrysene+Triphenylene	<LOQ
C1-Benzo[a]anthracene/Chrysene	<LOQ
C2-Benzo[a]anthracene/Chrysene	<LOQ
C3-Benzo[a]anthracene/Chrysene	<LOQ
C4-Benzo[a]anthracene/Chrysene	<LOQ
Benzo(b)fluoranthene	<LOQ
Benzo(j+k)fluoranthene	<LOQ
Benzo(a)fluoranthene	<LOQ
Benzo(e)pyrene	<LOQ
Benzo(a)pyrene	<LOQ
Dibenzo(a,h)anthracene	<LOQ
Indeno(1,2,3-cd)pyrene	<LOQ
Benzo(g,h,i)perylene	<LOQ
tPAH50	0.0261±0.0008
Volatile Organic Compounds	
Chloroform	<LOQ
Bromodichloromethane	<LOQ
Dibromochloromethane	<LOQ
Bromoform	<LOQ

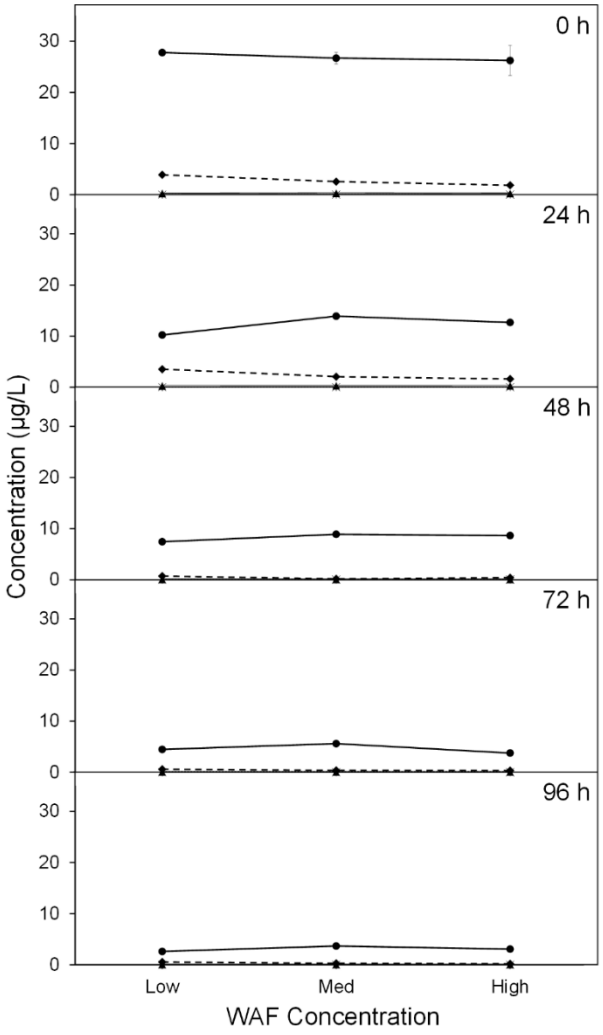

Appendix 8. The distribution of the PAHs grouped by number of aromatic rings is consistent between all LSMD WAF concentrations over time. The sum of PAH concentrations grouped by aromatic ring composition for Low, medium (Med), and High concentration WAF (equivalent to 100, 320, or 1000 mg/L LSMD, respectively) at the indicated exposure times are shown. Points and errors bars represent the median and median absolute deviation. Ring composition representation: 2 ring (circle and solid line), 3 ring (diamond and dashed line), 4 ring (triangle and solid line), 5-6 ring (X with dotted line).

Appendix 9. Weight and fork length of LSMD, HSFO, dilbit, and Alaskan crude WAF-exposed juvenile coho salmon prior to tissue sampling. Average ± standard deviation is shown. SW, seawater.

Treatment	Weight (g)	Fork Length (cm)
LSMD WAF		
SW Control (n=40)	7.4±1.6	8.6±0.6
Low (n=40)	7.2±1.9	8.5±0.6
Medium (n=40)	7.1±1.4	8.5±0.5
High (n=40)	6.7±1.2	8.4±0.5
HSFO WAF		
Control (n=40)	8.2±1.4	9.0±1.4
Low (n=40)	7.3±1.0	8.8±1.0
Mid (n=40)	7.7±1.3	8.8±1.3
High (n=40)	8.2±1.3	9.0±1.3
Dilbit WAF		
Control (n=40)	10.4±2.4	9.6±0.6
Low (n=40)	9.9±1.6	9.6±0.4
Mid (n=39)	10.9±1.3	9.8±0.4
High (n=40)	11.0±1.7	10.0±0.6
Alaskan crude WAF		
Control (n=40)	12.7±2.0	10.4±0.6
Low (n=40)	11.6±1.5	10.1±0.5
Mid (n=40)	13.2±2.4	10.5±0.6
High (n=40)	12.4±2.6	10.4±0.6

Appendix 10. Distribution of male and female juvenile coho salmon from the LSMD, HSFO, dilbit, and Alaskan crude WAF exposures according to treatment condition as determined by sex genotyping. SW, seawater.

Sex	WAF Concentrations				Totals
	SW Control	Low	Med	High	
LSMD WAF					
Male	26	23	16	18	83
Female	14	17	24	22	77
Totals	40	40	40	40	160
HSFO WAF					
Male	18	19	19	17	73
Female	22	21	21	23	87
Totals	40	40	40	40	160
Dilbit WAF					
Male	17	19	25	19	80
Female	23	21	14	21	79
Totals	40	40	39	40	159
Alaskan crude WAF					
Male	25	20	24	18	87
Female	15	20	16	22	73
Totals	40	40	40	40	160

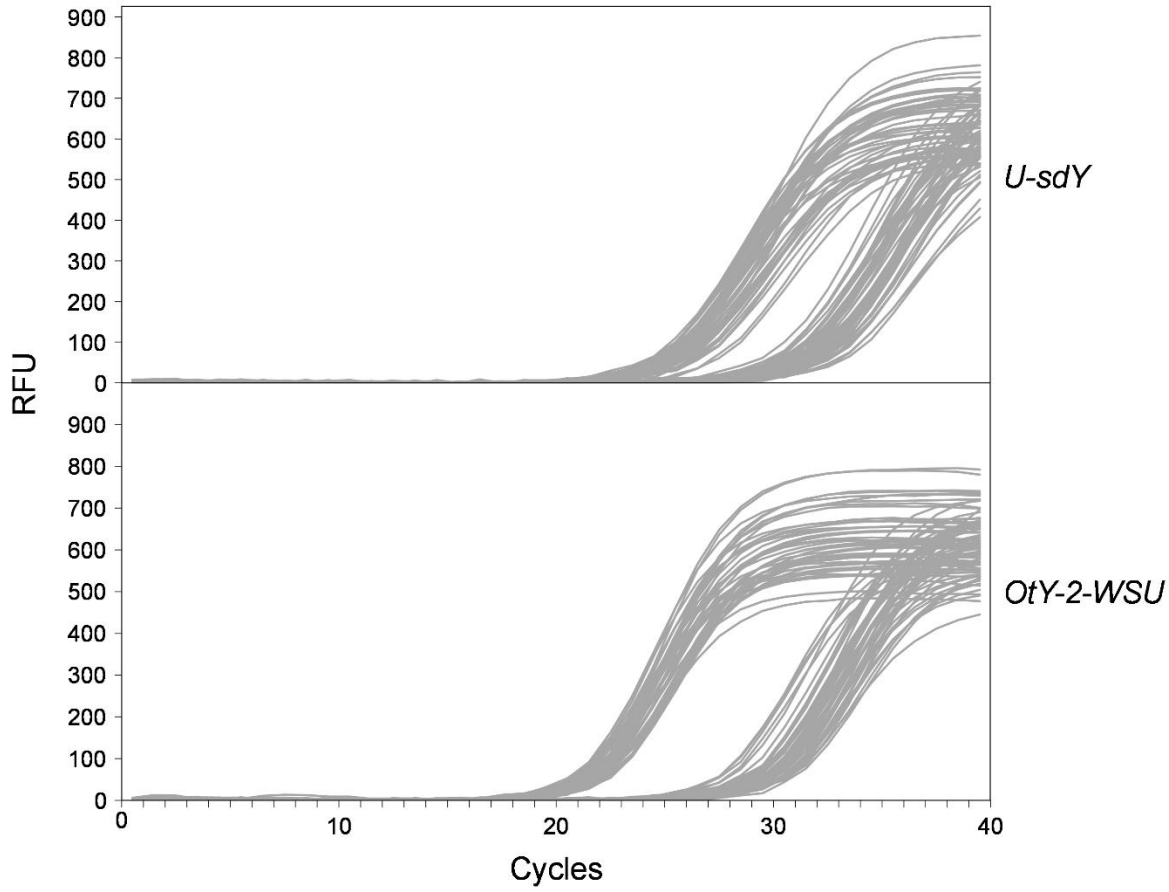

Appendix 11. *OtY2* genotyping results in a greater separation of male and female coho salmon than *sdY*. The qPCR amplification curves of juvenile coho salmon gDNA using *U-sdY* and *OtY2-WSU* primer sets. These data are from a representative 47 salmon (analysed in duplicate). RFU, relative fluorescence units.

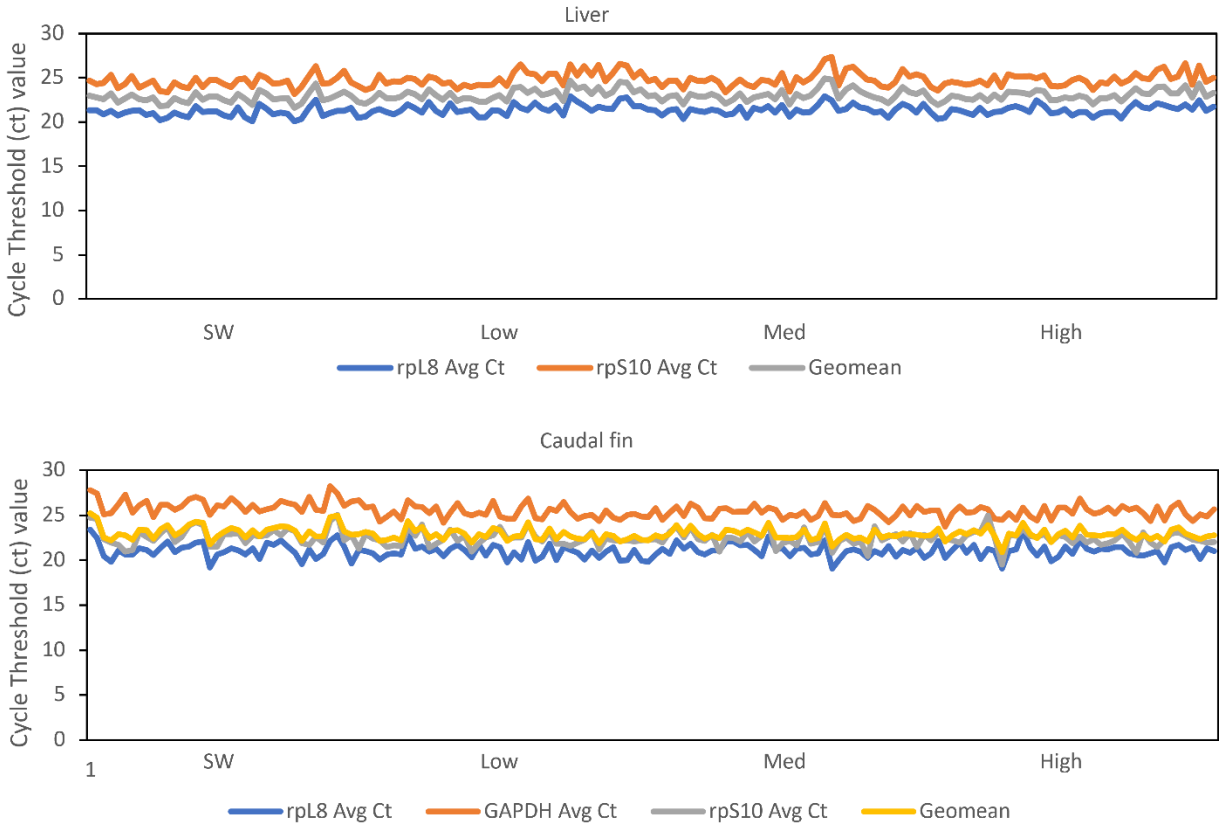

Appendix 12. Distribution of C_t values of normalizer genes used for the HSFO WAF exposure.

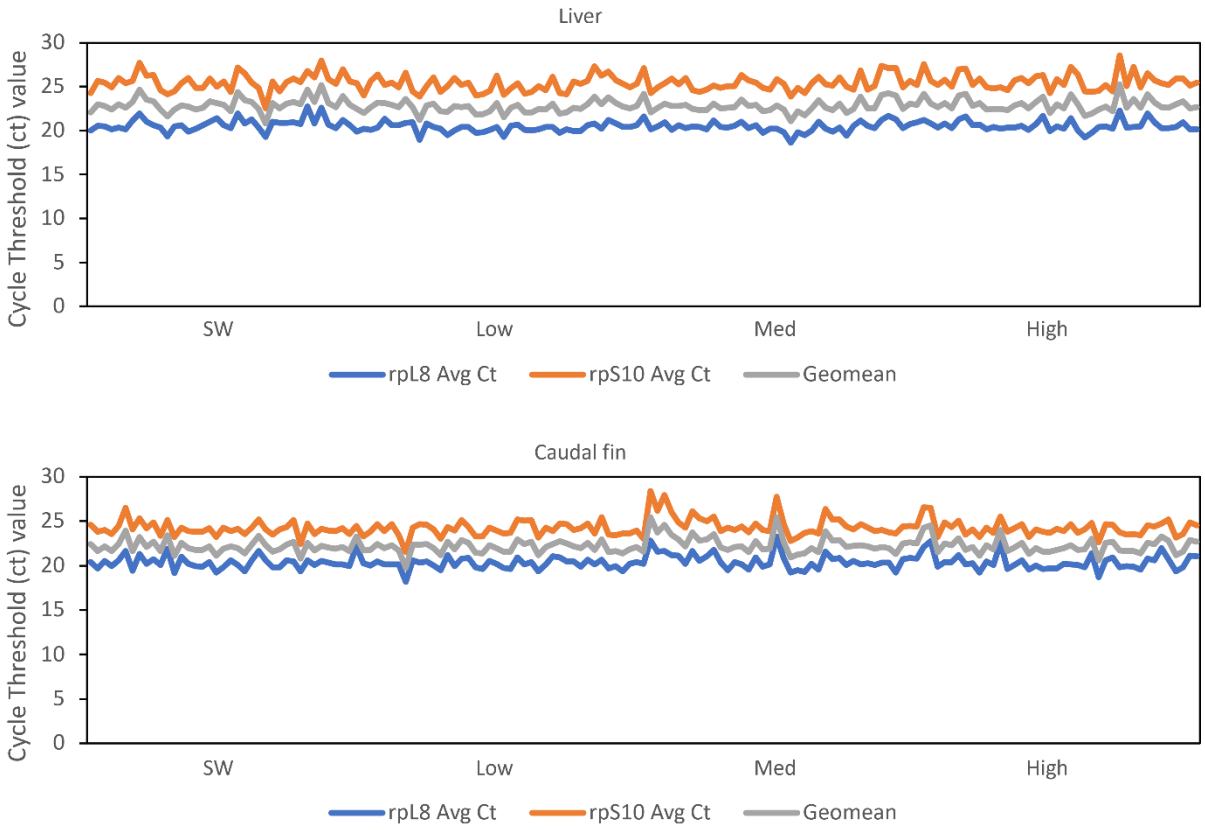

Appendix 13. Distribution of C_t values of normalizer genes used for the dilbit WAF exposure.

Appendix 14. Distribution of C_t values of normalizer genes used for the Alaskan crude WAF exposure.

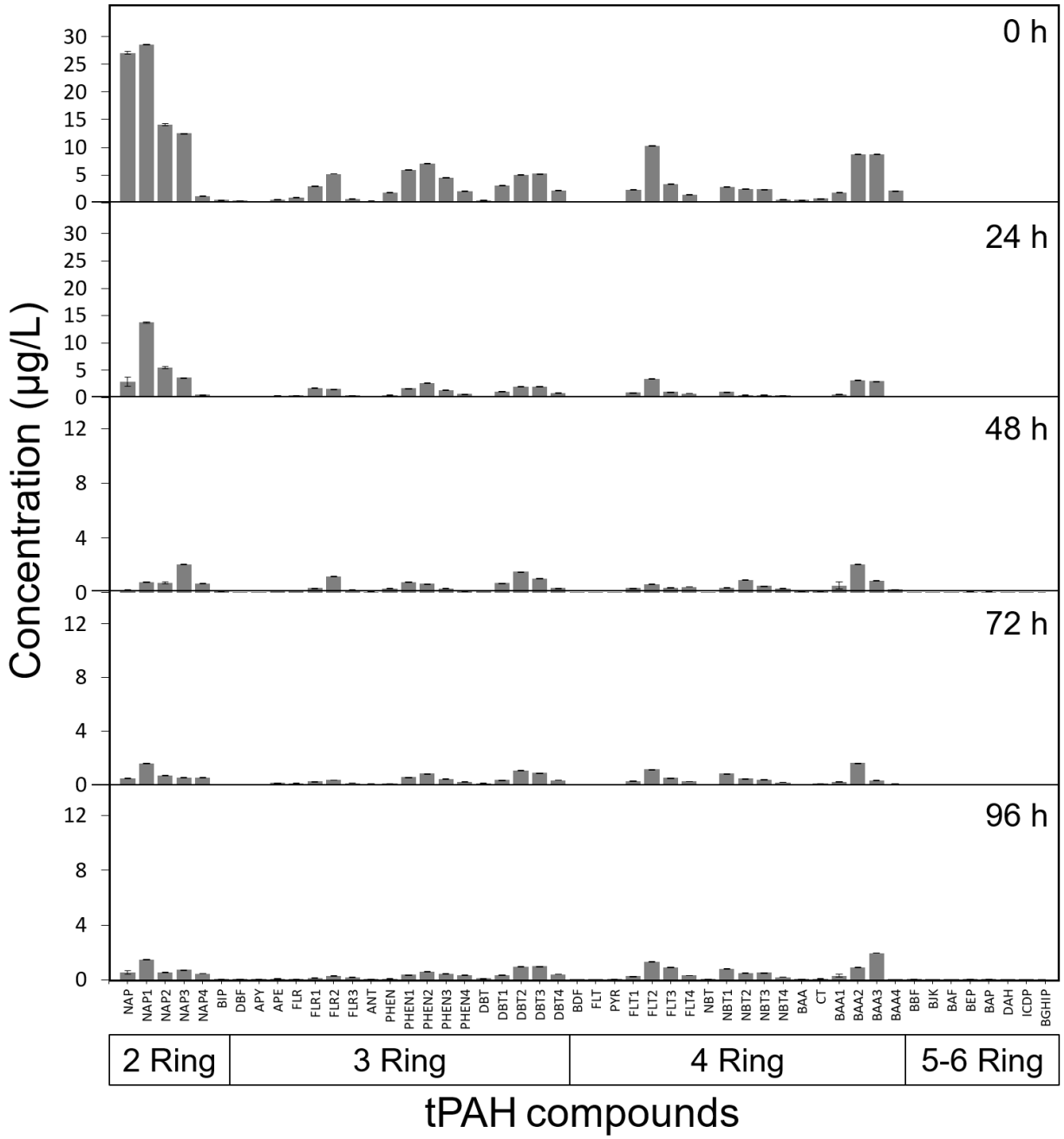

Appendix 15. PAH composition of HSFO WAF over time. Initially, HSFO WAFs are composed of primarily 2 ring PAHs, that rapidly weather out of solution and leave a majority of larger PAH compounds towards the end of the 96-h exposure. The concentrations of PAH analytes grouped by number of rings quantified from the High (1000 mg/L HSFO) WAF concentration over time are shown. The minimum quantifiable limit of PAH concentration was 0.04 µg/L. The low and med WAF concentrations show similar PAH distributions as grouped by ring size. Medians (bars) and median absolute deviation (whiskers) are depicted. Values for individual PAH data not shown.

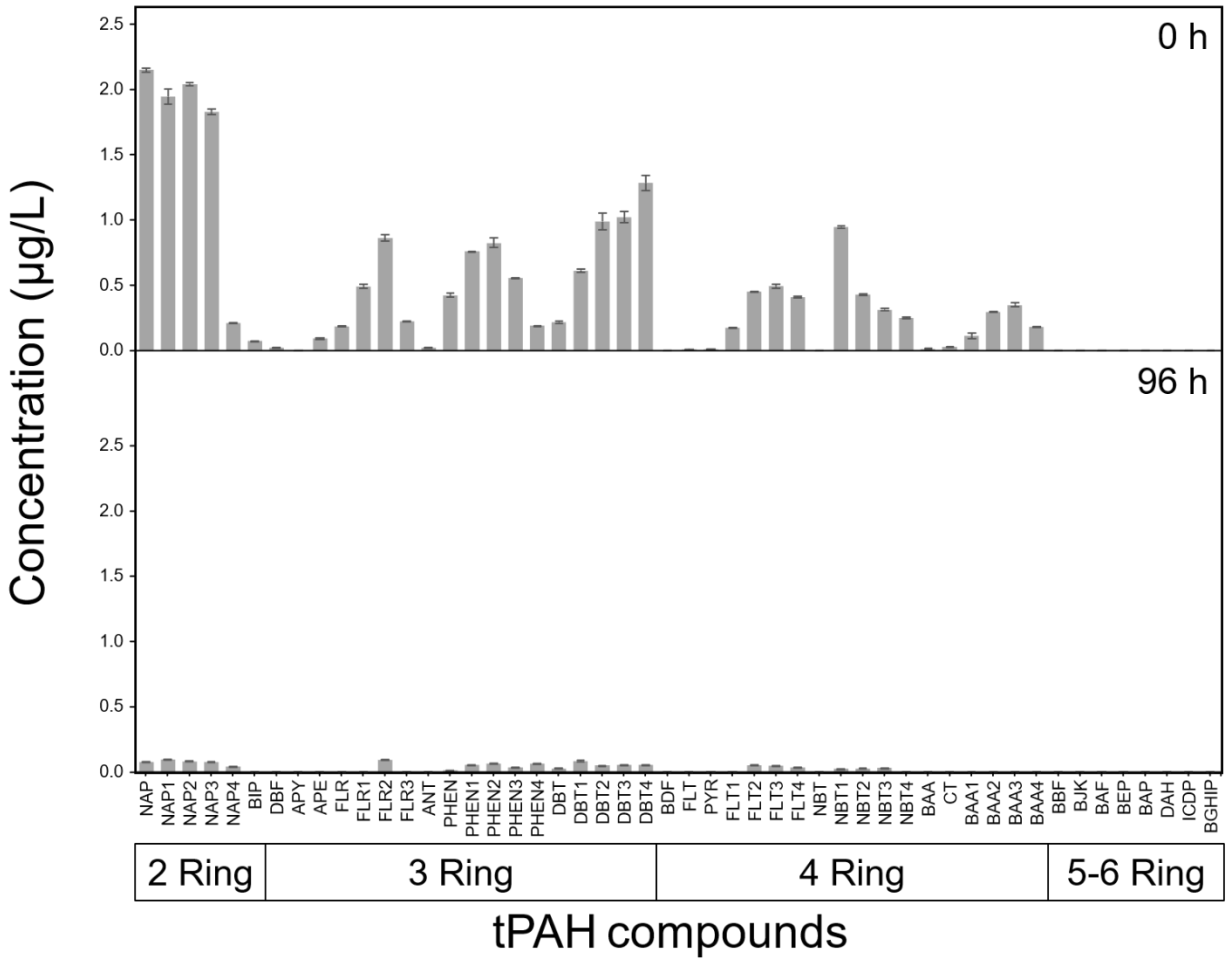

Appendix 16. PAH composition of dilbit WAF during the beginning and end of the 96 h exposures. The concentrations of PAH analytes grouped by number of rings quantified from the medium (320 mg/L dilbit) WAF concentration over time are shown. Values for individual PAH data not shown. For more details, see **Appendix 15** legend.

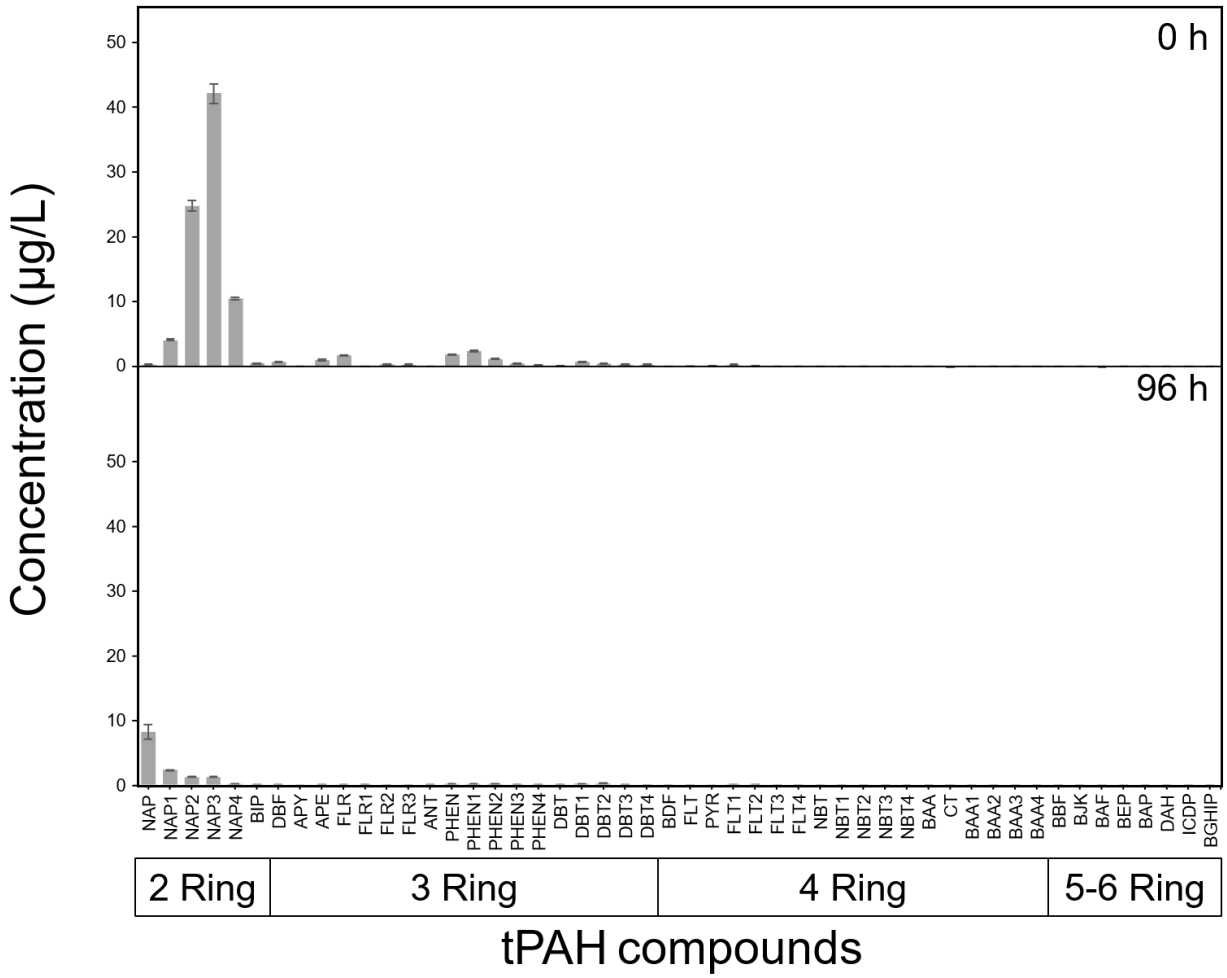

Appendix 17. PAH composition of Alaskan crude WAF during the beginning and end of the 96 h exposures. The concentrations of PAH analytes grouped by number of rings quantified from the medium (320 mg/L Alaskan crude) WAF concentration over time are shown. For more details, see **Appendix 15** legend.

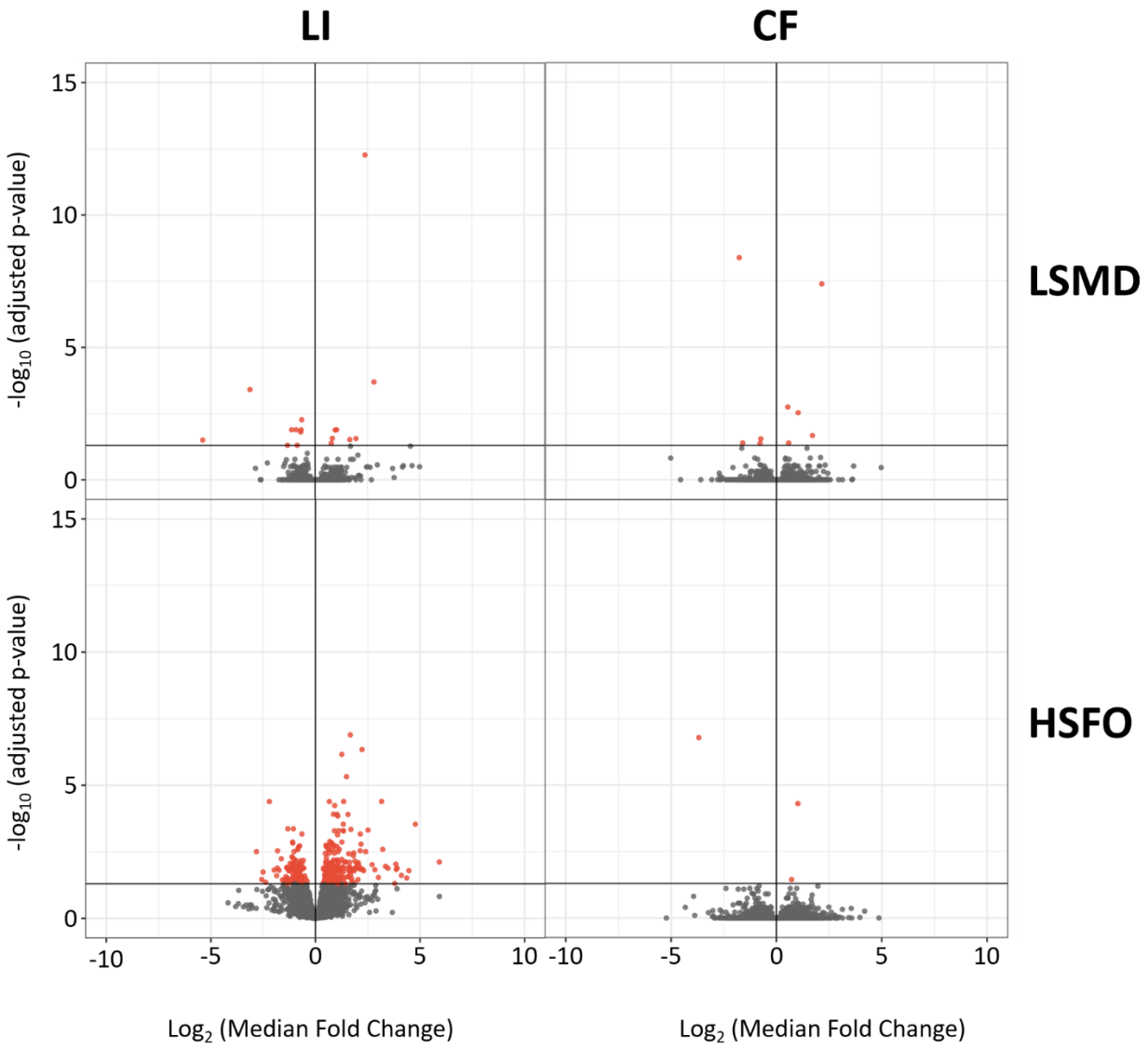

Appendix 18. Volcano plots contrasting 5 males to 5 female transcript profiles in the liver and caudal fin in the seawater control exposures. Differentially expressed genes as determined by DESEQ2 are represented by red dots and not differentially expressed genes are represented by grey dots ($p_{adj} < 0.05$). Individual isoform abundance was grouped to give counts of gene expression rather than individual transcript expression. Significance cut-off is represented by the horizontal bar separating the red and grey dots. Degree of differential expression is depicted by an increasing –log10 of the p_{adj} value for each transcript. Median fold change in transcript abundance is expressed in a log2 scale.

Appendix 19. High concentration LSMD WAF exposure results in six genes that are differentially expressed in all tissues. Fold-change (FC) and adjusted p-value (p_{adj}) are displayed for each transcript. Annotations are based on Blastn results of each transcript against NCBI's nucleotide (nt) database and represented as Accession number of the top hit, percent identity (%id) of the query sequence to the result, and the annotated name of the result.

ContigID	LI-F		LI-M		CF-F		CF-M		Accession number	%id	Blastn Annotation
	FC	P_{adj}	FC	P_{adj}	FC	P_{adj}	FC	P_{adj}			
COHO.12578	15	6.29 E-12	5	7.33 E-04	4	2.57 E-08	6	3.50 E-18	BT045022.1	95.8	Salmo salar clone ssal-rgf-510-032 Cytochrome P450 1B1 putative mRNA, complete cds
COHO.29488	1	3.98 E-02	2	1.54 E-02	2	4.01 E-02	3	4.75 E-05	XM 20478960.1	100	PREDICTED: Oncorhynchus kisutch UDP-glucuronosyltransferase-like (LOC109887636), mRNA
COHO.7107	6	9.09 E-18	10	1.20 E-16	11	9.43 E-05	7	9.83 E-08	XM 20488935.1	100	PREDICTED: Oncorhynchus kisutch cytochrome P450 1A1 (LOC109895321), mRNA
gene36783	2	2.13 E-02	2	8.98 E-03	3	1.46 E-07	4	2.74 E-09	XM 21578846.1	97.8	PREDICTED: Oncorhynchus mykiss UDP-glucuronosyltransferase-like (LOC110501343), mRNA
gene4427	6	2.43 E-13	8	1.46 E-17	12	2.08 E-05	6	9.45 E-07	XR 2252757.1	100	PREDICTED: Oncorhynchus kisutch cytochrome P450 1A1-like (LOC109874903), misc RNA
gene44441	1	4.13 E-02	2	7.33 E-04	3	4.22 E-09	4	1.75 E-10	XR 2254784.1	100	PREDICTED: Oncorhynchus kisutch UDP-glucuronosyltransferase-like (LOC109886608), misc RNA

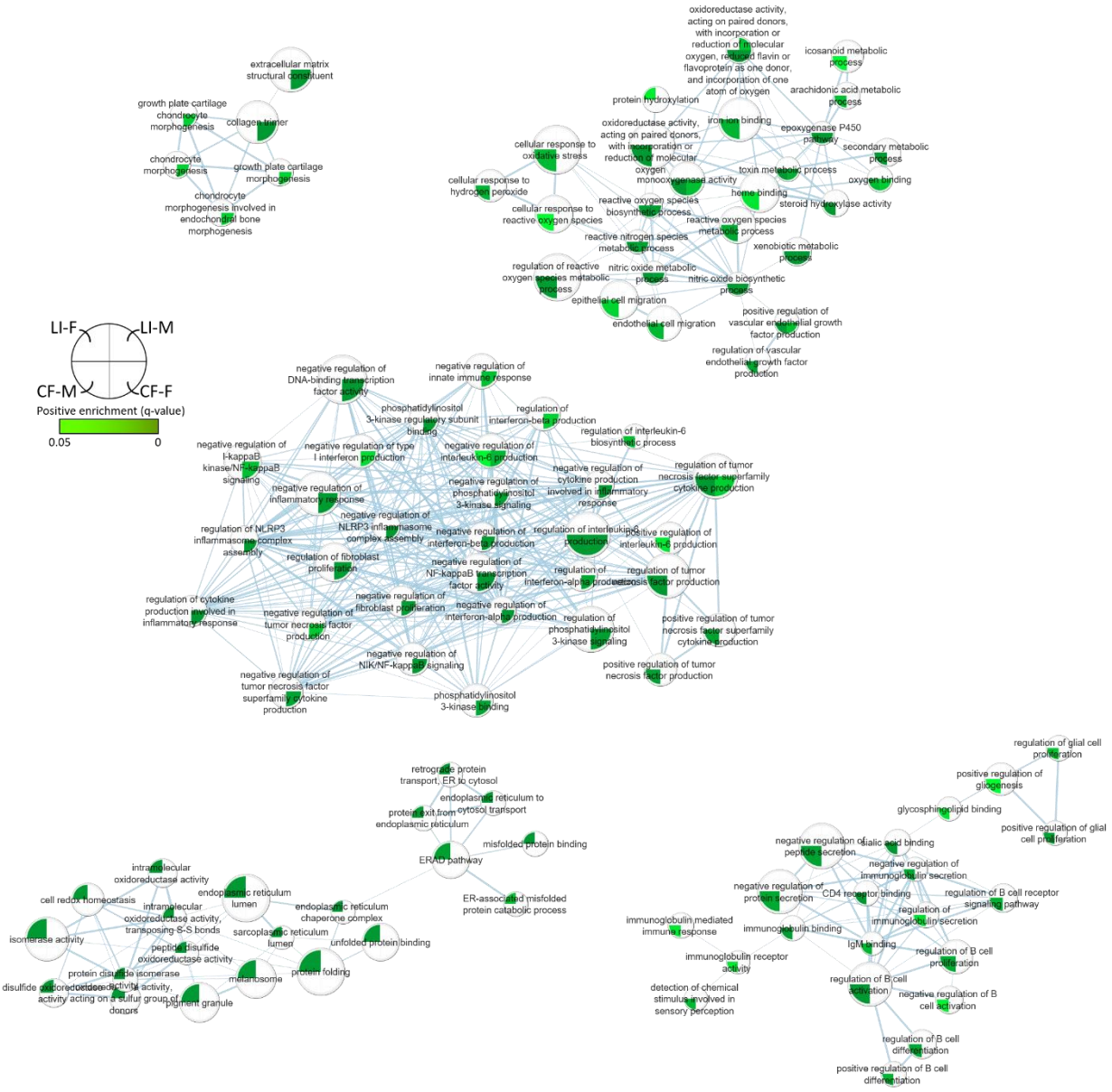

Appendix 20-1. Map of enriched GO terms from LSMD WAF after applying an extremes filter (minimum ten, maximum 300 annotated genes). Significantly enriched GO terms (p_{adj}, FDR<0.05) were visualized using the Cytoscape Enrichment Map plugin. Enrichment is relative to a background containing GO-terms represented from all genes expressed from their respective tissue-types (males and females combined). Each node represents a GO term. Each tissue is represented by a single quadrant of GO term nodes. If a tissues quadrant is a shade of green, this indicates this GO-term was enriched in that tissue set where a darker shade of green indicates a lower q-value enrichment. Node size is indicative of the number of genes annotated with that GO term. The thickness of each line is indicative of the number of genes shared between the

connected gene sets (minimum 50% overlap). White shading indicates that the GO term was missing for a given tissue.

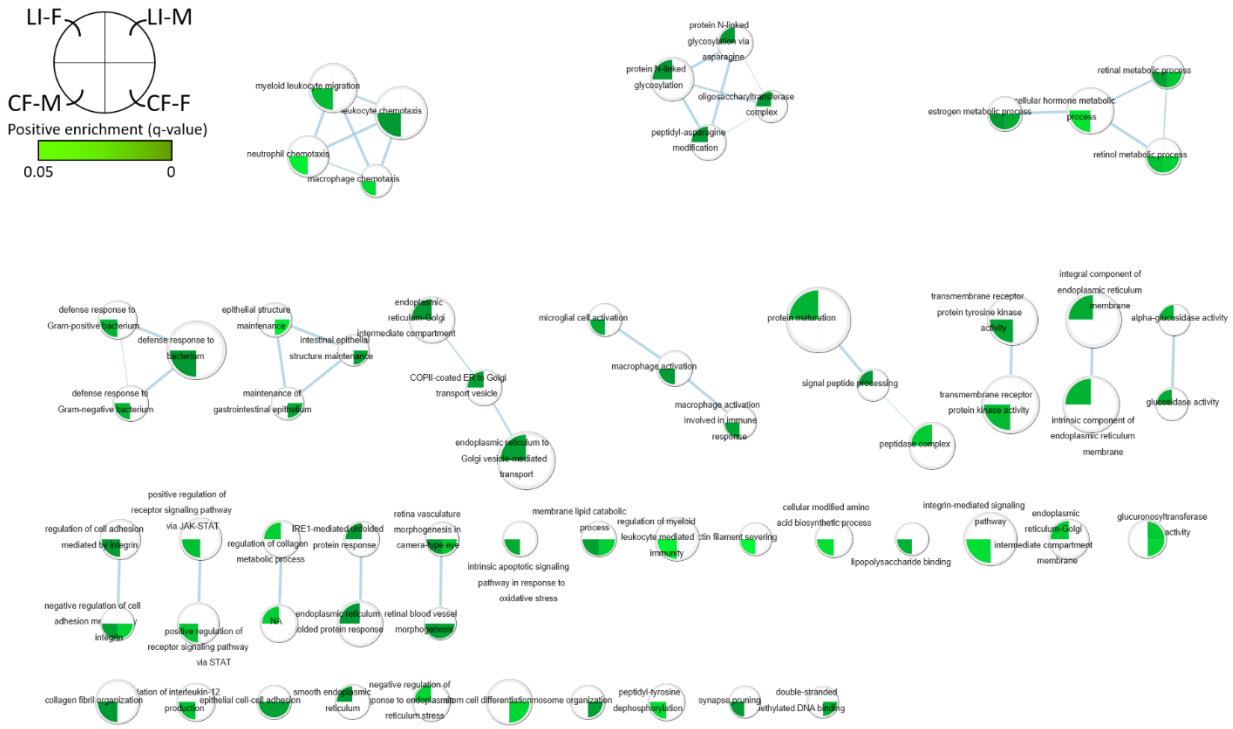

Appendix 20-2. Continued map of enriched GO terms from LSMD WAF exposure. See **Appendix 20-1 legend** for more details.

Appendix 21. High concentration HSFO WAF exposure results in 312 genes that are differentially expressed in all tissues. See **Appendix 19** legend for more details.

ContigID	LI-F		LI-M		CF-F		CF-M		Accession number	%id	Blastn Annotation
	FC	p_{adj}	FC	p_{adj}	FC	p_{adj}	FC	p_{adj}			
COHO.12457	Inf	1.37E-29	25	2.33E-23	8	1.02E-19	10	1.13E-11	XM_20479494.1	99	PREDICTED: Oncorhynchus kisutch cytochrome P450 1B1-like (LOC109888318), mRNA
COHO.15178	Inf	2.16E-22	35	6.72E-26	5	1.43E-16	3	4.75E-08	XM_20508873.1	100	PREDICTED: Oncorhynchus kisutch uncharacterized LOC109909829 (LOC109909829), mRNA
gene36962	Inf	4.09E-02	Inf	1.90E-07	4	3.52E-04	2	3.48E-02	XM_20470778.1	100	PREDICTED: Oncorhynchus kisutch coiled-coil domain-containing protein 87-like (LOC109878569), mRNA
COHO.28078	446	1.10E-09	Inf	6.30E-04	5	2.68E-23	3	2.55E-08	XM_20477292.1	100	PREDICTED: Oncorhynchus kisutch heat shock protein HSP 90-alpha-like (LOC109885446), mRNA
COHO.6785	271	3.86E-06	Inf	2.66E-10	38	2.40E-84	58	3.42E-07	XR_2255882.1	100	PREDICTED: Oncorhynchus kisutch cytochrome P450 1B1 pseudogene (LOC109894533), misc RNA
COHO.6783	203	2.94E-11	331	########	17	3.70E-22	11	8.58E-13	XR_2255881.1	100	PREDICTED: Oncorhynchus kisutch cytochrome P450 1B1 pseudogene (LOC109894532), misc RNA
COHO.12458	82	4.96E-47	48	5.66E-82	10	3.09E-20	9	3.22E-10	BT045022.1_BT045022.1	96	Salmo salar clone ssal-rgf-510-032 Cytochrome P450 1B1 putative mRNA, complete cds
COHO.3920	46	7.21E-42	66	7.62E-42	11	5.06E-44	7	8.47E-03	XM_20481515.1	100	PREDICTED: Oncorhynchus kisutch cytochrome P450 1B1-like (LOC109889798), transcript variant X1, mRNA
COHO.13762	36	4.50E-14	35	2.32E-16	7	8.11E-19	3	2.00E-06	XM_20504111.1	100	PREDICTED: Oncorhynchus kisutch thioredoxin-like (LOC109906425), mRNA
COHO.4795	23	6.64E-08	45	9.61E-16	3	2.10E-14	2	1.84E-03	XM_20483514.1	100	PREDICTED: Oncorhynchus kisutch glutathione peroxidase 2-like (LOC109891177), mRNA
COHO.26461	20	1.75E-45	14	3.05E-18	3	6.19E-16	2	1.38E-04	XM_20474289.1	100	PREDICTED: Oncorhynchus kisutch glutamate--cysteine ligase regulatory subunit-like (LOC109882206), mRNA
COHO.9763	19	9.00E-36	8	6.93E-19	2	4.81E-13	2	1.48E-02	XM_20495192.1	100	PREDICTED: Oncorhynchus kisutch glutathione S-transferase omega 1 (gsto1), mRNA
COHO.29676	16	8.83E-19	25	6.14E-39	9	1.35E-24	14	4.15E-10	XM_20479494.1	100	PREDICTED: Oncorhynchus kisutch cytochrome P450 1B1-like (LOC109888318), mRNA
COHO.9475	16	7.30E-05	58	3.40E-25	4	1.67E-28	6	1.90E-11	XM_20494565.1	100	PREDICTED: Oncorhynchus kisutch putative inactive phenolphthiocerol synthesis polyketide synthase type I Pks15 (LOC109899378), transcript variant X1, mRNA
COHO.11697	14	2.95E-18	10	2.67E-11	2	2.41E-22	2	1.52E-02	XM_20499414.1	100	PREDICTED: Oncorhynchus kisutch proteasome subunit alpha type-7-like (LOC109902778), mRNA
COHO.3194	14	2.71E-04	3	2.24E-04	3	2.28E-11	3	8.85E-05	XR_2252564.1	100	PREDICTED: Oncorhynchus kisutch uncharacterized LOC109873228 (LOC109873228), ncRNA
COHO.16461	13	5.09E-25	7	1.10E-09	2	1.82E-12	2	1.51E-06	XM_20452892.1	100	PREDICTED: Oncorhynchus kisutch glutathione S-transferase P-like (LOC109864869), mRNA
COHO.7899	13	2.96E-05	11	2.44E-02	2	2.26E-05	2	3.49E-02	XM_20490548.1	100	PREDICTED: Oncorhynchus kisutch small nuclear ribonucleoprotein F-like (LOC109896284), partial mRNA
COHO.16528	11	5.77E-31	9	2.61E-12	2	1.24E-06	2	4.35E-04	XM_20509379.1	100	PREDICTED: Oncorhynchus kisutch thiosulfate sulfurtransferase/rhodanese-like domain-containing protein 1 (LOC109910248), mRNA
COHO.12591	10	1.78E-12	10	5.15E-20	2	5.55E-05	3	2.06E-02	XM_20501343.1	100	PREDICTED: Oncorhynchus kisutch ornithine decarboxylase 1-like (LOC109904160), mRNA
gene44441	9	9.44E-40	19	2.59E-57	47	8.04E-66	36	8.16E-07	XR_2254784.1	100	PREDICTED: Oncorhynchus kisutch UDP-glucuronosyltransferase-like (LOC109886608), misc RNA
COHO.24028	9	3.04E-26	5	1.47E-21	1	7.15E-06	1	8.60E-03	XM_20469859.1	100	PREDICTED: Oncorhynchus kisutch mitochondrial-processing peptidase subunit beta-like (LOC109877651), mRNA

COHO.9990	9	1.26E-19	10	4.95E-29	2	5.82E-09	1	1.69E-02	XM_20495671.1	100	PREDICTED: Oncorhynchus kisutch desumoylating isopeptidase 1-like (LOC109899982), transcript variant X1, mRNA
COHO.18163	9	6.82E-20	10	4.04E-14	-1	6.66E-03	-2	5.65E-05	XM_20457151.1	100	PREDICTED: Oncorhynchus kisutch caveolin-2-like (LOC109867831), mRNA
COHO.21802	8	2.84E-08	8	4.63E-10	4	1.62E-09	2	3.67E-02	XM_20466266.1	100	PREDICTED: Oncorhynchus kisutch sarcoplasmic/endoplasmic reticulum calcium ATPase 2 (LOC109874383), mRNA
COHO.3983	8	5.68E-18	6	7.73E-12	2	9.73E-09	2	6.16E-05	XM_20481623.1	100	PREDICTED: Oncorhynchus kisutch apoptosis inducing factor, mitochondria associated 2 (aifm2), mRNA
COHO.20848	8	1.64E-22	3	1.61E-02	3	1.93E-09	2	2.60E-02	XM_20463436.1	100	PREDICTED: Oncorhynchus kisutch growth arrest and DNA damage-inducible protein GADD45 alpha-like (LOC109872257), mRNA
gene5657	8	6.26E-07	5	5.68E-07	2	1.07E-09	2	4.97E-02	XM_20481722.1	100	PREDICTED: Oncorhynchus kisutch protein FAM98A-like (LOC109889907), mRNA
COHO.28541	8	6.81E-26	5	7.43E-07	3	1.38E-24	3	5.02E-12	XM_20478010.1	100	PREDICTED: Oncorhynchus kisutch pirin (pir), mRNA
COHO.11280	8	1.85E-10	6	1.72E-12	2	1.41E-04	2	2.11E-02	XM_20498528.1	100	PREDICTED: Oncorhynchus kisutch transmembrane protein 47-like (LOC109902282), mRNA
gene35662	8	4.15E-24	4	1.11E-19	1	1.30E-07	1	3.86E-02	XM_20469462.1	100	PREDICTED: Oncorhynchus kisutch mitochondrial-processing peptidase subunit beta-like (LOC109877143), mRNA
COHO.7838	8	1.21E-14	4	2.05E-05	2	1.76E-02	2	8.71E-03	XM_20490874.1	100	PREDICTED: Oncorhynchus kisutch normal mucosa of esophagus-specific gene 1 protein-like (LOC109896594), transcript variant X2, mRNA
COHO.5418	7	1.68E-43	10	4.47E-31	3	4.84E-17	3	8.75E-10	XM_20485324.1	100	PREDICTED: Oncorhynchus kisutch UDP-glucuronosyltransferase-like (LOC109892642), mRNA
COHO.29671	7	5.91E-10	3	3.81E-07	2	9.19E-10	2	3.68E-02	XM_20479484.1	100	PREDICTED: Oncorhynchus kisutch mitochondrial import receptor subunit TOM40 homolog (LOC109888304), mRNA
gene36783	7	1.01E-24	12	1.39E-20	45	2.40E-84	43	1.08E-05	XM_21578846.1	97	PREDICTED: Oncorhynchus mykiss UDP-glucuronosyltransferase-like (LOC110501343), mRNA
COHO.29242	7	1.45E-19	11	8.71E-16	26	1.21E-60	25	1.49E-06	XM_20478960.1	100	PREDICTED: Oncorhynchus kisutch UDP-glucuronosyltransferase-like (LOC109887636), mRNA
COHO.2000	7	2.08E-04	6	1.43E-03	3	2.64E-16	2	2.92E-02	XM_20457111.1	100	PREDICTED: Oncorhynchus kisutch dnaJ homolog subfamily B member 11-like (LOC109867805), mRNA
COHO.23171	7	6.30E-12	10	1.96E-31	2	2.30E-03	2	3.61E-02	XM_20468668.1	100	PREDICTED: Oncorhynchus kisutch 26S proteasome non-ATPase regulatory subunit 1-like (LOC109876207), mRNA
COHO.7580	7	8.17E-03	5	3.28E-04	2	3.13E-11	1	3.93E-02	XM_20490105.1	100	PREDICTED: Oncorhynchus kisutch FIC domain containing (ficd), mRNA
COHO.24111	7	1.36E-11	3	1.68E-05	1	9.70E-04	1	3.57E-02	XM_20469988.1	100	PREDICTED: Oncorhynchus kisutch dnaJ homolog subfamily C member 15-like (LOC109877788), transcript variant X1, mRNA
COHO.22572	6	1.14E-13	7	6.28E-29	3	6.15E-22	1	4.63E-02	XM_20466404.1	100	PREDICTED: Oncorhynchus kisutch ubiquitin carboxyl-terminal hydrolase 14-like (LOC109874492), transcript variant X2, mRNA
COHO.22990	6	4.68E-35	4	1.01E-10	3	4.09E-26	3	3.77E-12	XM_20468319.1	100	PREDICTED: Oncorhynchus kisutch cytochrome b5-like (LOC109875882), mRNA
COHO.2677	6	3.23E-10	6	6.29E-13	3	2.50E-15	2	4.50E-02	XM_20473069.1	100	PREDICTED: Oncorhynchus kisutch transitional endoplasmic reticulum ATPase-like (LOC109880883), mRNA
COHO.27767	6	5.67E-03	4	1.54E-06	4	6.12E-03	5	5.24E-04	XR_2254439.1	100	PREDICTED: Oncorhynchus kisutch uncharacterized LOC109884845 (LOC109884845), ncRNA
COHO.1784	6	4.15E-24	14	6.94E-24	3	1.08E-25	4	8.76E-08	XM_20498474.1	100	PREDICTED: Oncorhynchus kisutch glucocorticoid modulatory element-binding protein 1-like (LOC109902252), transcript variant X2, mRNA
COHO.11668	6	2.01E-10	2	3.08E-02	2	3.86E-03	2	3.14E-02	XM_20499349.1	100	PREDICTED: Oncorhynchus kisutch glutaredoxin 2 (glrx2), transcript variant X4, mRNA
COHO.23698	5	2.20E-12	4	1.93E-05	2	1.26E-03	2	1.27E-02	XM_24437998.1	95	PREDICTED: Oncorhynchus tshawytscha transmembrane protein 60-like (LOC112262323), mRNA

COHO.3700	5	2.41E-10	3	1.33E-02	2	4.63E-04	2	1.92E-02	XM_20481030.1	100	PREDICTED: Oncorhynchus kisutch protein C19orf12 homolog (LOC109889538), mRNA
COHO.8794	5	4.96E-06	3	4.89E-02	2	1.40E-04	1	2.25E-02	XM_20492939.1	100	PREDICTED: Oncorhynchus kisutch cAMP-specific 3',5'-cyclic phosphodiesterase 4B-like (LOC109898126), transcript variant X1, mRNA
gene18532	5	1.37E-06	4	8.84E-09	-2	3.76E-04	-2	4.40E-02	XM_20501080.1	100	PREDICTED: Oncorhynchus kisutch formin-1-like (LOC109904018), mRNA
COHO.7016	5	1.02E-11	4	3.98E-11	3	1.42E-16	4	7.32E-15	XM_20488636.1	100	PREDICTED: Oncorhynchus kisutch collagen and calcium-binding EGF domain-containing protein 1-like (LOC109894979), mRNA
COHO.28579	5	1.93E-09	4	8.92E-16	2	2.17E-17	1	1.56E-02	XM_20478062.1	100	PREDICTED: Oncorhynchus kisutch 26S proteasome non-ATPase regulatory subunit 13-like (LOC109886365), partial mRNA
COHO.13556	5	9.95E-06	3	7.96E-07	-2	1.27E-03	-2	4.20E-02	XM_20503470.1	100	PREDICTED: Oncorhynchus kisutch serpin H1-like (LOC109905838), transcript variant X1, mRNA
COHO.8484	5	1.33E-12	3	8.40E-08	2	1.05E-15	2	4.66E-02	XM_20492376.1	100	PREDICTED: Oncorhynchus kisutch AFG3-like protein 1 (LOC109897802), mRNA
COHO.9223	5	8.77E-11	2	2.58E-05	3	3.92E-25	2	2.24E-02	XM_20493721.1	100	PREDICTED: Oncorhynchus kisutch probable ATP-dependent RNA helicase DDX5 (LOC109898664), transcript variant X2, mRNA
COHO.13178	5	1.58E-14	3	1.15E-09	2	2.77E-10	1	2.96E-02	XM_20502764.1	100	PREDICTED: Oncorhynchus kisutch cleft lip and palate transmembrane protein 1 homolog (LOC109905408), mRNA
gene37057	5	3.15E-05	3	1.79E-02	2	1.95E-10	2	2.60E-02	XM_21625602.1	97	PREDICTED: Oncorhynchus mykiss solute carrier family 35 member B1 (LOC110538649), mRNA
COHO.6471	5	1.05E-18	2	3.34E-03	Inf	9.60E-06	14	1.03E-06	XM_20487535.1	100	PREDICTED: Oncorhynchus kisutch type II iodothyronine deiodinase-like (LOC109894226), mRNA
COHO.25300	5	1.69E-39	2	1.58E-12	1	3.84E-02	1	1.66E-02	XM_20472216.1	100	PREDICTED: Oncorhynchus kisutch abhydrolase domain containing 4 (abhd4), mRNA
COHO.27878	5	8.13E-08	9	4.75E-18	4	6.24E-04	3	8.27E-03	XM_20476944.1	100	PREDICTED: Oncorhynchus kisutch NAD(P)H dehydrogenase [quinone] 1-like (LOC109885081), mRNA
COHO.27880	4	3.92E-08	11	2.85E-23	4	1.10E-03	3	1.17E-03	XM_20476945.1	100	PREDICTED: Oncorhynchus kisutch NAD(P)H dehydrogenase [quinone] 1-like (LOC109885082), mRNA
COHO.11053	4	4.39E-14	3	9.78E-41	2	8.91E-13	1	3.57E-02	XM_20498091.1	100	PREDICTED: Oncorhynchus kisutch ubiquilin-4-like (LOC109902037), mRNA
COHO.12029	4	6.53E-11	3	1.77E-08	2	4.10E-10	2	4.25E-02	XM_20500280.1	100	PREDICTED: Oncorhynchus kisutch nuclear migration protein nudC-like (LOC109903513), mRNA
COHO.21924	4	5.10E-08	2	4.33E-05	2	2.60E-08	2	4.90E-02	XM_20465521.1	100	PREDICTED: Oncorhynchus kisutch developmentally-regulated GTP-binding protein 1 (LOC109873803), mRNA
gene4431	4	4.44E-12	12	4.34E-18	1	2.15E-03	1	2.94E-02	XR_2252763.1	100	PREDICTED: Oncorhynchus kisutch tyrosine-protein kinase CSK-like (LOC109874928), misc RNA
COHO.23790	4	3.16E-13	2	1.32E-03	2	2.84E-03	2	3.97E-02	XM_20469589.1	100	PREDICTED: Oncorhynchus kisutch NADH:ubiquinone oxidoreductase subunit B6 (ndufb6), mRNA
COHO.24429	4	4.90E-07	2	1.84E-03	2	2.72E-07	2	2.14E-02	XM_20470638.1	100	PREDICTED: Oncorhynchus kisutch eukaryotic peptide chain release factor subunit 1-like (LOC109878411), transcript variant X1, mRNA
COHO.11549	4	2.19E-09	3	4.80E-10	2	2.23E-07	1	2.19E-02	XM_20499109.1	100	PREDICTED: Oncorhynchus kisutch glutamate--cysteine ligase regulatory subunit-like (LOC109902612), transcript variant X2, mRNA
COHO.4998	4	1.83E-16	4	1.04E-13	2	6.74E-04	1	3.60E-02	XM_20483888.1	100	PREDICTED: Oncorhynchus kisutch thioredoxin reductase 1, cytoplasmic-like (LOC109891395), mRNA
COHO.18098	4	3.72E-08	3	5.61E-05	4	3.17E-05	3	1.49E-02	XM_20457097.1	100	PREDICTED: Oncorhynchus kisutch fibroblast growth factor 23-like (LOC109867799), mRNA
COHO.26464	4	1.65E-04	3	4.68E-02	2	3.47E-15	2	3.17E-02	XM_20474311.1	100	PREDICTED: Oncorhynchus kisutch solute carrier family 35 member B1 (LOC109882219), mRNA
COHO.9061	4	2.72E-11	3	2.92E-06	2	7.54E-09	1	1.62E-02	XM_21557822.1	99	PREDICTED: Oncorhynchus mykiss ubiquitin domain-containing protein UBFD1-like (LOC110486317), transcript variant X1, mRNA

COHO.27047	4	7.06E-31	2	6.50E-06	3	3.06E-32	2	3.33E-06	XM_20475398.1	100	PREDICTED: Oncorhynchus kisutch glutathione S-transferase A-like (LOC109883379), mRNA
COHO.23699	4	1.66E-07	3	4.93E-10	2	1.97E-12	1	2.37E-02	XM_20469474.1	100	PREDICTED: Oncorhynchus kisutch 26S proteasome non-ATPase regulatory subunit 13-like (LOC109877163), partial mRNA
COHO.22821	4	2.76E-14	2	7.84E-03	2	3.51E-07	2	1.37E-02	XM_20467939.1	100	PREDICTED: Oncorhynchus kisutch ribosome maturation protein SBDS-like (LOC109875584), mRNA
COHO.20966	3	4.40E-08	7	4.78E-13	2	1.85E-05	3	3.90E-03	XM_20463400.1	100	PREDICTED: Oncorhynchus kisutch C-C chemokine receptor type 9-like (LOC109872235), mRNA
COHO.20808	3	5.73E-11	2	4.76E-06	2	1.06E-13	1	1.57E-02	XM_20462762.1	100	PREDICTED: Oncorhynchus kisutch AP-2 complex subunit mu-A (LOC109871770), transcript variant X2, mRNA
COHO.18162	3	2.80E-15	4	8.24E-22	-2	1.80E-12	-2	1.71E-07	XM_20456004.1	100	PREDICTED: Oncorhynchus kisutch caveolin-1 (LOC109867090), mRNA
COHO.15001	3	1.69E-11	2	5.57E-08	1	4.43E-03	1	2.86E-02	XM_20506740.1	100	PREDICTED: Oncorhynchus kisutch ubiquitin-conjugating enzyme E2 variant 1 (LOC109908191), mRNA
COHO.5546	3	3.06E-07	2	2.41E-04	2	1.05E-09	1	4.64E-02	XM_20483330.1	100	PREDICTED: Oncorhynchus kisutch endoplasmic reticulum-Golgi intermediate compartment protein 3 (LOC109891044), transcript variant X1, mRNA
COHO.3605	3	9.82E-05	2	5.54E-03	1	2.88E-02	1	2.98E-02	XM_20480864.1	100	PREDICTED: Oncorhynchus kisutch CDP-diacylglycerol--glycerol-3-phosphate 3-phosphatidyltransferase, mitochondrial-like (LOC109889438), mRNA
COHO.7532	3	2.07E-05	3	7.46E-05	2	6.16E-15	2	1.08E-03	XM_20490015.1	100	PREDICTED: Oncorhynchus kisutch BCL tumor suppressor 7A (bcl7a), transcript variant X1, mRNA
COHO.16779	3	9.03E-03	3	4.84E-03	-2	5.83E-03	-2	3.78E-04	XM_20454552.1	100	PREDICTED: Oncorhynchus kisutch pyruvate dehydrogenase (acetyl-transferring) kinase isozyme 2, mitochondrial-like (LOC109866016), mRNA
COHO.20522	3	5.99E-07	2	3.45E-04	2	3.10E-09	2	3.21E-02	XM_20462975.1	100	PREDICTED: Oncorhynchus kisutch protein arginine N-methyltransferase 5-like (LOC109871938), mRNA
COHO.24060	3	3.16E-05	4	5.13E-13	2	4.93E-07	3	6.58E-17	XR_2253267.1	100	PREDICTED: Oncorhynchus kisutch uncharacterized LOC109877694 (LOC109877694), ncRNA
COHO.25776	3	4.41E-04	3	1.42E-02	2	5.03E-11	2	2.76E-02	XM_20473035.1	100	PREDICTED: Oncorhynchus kisutch phosphoglycerate mutase 1 (LOC109880855), mRNA
COHO.8229	3	2.14E-04	2	8.83E-03	2	3.68E-12	1	4.38E-02	XM_20491495.1	100	PREDICTED: Oncorhynchus kisutch dnaJ homolog subfamily C member 3-like (LOC109897010), mRNA
COHO.10504	3	8.27E-08	2	1.89E-02	2	3.31E-02	2	7.97E-04	XM_20496932.1	100	PREDICTED: Oncorhynchus kisutch peptidyl-prolyl cis-trans isomerase FKBP1B (LOC109900984), mRNA
COHO.22085	3	2.79E-05	2	2.41E-03	2	4.58E-05	2	2.60E-02	XM_20466182.1	100	PREDICTED: Oncorhynchus kisutch leucine-rich repeat neuronal protein 4-like (LOC109874320), transcript variant X2, mRNA
COHO.812	3	5.02E-12	3	4.90E-08	-2	3.63E-11	-2	4.24E-03	XM_20487853.1	100	PREDICTED: Oncorhynchus kisutch NADH-cytochrome b5 reductase 1-like (LOC109894389), transcript variant X2, mRNA
COHO.18823	3	7.80E-08	2	2.81E-06	2	1.35E-10	2	2.56E-03	XM_20458373.1	100	PREDICTED: Oncorhynchus kisutch growth arrest-specific protein 1-like (LOC109868660), mRNA
COHO.23842	3	9.42E-06	2	1.28E-06	2	5.33E-04	2	9.24E-03	XM_20469653.1	100	PREDICTED: Oncorhynchus kisutch soluble calcium-activated nucleotidase 1-like (LOC109877380), mRNA
COHO.17405	3	9.53E-04	2	2.05E-02	2	3.94E-09	2	3.27E-02	XM_20455046.1	100	PREDICTED: Oncorhynchus kisutch ARV1 homolog, fatty acid homeostasis modulator (arv1), mRNA
COHO.13074	3	3.08E-13	2	1.71E-03	1	2.89E-02	2	9.83E-03	XM_20502575.1	100	PREDICTED: Oncorhynchus kisutch dihydropteridine reductase-like (LOC109905290), mRNA
gene29815	3	3.65E-07	4	4.63E-27	1	1.04E-07	2	1.82E-02	XM_20460455.1	100	PREDICTED: Oncorhynchus kisutch nuclear protein localization protein 4 homolog (LOC109870108), mRNA
COHO.19339	3	9.81E-12	2	3.19E-03	2	1.64E-14	2	2.14E-03	XM_20459445.1	100	PREDICTED: Oncorhynchus kisutch WD repeat domain 46 (wdr46), mRNA
COHO.11866	3	7.04E-04	2	1.89E-03	2	2.03E-07	2	4.65E-02	XM_20499985.1	100	PREDICTED: Oncorhynchus kisutch coiled-coil domain-containing protein 126-like

											(LOC109903346), transcript variant X1, mRNA
COHO.20167	3	3.94E-05	2	1.17E-04	3	3.52E-08	2	4.92E-04	XM_20462293.1	100	PREDICTED: Oncorhynchus kisutch G protein-coupled receptor 161 (gpr161), transcript variant X2, mRNA
gene23282	3	4.31E-04	3	2.05E-07	2	2.97E-17	2	4.08E-02	XM_20507787.1	100	PREDICTED: Oncorhynchus kisutch bleomycin hydrolase-like (LOC109908965), mRNA
COHO.13485	3	2.29E-06	2	8.75E-03	1	2.23E-03	1	7.76E-03	XM_20503330.1	100	PREDICTED: Oncorhynchus kisutch ribosomal protein S6 kinase beta-1-like (LOC109905765), mRNA
COHO.26253	3	2.36E-07	2	7.30E-03	2	5.83E-14	1	3.75E-02	XM_20473889.1	100	PREDICTED: Oncorhynchus kisutch 39S ribosomal protein L17, mitochondrial-like (LOC109881775), transcript variant X2, mRNA
COHO.26724	3	3.85E-09	2	7.72E-03	1	1.59E-04	1	4.94E-02	XM_20474803.1	100	PREDICTED: Oncorhynchus kisutch high mobility group protein B2-like (LOC109882714), mRNA
COHO.11843	2	1.39E-06	2	1.06E-09	2	1.22E-02	2	3.18E-02	XM_20499956.1	100	PREDICTED: Oncorhynchus kisutch chromobox protein homolog 3-like (LOC109903322), transcript variant X2, mRNA
COHO.425	2	1.46E-04	2	2.92E-04	2	2.33E-05	2	4.45E-02	XM_20481228.1	100	PREDICTED: Oncorhynchus kisutch exportin-1-like (LOC109889643), mRNA
COHO.4255	2	3.34E-08	2	1.57E-03	2	1.92E-11	1	1.54E-02	XM_20482507.1	100	PREDICTED: Oncorhynchus kisutch small ubiquitin-related modifier 3 (LOC109890574), mRNA
COHO.19501	2	6.82E-20	2	4.16E-13	1	1.03E-04	1	8.40E-03	XM_20460238.1	100	PREDICTED: Oncorhynchus kisutch nuclear factor erythroid 2-related factor 1-like (LOC109869925), transcript variant X2, mRNA
COHO.14756	2	6.35E-07	2	3.61E-03	2	9.86E-06	1	4.74E-02	XM_20506174.1	100	PREDICTED: Oncorhynchus kisutch acyl-CoA thioesterase 7 (acot7), transcript variant X3, mRNA
COHO.20226	2	5.99E-07	2	8.53E-04	1	2.43E-05	1	4.42E-02	XM_20461322.1	100	PREDICTED: Oncorhynchus kisutch protein ABHD13 (LOC109870711), mRNA
COHO.16425	2	4.61E-05	3	1.49E-05	2	1.55E-06	2	1.69E-02	XM_20452797.1	100	PREDICTED: Oncorhynchus kisutch calnexin-like (LOC109864822), transcript variant X3, mRNA
gene37870	2	1.78E-02	2	9.39E-03	2	3.66E-02	5	1.91E-04	XR_2253555.1	100	PREDICTED: Oncorhynchus kisutch elongation factor 2-like (LOC109879533), misc RNA
COHO.14040	2	5.48E-07	2	1.61E-04	2	2.41E-18	1	5.93E-03	XM_20504599.1	100	PREDICTED: Oncorhynchus kisutch small ubiquitin-related modifier 3 (LOC109906732), mRNA
COHO.15446	2	1.26E-11	2	2.40E-15	2	1.82E-12	1	3.91E-03	XM_20507441.1	100	PREDICTED: Oncorhynchus kisutch ubiquitin-protein ligase E3C-like (LOC109908761), mRNA
COHO.3434	2	5.90E-03	2	5.03E-03	1	2.67E-02	2	3.60E-02	XM_20480554.1	100	PREDICTED: Oncorhynchus kisutch large neutral amino acids transporter small subunit 1-like (LOC109889252), mRNA
COHO.25168	2	5.39E-08	2	1.92E-03	2	1.60E-07	2	1.97E-04	XM_20471898.1	100	PREDICTED: Oncorhynchus kisutch kelch-like ECH-associated protein 1 (LOC109879738), mRNA
COHO.24388	2	8.66E-05	3	1.41E-08	2	4.08E-05	2	2.95E-02	XR_2253366.1	100	PREDICTED: Oncorhynchus kisutch uncharacterized LOC109878285 (LOC109878285), ncRNA
COHO.13182	2	1.36E-06	2	8.07E-04	4	3.80E-05	2	2.11E-02	XM_20502772.1	100	PREDICTED: Oncorhynchus kisutch bone morphogenetic protein 4-like (LOC109905415), mRNA
COHO.15272	2	1.33E-04	2	2.13E-03	1	9.65E-04	1	3.85E-02	XM_20508917.1	100	PREDICTED: Oncorhynchus kisutch COP9 signalosome complex subunit 5 (LOC109909855), mRNA
COHO.21954	2	9.04E-05	3	4.09E-05	2	1.39E-04	2	2.30E-02	XM_20466065.1	100	PREDICTED: Oncorhynchus kisutch steroid receptor RNA activator 1 (sra1), transcript variant X2, mRNA
COHO.5977	2	4.40E-05	2	4.32E-04	2	2.04E-17	1	2.29E-02	XM_20486445.1	100	PREDICTED: Oncorhynchus kisutch protein HEXIM-like (LOC109893287), mRNA
COHO.9568	2	1.04E-05	2	7.29E-06	2	9.84E-11	1	1.18E-02	XM_20494776.1	100	PREDICTED: Oncorhynchus kisutch tyrosine-protein kinase yes (LOC109899488), mRNA
COHO.12734	2	4.88E-10	1	1.50E-02	2	8.28E-11	2	3.85E-03	XM_20501581.1	100	PREDICTED: Oncorhynchus kisutch tumor protein p53 inducible protein 3 (tp53i3), mRNA
COHO.25016	2	2.41E-03	2	2.45E-03	-2	1.91E-02	-3	3.89E-02	XM_20471637.1	100	PREDICTED: Oncorhynchus kisutch pleiotrophin-like (LOC109879469), mRNA

COHO.1128	2	3.24E-03	2	1.81E-04	2	2.32E-06	1	1.73E-02	XM_20493657.1	100	PREDICTED: Oncorhynchus kisutch hyaluronidase-2-like (LOC109898618), mRNA
COHO.953	2	1.09E-04	2	1.98E-04	1	1.01E-02	1	2.75E-02	XM_20490298.1	100	PREDICTED: Oncorhynchus kisutch SSU72 homolog, RNA polymerase II CTD phosphatase (ssu72), mRNA
COHO.1869	2	4.52E-03	2	3.20E-04	1	4.87E-02	1	3.55E-02	XM_20454492.1	100	PREDICTED: Oncorhynchus kisutch activin receptor type-1-like (LOC109865973), transcript variant X1, mRNA
COHO.9635	2	1.21E-04	2	1.67E-03	2	6.58E-06	2	1.69E-02	XM_20494921.1	100	PREDICTED: Oncorhynchus kisutch cytochrome c oxidase assembly protein COX15 homolog (LOC109899574), mRNA
gene5142	2	1.02E-02	2	1.77E-02	-2	3.17E-03	-2	1.84E-03	XM_20480046.1	100	PREDICTED: Oncorhynchus kisutch uncharacterized LOC109888885 (LOC109888885), mRNA
COHO.19884	2	3.00E-03	2	9.17E-04	1	2.16E-07	1	8.98E-03	XM_20460686.1	100	PREDICTED: Oncorhynchus kisutch endoplasmic reticulum lectin 1-like (LOC109870259), transcript variant X2, mRNA
gene42789	2	7.08E-04	2	4.18E-03	3	9.58E-13	3	4.93E-05	XM_20476753.1	100	PREDICTED: Oncorhynchus kisutch 5-aminolevulinate synthase, nonspecific, mitochondrial-like (LOC109884843), mRNA
COHO.12805	2	6.45E-06	2	2.94E-04	1	1.54E-03	1	4.67E-02	XM_20502064.1	100	PREDICTED: Oncorhynchus kisutch protein FAM122A-like (LOC109904974), transcript variant X1, mRNA
COHO.13052	2	3.80E-03	3	3.77E-04	2	2.61E-04	2	3.99E-02	XM_20502537.1	100	PREDICTED: Oncorhynchus kisutch calnexin-like (LOC109905261), transcript variant X1, mRNA
COHO.14887	2	6.35E-04	2	3.06E-04	2	2.85E-02	1	6.06E-03	XM_20506480.1	100	PREDICTED: Oncorhynchus kisutch von Willebrand factor A domain-containing protein 1-like (LOC109908058), mRNA
COHO.1906	2	8.74E-04	2	6.61E-03	2	5.13E-10	1	2.21E-02	XM_20455397.1	100	PREDICTED: Oncorhynchus kisutch DDB1 and CUL4 associated factor 17 (dcaf17), mRNA
COHO.6885	2	3.49E-04	2	1.39E-02	1	5.51E-03	1	2.86E-02	XM_20488251.1	100	PREDICTED: Oncorhynchus kisutch ADP-dependent glucokinase-like (LOC109894635), mRNA
COHO.24947	2	2.30E-04	2	3.23E-07	2	2.07E-05	2	4.25E-03	XM_20471510.1	100	PREDICTED: Oncorhynchus kisutch fragile X mental retardation syndrome-related protein 1-like (LOC109879338), transcript variant X2, mRNA
COHO.27190	2	5.60E-04	2	1.54E-03	2	4.81E-06	1	4.19E-02	XR_2254213.1	100	PREDICTED: Oncorhynchus kisutch nucleobindin-1-like (LOC109883674), misc RNA
COHO.27766	2	1.08E-02	4	1.64E-02	3	8.13E-07	2	4.90E-03	XM_24403538.1	97	PREDICTED: Oncorhynchus tshawytscha 5-aminolevulinate synthase, nonspecific, mitochondrial-like (LOC112235146), mRNA
COHO.19791	2	4.83E-02	2	2.31E-02	-2	7.10E-04	-1	3.47E-02	XM_20460216.1	100	PREDICTED: Oncorhynchus kisutch ras-related C3 botulinum toxin substrate 3 (rho family, small GTP binding protein Rac3) (rac3), transcript variant X1, mRNA
COHO.19733	2	7.66E-06	1	4.82E-03	1	1.79E-05	1	4.92E-02	XM_20461022.1	100	PREDICTED: Oncorhynchus kisutch transcription factor MafF-like (LOC109870498), transcript variant X3, mRNA
COHO.17211	2	1.04E-04	2	1.45E-05	2	3.82E-10	1	1.41E-06	XM_24396388.1	97	PREDICTED: Oncorhynchus tshawytscha kelch like ECH associated protein 1 (keap1), mRNA
COHO.3367	2	7.93E-04	2	2.80E-04	1	7.65E-05	1	8.64E-06	XM_20480387.1	100	PREDICTED: Oncorhynchus kisutch nicalin-1 (LOC109889165), transcript variant X3, mRNA
COHO.26508	2	1.15E-02	2	6.73E-03	-2	4.51E-06	-2	3.27E-02	XR_2253989.1	100	PREDICTED: Oncorhynchus kisutch uncharacterized LOC109882293 (LOC109882293), transcript variant X3, misc RNA
COHO.18486	2	1.25E-07	2	3.41E-06	1	3.10E-05	1	2.76E-02	XM_20457591.1	100	PREDICTED: Oncorhynchus kisutch set1/Ash2 histone methyltransferase complex subunit ASH2-like (LOC109868135), mRNA
COHO.7013	2	2.07E-07	4	2.65E-12	1	1.35E-04	1	2.39E-02	XM_20488933.1	100	PREDICTED: Oncorhynchus kisutch tyrosine-protein kinase CSK-like (LOC109895319), mRNA
COHO.10144	2	6.01E-03	1	8.56E-03	2	1.76E-05	2	2.93E-02	XM_20496240.1	100	PREDICTED: Oncorhynchus kisutch zinc transporter 1-like (LOC109900566), mRNA
COHO.28266	2	4.22E-04	2	4.20E-04	3	9.57E-10	3	5.06E-04	XM_20477596.1	100	PREDICTED: Oncorhynchus kisutch 5-aminolevulinate synthase, nonspecific, mitochondrial-like (LOC109885790), partial mRNA

COHO.6386	2	1.44E-02	2	1.74E-03	3	8.57E-15	2	3.93E-07	XM_20487371.1	100	PREDICTED: Oncorhynchus kisutch cleavage and polyadenylation specificity factor subunit 6-like (LOC109894135), transcript variant X2, mRNA
COHO.11231	2	4.04E-02	1	3.25E-02	1	3.30E-04	1	3.02E-02	XM_20498397.1	100	PREDICTED: Oncorhynchus kisutch prolactin regulatory element-binding protein-like (LOC109902226), transcript variant X1, mRNA
COHO.1782	2	2.65E-02	2	1.66E-05	6	1.47E-52	6	2.34E-08	XM_20453106.1	100	PREDICTED: Oncorhynchus kisutch discoidin, CUB and LCCL domain-containing protein 1-like (LOC109864994), transcript variant X1, mRNA
COHO.23861	2	4.65E-02	1	4.39E-02	1	2.79E-06	2	2.13E-03	GU129139.1_GU129139.1	89	Salmo salar IgH locus A genomic sequence
gene39561	1	7.75E-03	1	5.12E-03	2	7.16E-07	2	9.54E-03	XM_20473516.1	100	PREDICTED: Oncorhynchus kisutch Wilms tumor protein 1-interacting protein homolog (LOC109881366), mRNA
COHO.4282	1	2.22E-03	2	2.93E-02	-1	4.06E-03	-2	1.62E-02	XR_2255434.1	100	PREDICTED: Oncorhynchus kisutch uncharacterized LOC109890600 (LOC109890600), ncRNA
COHO.24109	1	1.28E-02	1	4.65E-02	2	2.23E-14	2	1.06E-04	XM_20469980.1	100	PREDICTED: Oncorhynchus kisutch TSC22 domain family protein 1-like (LOC109877784), transcript variant X3, mRNA
COHO.18476	1	8.57E-03	2	5.67E-03	-2	2.76E-08	-2	3.50E-03	XM_20457336.1	100	PREDICTED: Oncorhynchus kisutch collagen alpha-1(XI) chain-like (LOC109867989), mRNA
COHO.8837	1	4.24E-02	2	4.49E-04	2	7.22E-03	Inf	8.99E-04	XM_20492048.1	100	PREDICTED: Oncorhynchus kisutch transmembrane 4 L6 family member 1-like (LOC109897543), transcript variant X2, mRNA
COHO.1332	-1	4.20E-02	-2	1.19E-03	-3	6.50E-05	-3	7.69E-05	XM_20503853.1	100	PREDICTED: Oncorhynchus kisutch complement C1r subcomponent-like (LOC109906229), mRNA
COHO.5205	-1	1.21E-02	-2	8.13E-09	-2	8.59E-03	-3	3.64E-02	XM_20484905.1	100	PREDICTED: Oncorhynchus kisutch protein prune homolog 2-like (LOC109892403), transcript variant X3, mRNA
COHO.7254	-1	4.67E-02	-2	1.18E-03	-2	1.14E-03	-2	1.99E-02	XM_20489425.1	100	PREDICTED: Oncorhynchus kisutch ras and EF-hand domain-containing protein homolog (LOC109895593), mRNA
COHO.16477	-1	7.33E-03	-1	4.16E-02	-1	2.25E-02	-2	1.26E-02	XM_20452924.1	100	PREDICTED: Oncorhynchus kisutch septin-6-like (LOC109864886), transcript variant X3, mRNA
COHO.14315	-1	1.67E-02	-2	2.36E-02	2	3.31E-04	2	3.72E-03	XM_20505312.1	100	PREDICTED: Oncorhynchus kisutch ubiquitin-conjugating enzyme E2 E2-like (LOC109907382), mRNA
COHO.7821	-1	4.30E-05	-2	4.72E-07	-1	2.81E-04	-1	3.82E-02	XM_20490530.1	100	PREDICTED: Oncorhynchus kisutch differentially expressed in FDCP 6 homolog (LOC109896254), mRNA
COHO.6384	-1	1.26E-02	-3	1.96E-02	-2	4.35E-03	-3	2.18E-04	XM_20487044.1	100	PREDICTED: Oncorhynchus kisutch membrane-spanning 4-domains subfamily A member 12-like (LOC109893845), transcript variant X3, mRNA
COHO.2152	-1	1.83E-02	-2	3.79E-03	-2	8.39E-03	-2	4.04E-02	XM_20459961.1	100	PREDICTED: Oncorhynchus kisutch uncharacterized LOC109869688 (LOC109869688), mRNA
COHO.26411	-1	1.49E-03	-2	1.54E-05	-3	1.27E-03	-2	1.88E-02	XM_20474203.1	100	PREDICTED: Oncorhynchus kisutch 1-acyl-sn-glycerol-3-phosphate acyltransferase delta-like (LOC109882111), mRNA
COHO.17658	-2	4.58E-02	-2	5.71E-03	-2	7.88E-07	-2	9.14E-03	XM_20456056.1	100	PREDICTED: Oncorhynchus kisutch GRAM domain-containing protein 4-like (LOC109867123), transcript variant X4, mRNA
COHO.8332	-2	3.18E-02	-2	1.00E-16	-2	3.20E-08	-1	3.63E-02	XM_20491679.1	100	PREDICTED: Oncorhynchus kisutch calcium/calmodulin-dependent protein kinase type II delta chain (LOC109897118), transcript variant X3, mRNA
COHO.10771	-2	3.60E-02	-2	1.16E-02	-2	1.85E-08	-1	3.25E-02	XM_20497293.1	100	PREDICTED: Oncorhynchus kisutch uncharacterized LOC109901250 (LOC109901250), mRNA
COHO.25978	-2	3.24E-04	-2	4.59E-05	2	3.64E-35	2	3.56E-03	XM_20473417.1	100	PREDICTED: Oncorhynchus kisutch GRAM domain-containing protein 3-like (LOC109881257), transcript variant X2, mRNA
COHO.7991	-2	1.13E-02	-2	2.32E-03	-2	1.61E-07	-2	2.08E-05	XM_20491083.1	100	PREDICTED: Oncorhynchus kisutch prosaposin receptor GPR37-like (LOC109896751), mRNA

gene22017	-2	2.82E-02	-2	1.81E-02	-1	7.68E-04	-1	8.41E-03	XM_20504800.1	100	PREDICTED: Oncorhynchus kisutch coiled-coil domain containing 30 (ccdc30), mRNA
COHO.17640	-2	3.27E-02	-4	3.00E-06	-1	1.75E-06	-2	1.18E-03	XR_2469105.1	99	PREDICTED: Oncorhynchus mykiss mixed lineage kinase domain-like protein (LOC110493186), transcript variant X4, misc RNA
COHO.18680	-2	1.18E-02	-2	1.27E-04	-2	8.12E-06	-2	1.83E-04	XM_20457729.1	100	PREDICTED: Oncorhynchus kisutch gamma-glutamyltransferase 5-like (LOC109868289), mRNA
COHO.6632	-2	6.25E-03	-2	8.44E-04	-1	2.03E-02	-2	1.74E-03	XM_20487847.1	100	PREDICTED: Oncorhynchus kisutch protein LBH-like (LOC109894394), mRNA
COHO.20385	-2	2.06E-03	-3	2.34E-04	-2	4.57E-03	-2	1.01E-02	XM_20461627.1	100	PREDICTED: Oncorhynchus kisutch rho GTPase-activating protein 15-like (LOC109870921), transcript variant X3, mRNA
COHO.15135	-2	3.82E-02	-3	2.36E-11	-2	2.30E-07	-2	9.62E-03	XM_20506998.1	100	PREDICTED: Oncorhynchus kisutch Krueppel-like factor 15 (LOC109908347), transcript variant X2, mRNA
COHO.7708	-2	1.02E-03	-1	4.51E-02	-3	2.12E-03	-2	1.13E-03	XM_20485861.1	100	PREDICTED: Oncorhynchus kisutch differentially expressed in FDCP 6 homolog (LOC109892942), transcript variant X1, mRNA
COHO.19669	-2	4.10E-03	-2	4.02E-02	-3	9.06E-08	-2	7.32E-03	XM_20461148.1	100	PREDICTED: Oncorhynchus kisutch uncharacterized LOC109870581 (LOC109870581), mRNA
COHO.17388	-2	3.33E-07	-2	4.44E-05	1	2.44E-03	1	4.75E-02	XM_20455609.1	100	PREDICTED: Oncorhynchus kisutch mannosyl-oligosaccharide 1,2-alpha-mannosidase IA-like (LOC109866767), mRNA
COHO.4283	-2	8.33E-05	-3	1.16E-14	-2	2.08E-09	-1	2.58E-02	XM_20482547.1	100	PREDICTED: Oncorhynchus kisutch ribose-phosphate pyrophosphokinase 2 (LOC109890601), mRNA
gene12495	-2	4.98E-04	-2	3.86E-03	-4	2.12E-06	-3	2.08E-02	XM_20493418.1	100	PREDICTED: Oncorhynchus kisutch harmonin-like (LOC109898449), mRNA
COHO.6742	-2	3.00E-04	-3	4.17E-10	-1	3.73E-02	-2	2.27E-02	XM_20488017.1	100	PREDICTED: Oncorhynchus kisutch aldehyde dehydrogenase 6 family member A1 (aldh6a1), transcript variant X1, mRNA
COHO.18744	-2	2.44E-04	-2	1.48E-02	-4	1.60E-03	-3	6.36E-04	XM_20457383.1	100	PREDICTED: Oncorhynchus kisutch granzyme K-like (LOC109868017), mRNA
COHO.22037	-2	4.39E-03	-2	2.10E-04	-1	2.41E-03	-1	2.80E-02	XM_20465788.1	100	PREDICTED: Oncorhynchus kisutch peroxiredoxin-4-like (LOC109874044), mRNA
COHO.13297	-2	7.75E-06	-2	1.20E-02	-2	2.74E-05	-2	2.69E-02	XM_20502986.1	100	PREDICTED: Oncorhynchus kisutch mitogen-activated protein kinase 5-like (LOC109905557), mRNA
COHO.15174	-2	1.09E-06	-2	6.17E-10	-2	1.42E-02	-1	7.44E-03	XM_20507041.1	100	PREDICTED: Oncorhynchus kisutch enolase 1 (eno1), mRNA
COHO.14959	-2	3.34E-03	-2	1.13E-02	2	1.13E-06	2	3.18E-02	XM_20506656.1	100	PREDICTED: Oncorhynchus kisutch matrix-remodeling-associated protein 8-like (LOC109908147), transcript variant X2, mRNA
COHO.17366	-2	1.80E-06	-2	1.71E-03	-2	6.14E-08	-2	4.92E-04	XM_20455533.1	100	PREDICTED: Oncorhynchus kisutch rho GTPase-activating protein 18-like (LOC109866722), transcript variant X1, mRNA
COHO.19497	-2	1.79E-03	-2	3.02E-04	-2	2.75E-06	-2	2.56E-02	XM_20460483.1	100	PREDICTED: Oncorhynchus kisutch calcium-binding and coiled-coil domain-containing protein 2-like (LOC109870124), transcript variant X4, mRNA
COHO.6136	-2	4.61E-02	-2	2.24E-05	-2	4.90E-07	-1	2.04E-02	XM_20486662.1	100	PREDICTED: Oncorhynchus kisutch uncharacterized LOC109893435 (LOC109893435), mRNA
COHO.3309	-2	3.10E-05	-2	3.98E-05	-2	1.09E-08	-2	5.07E-03	XM_20480303.1	100	PREDICTED: Oncorhynchus kisutch interferon induced protein 44 like (ifi44l), transcript variant X3, mRNA
gene41908	-2	5.50E-03	-2	4.55E-05	-2	9.92E-16	-2	1.13E-02	XM_20475901.1	100	PREDICTED: Oncorhynchus kisutch decorin-like (LOC109883887), mRNA
COHO.18828	-2	8.60E-03	-1	2.58E-03	-2	5.81E-05	-2	4.04E-02	XR_2251869.1	100	PREDICTED: Oncorhynchus kisutch uncharacterized LOC109867979 (LOC109867979), ncRNA
COHO.13514	-2	1.04E-05	-2	1.21E-06	-2	1.70E-03	-1	1.99E-02	XM_20503401.1	100	PREDICTED: Oncorhynchus kisutch protein C-ets-1-like (LOC109905795), transcript variant X3, mRNA
COHO.29047	-2	3.55E-04	-3	3.54E-02	-2	2.70E-03	-2	4.19E-05	XM_20478713.1	100	PREDICTED: Oncorhynchus kisutch transforming growth factor-beta-induced protein ig-h3-like (LOC109887281), partial mRNA

COHO.5583	-2	4.73E-03	-2	2.46E-02	-2	1.99E-04	-1	2.52E-02	XM_20485630.1	100	PREDICTED: Oncorhynchus kisutch tetratricopeptide repeat domain 3 (ttc3), transcript variant X1, mRNA
COHO.24532	-2	4.55E-03	-2	7.85E-05	-2	6.08E-16	-2	5.66E-03	XM_20470775.1	100	PREDICTED: Oncorhynchus kisutch decorin-like (LOC109878563), mRNA
gene10922	-2	2.40E-03	-2	3.23E-02	-4	7.41E-17	-4	5.55E-03	XM_20489783.1	100	PREDICTED: Oncorhynchus kisutch citron Rho-interacting kinase-like (LOC109895792), mRNA
COHO.9190	-2	4.78E-06	-2	7.91E-04	-2	1.57E-08	-2	9.73E-04	XM_20493655.1	100	PREDICTED: Oncorhynchus kisutch CD9 antigen-like (LOC109898620), mRNA
COHO.9941	-2	5.25E-03	-2	8.54E-03	-1	1.38E-04	-2	2.86E-02	XM_20495553.1	100	PREDICTED: Oncorhynchus kisutch complement C1q tumor necrosis factor-related protein 1-like (LOC109899920), transcript variant X1, mRNA
gene10970	-14	1.02E-04	-12	2.64E-05	-4	1.47E-04	-3	3.72E-04	XM_20489848.1	100	PREDICTED: Oncorhynchus kisutch RIMS-binding protein 2-like (LOC109895829), mRNA
COHO.8804	-2	1.24E-03	-2	1.29E-02	-2	1.41E-11	-2	7.15E-03	XM_20492953.1	100	PREDICTED: Oncorhynchus kisutch uncharacterized LOC109898140 (LOC109898140), transcript variant X1, mRNA
COHO.9844	-2	6.98E-07	-2	3.52E-10	-2	8.24E-05	-1	3.09E-02	XM_20495373.1	100	PREDICTED: Oncorhynchus kisutch annexin A5-like (LOC109899815), mRNA
COHO.3693	-2	1.23E-02	-3	8.84E-08	6	1.99E-20	2	4.95E-03	XM_20481018.1	100	PREDICTED: Oncorhynchus kisutch dihydrofolate reductase-like (LOC109889530), mRNA
COHO.13930	-2	3.65E-09	-2	1.04E-02	-3	2.62E-05	-2	3.94E-02	XM_20504405.1	100	PREDICTED: Oncorhynchus kisutch cGMP-specific 3',5'-cyclic phosphodiesterase-like (LOC109906607), transcript variant X2, mRNA
COHO.19811	-2	1.53E-04	-2	4.41E-02	-1	2.15E-03	-2	8.52E-03	XM_20460575.1	100	PREDICTED: Oncorhynchus kisutch neurabin-2-like (LOC109870182), transcript variant X1, mRNA
COHO.9967	-6	3.29E-06	-12	7.97E-09	-2	6.33E-04	-3	3.13E-02	XM_20493979.1	100	PREDICTED: Oncorhynchus kisutch MACRO domain containing 2 (macrod2), partial mRNA
gene6931	-2	3.19E-03	-2	6.20E-04	-2	3.32E-05	-2	1.48E-04	XM_20484122.1	100	PREDICTED: Oncorhynchus kisutch uncharacterized LOC109891583 (LOC109891583), mRNA
COHO.3850	-2	1.84E-04	-2	9.51E-03	-2	2.68E-11	-1	1.34E-02	XM_20481333.1	100	PREDICTED: Oncorhynchus kisutch fibroblast growth factor receptor 2 (fgfr2), transcript variant X2, mRNA
COHO.22416	-2	1.11E-02	-2	1.90E-05	-2	4.50E-05	-2	2.62E-04	XM_20466667.1	100	PREDICTED: Oncorhynchus kisutch cyclin-Y-like (LOC109874663), transcript variant X2, mRNA
COHO.11841	-2	3.86E-02	-3	1.56E-03	-2	2.29E-06	-1	4.08E-02	XM_20499953.1	100	PREDICTED: Oncorhynchus kisutch collagen alpha-1(XVI) chain-like (LOC109903320), mRNA
COHO.26768	-2	1.14E-02	-2	2.71E-02	-2	3.03E-16	-2	2.04E-02	XM_20474902.1	100	PREDICTED: Oncorhynchus kisutch glia-derived nexin-like (LOC109882818), transcript variant X1, mRNA
COHO.27254	-2	7.52E-04	-3	4.48E-06	-2	6.33E-04	-2	2.63E-03	XM_20475830.1	100	PREDICTED: Oncorhynchus kisutch ras association domain-containing protein 6-like (LOC109883798), transcript variant X2, mRNA
COHO.3334	-2	3.65E-09	-2	4.19E-02	-3	4.74E-04	-2	3.51E-02	XM_20480339.1	100	PREDICTED: Oncorhynchus kisutch FYN-binding protein-like (LOC109889133), mRNA
COHO.14422	-2	4.23E-17	-3	2.09E-11	3	1.81E-06	2	1.05E-02	XM_20505483.1	100	PREDICTED: Oncorhynchus kisutch ectonucleotide pyrophosphatase/phosphodiesterase family member 2-like (LOC109907496), mRNA
COHO.394	-2	8.72E-06	-2	2.08E-03	-1	3.81E-02	-2	7.52E-03	XR_2255270.1	100	PREDICTED: Oncorhynchus kisutch uncharacterized LOC109889355 (LOC109889355), ncRNA
COHO.12886	-2	7.17E-05	-2	4.05E-03	-2	9.42E-05	-2	3.27E-02	XM_20502228.1	100	PREDICTED: Oncorhynchus kisutch platelet-derived growth factor receptor beta-like (LOC109905074), transcript variant X1, mRNA
COHO.22451	-2	1.27E-04	-2	1.33E-02	-2	1.43E-03	-2	8.86E-03	XM_20466966.1	100	PREDICTED: Oncorhynchus kisutch uncharacterized LOC109874909 (LOC109874909), mRNA
COHO.6881	-2	4.87E-05	-3	6.90E-13	-2	4.20E-07	-2	4.34E-03	XM_20487185.1	100	PREDICTED: Oncorhynchus kisutch cyclin dependent kinase like 1 (cdkl1), transcript variant X1, mRNA
gene215	-2	1.45E-04	-2	8.08E-05	-1	3.53E-02	-2	4.37E-02	XM_20475252.1	100	PREDICTED: Oncorhynchus kisutch integrin alpha-L-like (LOC109882882), mRNA

COHO.13745	-2	2.06E-05	-1	2.69E-02	-2	1.47E-07	-2	1.55E-04	XM_20503843.1	100	PREDICTED: Oncorhynchus kisutch uncharacterized LOC109906219 (LOC109906219), mRNA
COHO.609	-2	4.01E-03	-2	2.54E-03	5	1.28E-13	4	6.40E-05	XM_20484383.1	100	PREDICTED: Oncorhynchus kisutch uncharacterized LOC109891923 (LOC109891923), mRNA
COHO.21753	-2	4.32E-03	-2	5.70E-03	-4	7.67E-07	-3	1.92E-03	XM_20465340.1	100	PREDICTED: Oncorhynchus kisutch prostaglandin E2 receptor EP4 subtype-like (LOC109873683), mRNA
COHO.5692	-2	1.70E-04	-2	2.48E-03	-3	3.31E-26	-2	7.37E-09	XM_20485887.1	100	PREDICTED: Oncorhynchus kisutch prolyl 4-hydroxylase subunit alpha 2 (p4ha2), transcript variant X1, mRNA
gene13450	-2	2.08E-04	-2	2.35E-05	-2	8.66E-04	-1	8.12E-03	XR_2256362.1	100	PREDICTED: Oncorhynchus kisutch 3-phosphoinositide-dependent protein kinase 1-like (LOC109898469), misc RNA
gene23938	-2	4.06E-06	-1	9.99E-03	-3	1.33E-04	-2	1.39E-02	XM_20509524.1	100	PREDICTED: Oncorhynchus kisutch protein kinase C theta type-like (LOC109910350), mRNA
COHO.7449	-2	1.19E-04	-2	1.50E-03	-1	4.19E-02	-2	2.59E-02	XM_20489828.1	100	PREDICTED: Oncorhynchus kisutch deltex E3 ubiquitin ligase 1 (dtx1), transcript variant X2, mRNA
COHO.10043	-2	8.90E-03	-3	4.05E-06	-1	1.94E-02	-2	1.52E-03	XM_20495766.1	100	PREDICTED: Oncorhynchus kisutch WD repeat domain phosphoinositide-interacting protein 1-like (LOC109900046), mRNA
COHO.9966	-3	6.31E-03	-5	1.47E-04	-2	2.72E-02	-3	2.20E-02	XR_2256530.1	100	PREDICTED: Oncorhynchus kisutch uncharacterized LOC109899955 (LOC109899955), ncRNA
gene36220	-3	4.32E-09	-2	4.32E-03	-2	1.19E-05	-1	1.82E-03	XM_20469946.1	100	PREDICTED: Oncorhynchus kisutch interleukin-6 receptor subunit beta-like (LOC109877746), mRNA
gene34680	-3	1.52E-05	-3	2.98E-07	-1	2.02E-04	-1	1.74E-02	XM_24407814.1	98	PREDICTED: Oncorhynchus tshawytscha androgen receptor-like (LOC112239336), mRNA
COHO.378	-3	3.10E-10	-2	3.80E-02	-2	4.77E-03	-1	1.81E-02	XM_20480495.1	100	PREDICTED: Oncorhynchus kisutch protein AF-17-like (LOC109889223), mRNA
COHO.7090	-3	1.23E-03	-2	7.69E-03	-2	1.35E-02	-2	3.79E-03	XM_20489060.1	100	PREDICTED: Oncorhynchus kisutch nuclear factor of activated T-cells 5-like (LOC109895403), mRNA
COHO.22207	-3	6.94E-04	-2	2.45E-02	-2	2.87E-03	-1	2.00E-02	XM_20467159.1	100	PREDICTED: Oncorhynchus kisutch transmembrane protein 71 (tmem71), transcript variant X4, mRNA
COHO.12659	-3	1.39E-04	-3	5.26E-05	-1	3.32E-04	-2	3.37E-03	XM_20501456.1	100	PREDICTED: Oncorhynchus kisutch EH domain-containing protein 4-like (LOC109904230), mRNA
COHO.11915	-3	8.05E-07	-2	7.67E-04	-2	2.69E-04	-2	4.13E-03	XM_20500066.1	100	PREDICTED: Oncorhynchus kisutch engulfment and cell motility protein 1-like (LOC109903395), mRNA
COHO.16150	-3	1.31E-05	-2	2.92E-02	-2	6.70E-10	-1	5.85E-03	XM_20452204.1	100	PREDICTED: Oncorhynchus kisutch stromal interaction molecule 1-like (LOC109864423), transcript variant X1, mRNA
COHO.4473	-3	1.98E-02	-4	3.00E-06	-2	8.21E-04	-2	9.44E-09	XM_20482842.1	100	PREDICTED: Oncorhynchus kisutch mitogen-activated protein kinase 14A-like (LOC109890804), transcript variant X2, mRNA
gene8779	-3	2.50E-03	-3	1.95E-03	-2	3.82E-03	-1	4.29E-02	XM_21624922.1	98	PREDICTED: Oncorhynchus mykiss beta-1,3-N-acetylglucosaminyltransferase lunatic fringe-like (LOC110538231), mRNA
gene27025	-3	1.56E-02	-3	1.63E-03	-2	1.43E-02	-1	1.69E-02	XM_20455911.1	100	PREDICTED: Oncorhynchus kisutch inositol 1,4,5-trisphosphate receptor type 2-like (LOC109866991), mRNA
COHO.4748	-3	4.03E-05	-2	1.93E-02	-2	4.59E-03	-2	1.46E-02	XM_20483440.1	100	PREDICTED: Oncorhynchus kisutch TRAF3-interacting JNK-activating modulator-like (LOC109891119), transcript variant X2, mRNA
COHO.8916	-7	1.07E-05	-5	4.49E-05	-19	1.58E-03	-5	1.84E-04	XM_20491794.1	100	PREDICTED: Oncorhynchus kisutch uncharacterized LOC109897257 (LOC109897257), mRNA
COHO.2543	-3	1.50E-07	-2	4.28E-02	-2	2.28E-02	-1	3.00E-03	XM_20470934.1	100	PREDICTED: Oncorhynchus kisutch E3 ubiquitin-protein ligase DTX1-like (LOC109878726), mRNA
COHO.5019	-3	2.13E-07	-3	7.80E-08	-1	4.84E-02	-3	1.27E-05	XM_20483916.1	100	PREDICTED: Oncorhynchus kisutch helicase with zinc finger 2 (helz2), transcript variant X3, mRNA
COHO.26179	-3	1.72E-07	-4	2.24E-23	-2	8.46E-08	-2	4.45E-02	XM_20473766.1	100	PREDICTED: Oncorhynchus kisutch membrane-spanning 4-domains subfamily A member 4A-like (LOC109881660), transcript variant X1, mRNA

COHO.19982	-3	7.31E-09	-2	4.57E-03	-2	2.85E-14	-2	9.22E-04	XM_20461212.1	100	PREDICTED: Oncorhynchus kisutch collagen alpha-3(VI) chain-like (LOC109870641), transcript variant X4, mRNA
COHO.3561	-3	7.29E-06	-2	7.06E-03	-2	1.59E-06	-2	1.66E-04	XR_2255277.1	100	PREDICTED: Oncorhynchus kisutch uncharacterized LOC109889391 (LOC109889391), ncRNA
COHO.9298	-3	2.68E-06	-2	4.85E-02	-5	3.79E-24	-8	6.06E-18	XM_20493843.1	100	PREDICTED: Oncorhynchus kisutch transcription factor Sox-9-B-like (LOC109898744), transcript variant X1, mRNA
COHO.26430	-3	2.58E-04	-2	5.91E-04	-2	4.88E-02	-2	6.31E-03	XM_20474231.1	100	PREDICTED: Oncorhynchus kisutch up-regulator of cell proliferation-like (LOC109882137), mRNA
COHO.4921	-3	1.26E-06	-2	3.71E-03	-3	7.87E-05	-2	1.27E-02	XM_20483759.1	100	PREDICTED: Oncorhynchus kisutch differentially expressed in FDCP 6 homolog (LOC109891317), transcript variant X3, mRNA
COHO.29479	-3	9.16E-04	-2	2.65E-04	-2	4.47E-05	-2	3.07E-02	XM_20479248.1	100	PREDICTED: Oncorhynchus kisutch uncharacterized protein C1orf43 homolog (LOC109888004), partial mRNA
COHO.10298	-4	4.54E-02	-5	5.82E-04	-3	9.44E-14	-3	4.92E-04	XM_20496534.1	100	PREDICTED: Oncorhynchus kisutch scavenger receptor class A member 5-like (LOC109900746), mRNA
COHO.1719	-3	3.84E-04	-4	4.03E-05	-2	7.39E-06	-2	1.28E-02	XM_20509375.1	100	PREDICTED: Oncorhynchus kisutch prolyl 3-hydroxylase 3-like (LOC109910242), mRNA
COHO.18669	-3	2.99E-09	-3	4.04E-04	-2	5.56E-14	-2	3.86E-03	XM_20457819.1	100	PREDICTED: Oncorhynchus kisutch apelin receptor B-like (LOC109868348), mRNA
COHO.3352	-3	1.54E-06	-2	1.41E-02	-2	7.43E-03	-2	3.05E-02	XM_20480369.1	100	PREDICTED: Oncorhynchus kisutch tyrosine-protein kinase JAK2-like (LOC109889150), transcript variant X3, mRNA
COHO.19350	-3	1.00E-07	-2	2.11E-02	-2	6.02E-07	-2	2.50E-02	XM_20458850.1	100	PREDICTED: Oncorhynchus kisutch membrane-associated guanylate kinase, WW and PDZ domain-containing protein 1-like (LOC109869032), transcript variant X3, mRNA
COHO.14274	-3	3.16E-05	-4	1.82E-03	3	1.77E-07	2	7.25E-03	XM_20505246.1	100	PREDICTED: Oncorhynchus kisutch growth factor receptor-bound protein 10-like (LOC109907342), transcript variant X1, mRNA
COHO.8770	-3	1.26E-09	-2	1.82E-04	-2	2.98E-05	-2	1.82E-02	XM_20491759.1	100	PREDICTED: Oncorhynchus kisutch desmoplakin-like (LOC109897206), partial mRNA
COHO.21655	-3	2.82E-02	-3	3.04E-02	12	9.96E-60	7	2.93E-12	XM_20466304.1	100	PREDICTED: Oncorhynchus kisutch prostaglandin E synthase-like (LOC109874417), mRNA
COHO.7012	-3	1.44E-04	-3	1.40E-06	-2	4.40E-07	-2	4.63E-02	XM_20488934.1	100	PREDICTED: Oncorhynchus kisutch enhancer of mRNA-decapping protein 3-like (LOC109895320), mRNA
COHO.21931	-3	2.68E-08	-2	6.60E-04	-2	5.58E-03	-2	6.50E-04	XM_20465764.1	100	PREDICTED: Oncorhynchus kisutch protein-lysine 6-oxidase-like (LOC109874026), transcript variant X2, mRNA
COHO.16490	-3	9.89E-05	-3	4.64E-02	-2	4.05E-03	-2	8.77E-03	XM_20452958.1	100	PREDICTED: Oncorhynchus kisutch uncharacterized LOC109864902 (LOC109864902), transcript variant X2, mRNA
gene31427	-3	3.59E-05	-3	4.60E-03	-2	1.15E-05	-2	1.56E-03	XM_20462868.1	100	PREDICTED: Oncorhynchus kisutch collagen alpha-1(VI) chain-like (LOC109871859), mRNA
COHO.21174	-3	5.10E-04	-4	1.73E-03	-2	4.51E-03	-2	1.77E-02	XM_20464517.1	100	PREDICTED: Oncorhynchus kisutch cytotoxic and regulatory T-cell molecule (crtam), transcript variant X2, mRNA
COHO.14509	-3	1.71E-02	-4	7.18E-03	-3	1.16E-04	-2	2.92E-02	XM_20505666.1	100	PREDICTED: Oncorhynchus kisutch exostosin-1c (LOC109907601), transcript variant X4, mRNA
gene24352	-3	2.06E-08	-2	7.59E-03	-2	2.38E-03	-2	3.38E-02	XM_20452539.1	100	PREDICTED: Oncorhynchus kisutch dedicator of cytokinesis protein 2-like (LOC109864674), mRNA
gene29539	-3	9.08E-03	-2	3.47E-02	-2	1.64E-03	-3	2.34E-02	XM_24433060.1	86	PREDICTED: Oncorhynchus tshawytscha zinc finger CCCH domain-containing protein 7B-like (LOC112258593), mRNA
gene30402	-3	4.67E-09	-2	1.24E-06	-2	2.12E-03	-2	1.61E-03	XM_20461430.1	100	PREDICTED: Oncorhynchus kisutch unconventional myosin-Ib-like (LOC109870799), mRNA

COHO.3748	-3	5.65E-03	-2	3.03E-02	-2	6.80E-04	-2	1.66E-03	XM_20481149.1	100	PREDICTED: Oncorhynchus kisutch AMP deaminase 3-like (LOC109889597), transcript variant X2, mRNA
COHO.17900	-3	1.79E-04	-5	3.28E-02	-1	2.33E-02	-2	3.98E-02	XM_20456186.1	100	PREDICTED: Oncorhynchus kisutch protein NLRC5-like (LOC109867189), transcript variant X3, mRNA
COHO.14692	-4	1.68E-13	-4	1.30E-09	-3	1.12E-08	-2	4.63E-02	XM_20506058.1	100	PREDICTED: Oncorhynchus kisutch choline dehydrogenase (chdh), mRNA
COHO.15386	-5	1.80E-08	-5	2.96E-07	-3	1.54E-08	-3	1.91E-04	XM_20509115.1	100	PREDICTED: Oncorhynchus kisutch vimentin (vim), mRNA
gene42166	-2	1.82E-05	-5	3.04E-16	-4	5.54E-13	-2	6.17E-04	XR_2474308.1	96	PREDICTED: Oncorhynchus mykiss insulin-like growth factor-binding protein 2-A (LOC110528844), transcript variant X2, misc RNA
COHO.10244	-4	2.33E-03	-3	8.69E-04	-2	4.92E-04	-1	3.23E-02	XM_20496433.1	100	PREDICTED: Oncorhynchus kisutch mitogen-activated protein kinase 5-like (LOC109900687), transcript variant X3, mRNA
COHO.26532	-4	1.23E-10	-5	2.80E-08	-2	1.92E-02	-2	4.84E-03	XM_20474454.1	100	PREDICTED: Oncorhynchus kisutch plexin-A4-like (LOC109882352), mRNA
COHO.8205	-30	4.40E-09	-4	5.29E-03	-5	2.47E-17	-3	1.24E-06	XR_2256167.1	100	PREDICTED: Oncorhynchus kisutch uncharacterized LOC109896985 (LOC109896985), ncRNA
COHO.14148	-4	8.99E-05	-3	6.75E-04	-2	1.83E-11	-2	4.63E-04	XM_20505055.1	100	PREDICTED: Oncorhynchus kisutch uncharacterized LOC109907218 (LOC109907218), mRNA
gene41715	-4	1.01E-03	-3	1.15E-06	-3	5.89E-17	-2	4.01E-04	XM_20475713.1	100	PREDICTED: Oncorhynchus kisutch protein Jumonji-like (LOC109883683), partial mRNA
COHO.7541	-4	2.01E-08	-4	7.76E-07	-2	1.34E-13	-2	2.45E-02	XM_20490038.1	100	PREDICTED: Oncorhynchus kisutch RILP-like protein 1 (LOC109895926), transcript variant X1, mRNA
COHO.11518	-4	9.03E-08	-4	8.08E-06	-3	5.54E-06	-2	3.06E-02	XM_20499025.1	100	PREDICTED: Oncorhynchus kisutch A disintegrin and metalloproteinase with thrombospondin motifs 10-like (LOC109902569), transcript variant X2, mRNA
COHO.21560	-4	7.22E-07	-2	3.66E-02	-2	1.06E-03	-2	2.10E-02	XM_20464447.1	100	PREDICTED: Oncorhynchus kisutch rho guanine nucleotide exchange factor 15-like (LOC109872994), transcript variant X3, mRNA
COHO.23344	-4	4.53E-02	-4	5.29E-05	-3	5.40E-12	-2	5.33E-03	XR_2253019.1	100	PREDICTED: Oncorhynchus kisutch uncharacterized LOC109876517 (LOC109876517), ncRNA
gene189110	-19	1.39E-12	-4	4.75E-06	-4	1.01E-05	-3	1.37E-02	XM_20501531.1	100	PREDICTED: Oncorhynchus kisutch SAM and SH3 domain-containing protein 1-like (LOC109904287), transcript variant X2, mRNA
COHO.10099	-4	2.64E-03	-2	3.61E-04	-3	7.80E-15	-1	2.92E-02	XM_20496170.1	100	PREDICTED: Oncorhynchus kisutch zinc finger and BTB domain-containing protein 25-like (LOC109900517), mRNA
COHO.23654	-4	2.59E-04	-3	5.38E-03	-2	4.88E-21	-2	2.83E-03	XM_20469393.1	100	PREDICTED: Oncorhynchus kisutch serum paraoxonase/arylesterase 2-like (LOC109877072), mRNA
COHO.19942	-4	1.68E-09	-3	9.25E-05	2	1.85E-03	2	1.66E-04	XM_20460808.1	100	PREDICTED: Oncorhynchus kisutch zinc finger protein 503-like (LOC109870327), mRNA
COHO.20435	-4	3.90E-04	-4	1.29E-08	-1	1.82E-03	-1	2.24E-03	XM_20461684.1	100	PREDICTED: Oncorhynchus kisutch ATP-dependent 6-phosphofructokinase, liver type-like (LOC109870961), mRNA
COHO.18225	-4	3.24E-10	-6	1.32E-07	-3	1.63E-02	-2	9.13E-03	XM_20455960.1	100	PREDICTED: Oncorhynchus kisutch coiled-coil domain-containing protein 136-like (LOC109867051), mRNA
gene36265	-5	3.01E-02	-3	2.54E-02	-2	2.56E-09	-2	3.27E-03	XM_24388602.1	99	PREDICTED: Oncorhynchus tshawytscha tumor necrosis factor receptor superfamily member EDAR-like (LOC112225042), mRNA
COHO.15920	0	4.11E-02	-3	1.96E-03	-2	2.08E-02	-3	1.99E-04	XM_20453211.1	100	PREDICTED: Oncorhynchus kisutch plexin-A4-like (LOC109865081), partial mRNA
COHO.12337	-4	1.08E-16	-3	6.74E-09	-2	3.16E-08	-2	1.65E-03	XM_20500892.1	100	PREDICTED: Oncorhynchus kisutch kinase D-interacting substrate of 220 kDa-like (LOC109903884), transcript variant X4, mRNA
COHO.2728	-5	5.03E-08	-3	2.15E-03	-2	2.91E-07	-2	2.97E-02	XM_20473805.1	100	PREDICTED: Oncorhynchus kisutch autism susceptibility gene 2 protein-like (LOC109881677), transcript variant X3, mRNA

COHO.13351	-5	5.90E-03	-3	2.97E-02	2	8.69E-04	2	2.86E-02	XM_20503101.1	100	PREDICTED: Oncorhynchus kisutch protein phosphatase 1L-like (LOC109905619), transcript variant X1, mRNA
COHO.10623	-5	1.80E-07	-3	1.43E-02	-2	3.43E-02	-5	1.49E-06	XM_20497131.1	100	PREDICTED: Oncorhynchus kisutch uncharacterized LOC109901106 (LOC109901106), mRNA
COHO.7661	-5	2.23E-09	-2	3.42E-03	-2	2.58E-05	-2	1.13E-02	XM_20488582.1	100	PREDICTED: Oncorhynchus kisutch autism susceptibility gene 2 protein-like (LOC109894924), mRNA
COHO.15083	-5	9.62E-03	-3	2.93E-02	-2	3.47E-02	-2	2.82E-02	XM_20506891.1	100	PREDICTED: Oncorhynchus kisutch arf-GAP with GTPase, ANK repeat and PH domain-containing protein 2-like (LOC109908288), mRNA
COHO.27195	-5	1.29E-08	-2	2.74E-06	-2	3.28E-24	-2	3.23E-02	XM_20475712.1	100	PREDICTED: Oncorhynchus kisutch protein Jumonji-like (LOC109883682), mRNA
COHO.3312	-5	1.02E-07	-3	2.77E-03	-2	2.56E-06	-2	3.65E-03	XM_20480306.1	100	PREDICTED: Oncorhynchus kisutch interferon-induced protein 44-like (LOC109889108), transcript variant X2, mRNA
gene11663	-5	1.78E-14	-3	3.22E-05	11	1.63E-02	10	4.03E-02	XM_20490958.1	100	PREDICTED: Oncorhynchus kisutch myosin-binding protein C, slow-type-like (LOC109896661), mRNA
COHO.17434	-6	5.57E-06	-3	5.65E-05	-2	6.78E-05	-2	4.31E-05	XM_20454700.1	100	PREDICTED: Oncorhynchus kisutch uncharacterized LOC109866141 (LOC109866141), transcript variant X7, mRNA
COHO.17202	-13	1.58E-10	-3	2.70E-05	-4	1.11E-29	-2	1.46E-04	XM_20454302.1	100	PREDICTED: Oncorhynchus kisutch probable ATP-dependent RNA helicase DDX17 (LOC109865835), mRNA
gene43513	-6	2.04E-04	-7	3.45E-05	3	2.13E-06	2	5.28E-03	XM_20477435.1	100	PREDICTED: Oncorhynchus kisutch hephaestin-like protein 1 (LOC109885602), mRNA
gene34864	-6	2.93E-02	-6	4.62E-03	3	2.95E-14	2	6.26E-05	XM_20468727.1	100	PREDICTED: Oncorhynchus kisutch cell migration-inducing and hyaluronan-binding protein-like (LOC109876289), mRNA
COHO.1836	-3	2.43E-03	-3	2.00E-07	-3	1.82E-05	-4	3.13E-02	XM_20453957.1	100	PREDICTED: Oncorhynchus kisutch villin-1-like (LOC109865618), transcript variant X3, mRNA
COHO.267	-7	1.80E-06	-3	3.44E-05	-3	3.33E-13	-2	4.99E-04	XR_2254114.1	100	PREDICTED: Oncorhynchus kisutch probable ATP-dependent RNA helicase DDX17 (LOC109883060), misc RNA
COHO.9325	-4	7.79E-05	-3	5.39E-05	-2	9.30E-08	-3	1.49E-06	XM_20494260.1	100	PREDICTED: Oncorhynchus kisutch lisH domain and HEAT repeat-containing protein KIAA1468 homolog (LOC109899208), mRNA
gene40489	-7	8.99E-03	-11	4.54E-05	-2	1.47E-02	-2	6.78E-04	XM_20474456.1	100	PREDICTED: Oncorhynchus kisutch plexin-A4-like (LOC109882353), mRNA
gene15134	-4	9.29E-04	-3	4.84E-09	-3	1.63E-06	-3	6.83E-09	XM_20497363.1	100	PREDICTED: Oncorhynchus kisutch papilin-like (LOC109901324), mRNA
COHO.6422	-6	2.68E-06	-3	2.07E-02	-5	7.80E-05	-3	1.80E-07	XM_20487442.1	100	PREDICTED: Oncorhynchus kisutch uncharacterized LOC109894172 (LOC109894172), transcript variant X1, mRNA
COHO.6740	-14	4.54E-04	-30	4.62E-03	-2	3.54E-06	-3	5.82E-03	XM_20488016.1	100	PREDICTED: Oncorhynchus kisutch ectonucleoside triphosphate diphosphohydrolase 5-like (LOC109894489), mRNA
COHO.18516	-3	1.11E-08	-3	1.97E-08	-4	2.96E-22	-2	1.84E-03	XM_20457261.1	100	PREDICTED: Oncorhynchus kisutch dimethylglycine dehydrogenase (dmgdh), mRNA
COHO.26754	-2	3.28E-08	-3	1.12E-20	-4	5.63E-22	-3	5.06E-05	XM_20474863.1	100	PREDICTED: Oncorhynchus kisutch insulin-like growth factor-binding protein 2-A (LOC109882775), mRNA
gene2534	-4	5.98E-06	-2	1.48E-05	-3	7.40E-11	-3	1.84E-03	XM_20455906.1	100	PREDICTED: Oncorhynchus kisutch disintegrin and metalloproteinase domain-containing protein 23-like (LOC109866979), mRNA

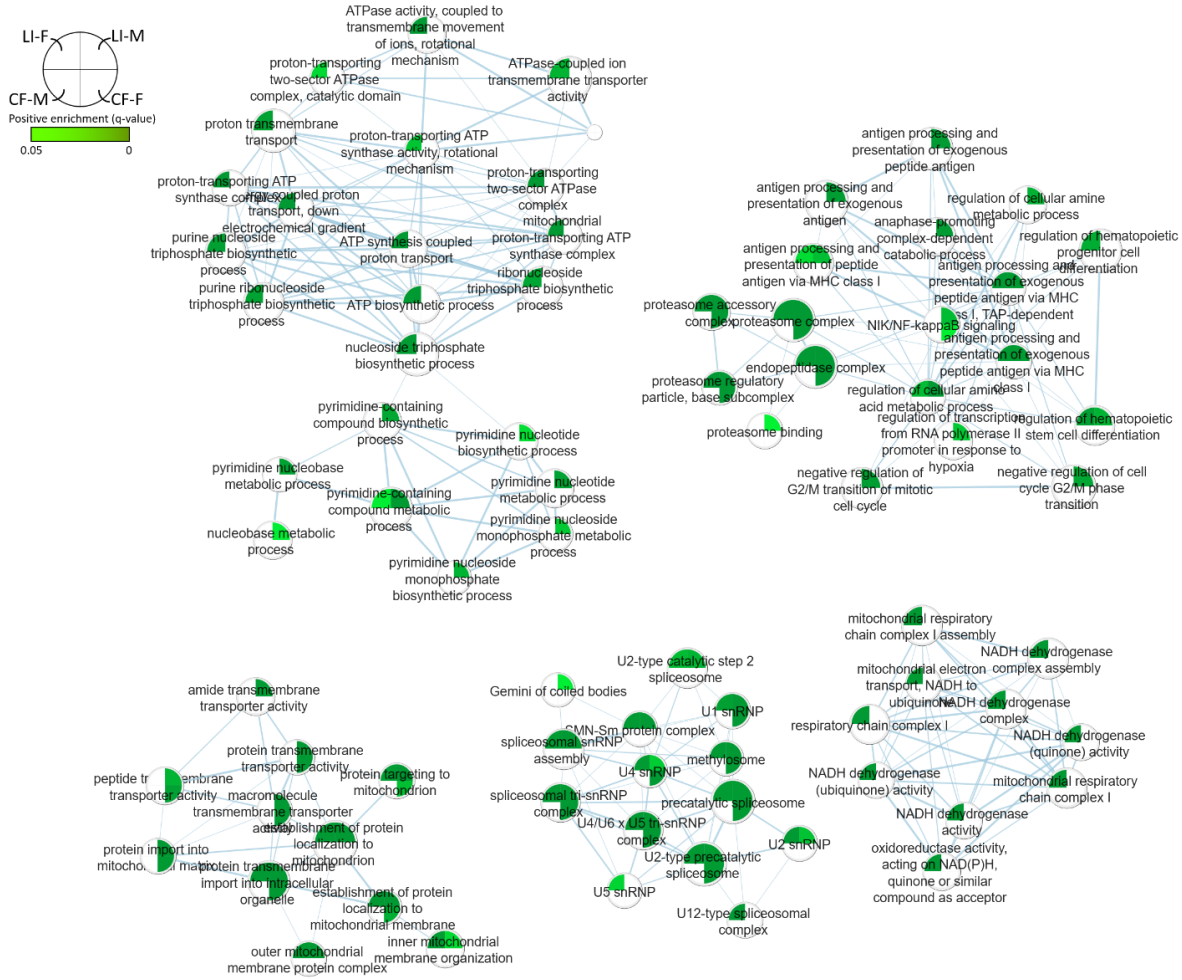

Appendix 22-1. Map of enriched GO terms from HSFO WAF after applying an extremes filter (minimum 20, maximum 100 annotated genes). See **Appendix 20-1** figure legend for more details.

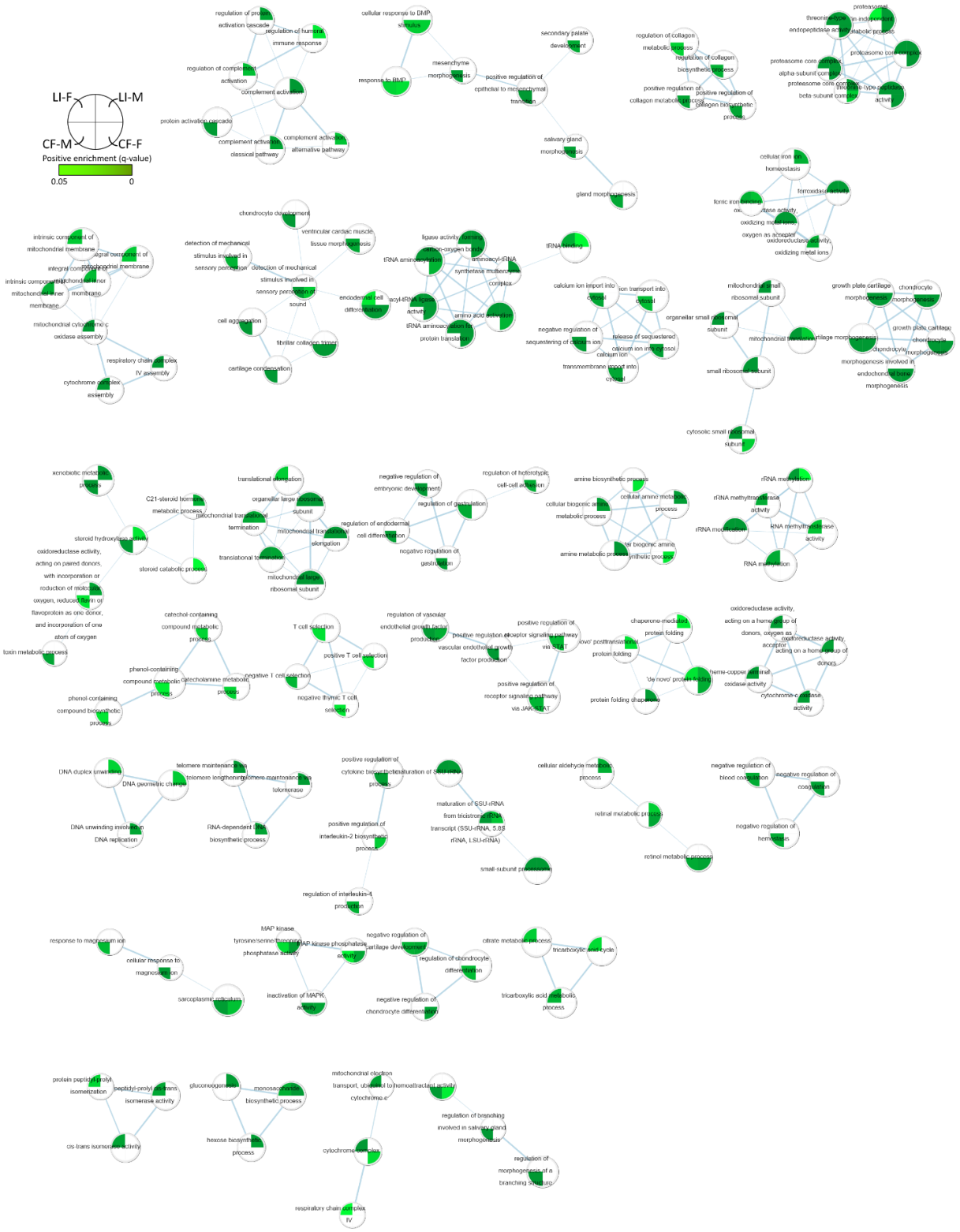

Appendix 22-2. Continued map of enriched GO terms from HSFO WAF. See **Appendix 20-1** figure legend for more details.

Appendix 22-3. Continued map of enriched GO terms from HSFO WAF. See **Appendix 20-1** figure legend for more details.

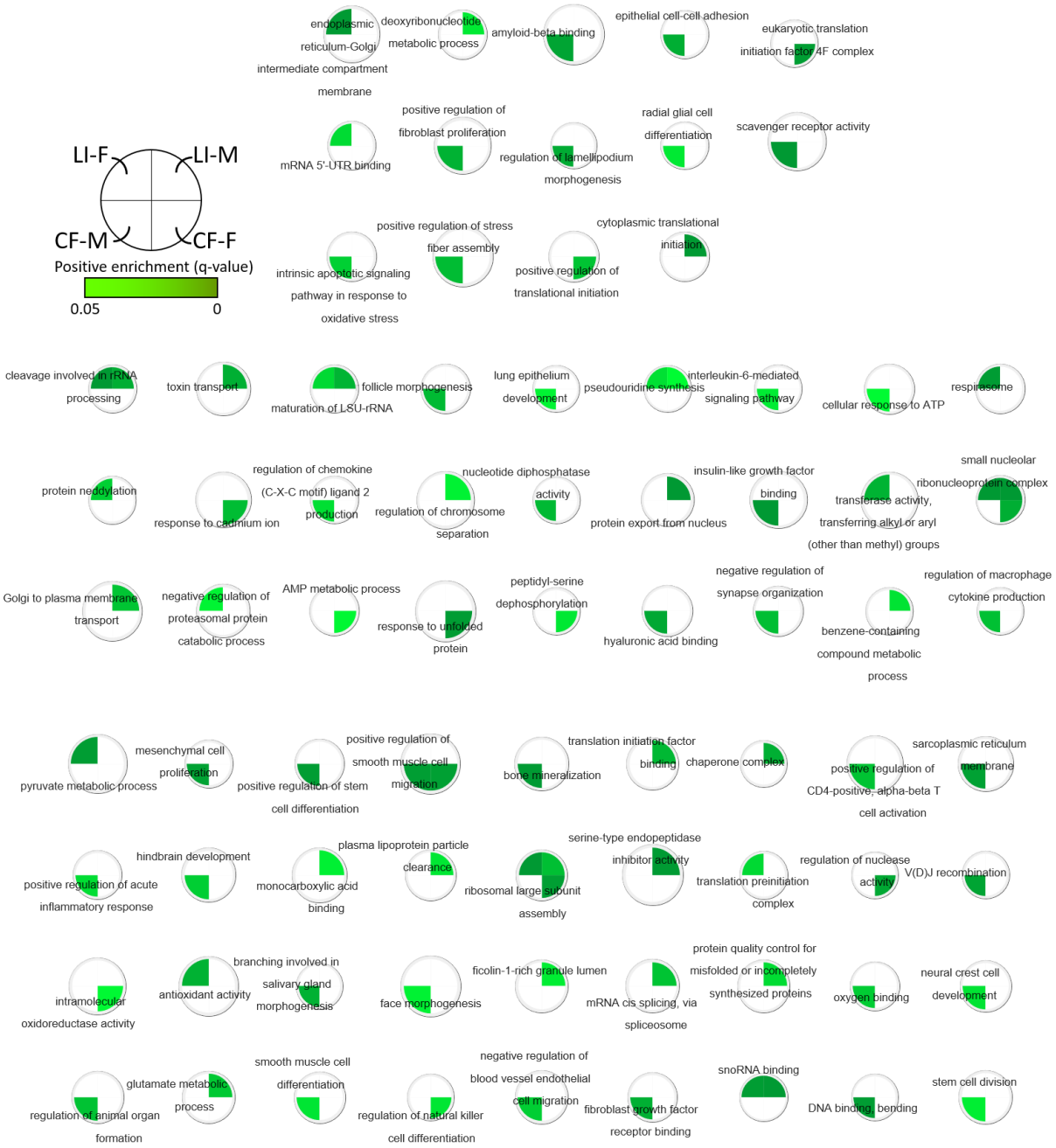

Appendix 22-4. Continued map of enriched GO terms from HSFO WAF. See **Appendix 20-1** figure legend for more details.

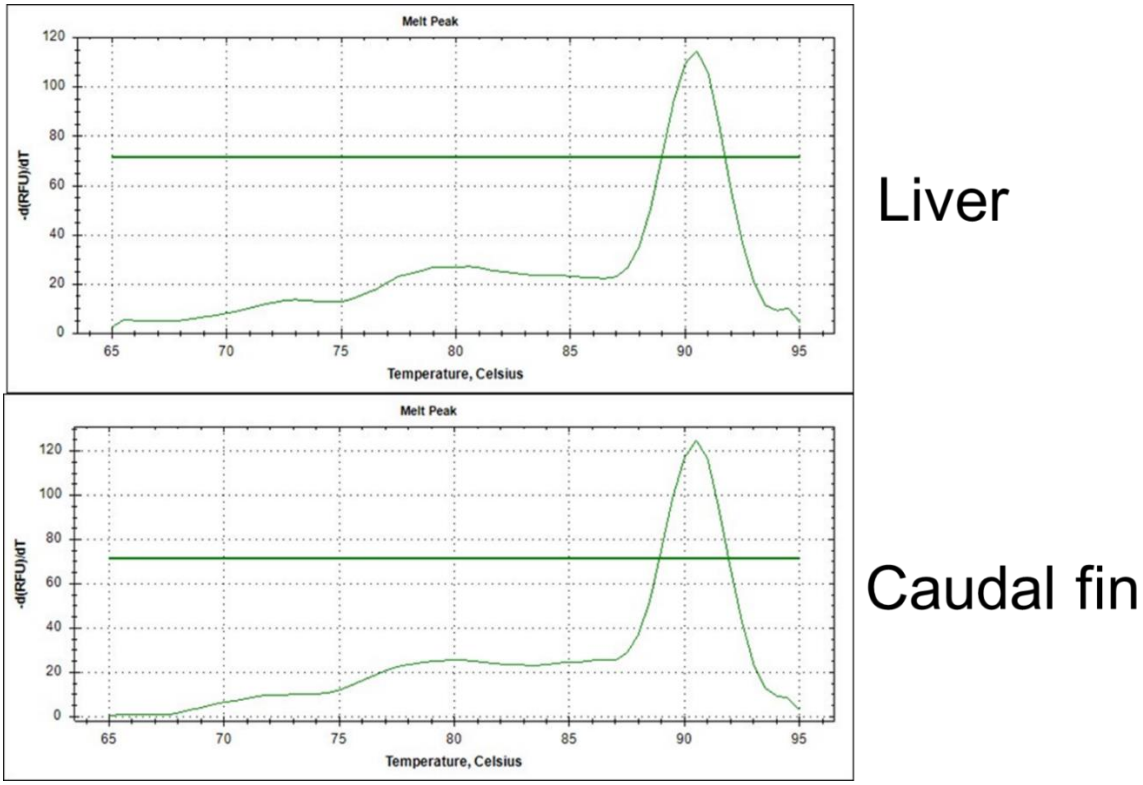

Appendix 23. qPCR amplification using *cyp1a1* primer sets results in a single thermodenaturation peak identifying that only a single transcript is primarily amplified using this primer set. Differential relative fluorescence compared to the heat of denaturation is compared during heat denaturation cycle. C*yp1a1* specificity is further confirmed through gel banding patterns after restriction digest of amplicon using FokI (data not shown).

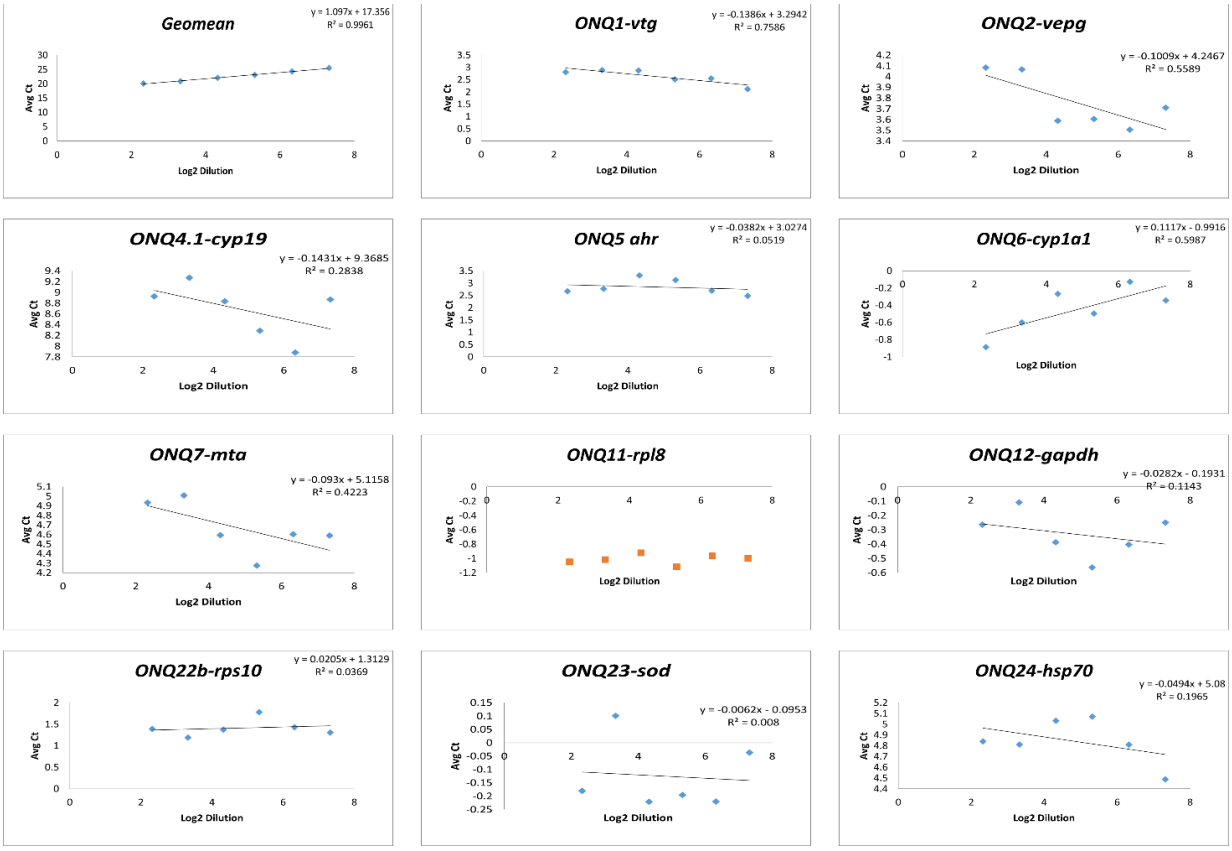

Appendix 24. Primer efficiencies with amplification of five-fold to 160-fold diluted liver cDNA. C_t values are normalized against the geometric mean of *rpl8* and *rps10* normalizers.

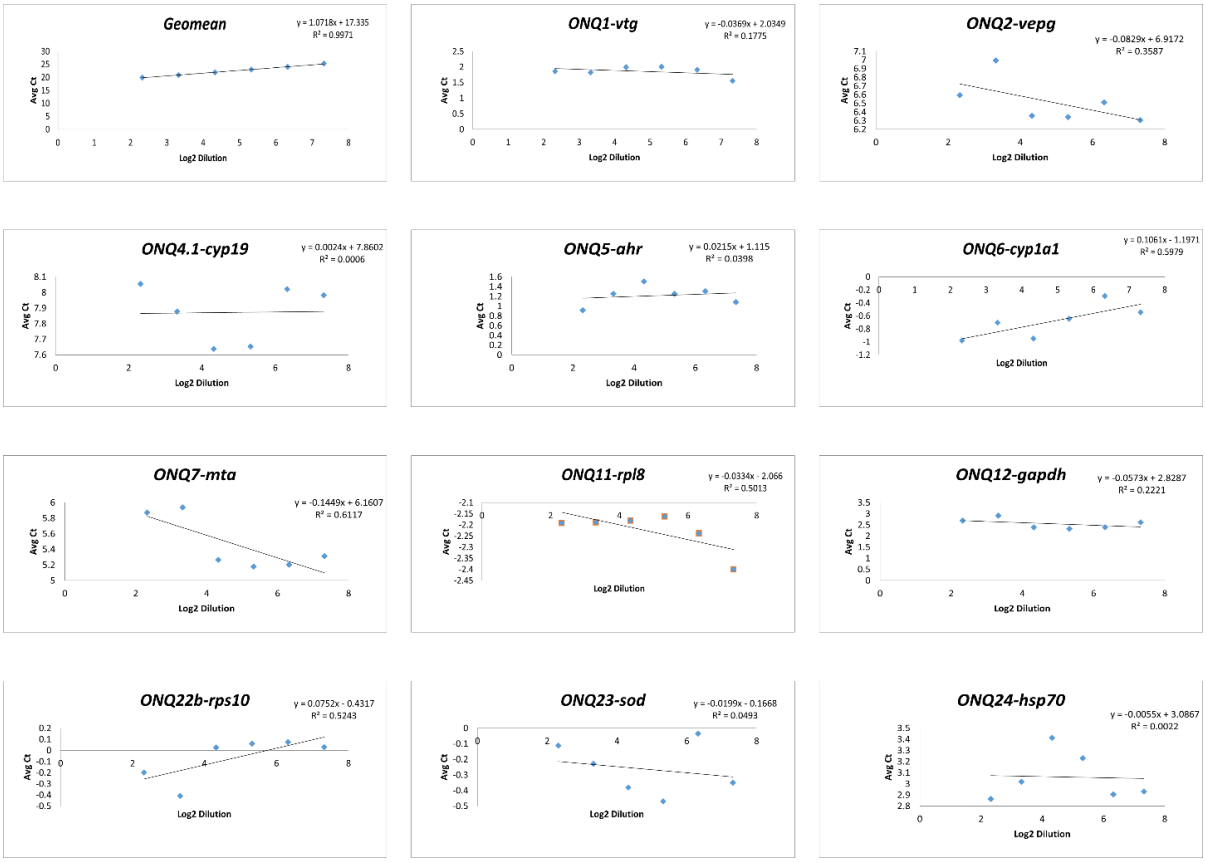

Appendix 25. Primer efficiencies with amplification of five-fold to 160-fold diluted caudal fin cDNA. C_t values are normalized against the geometric mean of *rpl8* and *rps10* normalizers.